Adaptive distributed control of uncertain multi-agent systems in the power-chained form

Lyu, Maolong

DOI
10.4233/uuid:183c7014-a4cb-41b7-a107-0fd4b1a672d7

Publication date
2021

Document Version
Final published version

Citation (APA)
Lyu, M. (2021). *Adaptive distributed control of uncertain multi-agent systems in the power-chained form*. [Dissertation (TU Delft), Delft University of Technology]. https://doi.org/10.4233/uuid:183c7014-a4cb-41b7-a107-0fd4b1a672d7

Adaptive Distributed Control of Uncertain Multi-Agent Systems in the Power-Chained Form

ADAPTIVE DISTRIBUTED CONTROL OF UNCERTAIN MULTI-AGENT SYSTEMS IN THE POWER-CHAINED FORM

Proefschrift

ter verkrijging van de graad van doctor
aan de Technische Universiteit Delft,
op gezag van de Rector Magnificus Prof.dr.ir. T.H.J.J. van der Hagen
voorzitter van het College voor Promoties,
in het openbaar te verdedigen op
vrijdag 1 oktober 2021 om 10:00 uur

door

Maolong LYU

Master of Engineering in Control Science and Engineering,
Air Force Engineering University, Xi'an, China,
geboren te Mianyang, China.

Dit proefschrift is goedgekeurd door de promotoren.

Samenstelling promotiecommissie bestaat uit:

Rector Magnificus	voorzitter
Prof.dr. S. Baldi,	Southeast University & Technische Universiteit Delft, promotor
Prof.dr.ir. B. De Schutter	Technische Universiteit Delft, promotor
Onafhankelijke leden:	
Prof. dr. ir. J. Hellendoorn	Technische Universiteit Delft
Prof. dr. ir. T. Keviczky	Technische Universiteit Delft
Prof. dr. ir. M. Cao	Universiteit van Groningen
Prof. dr. Z. D. Wang,	Brunel-universiteit, Engeland
Overig lid:	
Prof. dr. Z. Y. Chen	Universiteit van Newcastle, Australië

Keywords:	Distributed control, multi-agent systems, power-chained form.
Front & Back:	Representative application of multi-agent systems.
Cover designed by:	Maolong Lyu.
Printed by:	Gildeprint.

ISBN 978-94-6419-299-5

An electronic version of this dissertation is available at
http://repository.tudelft.nl/.

If you don't accumulate steps, you can't reach a thousand miles; if you don't accumulate small currents, you can't become a river!

– Xunzi

CONTENTS

ACKNOWLEDGEMENTS

Four years of PhD time is fleeting, and it is time to thank the people who made this journey possible and fantastic. This journey was full of ups and downs, but with the help of many people, it was perfect and meaningful in the end.

First of all, I want to thank my daily supervisor dr. Simone Baldi for giving me the sufficient trust of truly independent research. I would like to thank him on a personal level. Four years ago, we met in Xi'an, China, and had a great time. In the second year of my PhD, I decided to change the PhD topic to a new and challenging field that we both were not familiar with. He not only gave me full trust, but also helped me to refine the problem. Facing new research topics, there was a period of time when I was very stressed and often suffered from insomnia and health problems. At this time, he always comforted me and gave me encouragement and strength. Whenever I formulated an idea or finished paper drafts, he can always give me some insightful comments which improved the quality of the papers quite a lot. All the help he provided throughout these years, the assistance with presentations, and the suggestions about research or on how to reply to reviewers has been precious to me, both for my personal growth and for my PhD topic.

Besides, I truly intend to express my sincere gratitude to my promotor Prof. Bart De Schutter for his constant support and encouragement. His critical attitude towards research helped me to find the pitfalls and issues with my work. Due to long hours of work and sitting, I had a problem with my back two years ago. Prof. Bart took the initiative to care about me and contacted the secretary to provide me with a height-adjustable table. No matter when I encountered difficulties, he always stood by me and offered me a hand. I would personally thank Prof. Bart for all of this. Thank you for creating a relaxing and pleasant research atmosphere for our team. Overall, it was a super nice experience to work with you.

Secondly, I would like to thank my PhD committee members, Prof. Hans Hellendoorn, Prof. Zhiyong Chen, Prof. Ming Cao, Prof. Zidong Wang, and Prof. Tamas Keviczky for their constructive comments and for their valuable time. They helped me greatly to improve the quality of this dissertation.

Next, special thanks go to my good friends: thanks Shuai, Fan, and Hai for sharing their research experiences in the early stages of my PhD; thanks Yaoling and Nan for helping me to get to know the new study and living environment; thanks Kim for cheering me up when I face difficulties; thanks Umur, Diego and Martinmy for creating a lot of happy and relaxing moments during my internship in the University of Grenoble; thanks our basketball team members Jingwei, Jianing, Dingshan, Dongdong, Zehang, Junda, Shuaidong, Jinshan, Hao, Qichen, and Hanqing for many happy times to sweat together; thanks our table football team members Tomas, Prof. Momo, Carlos R., Carlos C., Jesus, Alejandro, and Abhimanyu for many joyous moments; thanks our football team members Qiang, Changyi, Kun, Heng, Jinbing, and Bin for some exciting moments; thanks

my flatmates Kaikai, Sihao, Zhi, Congbiao, Yihan, Xiaojuan, Lu, Yaoling, and Nan for offering me the opportunity to taste all sorts of delicious food; thanks Prof. Chen, Prof. Wang, Prof. Cao, Prof. Yu, Prof. Tong, Prof. Li, Prof. Liu, Prof. Zhao, Xuerui, Zongcheng, Shuai, Fan, and Wei for valuable academic discussions and collaborations. I would also like to take this opportunity to thank the DCSC secretaries Heleen, Marieke, and Francy for organizing the nice events.

Then, I would like to thank all the colleagues and friends I met in Delft and in particular at DCSC. A warm thanks goes to Tomas, Carlos Andres, Momo, Mahdiyeh, Carlos R., Carlos C., Fernando, Camilo, Alfiya, Suad, Barbara, Rodrigo, Giovanni, Manyu, Mattia, Aitazaz, Facundo, Filippo, Clara, Alejandro, Shuai, Hai, Kim, Anqi, Arman, Hongpeng, Hao, Kai, Na, Yang, Dingshan, Jianfeng, Jianing, Yongxia, Huichen, Ping, Rui, Langzi, Qingrui, Chengwei, Haohua, Jingwei, Xiaoyu, and Tian. I extend my appreciation to the “Chili con Carne" community founded by the dictator Tomas.

Last but not least, I would like to express my gratitude to my wife, my parents, and my parents-in-law. Thank all of you for your endless love, understanding, and unconditional support during the last four years. Despite being thousands miles away, you are always there to encourage me and cheer me up when I encountered problems. Thank you so much for standing behind me during my PhD study. Without your support I would have never seen the end of this voyage.

SUMMARY

Power-chained form systems are a generalization of strict-feedback and pure-feedback systems since integrators with positive odd-powers can appear in the dynamics (chain of positive-odd power integrators) and they are extremely challenging to deal with, as their linearized dynamics might possess uncontrollable modes whose eigenvalues are in the right-hand-side plane, making standard feedback linearization or standard backstepping methodologies fail. The adding-one-power-integrator technique was proposed to handle power-chained form systems. Progress made for power-chained form systems includes employing universal approximators to handle completely unknown nonlinearities. However, state-of-the-art results on power-chained form systems are mainly focused on the single-agent case since a direct extension of the existing design to a distributed setting is not very meaningful on account of the facts that: i) the control gain of each virtual control is incorporated into the next virtual control law iteratively, possibly leading to high-gain issues; ii) state-of-the-art results rely on the assumption that the agents' control directions are known a priori and are available for control design; iii) universal approximators often used in the adding-one-power-integrator procedure inevitably increase the complexity in the sense that extra adaptive parameters have to be updated (i.e. extra nonlinear differential equations need to be solved numerically), thus making their distributed implementation difficult.

In the first part of this thesis, we propose a reduced-complexity adaptive methodology for multi-agent power-chained form systems. Complexity is reduced in a twofold sense: the control gain of each virtual control law does not have to be incorporated iteratively in the next virtual control law, thus leading to a simpler expression of the control laws; the power of the virtual and actual control laws increases only proportionally (rather than exponentially) with the order of the systems, dramatically reducing high-gain issues.

In the second part of this thesis, we consider multi-agent in power-chained form systems with multiple control directions, some being known, some being unknown. We develop a new conditional inequality composed by multiple hybrid Nussbaum functions for dealing with such mixed a priori knowledge.

In the third part of this thesis, we address the problem of removing the large transients in learning caused by the use of Nussbaum functions. As a consequence, we propose a logic-based switching control method tailored for multi-agent in power-chained form systems. Logic-based control refers to the fact that a switching logic (in place of a Nussbaum mechanism) is in charge of estimating online the control directions, assumed to be unknown a priori for all agents.

In the fourth part of this thesis, we address the problem of avoiding any universal approximators (e.g. neural networks, fuzzy logic systems, etc.) in the control design. Accordingly, we design a low-complexity prescribed-performance controller for a single-agent power-chained form system, guaranteeing minimum convergence rate, maximum

overshoot, and maximum steady-state error. In this scenario, the control coefficients are not only taken to be unknown, but also time-varying. In order to solve this problem, we resort to the Nussbaum approach, and we show via a counterexample and a positive example that only some particular type B Nussbaum functions are still type B Nussbaum functions even when elevated to a positive-odd integer power. These latter functions can be used for handling time-varying unknown control coefficients. Correspondingly, a new switching conditional inequality is proposed. This inequality encompasses existing ones as special cases: instead of always increasing the Nussbaum gain, its design is based on increasing the Nussbaum gain only when the tracking error is close to violating the performance bounds.

SAMENVATTING

Power-chained form systemen zijn een generalisatie van strict feedback en pure feedback systemen, aangezien integrators met positive oneven krachten in de dynamiek kunnen verschijnen (keten van positieve odd power-integratoren) en ze zijn buitengewoon uitdagend om mee om te gaan, omdat hun gelineariseerde dynamiek kan bezitten. Oncontroleerbare modi waarvan de eigenwaarden zich in het rechterzijvlak bevinden, waardoor standaard feedbacklinearisering of standaard backstepping-methodologieën mislukken. De-add-one-power-integrator techniek werd voorgesteld om een bekrachtigde vorm aan te kunnen. Vooruitgang die is geboekt voor vorm met een stroomketen omvat het gebruik van universele benaderingen om volledig onbekende niet-lineariteiten aan te pakken. State-of-the-art resultaten op het gebied van power chained-vorm zijn echter voornamelijk gericht op single agent-gevallen, aangezien een directe uitbreiding van het bestaande ontwerp naar een gedistribueerde setting niet erg zinvol is vanwege het feit dat: i) de add-one-power- de integratortechniek vertoont een aantal complexe aspecten aangezien de controleversterking van elke virtuele controle iteratief wordt opgenomen in de volgende virtuele controlewet, wat mogelijk leidt tot een probleem met een hoge gain; ii) state-of-the-art resultaten berusten op de aanname dat de controlerichtingen van de agenten a priori bekend zijn en beschikbaar zijn voor het ontwerp van de controle; iii) universele benaderingen die vaak worden gebruikt bij het toevoegen van één kracht-integratorprocedure verhogen onvermijdelijk de complexiteit in die zin dat extra adaptieve parameters moeten worden bijgewerkt (d.w.z. extra niet-lineaire differentiaalvergelijkingen moeten numeriek worden opgelost), waardoor hun gedistribueerde implementatie moeilijk wordt.

In het eerste deel van dit proefschrift stellen we een adaptieve methodologie voor met verminderde complexiteit voor een multi agentversie van een vorm met een stroomketen. De complexiteit wordt in tweevoudige zin verminderd: de controlewinst van elke virtuele controlewet hoeft niet iteratief in de volgende virtuele controlewet te worden opgenomen, wat leidt tot een eenvoudigere uitdrukking van de controlewetten; de kracht van de virtuele en feitelijke controlewetten neemt slechts proportioneel (in plaats van exponentieel) toe met de volgorde van de systemen, waardoor de problemen met hoge versterking drastisch worden verminderd.

In het tweede deel van dit proefschrift kijken we naar agenten in de vorm van een stroomketen met meerdere controlerichtingen, waarvan sommige bekend zijn, andere onbekend. We ontwikkelen een nieuwe voorwaardelijke ongelijkheid die bestaat uit meerdere hybride Nussbaum functies voor het omgaan met dergelijke gemengde a priori kennis. In het derde deel van dit proefschrift behandelen we het probleem van het verwijderen van de grote transiënten die leren veroorzaakt door het gebruik van Nussbaumfuncties. Daarom stellen we een op logica gebaseerde schakelbesturingsmethode voor, op maat gemaakt voor agenten in de vorm van een stroomketen. Op logica gebaseerde besturing verwijst naar het feit dat een schakellogica (in plaats van een Nussbaum mech-

anisme) verantwoordelijk is voor het online schatten van de besturingsrichtingen, waarvan wordt aangenomen dat deze voor alle agents onbekend zijn.

In het vierde deel van dit proefschrift behandelen we het probleem van het vermijden van universele benaderingen (bijv. Neurale netwerken, fuzzy logic-systemen, enz.) In het besturingsontwerp. Dienovereenkomstig ontwerpen we een voorgeschreven prestatiecontroller met een lage complexiteit voor een enkele vorm met een stroomketen, waardoor minimale convergentie wordt gegarandeerd snelheid, maximale overschrijding en stabiele fout. In dit scenario worden de controlecoëfficiënten niet alleen als onbekend beschouwd, maar ook in de tijd variërend. Om dit probleem op te lossen, nemen we onze toevlucht tot de Nussbaum-benadering en laten we via een tegenvoorbeeld en een positief voorbeeld zien dat slechts enkele bepaalde Nussbaum-functies hun eigenschap behouden, zelfs wanneer ze worden verhoogd tot een positieve oneven-integermacht. Deze laatste functies kunnen worden gebruikt voor het verwerken van in de tijd variërende onbekende stuurcoëfficiënten. Er wordt een nieuwe voorwaardelijke ongelijkheid voorgesteld. Deze ongelijkheid omvat bestaande als speciale gevallen: in plaats van altijd de Nussbaum-versterking te verhogen, is het ontwerp ervan gebaseerd op het alleen verhogen van de Nussbaum-versterking wanneer de tracking error de prestatiegrenzen bijna overschrijdt.

NOTATIONS

$\mathbb{R}$	set of real numbers
$\mathbb{R}^n$	set of n component real vectors
$\mathbb{R}^+$	set of positive real numbers
$\mathbb{R}^{n\times n}$	set of n by n real matrices
x^T	transpose of vector x
$\mathbb{N}_{\text{odd}}$	set of positive odd integers
$\|\cdot\|$	Euclidean norm
■	end of proof
$\triangleq$	equal by definition
$\sigma_{\min}(\cdot)$	minimum singular value of a matrix
$\text{sign}(\cdot)$	sign of a number
$x(t^-)$	left limit of $x(t)$, i.e., $x(t^-) = \lim_{\tau\to t^-} x(\tau)$
Class $\mathcal{K}$	An function $\alpha : [0,\infty) \to [0,\infty)$ is of *class* $\mathcal{K}$, written as $\alpha \in \mathcal{K}$ when α is continuous, strictly increasing, and $\alpha(0) = 0$
Class $\mathcal{KL}$	An function $\beta : [0,\infty) \times [0,\infty) \to [0,\infty)$ is of *class* $\mathcal{KL}$, written as $\beta \in \mathcal{KL}$ when $\beta(\cdot, t)$ is of *class* $\mathcal{K}$ for each fixed $t \geq 0$ and $\beta(s, t)$ decreases to 0 as $t \to \infty$ for each fixed $s \geq 0$
Class $\mathcal{K}_\infty$	An function ζ: $[0,\infty) \to [0,\infty)$ is of *class* $\mathcal{K}_\infty$ if it is continuous, strictly increasing, unbounded, and $\zeta(0) = 0$

1

INTRODUCTION

This chapter presents the main motivation of the research of this thesis. The research questions and main contributions of this thesis are given. After that, the chapter is concluded with an outline of the thesis.

1.1. Motivation of the Research

1.1.1. Distributed Control of Multi-Agent Systems

A typical setting of distributed control is to steer a team of agents to a not globally known leader signal y_r using only locally available information, which is collected from neighboring agents [84, 90, 131] according to the graph theory given below.

The communication topology used in this thesis is described by a directed graph $\mathcal{G} \triangleq (\mathcal{V}, \mathcal{E})$, with $\mathcal{V} \triangleq \{0, 1, \ldots, N\}$ being the set of nodes (agents) and with $\mathcal{E} \subseteq \mathcal{V} \times \mathcal{V}$ being the set of directed edges between two distinct agents (self-edges are not allowed). A directed edge $(j, i) \in \mathcal{E}$ represents that agent i can obtain information from agent j. The neighbor set of agent i is denoted by $\mathcal{N}_i = \{j | (j, i) \in \mathcal{E}\}$: this is the set of agents from which agent i can obtain information. We reserve index 0 to the so-called leader agent: because agent 0 plays a special role, let us consider the subgraph defined by $\overline{\mathcal{G}} \triangleq (\overline{\mathcal{V}}, \overline{\mathcal{E}})$ with $\overline{\mathcal{V}} \triangleq \{1, 2 \ldots, N\}$ and $\overline{\mathcal{E}}$ defined accordingly. For this subgraph, let us define

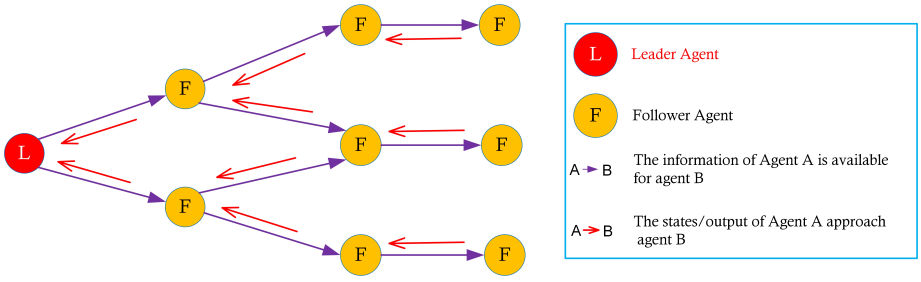

Figure 1.1: A schematic diagram of distributed consensus tracking

the connectivity matrix $\overline{\mathscr{A}} = [a_{ij}] \in \mathbb{R}^{N\times N}$: if $(j,i) \in \overline{\mathscr{E}}$ with $i \neq j$, then $a_{ij} = 1$, otherwise $a_{ij} = 0$ (note that $a_{ii} = 0$). The Laplacian matrix $\mathscr{L}$ associated with $\mathscr{G}$ is defined as

$$\mathscr{L} = \begin{bmatrix} 0 & \mathbf{0}_{1\times N} \\ -\boldsymbol{\mu} & \overline{\mathscr{L}} + \mathscr{B} \end{bmatrix}$$

with $\boldsymbol{\mu} = [\mu_1, \ldots, \mu_N]^{\mathrm{T}}$, where $\mu_i = 1$ if the leader $0 \in \mathscr{N}_i$, and $\mu_i = 0$ otherwise. Also, $\mathscr{B} = \mathrm{diag}[\mu_1, \ldots, \mu_N]^T$ and $\overline{\mathscr{L}} = \overline{\mathscr{D}} - \overline{\mathscr{A}}$ is the Laplacian matrix related to $\overline{\mathscr{G}}$ with $\overline{\mathscr{D}} = \mathrm{diag}[d_1, \ldots, d_N]$, where $d_i = \sum_{j\in\mathscr{N}_i} a_{ij}$. A direct path from agent i to agent j is a sequence of successive edges in the form $\{(v_i, v_l), (v_l, v_m), \ldots, (v_k, v_j)\}$. A graph has a spanning tree, if the leader agent is such that there is a directed path from the leader to each follower agent in the graph.

The following standard assumptions are typically made in the literature.

Assumption 1.1 [127] The leader agent 0 is represented by a leader output signal y_{r}, which is continuously differentiable, bounded, and available only to a subset of the follower agents. Furthermore, $\dot{y}_{\mathrm{r}}$ is bounded and not available to any follower agent. The bounds for y_{r} and $\dot{y}_{\mathrm{r}}$ are unknown.

Assumption 1.2 [111] The directed graph $\mathscr{G} = (\mathscr{V}, \mathscr{E})$ representing the multi-agent communication contains at least one directed spanning tree with the leader agent as the root.

Remark 1.1 Assumption 1.1 implies that the leader information is only available to a small fraction of followers. Assumption 1.2 implies that $\overline{\mathscr{L}} + \mathscr{B}$ is a nonsingular $\mathscr{M}$-matrix[1] and guarantees the feasibility of consensus [132].

Distributed consensus is one of the most studied problems in distributed control [3, 16, 19–21, 24, 26, 35, 42, 50, 67, 69–71, 74, 76, 79, 85, 85, 87, 88, 110, 111, 113, 114, 119–121, 127, 128, 130, 140, 141] and it aims at achieving an agreement for the states or the outputs of subsystems connected via a network by designing a control protocol for each agent based on locally available information. Distributed control of nonlinear multi-agent systems is more challenging but also potentially more applicable than its linear counterpart. In recent years, leaderless (i.e. the convergence of agents states toward an *a priori* unknown common value) or leader-following (i.e. the convergence of agents states toward the desired trajectory of a leader, as shown in Fig. 1.1) consensus results have been obtained for two large families of nonlinear multi-agent systems: strict-feedback [16, 21, 24, 26, 35, 50, 69, 87, 88, 110, 111, 114, 119–121, 130, 140, 141] (cf. the expression in (1.1)) and pure-feedback multi-agent systems [70, 113, 127, 128], which can be equivalently transformed into strict-feedback systems. For these families, the commonly adopted approach is an extension of the well-known backstepping technique [44] in a distributed sense. When the nonlinear functions are unknown, approximators such as neural networks (cf. the Section 2.2.1) and fuzzy logic systems have been incorporated in such a design. Switching dynamics can also be handled via the common Lyapunov function method [127, 128, 140]. Although strict-feedback and pure-feedback systems

[1] An $\mathscr{M}$-matrix is a square matrix with non-positive off-diagonal entries and non-negative principal minors.

are popular dynamics in the nonlinear control field, there exist extensions to these dynamics: most notably, power-chained form systems (cf. the expression in (1.2)) are such a class of systems.

$$\text{Strict feedback systems}: \begin{cases} \dot{\chi}_1 = \phi_1(\chi_1) + \psi_1(\chi_1)\chi_2, \\ \dot{\chi}_2 = \phi_2(\overline{\chi}_2) + \psi_2(\overline{\chi}_2)\chi_3, \\ \quad \vdots \\ \dot{\chi}_m = \phi_m(\overline{\chi}_m) + \psi_m(\overline{\chi}_m)\chi_{m+1}, \quad m = 3, \ldots, n-1 \\ \dot{\chi}_n = \phi_n(\overline{\chi}_n) + \psi_n(\overline{\chi}_n)u, \end{cases} \tag{1.1}$$

$$\text{Power chained form}: \begin{cases} \dot{\chi}_1 = \phi_1(\chi_1) + \psi_1(\chi_1)\chi_2^{p_1}, \\ \dot{\chi}_2 = \phi_2(\overline{\chi}_2) + \psi_2(\overline{\chi}_2)\chi_3^{p_2}, \\ \quad \vdots \\ \dot{\chi}_m = \phi_m(\overline{\chi}_m) + \psi_m(\overline{\chi}_m)\chi_{m+1}^{p_m}, \quad m = 3, \ldots, n-1 \\ \dot{\chi}_n = \phi_n(\overline{\chi}_n) + \psi_n(\overline{\chi}_n)u^{p_n}, \end{cases} \tag{1.2}$$

where $\overline{\chi}_m = [\chi_1, \chi_2, \ldots, \chi_m]^T \in \mathbb{R}^m$, p_1, p_2, p_m, and p_n are positive odd integers; $\phi_m(\cdot)$ is unknown continuous function (referred to as system nonlinearity), $\psi_m(\cdot)$ is unknown continuous function (referred to as control gain function whose sign is the so-called control direction) and is assumed to be such that

$$\underline{\psi}_m \leq |\psi_m(\cdot)| \leq \overline{\psi}_m \tag{1.3}$$

with $\underline{\psi}_m$ and $\overline{\psi}_m$ being positive constants. Inequality (1.3) is a general controllability condition for many classes of nonlinear dynamics, including strict-feedback, pure-feedback, and power-chained form systems [89, 135, 136]. In case only the sign of the control gain function $\psi_n(\cdot)$ is unknown, the system (1.2) is said to possess a *single unknown control direction*. In case the signs of more than one control gain functions $\psi_m(\cdot)$ are unknown, the system (1.2) is said to possess *multiple unknown control directions*. The main difficulty caused by unknown control directions is illustrated by Examples 6 and 7 in Section 2.2. It is worth noting that, in line with [55, 57, 83], p_m are odd positive integers since stabilization is not possible in general in the presence of even powers. This is because no matter whether the control signals are positive or negative, they would become positive as per effect of the even power [65].

1.1.2. Power-Chained Form Systems

Over the last decades, power-chained form systems (also called high-order nonlinear systems and systems in p-normal form) has been attracting great attention. The reason is twofold: from a mathematical point of view, power-chained form dynamics are a generalization of strict-feedback [14, 22, 106, 111] and pure-feedback dynamics [25, 113, 127] since they include more general integrators (with positive-odd-integer powers); from an engineering point of view, dynamics in the power-chained form can describe relevant classes of practical systems such as dynamical boiler-turbine units [15], hydraulic dynamics [66], aircraft wing dynamics [28] and some classes of under-actuated,

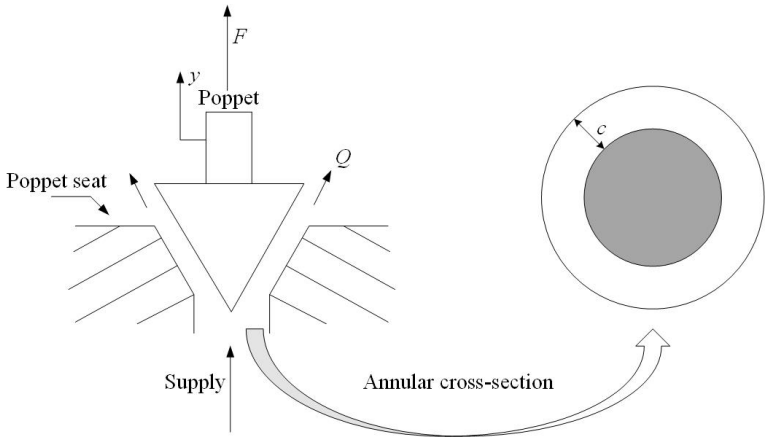

Figure 1.2: Poppet valve system

weakly coupled mechanical systems with cubic force deformation relations (nonlinear spring forces) [55, 57, 83]. In the following, we provide two concrete examples to show the relevance of power-chained form systems from practical engineering perspective.

Example 1. In hydraulic systems, a poppet valve is one of the most commonly used components. A poppet valve is typically used to control the timing and quantity of gas or vapor flow into an engine, and its behavior can be modeled by annular leakage equation. As shown in Fig. 1.2, the input force F drives the poppet to move along the $y-$axis, regulating the volumetric flow rate Q of oil from the high-pressure to the low-pressure chamber. The actual applications of poppet valve system typically arise in fulfilling aerial refueling mission and driving hydraulic actuator [66].

According to Navier-Stokes equations, the volumetric flow rate Q for annular laminar flow can be described as (cf. [66, pp. 54]):

$$Q = \frac{\pi r}{6\mu L}\Delta P c^3, \tag{1.4}$$

where r, μ, and L are constants independent of the axial motion of poppet, and ΔP is the pressure drop between two chambers and remains almost unchanged in the control process. c is the effective clearance of the annular passage. Then, relation (1.4) can be rewritten as $Q = \lambda c^3$ for convenience with λ being a lumped coefficient. In view of the geometric structure, $c = \alpha y$ with α being a constant related to the cone angle of poppet. The dynamics of oil volume V in upper chamber is given by

$$\frac{dV(t)}{dt} = Q - R(t), \tag{1.5}$$

where R is the lumped reduction rate of oil attributed to consumption and other leakages. Likewise, the equation of motion of the poppet is

$$m\frac{d^2y(t)}{dt^2} = -k\frac{dy(t)}{dt} + T(t) + F(t), \tag{1.6}$$

where m is the mass of the poppet, k is the viscous friction coefficient, T denotes the lumped elastic force, and F represents the input force. At this point, let us conduct the following notation substitution:

$$\chi_1 = V, \quad \chi_2 = y, \quad \chi_3 = \frac{dy}{dt}, \quad u = F. \tag{1.7}$$

Then, the dynamics of systems (1.7) comes down to

$$\dot{\chi}_1 = \phi_1 + \psi_1 \chi_2^3, \quad \dot{\chi}_2 = \phi_3, \quad \dot{\chi}_3 = \phi_3 + \psi_3 u, \tag{1.8}$$

where $\psi_1 = \lambda\alpha^3$, $\phi_1 = -R(t)$, $\psi_3 = \frac{1}{m}$, and $\phi_3 = \frac{1}{m}(T(t) - k\chi_3)$.

Example 2. Let us consider an underactuated weakly coupled mechanical benchmark [83], also shown in Fig. 1.3. The system includes a mass m_1 on a horizontal smooth surface and an inverted pendulum m_2 supported by a massless rod. The mass is connected to the wall surface by a linear spring and to the inverted pendulum by a nonlinear spring with a cubic force deformation relation. Thus, its mathematical model can be described by [83]

$$\begin{cases} \ddot{\theta} = \dfrac{g\sin(\theta)}{l} + \dfrac{k_2}{m_2 l}\big(x - l\sin(\theta)\big)^3\cos(\theta), \\ \ddot{x} = -\dfrac{k_1}{m_1}x - \dfrac{k_2}{m_1}\big(x - l\sin(\theta)\big)^3 + \dfrac{u}{m_1}, \end{cases} \tag{1.9}$$

where $\theta \in (-\frac{\pi}{2}, \frac{\pi}{2})$, x is the displacement of m_1, and u is the control force acting on m_1. Moreover, k_1 and k_2 are spring coefficients, and l is the pendulum length. The following change of coordinates

$$\chi_1 = \theta, \quad \chi_2 = \dot{\theta}, \quad \chi_3 = x, \quad \chi_4 = \dot{x}, \tag{1.10}$$

transforms (1.9) into

$$\begin{cases} \dot{\chi}_1 = \chi_2, \\ \dot{\chi}_2 = \phi_2(\overline{\boldsymbol{\chi}}_2) + \psi_2(\overline{\boldsymbol{\chi}}_2)\chi_3^3, \\ \dot{\chi}_3 = \chi_4, \\ \dot{\chi}_4 = \phi_4(\overline{\boldsymbol{\chi}}_4) + \psi_4(\overline{\boldsymbol{\chi}}_4)u, \end{cases} \tag{1.11}$$

where $\phi_2(\overline{\boldsymbol{\chi}}_2) = \frac{g}{l}\sin(\chi_1) + \frac{k_2}{m_2 l}\cos(\chi_1)\big[3\chi_3 l^2\sin^2(\chi_1) - 3\chi_3^2 l\sin(\chi_1) - l^3\sin^3(\chi_1)\big]$, $\phi_4(\overline{\boldsymbol{\chi}}_4) = -\frac{k_1}{m_1}\chi_3 - \frac{k_2}{m_1}\big[\chi_3^3 - l^3\sin^3(\chi_1) - 3\chi_3^2 l\sin(\chi_1) + 3\chi_3 l^2\sin^2(\chi_1)\big]$, $\psi_2(\overline{\boldsymbol{\chi}}_2) = \frac{k_2}{m_2 l}\cos(\chi_1)$, and $\psi_4(\overline{\boldsymbol{\chi}}_4) = \frac{1}{m_1}$.

1.1.3. Unique Challenges of Controlling Power-Chained Form Systems

There are mainly three challenges that will be considered when designing controller for power-chained form systems.

Challenge 1: Standard feedback linearization method fails to stabilize power-chained form systems. This is because the linearized dynamics of power-chained form systems around origin may contain uncontrollable modes whose eigenvalues are in the right half-plane [83].

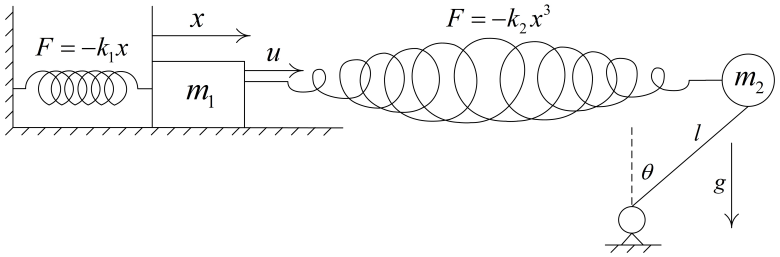

Figure 1.3: Underactuated weakly coupled mechanical system

Example 3. Let us take a four-dimensional nonlinear system to clarify this point:

$$\begin{cases} \dot{\chi}_1 = \chi_2, \\ \dot{\chi}_2 = \chi_3^3 + \chi_1, \\ \dot{\chi}_3 = \chi_4, \\ \dot{\chi}_4 = u, \end{cases} \tag{1.12}$$

The linearized matrices of (1.12) around the origin are

$$A = \begin{bmatrix} 0 & 1 & 0 & 0 \\ 1 & 0 & 0 & 0 \\ 0 & 0 & 0 & 1 \\ 0 & 0 & 0 & 0 \end{bmatrix}, \quad B = \begin{bmatrix} 0 \\ 0 \\ 0 \\ 1 \end{bmatrix}. \tag{1.13}$$

It is straightforward to obtain that $\text{rank}[B, AB, A^2B, A^3B] = 2 < 4$ and that there exists a positive eigenvalue (e.g. $\lambda_A = 1$) for the linearized matrix A. This implies that standard feedback linearization method fails to stabilize power-chained form systems.

Challenge 2: The standard backstepping method also fails for power-chained form systems [83]. The backstepping method is also known as adding-one-linear-integrator-technique [44]. It was successfully developed for strict-feedback and pure-feedback systems [16, 21, 24, 26, 35, 50, 69, 70, 87, 88, 110, 111, 113, 114, 119, 120, 127, 128, 130, 140], but it fails due to the presence of high powers as shown in the following example 4.

Example 4. Let us consider a two-dimensional power-chained form system

$$\begin{cases} \dot{\chi}_1 = \chi_1^3 \cos\chi_2 + \chi_2^3 \\ \dot{\chi}_2 = \chi_1^2 \chi_2 \sin\chi_1 + u^5. \end{cases} \tag{1.14}$$

The goal is to design control u such that (1.14) is stabilized. In what follows, we show that standard backstepping design fails to achieve such goal.

Backstepping control framework. Define the coordinate transformation

$$s_1 = \chi_1, \quad s_2 = \chi_2 - \alpha_1, \tag{1.15}$$

where α_1 is the smooth virtual control law to be designed. Substituting (1.15) into (1.14)

leads to

$$\begin{cases} \dot{s}_1 = \dot{\chi}_1 = (s_2+\alpha_1)^3 + s_1^3\cos(s_2+\alpha_1), \\ \dot{s}_2 = \dot{\chi}_2 - \dot{\alpha}_1 = u^5 + \chi_1^2\chi_2\sin\chi_1 - \dot{\alpha}_1 \\ \quad = u^5 + s_1^2(s_2+\alpha_1)\sin(s_1) - \dot{\alpha}_1. \end{cases} \tag{1.16}$$

If we choose Lyapunov candidate $V_1(s_1) = \frac{1}{2}s_1^2$, then, we have

$$\begin{aligned} \dot{V}_1(s_1) &= s_1(s_2+\alpha_1)^3 + s_1^4\cos(s_2+\alpha_1), \\ &= s_1(s_2^3 + 3s_2\alpha_1^2 + 3s_2^2\alpha_1 + \alpha_1^3) + s_1^4\cos(s_2+\alpha_1). \end{aligned} \tag{1.17}$$

Apparently, from (1.17) it can be seen that the virtual control law α_1 appears inside many different functions and it is quite difficult to design a virtual control $\alpha_1(\chi_1)$ to exactly cancel the term $s_1^4\cos(s_2+\alpha_1)$ via a standard backstepping procedure. In other words, backstepping also fails to work in this situation. This challenge is also detailed in [83].

Challenge 3: Asymptotic tracking for power-chained form systems is structurally impossible, even locally, because the linearized dynamics contain uncontrollable modes whose eigenvalues are in the right-half plane [83]. This point is shown in the following example.

Example 5. We take the two-dimensional planar system (see [83, Example 2.1])

$$\begin{cases} \dot{\chi}_1 = \chi_1^5 - \chi_1^4 + \chi_2^3 \\ \dot{\chi}_2 = u^3, \\ \quad y = \chi_1. \end{cases} \tag{1.18}$$

Let the output tracking error be $s = \chi_1 - y_r(t) = \chi_1 - 1$. Then, (1.18) can be represented by

$$\begin{cases} \quad \dot{s} = (1+s)^4 s + \chi_2^3 \\ \dot{\chi}_2 = u^3. \end{cases} \tag{1.19}$$

The linearized dynamics of (1.19) around the origin is characterized by

$$(A,B) = \left(\begin{bmatrix} 1 & 0 \\ 0 & 0 \end{bmatrix}, \begin{bmatrix} 0 \\ 0 \end{bmatrix} \right) \tag{1.20}$$

which is uncontrollable. The uncontrollable mode has a positive eigenvalue, and therefore system (1.19) cannot be stabilized, even locally, by any smooth state feedback control law according to [41]. Therefore, asymptotic output tracking for power-chained form systems is in general not achievable by smooth feedback. At this point, one may wonder whether asymptotic output tracking can be realized by non-smooth but continuous feedback. Unfortunately, the [82, Example 2.2] has shown that such conjecture is not true either.

1.2. Open Problems in the State-of-the-Art

In place of standard backstepping and feedback linearization methods, the adding-one-power-integrator technique was successfully proposed in [56] to handle power-chained form systems (cf. Section 2.2.2 in this thesis). Since then, several control methods have

been proposed to achieve stabilization to zero and output tracking for power-chained form systems in [55–57, 83, 95–98], where system nonlinearities are typically required to satisfy some growth conditions. To remove the restrictive growth conditions, universal approximators including neural networks (NNs) and fuzzy logic systems (FLSs) are exploited in [89, 107, 112, 135, 136] to handle unknown system nonlinearities. Nevertheless, the following four problems have not been solved in the-state-of-the-art.

The first problem is that the extension of the standard adding-one-power-integrator technique to a distributed setting is not very meaningful due to some complex aspects of the procedure. At least the following two complex aspects are worth mentioning: (a) the high-power terms are separated from the control gain functions via separation lemmas that make the power of the virtual control gains grow exponentially with the order of the system; (b) the control gain of each virtual control is incorporated into the next virtual control law iteratively, thus increasing the control complexity at each step. Such issues result in high-complexity and high-gain designs that might be prohibitive for multi-agent systems with low computational power and limited actuation. Therefore, the first open question naturally arises:

Question 1: how to design a reduced-complexity distributed methodology overcoming above-mentioned high control gains for nonlinear multi-agent systems in the power-chained form?

The second problem is that state-of-the-art results [89, 92–94, 112, 135, 136] rely on the assumption that the agents' control directions (i.e. the signs of control gain functions) are known *a priori* and are available for control design. However, it was shown in [106] that such a priori knowledge is not available in many practical scenarios such as visual servoing control systems [4], robotic systems [13] and so on. When such *a priori* knowledge is not available, a popular approach to tackle this challenge is continuous parameter adaptation via Nussbaum functions [18, 23, 37, 75, 106, 125] (cf. Section 2.2.3 of this thesis), which has been used also for distributed control of strict-feedback or pure-feedback dynamics [14, 17, 22, 25, 106]. The Nussbaum function method to handle single unknown control direction [23, 37, 75, 122, 125] and multiple unknown control directions [14, 22, 106] has not been explored for coordination of multi-agent systems with power-chained form dynamics. This is because addressing multiple unknown control directions requires novel conditional inequalities involving the summation of multiple Nussbaum function terms [37, 125], while avoiding cancellation of the multiple Nussbaum function terms. The aforementioned investigations open the following question:

Question 2: how to design Nussbaum functions-based techniques for handling nonlinear multi-agent systems in the power-chained form in the presence of multiple unknown control directions?

Furthermore, it is well-recognized [61] that Nussbaum functions-based methods require additional complexity in the control design and continuous parameter adaptation.

This may lead to large learning transients, so that several researchers have been engaged in the problem of overcoming continuous parameter adaptation by means of logic-based control [32, 54]. Notable settings where logic-based control was employed include overcoming conventional continuous tuning of control parameters [2, 27, 123, 124] and overcoming the conventional Nussbaum approach for strict-feedback dynamics [36, 115].

It is crucial to notice that the state-of-the-art logic-based mechanisms in [36, 115] for strict-feedback systems rely on monitor functions that monitor whether asymptotic tracking can be achieved (resulting in bounded energy of the tracking error) [36] or whether finite-time stabilization (i.e. the tracking error converges to zero in finite time) can be achieved [115]. Unfortunately, the same mechanism and monitor functions cannot be adopted for agents in the power-chained form due to the aforementioned structural difficulty in achieving asymptotic tracking, see also [83, Examples 2.1 and 2.2]. Therefore, a different logic-based mechanism and new monitor functions must be sought going beyond state-of-the-art for distributed control of power-chained form dynamics. This motivates the question:

Question 3: how to design a new logic-based mechanism for nonlinear multi-agent systems in the power-chained form with multiple unknown control directions even when asymptotic tracking cannot be structurally obtained?

The fourth problem is that universal approximators (e.g. neural networks and fuzzy logic systems) often used in the adding-one-power-integrator procedure in [89, 92–94, 112, 135, 136] are valid only within some compact sets where the capabilities of the universal approximators are guaranteed. Furthermore, the introduction of approximating structures unavoidably increases the complexity of the methods in [89, 92–94, 112, 135, 136], in the sense that extra adaptive parameters have to be updated (i.e. extra nonlinear differential equations need to be solved numerically) and extra calculations must be conducted to compute the control signal, thus making their distributed implementation difficult.

The technique called low-complexity prescribed performance control (PPC) (also called approximation-free PPC), first proposed in [5], aims to control systems without using any universal approximators, while at the same time imposing transient and steady-state specifications on the tracking error [52, 78, 101]. Nevertheless, the systems considered in [52, 78, 101] are confined to the strict-feedback form instead of the more general power-chained form systems. Inspired by above discussions, an interesting question arises:

Question 4: how to design an approximation-free prescribed performance control methodology for power-chained form systems, while taking into account unknown control directions?

This last question is investigated in this thesis for single-agent dynamics, but extension to multi-agent dynamics seems possible using the tools in [7].

1.3. Main Contributions of the Thesis

The main contributions of this thesis consist in solving the aforementioned open questions. To be specific:

- **A separation-based methodology for consensus tracking of nonlinear multi-agent systems in power-chained form systems.**

  We develop a reduced-complexity adaptive methodology to consensus tracking for a team of uncertain multi-agent systems in the power-chained form. At the core of the proposed distributed methodology is a newly proposed definition for separable functions: this definition allows the formulation of a separation-based lemma to handle the high-power terms with reduced complexity in the control design. Complexity is reduced in a twofold sense: the control gain of each virtual control law does not have to be incorporated in the next virtual control law iteratively, thus leading to a simpler expression of the control laws; the power of the virtual and actual control laws increases only proportionally (rather than exponentially) with the order of the systems, dramatically reducing high-gain issues.

- **Consensus for multi-agent systems in the power-chained form with mixed unknown control directions via hybrid Nussbaum-based control.**

  We solve the consensus tracking problem for multi-agent systems in the power-chained form with partially unknown control directions by proposing a hybrid Nussbaum technique that can handle uncertain agents in power-chained form dynamics with non-smooth behaviors (switching and quantization), and with multiple unknown control directions for each agent.

- **Logic-based distributed switching control for agents in the power-chained form with multiple unknown control directions.**

  We develop a new logic-based distributed switching control method for nonlinear agents in the power-chained form, where logic-based (switching) control arises from the online estimation of the control directions assumed to be unknown for all agents. Compared to the state-of-the-art logic-based mechanisms, the challenge of power-chained dynamics is that in general asymptotic tracking cannot be obtained, even for a single agent. To address this challenge, a new logic-based mechanism is proposed, which is orchestrated by a dynamic boundary function. The boundary function is decreasing in-between switching instants and monotonically increasing at the switching instants, depending on the jumps of an appropriately designed "Lyapunov-like" function. To remove chattering (i.e. two or more switching instants occurring consecutively with zero dwell time), a dynamic threshold is proposed, based on selecting the maximum values of the "Lyapunov-like" function before and after switching.

- **Approximation-free prescribed performance tracking control of power-chained form systems with unknown control directions.**

  We design a Nussbaum function-based low-complexity prescribed-performance controller for power-chained form systems. The peculiar features of the proposed design lie in not involving any universal approximators (e.g. neural networks,

fuzzy logic systems, etc), and in preserving some prescribed specifications (e.g. minimum convergence rate, maximum overshoot, and maximum steady state error). To be specific, a counterexample and a positive example are given to show two crucial points: a positive odd-integer-power of a type B Nussbaum function might not be a type B Nussbaum function; only some particular type B Nussbaum functions keep their property even when elevated to a positive odd-integer-power. These latter functions can be used for handling time-varying unknown control coefficients. A new switching conditional inequality is proposed. This inequality encompasses existing ones as special cases: instead of always increasing the Nussbaum gain, its design is based on increasing the Nussbaum gain only when the tracking error is close to violating the performance bounds.

1.4. Organization of the Thesis

This thesis consists of seven chapters whose organization and relationship are shown in Fig. 1.4. The content of each chapter is briefly summarized as follows.

Chapter 2: Some basic concepts and technical tools (including Nussbaum functions, the adding-one-power integrator method, neural network approximation, logic-based control, PPC and low-complexity PPC) used in this thesis are presented.

Chapter 3: A separation-based methodology is developed for a large class of uncertain nonlinear multi-agent systems in the power-chained form, which can exhibit heterogeneous nonlinearities and switched dynamics with possibly asynchronous switches among the agents. The core of the methodology is a newly proposed definition for separable functions and a new separation-based lemma to deal with the high-power terms. The results in this chapter are based on the work [62].

Chapter 4: A hybrid Nussbaum gains-based approach is proposed to handle mixed unknown control directions for each agent. The idea behind this choice is that in the mixed situation where some control directions are known and some are unknown, it is not appropriate to adopt the standard Nussbaum function for every agent since their effects might cancel each other, being unable to guarantee a boundedness of the summation of multiple Nussbaum integral terms. The results in this chapter are based on the work [61].

Chapter 5: A new logic-based mechanism is proposed, which is orchestrated by a dynamic boundary function. The boundary function is decreasing in-between switching instants and monotonically increasing at the switching instants, depending on the jumps of an appropriately designed "Lyapunov-like" function. Furthermore, a dynamic threshold is designed based on selecting the maximum values of the "Lyapunov-like" function before and after switching. The results in this chapter are based on the work [63].

Chapter 6: A Nussbaum function-based approximation-free PPC design is developed for power-chained form systems. To accomplish this, a new switching conditional inequality is proposed to avoid high gains in the sense that switching gain increases only when the tracking error is close to violating the performance bounds. We show with a counterexample and a positive example that only some Nussbaum functions are suited to handle time-varying unknown control coefficients for power-chained form dynamics. The results in this chapter are based on the work [64].

1

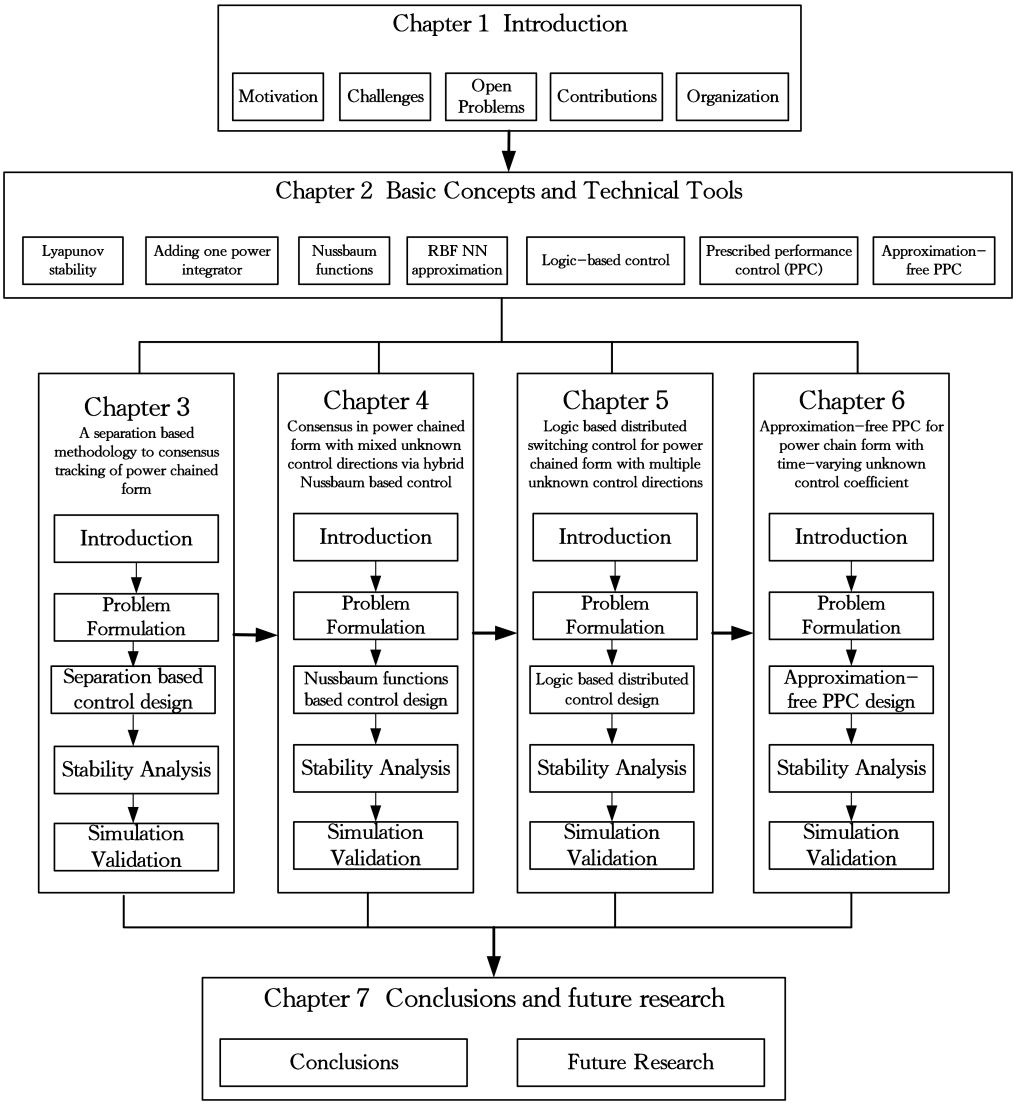

Figure 1.4: The overall structure of this thesis

Finally, conclusions and recommendations for future work are discussed in Chapter 7.

2

BASIC CONCEPTS AND TECHNICAL TOOLS

This chapter first gives a brief introduction on Lyapunov stability theory of ordinary differential equations. Then, some technical tools including the adding-power-integrator method, Nussbaum functions, radial basis function neural network approximators, logic-based control, prescribed performance control (PPC), and low-complexity PPC are presented.

2.1. Lyapunov Stability

Lyapunov stability concerns the behavior of trajectories around the equilibrium of a nonlinear differential equation. Consider systems described by ordinary differential equations of the form

$$\dot{x}(t) = f(t, x(t)), \quad x(t_0) = x_0, \tag{2.1}$$

where $x \in \mathbb{R}^n$, $f : \mathscr{T} \times \mathscr{B}(r) \to \mathbb{R}$ is continuous in t and locally Lipschitz in x uniformly over t, $\mathscr{T} = [t_0, \infty]$, and $\mathscr{B}(r) = \{x \in \mathbb{R}^n | \, \|x\| < r\}$. We assume that f is of such nature that for every $x_0 \in \mathscr{B}(r)$ and every $t_0 \in \mathbb{R}^+_{\geq 0}$. Then, system (2.1) possesses one and only one solution $x(t; t_0, x_0)$.

Definition 2.1 [41] A solution of (2.1) over the interval $[t_0, t_1] \subset \mathbb{R}$ is a continuous function

$$x(\cdot) : [t_0, t_1] \to \mathbb{R}^n \tag{2.2}$$

with $x(\cdot)$ piecewise continuous and satisfying (2.1) for all $t \in [t_0, t_1]$.

Definition 2.2 [41] A solution $x(t; t_0, x_0)$ of (2.1) is bounded if there exists a constant $\beta > 0$ such that $|x(t; t_0, x_0)| < \beta$ for all $t \geq t_0$.

Definition 2.3 [41] The solutions of (2.1) are uniformly bounded if for any $\alpha > 0$ and $t_0 \in \mathbb{R}^+$, there exists a $\beta = \beta(\alpha)$ independent of t_0 such that if $|x_0| < \alpha$, then $|x(t; t_0, x_0)| < \beta$ for all $t \geq t_0$.

Definition 2.4 [41] The solutions of (2.1) are uniformly ultimately bounded with ultimate bound β if there exist positive constants β and c, independent of $t_0 \geq 0$, and for every $\alpha \in (0, c)$, there exist a $T = T(\alpha, \beta) \geq 0$, independent of t_0, such that

$$|x(t_0)| \leq \alpha \;\Rightarrow\; |x(t; t_0, x_0)| \leq \beta, \;\; \forall\; t \geq t_0 + T \tag{2.3}$$

The following Lyapunov-like theorem is meant to show uniform boundedness and ultimate boundedness.

Theorem 2.1 [54] Let $D \subset \mathbb{R}^n$ be a domain that contains the origin and $V : [0, \infty) \times D \to \mathbb{R}$ be a continuously differentiable function such that

$$\alpha_1(||x||) \leq V(t, x) \leq \alpha_2(||x||) \tag{2.4}$$

$$\frac{\partial V}{\partial t} + \frac{\partial V}{\partial x} f(t, x) \leq -W_3(x), \;\; \forall x : \; ||x|| \geq \mu > 0, \tag{2.5}$$

where α_1 and α_2 are class $\mathcal{K}$ functions and W_3 is a continuous positive definite function. Take $r > 0$ and suppose that

$$\mu < \alpha_2^{-1}\big(\alpha_1(r)\big). \tag{2.6}$$

Then, there exists a class $\mathcal{KL}$ function β and for every initial state $x(t_0)$, satisfying $||x(t_0)|| \leq \alpha_2^{-1}\big(\alpha_1(r)\big)$, there exists a $T \geq 0$ (dependent on $x(t_0)$ and μ) such that the solution of (2.1) satisfies

$$||x(t)|| \leq \beta(||x(t_0)||, t - t_0), \;\; \forall\; t_0 \leq t \leq t_0 + T \tag{2.7}$$

$$||x(t)|| \leq \alpha_1^{-1}\big(\alpha_2(\mu)\big), \;\; \forall\; t \geq t_0 + T. \tag{2.8}$$

Moreover, if $D = \mathbb{R}^n$ and α_1 belongs to class $\mathcal{K}_\infty$, then (2.7) and (2.8) hold for any initial state $x(t_0)$, with no restriction on how large μ is.

Inequalities (2.7) and (2.8) show that $x(t)$ is uniformly bounded for all $t \geq t_0$ and uniformly ultimately bounded with the ultimate bound $\alpha_1^{-1}\big(\alpha_2(\mu)\big)$. The ultimate bound is a class $\mathcal{K}$ function of μ; hence, the smaller the value of μ, the smaller the ultimate bound.

The following invariant set notion is used in our thesis to ensure the validity of RBF NN approximators in the sense of confining relevant states within an invariant set all the time provided their initial conditions are located therein. The use of such a property can be observed in the stability analysis of Chapter 3.

Definition 2.5 [41] (Invariant Set) For a dynamic system (2.1) with state variable x, if all trajectories $x(t; t_0, x_0)$ initially starting in a set Ω remain in the set at any time in the future, i.e.

$$x(t_0) \in \Omega \Rightarrow x(t) \in \Omega, \;\; \forall t > t_0. \tag{2.9}$$

Then, the set Ω is called an invariant set of the dynamic system.

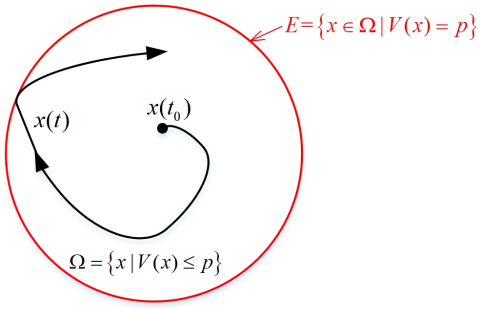

Figure 2.1: Schematic diagram of invariant set

Theorem 2.2 (Lyapunov-based Invariant Set) For a dynamic system $\dot{x} = f(x,t)$, let $V(\cdot): D \to \mathbb{R}^+$ be a continuously differentiable function satisfying $\alpha_1(x) \le V(x) \le \alpha_2(x)$, where α_1 and α_2 are class $\mathcal{K}_\infty$ functions. Define the compact set $\Omega = \{x|V(x) \le p\}$, where $p \in \mathbb{R}^+$ and $\Omega \subset D$. Let $E = \{x \in \Omega | V(x) = p\}$. If $V(x)$ satisfies $\dot{V}(x) \le 0$, $\forall x \in E$, then, Ω is an invariant set of $x(t)$, namely, it holds that

$$x(t_0) \in \Omega \Rightarrow x(t) \in \Omega, \quad \forall t > t_0. \tag{2.10}$$

A schematic diagram of Theorem 2.2 is depicted in Fig. 2.1.

2.2. Technical Tools

2.2.1. Radial Basis Function Neural Network Approximation

The radial basis function neural networks (RBF NNs) whose structure is given in Fig. 2.2 could be deemed as two-layer neural networks where the hidden layer carries out a fixed nonlinear transformation without tuneable parameters; i.e., the input space is mapped into a new space. The output layer then combines the outputs in the latter space linearly. Therefore, RBF NNs belong to a class of linearly parameterized networks, and can be described in the following form [30, 103, 104]:

$$F_{nn}(\boldsymbol{Z}) = \sum_{i=1}^{N} w_i \varphi_i(\boldsymbol{Z}) = \boldsymbol{W}^T \boldsymbol{\varphi}(\boldsymbol{Z}), \tag{2.11}$$

where $\boldsymbol{Z} \in \Omega_{\boldsymbol{Z}} \subset \mathbb{R}^q$ is the input vector, $\boldsymbol{W} = [w_1, \ldots, w_n]^T \in \mathbb{R}^N$ is the weight vector, $N > 1$ is the number of NN nodes, and $\boldsymbol{\varphi}(\boldsymbol{Z}) = [\varphi_1(||\boldsymbol{Z} - \boldsymbol{\xi}_1||), \ldots, \varphi_N(||\boldsymbol{Z} - \boldsymbol{\xi}_N||)]^T$ is the regressor vector, with φ_i a radial basis function, and $\boldsymbol{\xi}_i = [\xi_{i1}, \ldots, \xi_{in}]^T$ $(i = 1, \ldots, N)$ the center of the receptive field. In this thesis, $\varphi_i(||\boldsymbol{Z} - \boldsymbol{\xi}_i||)$ is chosen to be a Gaussian function in the form of

$$\varphi_i(||\boldsymbol{Z} - \boldsymbol{\xi}_i||) = \exp\left[\frac{-(\boldsymbol{Z} - \boldsymbol{\xi}_i)^T(\boldsymbol{Z} - \boldsymbol{\xi}_i)}{\eta^2}\right],$$

where η is the width of the receptive field of Gaussian function. It has been proved in [30, 103] that an RBF NN (2.11), with a sufficiently large number of nodes N and appropriately placed node centers and variances, can approximate any continuous function $F(\cdot): \Omega_{\boldsymbol{Z}} \to \mathbb{R}$ over a compact set $\Omega_{\boldsymbol{Z}}$ to arbitrary accuracy according to

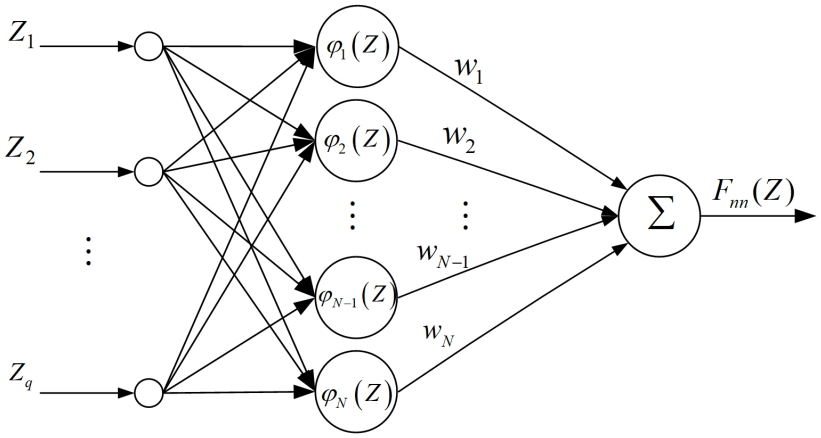

Figure 2.2: Structure of RBF neural network

$$F(\boldsymbol{Z}) = \boldsymbol{W}^{*T}\boldsymbol{\varphi}(\boldsymbol{Z}) + \epsilon(\boldsymbol{Z}), \quad \forall \boldsymbol{Z} \in \Omega_{\boldsymbol{Z}}, \tag{2.12}$$

where $\boldsymbol{W}^*$ is the ideal optimal weight vector, $\epsilon(\boldsymbol{Z})$ is the approximation error. It is normally assumed the ideal weight vector $\boldsymbol{W}^*$ exists such that $|\epsilon(\boldsymbol{Z})| \leq \epsilon^*$ with $\epsilon^* > 0$ a constant for all $\boldsymbol{Z} \in \Omega_{\boldsymbol{Z}}$. The ideal optimal vector $\boldsymbol{W}^*$ is an "artificial" quantity required for analytical purposes, and is defined as the value of $\boldsymbol{W}$ that minimizes $|\epsilon|$ for all $\boldsymbol{Z} \in \Omega_{\boldsymbol{Z}} \subset \mathbb{R}^q$, i.e.

$$\boldsymbol{W}^* \triangleq \arg\min_{\boldsymbol{W} \in \mathbb{R}^N} \left\{ \sup_{\boldsymbol{Z} \in \Omega_{\boldsymbol{Z}}} \left| F(\boldsymbol{Z}) - \boldsymbol{W}^T \boldsymbol{\varphi}(\boldsymbol{Z}) \right| \right\}. \tag{2.13}$$

Lemma 2.1 [135] Consider the Gaussian RBF network (2.11) and $h = \frac{1}{2}\min_{i \neq j} ||\xi_i - \xi_j||$. Then, we may take an upper bound of $\boldsymbol{\varphi}(\boldsymbol{Z})$ as

$$||\boldsymbol{\varphi}(\boldsymbol{Z})||^2 \leq \sum_{k=0}^{\infty} 3q(k+2)^{q-1} \exp(-2hk^2/\eta^2) \triangleq \Gamma, \tag{2.14}$$

where η is the width of the receptive field of Gaussian function and $\Gamma > 0$ is an unknown constant.

Remark 2.1 It can be easily proven that the sum $\sum_{k=0}^{\infty} 3q(k+2)^{q-1} \exp(-2hk^2/\eta^2)$ has limited value, because the infinite series $\{3q(k+2)^{q-1} \exp(-2hk^2/\eta^2)\}$, $(k = 0, \ldots, \infty)$, is convergent by the Ratio Test Theorem [103].

2.2.2. Adding-One-Power-Integrator Method

The adding-one-power-integrator method was initially proposed by Lin in [56] and is an extension of the standard backstepping control method. It cannot only handle the system classes for which backstepping works, but it is also able to stabilize a more general and challenging class of systems in the power-chained form for which backsteping fails to work. The core idea of the adding-one-power-integrator technique is the "domination".

The following lemmas are typically used in literature to achieve the "domination".

Lemma 2.2 [55] For any $x_1 \in \mathbb{R}$ and $x_2 \in \mathbb{R}$, and given positive integers b_1, b_2 and any real-valued function $\xi(\cdot,\cdot)$ with $\xi(x_1,x_2)>0$, it holds that

$$|x_1|^{b_1}|x_2|^{b_2} \le \frac{b_1\xi(x_1,x_2)|x_1|^{b_1+b_2}}{b_1+b_2} + \frac{b_2\xi^{-\frac{b_1}{b_2}}(x_1,x_2)|x_2|^{b_1+b_2}}{b_1+b_2}. \tag{2.15}$$

Lemma 2.3 [135] Let x_1 and x_2 be real-valued functions. There exist a positive odd integer $\bar{h}$ and a constant $\bar{\lambda} \ge 1$ such that

$$\left|x_1^{\bar{h}} - x_2^{\bar{h}}\right| \le \bar{h}\left|x_1 - x_2\right|\left|x_1^{\bar{h}-1} + x_2^{\bar{h}-1}\right| \tag{2.16a}$$

$$|x_1 + x_2|^{\bar{\lambda}} \le 2^{\bar{\lambda}-1}\left(|x_1|^{\bar{\lambda}} + |x_2|^{\bar{\lambda}}\right). \tag{2.16b}$$

Example 6. We take the following power-chained form systems (2.17) as an example to show the rationale of adding-one-power-integrator method.

$$\begin{cases} \dot{\chi}_1 = \chi_1^3\cos\chi_2 + \chi_2^3 \\ \dot{\chi}_2 = \chi_1^2\chi_2\sin\chi_1 + u^5, \end{cases} \tag{2.17}$$

which is the same system as Example 5. The goal is to design the control signal u such that (2.17) is stabilized.

Define the coordination transformation

$$s_1 = \chi_1, \quad s_2 = \chi_2 - \alpha_1, \tag{2.18}$$

where α_1 is the smooth virtual control law to be designed. Substituting (2.18) into (2.17) leads to

$$\begin{cases} \dot{s}_1 = \dot{\chi}_1 = (s_2+\alpha_1)^3 + s_1^3\cos(s_2+\alpha_1), \\ \dot{s}_2 = \dot{\chi}_2 - \dot{\alpha}_1 = u^5 + \chi_1^2\chi_2\sin\chi_1 - \dot{\alpha}_1 \\ \quad\ = u^5 + s_1^2(s_2+\alpha_1)\sin(s_1) - \dot{\alpha}_1. \end{cases} \tag{2.19}$$

If we choose the Lyapunov candidate $V_1(s_1) = \frac{1}{2}s_1^2$, then we have

$$\begin{aligned} \dot{V}_1(s_1) &= s_1(s_2+\alpha_1)^3 + s_1^4\cos(s_2+\alpha_1), \\ &= s_1(s_2^3 + 3s_2\alpha_1^2 + 3s_2^2\alpha_1 + \alpha_1^3) + s_1^4\cos(s_2+\alpha_1). \end{aligned} \tag{2.20}$$

In (2.20), we consider using $s_1\alpha_1^3$ to "dominate" $s_1^4\cos(s_2+\alpha_1)$ as follows:

$$\dot{V}_1(s_1) = s_1(s_2+\alpha_1)^3 - s_1\alpha_1^3 + s_1\alpha_1^3 + s_1^4\cos(s_2+\alpha_1). \tag{2.21}$$

Then, after selecting the virtual control law $\alpha_1 = -3^{\frac{1}{3}}s_1$, we arrive at

$$\dot{V}_1(s_1) = s_1(s_2+\alpha_1)^3 - s_1\alpha_1^3 + s_1\alpha_1^3 + s_1^4\cos(s_2+\alpha_1), \tag{2.22}$$

$$\le s_1s_2^3 - 3^{\frac{4}{3}}s_1^2s_2^2 + 3^{\frac{5}{3}}s_1^3s_2 - 2s_1^4 \tag{2.23}$$

Take the Lyapunov function candidate $V_2(s_1,s_2)=V_1(s_1)+\frac{1}{2}s_2^2$ and its derivative with respect to time satisfies

$$\begin{aligned}\dot{V}_2(s_1,s_2)\leq& s_1s_2^3-3^{\frac{4}{3}}s_1^2s_2^2+3^{\frac{5}{3}}s_1^3s_2-2s_1^4+s_2\Big[u^5+s_1^2\sin(s_1)\\&\times(s_2-3^{\frac{1}{3}}s_1)+3^{\frac{1}{3}}(s_2-3^{\frac{1}{3}}s_1)^3+3^{\frac{1}{3}}s_1^3\cos(s_2-3^{\frac{1}{3}}s_1)\Big]\\=&3^{\frac{1}{3}}s_2^4-2s_1^4+s_2u^5+(1-3^{\frac{5}{3}})s_1s_2^3+(9-3^{\frac{4}{3}}+\sin(s_1))s_1^2s_2^2\\&+\Big[3^{\frac{5}{3}}-3^{\frac{1}{3}}\sin(s_1)+3^{\frac{4}{3}}+3^{\frac{1}{3}}\cos(s_2-3^{\frac{1}{3}}s_1)\Big]s_1^3s_2.\end{aligned}\tag{2.24}$$

Using Lemma 2.2 to handle the last three terms of (2.24) gives

$$(1-3^{5/3})s_1s_2^3\leq 6\left|s_1s_2^3\right|\leq\frac{1}{3}s_1^4+8s_2^4,\tag{2.25}$$

$$(9-3^{4/3}+\sin(s_1))s_1^2s_2^2\leq 6\left|s_1^2s_2^2\right|\leq\frac{1}{3}s_1^4+27s_2^4,\tag{2.26}$$

$$\Big[3^{5/3}-3^{1/3}\sin s_1+3^{4/3}+3^{1/3}\cos(s_2-3^{1/3}s_1)\Big]s_1^3s_2\leq\frac{1}{3}s_1^4+9s_2^4.\tag{2.27}$$

In view of (2.25)-(2.27), we select $u=-10(s_2)^{3/5}$; then it follows that

$$\dot{V}_2(s_1,s_2)\leq -s_1^4-s_2^4.\tag{2.28}$$

This completes the design. ■

Although the adding-one-power-integrator method has been successfully applied in [89, 112, 135, 136] to stabilize power-chained form systems, the extension of the adding-one-power-integrator technique in [89, 112, 135, 136] to a distributed setting is not very meaningful due to the complexity of the controller structure, which is clarified by the following example.

Example 7. Let us revisit the power-chained form systems(1.2):

$$\begin{cases}\dot{\chi}_1=\phi_1(\chi_1)+\psi_1(\chi_1)\chi_2^{p_1},\\ \dot{\chi}_2=\phi_2(\overline{\chi}_2)+\psi_2(\overline{\chi}_2)\chi_3^{p_2},\\ \quad\vdots\\ \dot{\chi}_m=\phi_m(\overline{\chi}_m)+\psi_m(\overline{\chi}_m)\chi_{m+1}^{p_m},\quad m=3,\ldots,n-1\\ \dot{\chi}_n=\phi_n(\overline{\chi}_n)+\psi_n(\overline{\chi}_n)u^{p_n},\\ y=\chi_1.\end{cases}\tag{2.29}$$

In this example, we assume that the control directions of (2.29) are known *a priori* (i.e. the signs of $\psi_m(\cdot)$ are known *a priori*).

The control goal is to design a controller u such that the system output y tracks the reference signal y_r (bounded and differentiable), while ensuring the boundedness of all closed-loop signals.

Step 1: Define the coordination transformations

$$s_1=\chi_1-y_r,\ \ s_m=\chi_m-\alpha_{m-1},\tag{2.30}$$

where α_{m-1}, $m = 2,\ldots,n$, is the designed virtual control law specified later.

Then, we get the time derivative of s_1 as

$$\dot{s}_1 = \psi_1(\chi_1)\chi_2^{p_1} + \phi_1(\chi_1) - \dot{y}_r. \tag{2.31}$$

Take the Lyapunov function candidate as

$$V_1 = \frac{s_1^{p-p_1+2}}{p-p_1+2}. \tag{2.32}$$

Then, the time derivative of V_1 is

$$\dot{V}_1 = s_1^{p-p_1+1}\big(\psi_1(\chi_1)\chi_2^{p_1} + F_1(\boldsymbol{Z}_1)\big), \tag{2.33}$$

where $F_1(\boldsymbol{Z}_1) = \phi_1(\chi_1) - \dot{y}_r$ with $\boldsymbol{Z}_1 = [\chi_1, \dot{y}_r]^T$. Along the same lines as [135], we use a neural network to approximate $F_1(\boldsymbol{Z}_1)$ as

$$F_1(\boldsymbol{Z}_1) = \boldsymbol{W}_1^{*T}\boldsymbol{\varphi}_1(\boldsymbol{Z}_1) + \varepsilon_1(\boldsymbol{Z}_1), \quad |\varepsilon_1(\boldsymbol{Z}_1)| \le \bar{\varepsilon}_1, \quad \boldsymbol{Z}_1 \in \Omega_1, \tag{2.34}$$

where $\boldsymbol{W}_1^*$ is the optimal weight vector, $\boldsymbol{\varphi}_1(\cdot)$ is the activation function, and $\bar{\varepsilon}_1 > 0$ is an unknown constant. Similarly to [135, eq. (7)], it is possible to obtain the following inequalities:

$$\begin{aligned} s_1^{p-p_1+2}F_1(\boldsymbol{Z}_1) &= s_1^{p-p_1+2}\big(\boldsymbol{W}_1^{*T}\boldsymbol{\varphi}_1(\boldsymbol{Z}_1) + \varepsilon_1(\boldsymbol{Z}_1)\big) \\ &\le \frac{1}{\underline{p}_1}s_1^{-\underline{p}_1} + \frac{1}{\overline{p}_1}s_1^{\overline{p}_1}s_1^{p+1}\big(||\boldsymbol{W}_1^*||||\boldsymbol{\varphi}_1||\big)^{\overline{p}_1} + \frac{1}{\overline{p}_1}b_1^{\overline{p}_1}s_1^{p+1} + \frac{1}{\underline{p}_1}b_1^{-\underline{p}_1}\overline{\varepsilon}_1^{\underline{r}_1} \\ &\le s_1^{p+1}\left(b_1^{\overline{p}_1} + s_1^{\overline{r}_1}\Xi_1\Theta_1^{\overline{p}_1}\right) + \kappa_1, \end{aligned} \tag{2.35}$$

where $p = \max_{1\le m\le n}\{p_m\}$, $\overline{p}_1 = \frac{p+1}{p-p_1+1}$, $\underline{p}_1 = \frac{p+1}{p_1}$, $\Xi_1 = ||\boldsymbol{W}_1^*||^{\overline{p}_1}$, $\Theta_1 > 0$ is a known constant satisfying $\Theta_1 \ge ||\boldsymbol{\varphi}|| > 0$ according to [135, Lemma 2], and $\kappa_1 = \hbar_1^{-\underline{p}_1} + b_1^{-\underline{p}_1}\bar{\varepsilon}_1^{\underline{p}_1}$ with $\hbar_1 > 0$ and $b_1 > 0$ being design constants.

Substituting (2.35) into (2.33) leads to

$$\dot{V}_1 \le \psi_1(\chi_1)s_1^{p-p_1+1}\boxed{(s_2+\alpha_1)^{p_1}} + s_1^{p+1}\left(b_1^{\overline{p}_1} + s_1^{\overline{p}_1}\Xi_1\Theta_1^{\overline{p}_1}\right) + \kappa_1. \tag{2.36}$$

Adding and subtracting $\alpha_1^{p_1}$ on the right-hand side of (2.36) leads to

$$\begin{aligned} \dot{V}_1 &\le \psi_1(\chi_1)s_1^{p-p_1+1}\boxed{\left[(s_2+\alpha_1)^{p_1} - \alpha_1^{p_1} + \alpha_1^{p_1}\right]} + s_1^{p+1}\left(b_1^{\overline{p}_1} + s_1^{\overline{p}_1}\Xi_1\Theta_1^{\overline{p}_1}\right) + \kappa_1 \\ &\le \psi_1(\chi_1)s_1^{p-p_1+1}\alpha_1^{p_1} + s_1^{p-p_1+1}\boxed{\psi_1(\chi_1)\left[(s_2+\alpha_1)^{p_1} - \alpha_1^{p_1}\right]} \\ &\quad + s_1^{p+1}\left(b_1^{\overline{p}_1} + s_1^{\overline{p}_1}\Xi_1\Theta_1^{\overline{p}_1}\right) + \kappa_1. \end{aligned} \tag{2.37}$$

Then, we can design α_1 as

$$\alpha_1 = -s_1 \underbrace{\left\{ \frac{\text{sign}(\psi_1(\cdot))}{\overline{\psi}_1} \left(c_1 + s_1^{\overline{p}_1} \widehat{\Xi}_1 \Theta_1^{\overline{p}_1} + b_1^{\overline{p}_1} \right) \right\}^{\frac{1}{\overline{p}_1}}}_{\varsigma_1} = -s_1 \varsigma_1, \tag{2.38}$$

where $\widehat{\Xi}_1$ is the estimate of Ξ_1, and $c_1 > 0$ is a design constant.

Substituting (2.38) into (2.37) results in

$$\dot{V}_1 \leq -c_1 s_1^{p+1} + \psi_1(\chi_1) s_1^{p-p_1+1} \left(\chi_2^{p_1} - \alpha_1^{p_1} \right) + s_1^{p+1} s_1^{\overline{p}_1} \widetilde{\Xi}_1 \Theta_1^{\overline{p}_1} + \kappa_1. \tag{2.39}$$

Step 2: It follows from (2.29) and (2.30) that the derivative of s_2 is

$$\dot{s}_2 = F_2(\boldsymbol{Z}_2) + \psi_2(\chi_2) \chi_3^{p_2}, \tag{2.40}$$

where $F_2(\boldsymbol{Z}_2) = \phi_2(\overline{\boldsymbol{\chi}}_2) - \dot{\alpha}_1$.

Take the Lyapunov function candidate as

$$V_2 = V_1 + \frac{s_2^{p-p_2+2}}{p-p_2+2}. \tag{2.41}$$

Then, the derivative of V_2 satisfies

$$\begin{aligned} \dot{V}_2 \leq & -c_1 s_1^{p+1} + \boxed{\psi_1(\chi_1) s_1^{p-p_1+1} \left(\chi_2^{p_1} - \alpha_1^{p_1} \right)} + s_1^{p+1} s_1^{\overline{p}_1} \widetilde{\Xi}_1 \Theta_1^{\overline{p}_1} + \kappa_1 \\ & + s_2^{p-p_2+1} F_2(\boldsymbol{Z}_2) + \psi_2(\chi_2) s_2^{p-p_2+1} \chi_3^{p_2}. \end{aligned} \tag{2.42}$$

In the existing designs [135], the red term in (2.42) was handled by

$$\begin{aligned} & \left| \psi_1(\chi_1) s_1^{p-p_1+1} \left(\chi_2^{p_1} - \alpha_1^{p_1} \right) \right| \\ & \leq \overline{\psi}_1 p_1 \left| s_1^{p-p_1+1} \right| |s_2| \left(\chi_2^{p_1-1} + (s_1 \varsigma_1)^{p_1-1} \right) \\ & \leq s_1^{p+1} + s_2^{p+1} \overline{\varsigma}_1, \end{aligned} \tag{2.43}$$

where the above inequalities use Lemma 2.3, and $\overline{\varsigma}_1 = \left(2^{p_1-2} p_1 \overline{\psi}_1\right)^{\frac{p}{p_1}-1} + \left(2^{p_1-2} p_1 \varsigma_1^{p_1-1} \overline{\psi}_1\right)^{p+1}$.

Substituting (2.43) into (2.42) and using a neural network to approximate $F_2(\boldsymbol{Z}_2)$ leads to

$$\begin{aligned} \dot{V}_2 \leq & -c_1 s_1^{p+1} + s_1^{p+1} + \boxed{s_2^{p+1} \overline{\varsigma}_1} + s_1^{p+1} s_1^{\overline{p}_1} \widetilde{\Xi}_1 \Theta_1^{\overline{p}_1} + \kappa_1 + s_2^{p+1} \left(b_2^{\overline{p}_2} + s_2^{\overline{p}_2} \widetilde{\Xi}_2 \Theta_2^{\overline{p}_2} \right) + \kappa_2 \\ & + \psi_2(\chi_2) s_2^{p-p_2+1} \left(\chi_3^{p_2} - \alpha_2^{p_2} \right) + \psi_2(\chi_2) s_2^{p-p_2+1} \alpha_2^{p_2}, \end{aligned} \tag{2.44}$$

where $\overline{p}_2 = \frac{p+1}{p-p_2+1}$, $\underline{p}_2 = \frac{p+1}{p_2}$, $\Xi_2 = ||\boldsymbol{W}_2^*||^{\overline{p}_2}$, $\Theta_2 > 0$ is a known constant satisfying $\Theta_2 \geq ||\boldsymbol{\varphi}_2|| > 0$, and $\kappa_2 = \hbar_2^{-\underline{p}_2} + b_2^{-\underline{p}_2} \bar{\varepsilon}_2^{\underline{p}_2}$ with $\hbar_2 > 0$ and $b_2 > 0$ design constants.

Design the virtual controller α_2 as

$$\alpha_2 = -s_2 \underbrace{\left\{ \frac{\operatorname{sign}(\psi_2(\cdot))}{\overline{\psi}_2} \left(c_2 + \overline{\varsigma}_1 + s_2^{\overline{p}_2} \widehat{\Xi}_2 \Theta_2^{\overline{p}_2} + b_2^{\overline{p}_2} \right) \right\}^{\frac{1}{\overline{p}_2}}}_{\varsigma_2} = -s_2 \varsigma_2, \tag{2.45}$$

where $\widehat{\Xi}_2$ is the estimate of Ξ_2, and $c_2 > 0$ is a design constant.

Proceeding similarly and by induction, it is possible to obtain the expressions of virtual/actual controllers as

$$\alpha_m = -s_m \underbrace{\left\{ \frac{\operatorname{sign}(\psi_m(\cdot))}{\overline{\psi}_m} \left(c_m + \overline{\varsigma}_{m-1} + s_m^{\overline{p}_m} \widehat{\Xi}_m \Theta_m^{\overline{p}_m} + b_m^{\overline{p}_m} \right) \right\}^{\frac{1}{\overline{p}_m}}}_{\varsigma_m} = -s_m \varsigma_m, \tag{2.46}$$

$$u = -s_n \underbrace{\left\{ \frac{\operatorname{sign}(\psi_n(\cdot))}{\overline{\psi}_n} \left(c_n + \overline{\varsigma}_{n-1} + s_n^{\overline{p}_n} \widehat{\Xi}_n \Theta_n^{\overline{p}_n} + b_n^{\overline{p}_n} \right) \right\}^{\frac{1}{\overline{p}_n}}}_{\varsigma_n} = -s_n \varsigma_n, \tag{2.47}$$

where $\overline{\varsigma}_{m-1} = \left(2^{p_{m-1}-2} p_{m-1} \overline{\psi}_m\right)^{\frac{p}{p_{m-1}}} + \left(2^{p_{m-1}-2} p_{m-1} \varsigma_{m-1}^{p_{m-1}} \overline{\psi}_m\right)^{p+1}$, $\overline{\varsigma}_{n-1} = \left(2^{p_{n-1}-2} p_{n-1} \times \overline{\psi}_n\right)^{\frac{p}{p_{n-1}}} + \left(2^{p_{n-1}-2} p_{n-1} \varsigma_{n-1}^{p_n-1} \overline{\psi}_n\right)^{p+1}$, $\widehat{\Xi}_m$ is the estimate of Ξ_m, and $c_m > 0$ is a design constant for $m = 3, \ldots, n$.

The subsequent stability analysis is similar to that of [135] and we thus omit it here.

At this point, it can be seen from (2.46) and (2.47) that for the adding-one-power-integrator methods [55, 89, 112, 135, 136] to work, $\overline{\varsigma}_{m-1}$ is incorporated into the virtual controller α_m (2.46) to eliminate the extra term $\overline{\varsigma}_{m-1} s_m^{p+1}$: this inevitably increases the complexity of the controller structure. It is also worth mentioning that the power of the control gain $\overline{\varsigma}_{m-1}$ in (2.46) grows dramatically (exponentially) as the order of the subsystems grows, leading to possibly high control gains.

Remark 2.2 It can be seen that the signs of control gain functions $\psi_m(\cdot)$ (i.e. the control directions) are involved in the control designs (2.38), (2.45), (2.46), and (2.47). In other words, the above design is dependent on the priori knowledge of system control directions. In case the control directions of (1.2) are unknown (i.e. the signs of $\psi_m(\cdot)$ are unknown), Nussbaum functions (cf. the Section 2.2.3) are the commonly used tool to handle the absence of unknown control directions).

2.2.3. Nussbaum Functions and Corresponding Technical Lemmas

In case the control direction (i.e. the sign of a control gain function) of a control system is unknown a priori, designing a controller becomes challenging due to the fact that a control force with incorrect control direction might steer the system away from the desired behavior [18, 75]. A possible solution is to alternatively change the sign of the control gain function. Specifically, the negative effect accumulated during the periods

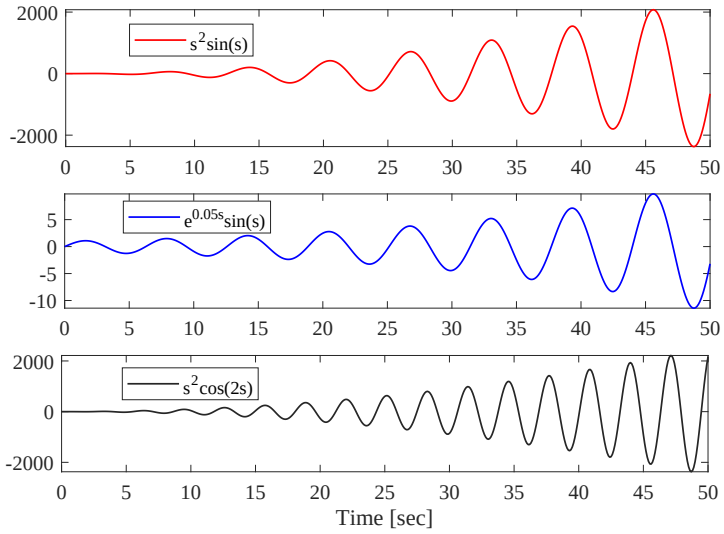

Figure 2.3: Trajectories of some typical Nussbaum functions

of incorrect control directions is counteracted by the positive effect accumulated during the periods of correct control directions.

The Nussbaum gain technique has been extensively exploited to tackle unknown control directions in [14, 22, 23, 75, 106, 122, 125] since it was originally proposed in [75]. A fundamental tool to prove closed-loop stability is the so-called conditional inequality, which consists in guaranteeing the boundedness of a Lyapunov-like function when its derivative along the system trajectories is upper bounded by an appropriate expression depending on the Nussbaum function.

In the sequel, we first introduce the definition of Nussbaum functions and some corresponding technical lemmas. Then, we show via an example how the issue of a single unknown control direction can be tackled by the Nussbaum functions-based technique.

Definition 2.6 [75] A continuously differentiable function $\mathcal{N}(\cdot) : [0,\infty) \to (-\infty,+\infty)$ is called a Nussbaum function if it satisfies

$$\lim_{y\to\infty} \sup \frac{1}{y}\int_0^y \mathcal{N}(s)ds = +\infty, \text{ and } \lim_{y\to\infty} \inf \frac{1}{y}\int_0^y \mathcal{N}(s)ds = -\infty. \tag{2.48}$$

The functions $s^2\sin(s)$, $\exp(0.05s)\sin(s)$, and $s^2\cos(2s)$ whose trajectories are shown in Fig. 2.3 are Nussabum functions since they satisfy the properties (2.48).

Lemma 2.4 [31] Consider two continuously differentiable functions $V(\cdot) : [0, t_s) \to \mathbb{R}^+$, $y(t) : [0, t_s) \to \mathbb{R}^+$. If $\mathcal{N}(\cdot)$ is a Nussbaum function with the following inequality holding:

$$V(t) \le c_0 + \exp(-c_1 t)\int_0^t \Big[g(\tau)\mathcal{N}(y) + 1\Big]\dot{y}\exp(c_1\tau)d\tau, \quad \forall\ t \in [0, t_s) \tag{2.49}$$

where c_0 and c_1 are positive constants; g is a function satisfying $g(t) \in [l_1, l_2]$ with $0 < l_1 < l_2$ or $0 > l_2 > l_1$ with l_1 and l_2 constants. Then, $V(\cdot)$ and $y(\cdot)$ remain bounded on any finite time interval $[0, t_s)$.

Lemma 2.5 [18] Consider two continuously differentiable functions $V(\cdot) : [0,\infty) \to \mathbb{R}^+$, $y(\cdot) : [0,\infty) \to \mathbb{R}^+$. If

$$\dot{V}(t) \leq \big(\lambda \mathscr{N}(y(t)) + a\big)\dot{y}(t) \tag{2.50}$$

for two constants a, $\lambda \in \mathbb{R}$ and a Nussbaum function $\mathscr{N}$, then $V(\cdot)$ and $y(\cdot)$ are bounded over $[0,\infty)$.

Remark 2.3 The fundamental difference between Lemma 2.4 and Lemma 2.5 consists in the fact that Lemma 2.4 can only ensure boundedness of $V(\cdot)$ and $y(\cdot)$ within finite time, i.e. $t_s < \infty$. When $t_s = \infty$, the boundedness of $V(\cdot)$ and $y(\cdot)$ is not guaranteed (cf. the discussion in [80, Remark 1]), whereas Lemma 2.5 ensures the boundedness of $V(\cdot)$ and $y(\cdot)$ on the entire time domain $[0,\infty)$.

We are now in the position to clarify how Lemmas 2.4 and 2.5 are used to solve the control design difficulty caused by a single unknown control direction.

Example 8. Let us consider the following first-order system in the power-chained form whose control direction (i.e. the sign of $\psi(\cdot)$) is unknown *a priori*:

$$\begin{cases} \dot{\chi} = \phi(\chi) + \psi(\chi)u^p, \\ y = \chi, \end{cases} \tag{2.51}$$

where χ and $y \in \mathbb{R}$ are the state and the output of the system, respectively; p is a positive odd integer, $\phi(\cdot)$ is an unknown continuous nonlinear function, $\psi(\cdot)$ is the control gain function with an unknown sign satisfying $\underline{\psi} \leq \big|\psi(\cdot)\big| \leq \bar{\psi}$ with $\underline{\psi}$ and $\bar{\psi}$ positive constants, and u is the control signal.

The control goal is to design u such that the output y tracks the reference signal y_r in spite of the unknown control direction.

To begin with the design, let us define the following change of coordinate:

$$s = \chi - y_r, \tag{2.52}$$

where y_r is the reference signal with continuous and bounded derivative.

Consider (2.51) and (2.52), the time derivative of s is

$$\dot{s} = \psi(\chi)u^p + F(\boldsymbol{Z}), \tag{2.53}$$

where $\boldsymbol{Z} = \big[\chi, \dot{y}_r\big]$ and $F(\boldsymbol{Z}) = \phi(\chi) - \dot{y}_r$.

Similarly to [135], we use an RBF NN to approximate the unknown continuous function $F(\cdot)$ as

$$F(\boldsymbol{Z}) = \boldsymbol{W}^{*T}\boldsymbol{\varphi}(\boldsymbol{Z}) + \varepsilon(\boldsymbol{Z}), \quad \boldsymbol{Z} \in \Omega_{\boldsymbol{Z}} \tag{2.54}$$

where $\big|\varepsilon(\boldsymbol{Z})\big| \leq \bar{\varepsilon}$ with $\bar{\varepsilon}$ a positive constant.

In light of Lemma 2.2, the following inequality holds:

$$\begin{aligned} s^3 F \leq & \frac{3}{p+3}\ell^{\frac{p+3}{3}} s^{p+3}\left\|\boldsymbol{W}^*\right\|^{\frac{p+3}{3}}\|\boldsymbol{\varphi}\|^{\frac{p+3}{3}} \\ & + \frac{p}{p+3}\varsigma^{-\frac{p+3}{p}}\bar{\varepsilon}^{\frac{p+3}{p}} + \frac{p}{p+3}\ell^{-\frac{p+3}{p}} \\ & + \frac{3}{p+3}\varsigma^{\frac{p+3}{3}} s^{p+3} \\ \leq & s^{p+3}\left(\ell^{\frac{p+3}{3}}\beta\|\boldsymbol{\varphi}\|^{\frac{p+3}{3}} + \varsigma^{\frac{p+3}{3}}\right) + \lambda, \end{aligned} \tag{2.55}$$

where $\beta = \left\|\boldsymbol{W}^*\right\|^{\frac{p+3}{3}}$ and $\lambda = \ell^{-\frac{p+3}{p}} + \varsigma^{-\frac{p+3}{p}}\bar{\varepsilon}^{\frac{p+3}{p}}$.

Consider the Lyapunov function candidate

$$V = \frac{s^4}{4} + \frac{1}{2\vartheta}\tilde{\beta}^2, \tag{2.56}$$

where $\tilde{\beta} = \beta - \hat{\beta}$ and $\vartheta > 0$ is a design constant.

The time derivative of V along (2.53), (2.55), and (2.56) satisfies

$$\begin{aligned} \dot{V} \leq & s^3\left(\psi(\chi)u^p + s^p\kappa\right) + s^{p+3}\varsigma^{\frac{p+3}{3}} - s^{p+3}\kappa \\ & - \frac{\tilde{\beta}\dot{\hat{\beta}}}{\vartheta} + s^{p+3}\ell^{\frac{p+3}{3}}\beta\|\boldsymbol{\varphi}\|^{\frac{p+3}{3}} + \lambda. \end{aligned} \tag{2.57}$$

Design the virtual controllers u and adaptive law $\hat{\beta}$ as

$$\boxed{u = \mathcal{N}_R^{\frac{1}{p}}(\xi)\kappa^{\frac{1}{p}}s,} \tag{2.58}$$

$$\kappa = \ell^{\frac{p+3}{3}}\hat{\beta}\|\boldsymbol{\varphi}\|^{\frac{p+3}{3}} + c + \varsigma^{\frac{p+3}{3}}, \tag{2.59}$$

$$\dot{\xi} = s^{p+3}\kappa, \tag{2.60}$$

$$\dot{\hat{\beta}} = \vartheta\ell^{\frac{p+3}{3}} s^{p+3}\|\boldsymbol{\varphi}\|^{\frac{p+3}{3}} - \gamma\hat{\beta}, \tag{2.61}$$

where $\mathcal{N}_R$ is a Nussbaum function, and where ℓ, c, γ, and ς are positive design parameters.

Substituting (2.58), (2.59), (2.60), and (2.61) into (2.57) gives

$$\dot{V} \leq \dot{\xi}\left(\psi(\chi)\mathcal{N}_R(\xi) + 1\right) - cs^{p+3} + \frac{\gamma}{2\vartheta}\left(\beta^2 - \tilde{\beta}^2\right) + \lambda. \tag{2.62}$$

Applying Lemma 2.2 to the term $\omega^{\frac{p-1}{p+3}}s^4$ with $\omega > 0$ a constant, it holds that

$$\omega^{\frac{p-1}{p+3}}s^4 \leq \omega + s^{p+3}. \tag{2.63}$$

Substituting (2.63) into (2.62) yields

$$\dot{V} \leq \dot{\xi}\big(\psi(\chi)\mathcal{N}_R(\xi)+1\big)-\mu V+\varrho, \tag{2.64}$$

where $\mu=\min\left\{4c\omega^{\frac{p-1}{p+3}},\gamma\right\}$ and $\varrho=c\omega+\lambda+\frac{\gamma}{2\vartheta}\beta^2$.

Multiplying both sides by $e^{\mu t}$, integrating it over $[0,t]$ and multiplying both sides by $e^{-\mu t}$, one has

$$\boxed{V(t)\leq\int_0^t\big(\psi(\chi)\mathcal{N}_R(\xi)+1\big)\dot{\xi}e^{\mu(\nu-t)}d\nu+c_0,} \tag{2.65}$$

where $c_0=V(0)+\Pi$ with $\Pi=\frac{\varrho}{\mu}$ a positive constant. Recalling Lemma 2.4 yields the boundedness of $V(\cdot)$. Following a similar reasoning to [61] one can prove the boundedness of closed-loop signals on the time interval $[0,t_s)$ with $t_s<+\infty$. ■

In contrast with the designs (2.46) and (2.47), the control law (2.58) does not rely on the sign of control gain function $\psi(\cdot)$ (i.e. the control direction). In place of the priori knowledge of the control direction, a Nussbaum function is utilized in (2.58) to facilitate the control design. Besides, it can be seen from (2.52)-(2.65) that Lemma 2.4 plays a crucial role in achieving closed-loop stability. The use of Lemma 2.5 is similar to Lemma 2.4, which can be observed in Chapter 6.

Note that the above Example 8 shows that Lemma 2.4 can be directly exploited to handle a single unknown control direction (i.e. the sign of control gain function $\psi(\cdot)$ is unknown). When considering higher-order (more than first-order) nonlinear systems with multiple unknown control directions (i.e. the signs of multiple control gain functions are unknown), multiple Nussbaum functions terms appear as shown in the following example 9.

Example 9. Let us consider the following third-order systems in the power-chained form with multiple unknown control directions (i.e. the signs of $\psi_m(\cdot)$, $m=1,2,3$) are unknown *a priori*.

$$\begin{cases}\dot{\chi}_1=\phi_1(\chi_1)+\psi_1(\chi_1)\chi_2^{p_1},\\ \dot{\chi}_2=\phi_2(\bar{\boldsymbol{\chi}}_2)+\psi_2(\bar{\boldsymbol{\chi}}_2)\chi_3^{p_2},\\ \dot{\chi}_3=\phi_3(\bar{\boldsymbol{\chi}}_3)+\psi_3(\bar{\boldsymbol{\chi}}_3)u^{p_3},\\ y=\chi_1,\end{cases} \tag{2.66}$$

where $\bar{\boldsymbol{\chi}}_2=[\chi_1,\chi_2]^T\in\mathbb{R}^2$, $\bar{\boldsymbol{\chi}}_3=[\chi_1,\chi_2,\chi_3]^T\in\mathbb{R}^3$ and $y\in\mathbb{R}$ are state variables and output of the system, respectively. For $m=1,2,3$, p_m is positive odd integer, $\phi_m(\cdot)$ is an unknown continuous nonlinear function, $\psi_m(\cdot)$ is a control gain function with unknown control direction satisfying $\underline{\psi}_m\leq|\psi_m(\cdot)|\leq\overline{\psi}_m$ with $\underline{\psi}_m$ and $\overline{\psi}_m$ being positive constants, and u is the control signal to be designed.

The aim is to devise u such that the output y follows the reference signal y_r in spite of multiple unknown control directions, while guaranteeing that all closed-loop signals are bounded.

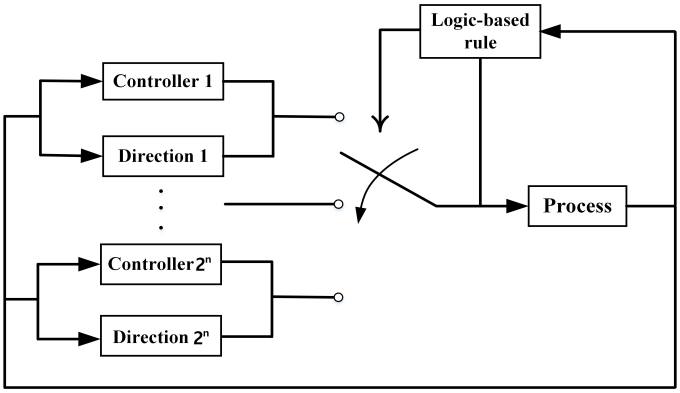

Figure 2.4: A schematic diagram of tuning control parameters and control directions via a logic-based rule

To begin with the design, let us define $p = \max_{1\le m\le 3}\{p_m\}$ and the following changes of coordinates

$$\begin{cases} s_1 = \chi_1 - y_r, \\ s_2 = \chi_2 - \alpha_2, \\ s_3 = \chi_3 - \alpha_3, \end{cases} \tag{2.67}$$

where α_2 and α_3 represent the virtual control laws, which will be specified later.

The subsequent design procedure contains 3 steps; the design of each step is similar to the design in Example 8. By induction, it is possible to reach the following inequality:

$$V(t) \le \sum_{m=1}^{3} \int_0^t \left(\psi_m(\bar{\chi}_m)\mathcal{N}_R(\xi_m) + 1\right)\dot{\xi}_m e^{\mu(\nu-t)}\, d\nu + c_0, \tag{2.68}$$

where c_0 is a positive constant.

In comparison with the inequality in (2.65), which contains only one Nussbaum function term, the inequality (2.68) contains multiple Nussbaum functions terms. Such a fact requires to propose new Nussbaum functions guaranteeing the boundedness of $V(\cdot)$ and $\xi_m(\cdot)$ under the framework of (2.68). This is because [37, 125] have shown that the summed versions of Lemma 2.4 (cf. (2.68)) does not necessarily hold for existing Nussbaum functions since their effects could counteract each other, making the boundedness of $V(\cdot)$ and $\xi_m(\cdot)$ non-existent.

2.2.4. State-of-the-Art in Logic-based Control

Logic-based control typically means to update parameters (including controller parameters, control directions, and unknown system parameters) in a discrete manner (rather than continuously) via a logic-based rule that is designed in such a way that closed-loop

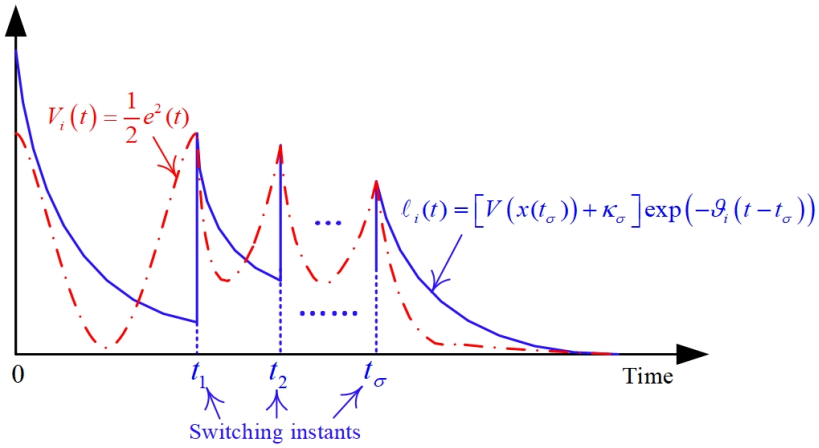

Figure 2.5: Logic-based switching mechanisms of [36, 115]

stability is guaranteed. A schematic diagram of tuning controller parameters and control directions is given in Fig. 2.4, where 2^n denotes the number of all possible combinations of n control directions.

State-of-the-art logic-based control methods have been successfully exploited to avoid conventional continuous tuning of controller parameters and conventional Nussabum functions-based approaches for strict-feedback systems in [36, 115]. However, it is worth pointing out that the logic-based mechanisms in [36, 115] depend on monitor functions that monitor whether asymptotic tracking can be achieved (leading to bounded energy of the tracking error) [36] or whether finite-time stabilization (i.e. the stabilization error converges to zero in finite time) can be obtained [115]. In other words, for the methods [36, 115] to work, tracking errors are required to converge to zero asymptotically, which is shown in Fig. 2.5 where $V(t)=\frac{1}{2}e^2(t)$ is the Lyapunov function and $\ell(t)=\left[V(x(t_\sigma))+\kappa_\sigma\right]\exp\left(-\vartheta_i(t-t_\sigma)\right)$ is the monitor function with κ_σ and ϑ_σ positive design constants. Unfortunately, the same mechanism and monitor functions in [36, 115] cannot be adopted for agents in power-chained form systems on account of the fact that asymptotic tracking in general cannot be achieved for power-chained form systems due to the aforementioned structural difficulty, as illustrated in Chapter 1. Therefore, a new logic-based mechanism as well as new monitor functions must be sought for power-chained form systems [83, Sect. 2].

2.2.5. Prescribed-Performance Control

The paradigm of prescribed-performance control (PPC) was originally proposed in [5] and utilized in [6, 52, 78, 101] to design controllers capable of guaranteeing prescribed performance bounds on the transient and steady-state output error *a priori* for a range of nonlinear system classes. Its key idea is to transform the considered system into one that takes into account some prescribed transient and steady-state specifications (e.g. convergence rate, overshoot, or steady-state error).

To explain the rationale of PPC, let us consider a generic tracking error $e\in\mathbb{R}$. Pre-

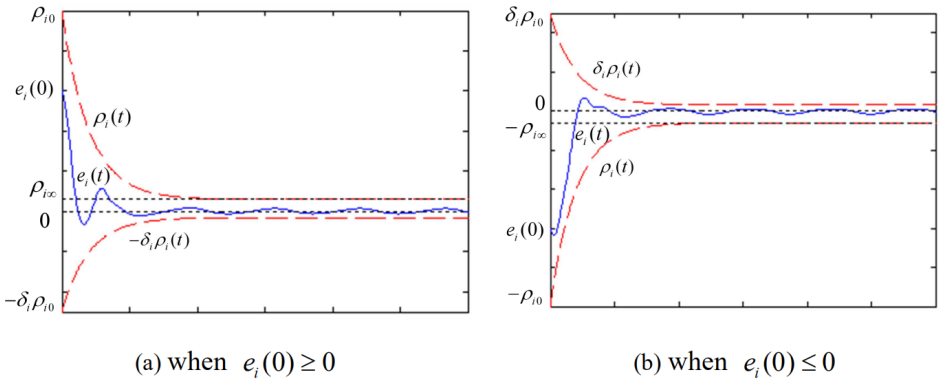

(a) when $e_i(0) \geq 0$ (b) when $e_i(0) \leq 0$

Figure 2.6: Graphical representation of (2.69)

scribed performance is achieved if the following two inequalities are satisfied for all $t \geq 0$:

$$\begin{cases} -\delta_i\rho_i(t) < e_i(t) < \rho_i(t), & \text{if } e_i(0) \geq 0 \\ -\rho_i(t) < e_i(t) < \delta_i\rho_i(t), & \text{if } e_i(0) \leq 0, \end{cases} \tag{2.69}$$

where $0 \leq \delta_i < 1$ is a non-negative design constant and $\rho_i(\cdot) : \mathbb{R}_{\geq 0} \to \mathbb{R}_{>0}$ is the *prescribed performance function* satisfying $\underline{\rho}_i \leq \rho_i(t) \leq \bar{\rho}_i$, $\forall t \geq 0$ for some constants $\underline{\rho}_i > 0$ and $\bar{\rho}_i > 0$. Note that (2.69) indicates that (i) when $e_i(0) > 0$, $\rho_i(0)$ is chosen to make $e_i(0) < \rho_i(0)$ hold; (ii) when $e_i(0) < 0$, $\rho_i(0)$ is chosen to make $-e_i(0) < \rho_i(0)$ hold; (iii) when $e_i(t) = 0$, for any $\rho_i(0) > 0$, δ_i should be chosen such that $\delta_i \neq 0$. In other words, the constant δ_i and function $\rho_i(\cdot)$ are utilized to show the desired performance metrics of $e_i(\cdot)$. Without loss of generality, prescribed performance function is defined as

$$\rho_i(t) = (\rho_{i,0} - \rho_{i,\infty}) \exp(-\mu_i t) + \rho_{i,\infty}, \tag{2.70}$$

where $\rho_{i,\infty} > 0$ corresponds to the maximum allowable tracking error at steady state and $\mu_i > 0$ to the minimum admissible convergence rate; the maximum overshoot is prescribed less than $\delta_i\rho_i(0) = \delta_i\rho_{i,0}$.

For a more vivid explanation, Fig. 2.6 depicts the evolution of the tracking error $e_i(\cdot)$ prescribed by the performance function $\rho_i(\cdot)$ and constant $\delta_i(\cdot)$.

2.2.6. Approximation-Free Prescribed-Performance Control

Approximation-free (also called low-complexity) PPC is a control methodology whose strongest feature is its structural simplicity: uncertainty can be handled without unknown parameter estimators nor approximation structures (neural networks, fuzzy logic, etc.) being involved in the control design. Remarkably, uncertain dynamics can be stabilized with a low-complexity structure, as the control action is a simple nonlinear static action without any approximation structure nor dynamic parametric adaptation.

Consider a continuous function $T_i : (L_i, U_i) \to \mathbb{R}$ that is strictly increasing and satisfies $\lim_{z \to U_i^-} T_i(z) = +\infty$ and $\lim_{z \to L_i^+} T_i(z) = -\infty$ with constants $U_i \geq 0$ and $L_i \leq 0$

defined as

$$(L_i, U_i) = \begin{cases} (-\delta_i, 1), & \text{if } e_i(0) \geq 0, \\ (-1, \delta_i), & \text{if } e_i(0) < 0. \end{cases} \tag{2.71}$$

It is straightforward to verify that the inverse function $T_i^{-1} : \mathbb{R} \to (L_i, U_i)$ is well-defined and strictly increasing as well. A representative example of T_i is given by

$$T_i(\star) = \log\left(\frac{-L_i + \star}{U_i - \star}\right). \tag{2.72}$$

It has been shown in [6, 101] that achieving the boundedness of $T_i\left(\frac{e_i(t)}{\rho_i(t)}\right)$ results in $L_i < \frac{e_i(t)}{\rho_i(t)} < U_i$, $\forall t \geq 0$, implying that the prescribed performance in the sense that (2.69) is guaranteed. In what follows, we provide an example to show the rationale of approximation free PPC.

Example 10. Consider the strict-feedback nonlinear system in the form of

$$\begin{cases} \dot{\chi} = \phi(\chi) + \psi(\chi)u, \\ y = \chi, \end{cases} \tag{2.73}$$

where $\chi \in \mathbb{R}$ and $y \in \mathbb{R}$ are the state and the output of the system, respectively; $\phi(\cdot)$ is an unknown continuous nonlinear function satisfying $\underline{\phi}(\cdot) \leq \left|\phi(\cdot)\right| \leq \bar{\phi}(\cdot)$ with $\underline{\phi}(\cdot)$ and $\bar{\phi}(\cdot)$ positive functions, $\psi(\cdot)$ is a control gain function satisfying $\underline{\psi} \leq \left|\psi(\cdot)\right| \leq \bar{\psi}$ with $\underline{\psi}$ and $\bar{\psi}$ positive constants, and u is the control signal specified later.

The control goal is to design $u \in \mathbb{R}$ such that (i) all closed-loop signals remain bounded, and (ii) the tracking error $e(t) = y(t) - y_{\mathrm{r}}(t)$ is such that $|e(t)| < \rho(t)$ for all $t \geq 0$, where $\rho(\cdot)$ is the prescribed performance function defined in (2.70), and $y_{\mathrm{r}}(\cdot)$ is a continuously differentiable and bounded signal with bounded derivative.

Define the transformed error surface $s(t) = \log\left(\frac{1+\zeta(t)}{1-\zeta(t)}\right)$, where

$$\zeta(t) = \frac{e(t)}{\rho(t)} \tag{2.74}$$

is normalized error and $\rho(t) = (\rho_0 - \rho_\infty)\exp(-\mu t) + \rho_\infty$ is the so-called prescribed performance function as defined in (2.70) , where ρ_0 satisfying $\rho_0 > |x(0) - y_r(0)| \geq 0$ is a design constant.

We are now at the position to design the control law u as

$$\boxed{u(t) = -\text{sign}\big(\psi(\cdot)\big)\kappa s(t) \triangleq u^\star(\zeta, t),} \tag{2.75}$$

with $\kappa > 0$ a design parameter.

It is not hard to arrive at

$$\chi(t) = e(t) + y_{\mathrm{r}}(t) = \rho(t)\zeta(t) + y_{\mathrm{r}}(t) \triangleq \chi^\star(\zeta, t). \tag{2.76}$$

Differentiating the normalized error $\zeta(t)$ in (2.74) w.r.t. time gives

$$\dot{\zeta}(t) = \frac{1}{\rho(t)}\left[\phi(\chi^\star, t) + \psi(\chi^\star, t)u^\star(\zeta, t) - \dot{y}_{\mathrm{r}} - \dot{\rho}(t)\zeta\right] \triangleq \beta(\zeta, t). \tag{2.77}$$

Define the open set $\Omega_\zeta = (-1,1)$, it is straightforward to verify that $\zeta(0) \in \Omega_\zeta$. Besides, note that $\beta(\cdot,\cdot) : \Omega_\zeta \times \mathbb{R}_+ \to \mathbb{R}$ is piecewise continuous in t and locally Lipschitz in Ω_ζ; $\phi(\cdot)$ and $\psi(\cdot)$ are piecewise continuous in t and locally Lipschitz in χ, and $y_r(\cdot)$ and $\rho(\cdot)$ are bounded and differentiable. Then, it follows from [6, Theorem 1] that there exists a unique maximal solution $\zeta(\cdot)$ of (2.76) on the time interval $[0,\tau_{\max})$ where $\tau_{\max} < +\infty$ is chosen such that $\zeta(t) \in \Omega_\zeta$ for all $t \in [0,\tau_{\max})$. In what follows, we first suppose $\tau_{\max} < +\infty$, and eventually we prove by a contradiction that $\tau_{\max}$ can be extended to $+\infty$.

Take the Lyapunov function

$$V = \frac{1}{2}s^2, \tag{2.78}$$

where V is positive definite and continuously differentiable over Ω_ζ. The following steps are conducted on the time interval $[0,\tau_{\max})$.

It follows from (2.73)-(2.77) that the time derivative of V satisfies

$$\dot{V} \le \gamma|s|\Big[F(t) - \kappa\psi(\chi)|s|\Big] \le \gamma\Big[\bar{F}|s| - \kappa\underline{\psi}|s|^2\Big], \quad t \in [0,\tau_{\max}) \tag{2.79}$$

where $\gamma = \frac{2}{\rho(t)(1-\zeta^2)}$ and $\bar{F}$ is the upper bound of the continuous function F defined by $F(t) = |\phi(\chi)| + |\dot{y}_r| + |\dot{\rho}(t)\zeta|$ according to extreme value theorem.

From (2.79), we have that $\dot{V}$ is negative when $|s| > \frac{\bar{F}}{\kappa\underline{\psi}}$. This indicates that

$$|s(t)| \le \max\left\{|s(0)|, \frac{\bar{F}}{\kappa\underline{\psi}}\right\} \triangleq \bar{s}, \quad t \in [0,\tau_{\max}), \tag{2.80}$$

which immediately implies that ζ is bounded on $[0,\tau_{\max})$ due to the monotonicity of function $s(\zeta)$. Furthermore, u remains bounded (i.e. $|u| \le \kappa\bar{s}$) for all $t \in [0,\tau_{\max})$. Up to this, what remains to show is that $\tau_{\max}$ can be extended to $+\infty$. In view of the expression of $s(t)$ and (2.80), we have that $\zeta(t) \in \Omega_\zeta^*$, $\forall t \in [0,\tau_{\max})$, where the set $\Omega_\zeta^* = \left[\underline{\zeta},\bar{\zeta}\right]$ is nonempty and compact with

$$-1 < \frac{\exp(-\bar{s})-1}{\exp(-\bar{s})+1} = \underline{\zeta} \le \zeta(t) \le \bar{\zeta} = \frac{\exp(\bar{s})-1}{\exp(\bar{s})+1} < 1, \quad t \in [0,\tau_{\max}) \tag{2.81}$$

which suggests that the prescribed performance $|e(t)| < \rho(t)$ has been guaranteed on $[0,\tau_{\max})$.

At this point, it is straightforward to verify that $\Omega_\zeta^* \subset \Omega_\zeta$. According to [6, Proposition 1], we have $\tau_{\max} = +\infty$. This completes the proof. ■

It can be seen from Example 10 that no universal approximators such as neural networks and fuzzy logic systems have been involved in the design and stability analysis, while guaranteeing the prescribed performance imposed on $e(\cdot)$.

2.2.7. Common Lyapunov Function Method

Prior to introducing common Lyapunov function method, we first present the definition of switched systems. Switched systems according to [54] are a special class of hybrid systems composed by collection of subsystems (cf. (2.82)), and a rule to regulate the switching behavior among them, called switching law or signal (referring to $\sigma(t)$ in Fig.

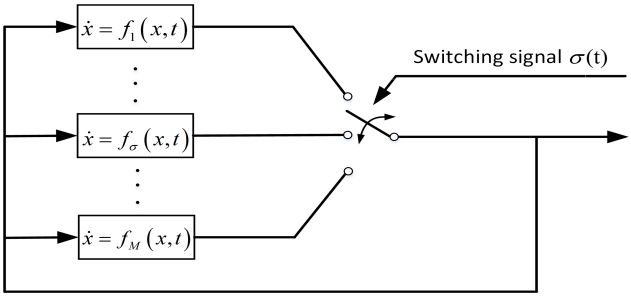

Figure 2.7: The framework of switched systems

2.7). In accordance with the essence of the switching signals, switched systems could be divided into two categories (i.e. time-driven switched systems and state-dependent switched systems). In this thesis, Chapters 3 and 4 focus on switched systems with time-driven switching signals whose framework is given in Fig. 2.7.

$$\dot{x} = f_\sigma(x,t),\ \forall \sigma \in \mathscr{P}, \tag{2.82}$$

where $\mathscr{P}$ is some index set (typically $\mathscr{P}$ is a subset of a finite-dimensional linear vector space). It has been shown in [54] that Lyapunov's stability theorem has a direct extension that provides a basic tool for studying uniform stability of the switched system (2.82). This extension is obtained by requiring the existence of a single Lyapunov function whose derivative along solutions of all systems in the family (2.82) satisfies suitable inequalities. We are particularly interested in obtaining a Lyapunov condition for uniform ultimate boundedness (UUB). To do this, we must special care in formulating an inequality that ensures a uniform rate of decay.

Given a positive definite continuously differentiable function $V : \mathbb{R}^n \to \mathbb{R}$, we say that it is a *common Lyapunov function* [54] for the family of switched systems $\dot{x} = f_\sigma(x,t)$ if it holds that

$$\frac{\partial V}{\partial x} f_\sigma(s) \le -\alpha V(x) + \beta, \quad \forall x, \tag{2.83}$$

where $\alpha > 0$ and $\beta \ge 0$ are constants.

The following theorem will be used in Chapters 3 and 4 of this thesis.

Theorem 2.3 If all systems in the family (2.82) share a radially unbounded common Lyapunov function such that (2.83) holds, then, the switched system (2.82) is UUB. In addition, if $\beta = 0$ in (2.83), asymptotic stability is obtained.

Theorem 2.3 is an extension of [54, Theorem 2.1] and can be derived in the same way as the standard Lyapunov stability theorem. The main idea of the theorem is that the rate of decrease of V along the solutions, given by (2.82), is not affected by switching, hence stability result is uniform with respect to switching signal σ.

3

A Separation-Based Methodology to Consensus Tracking of Switched Multi-Agent Systems in the Power-Chained Form

This chapter investigates a reduced-complexity adaptive methodology to consensus tracking for a team of uncertain power-chained form systems with switched (possibly asynchronous) dynamics. The organization of this chapter is as follows. The introduction is given in Section 3.1. The problem formulation and preliminaries are provided in Section 3.2. Sections 3.3 and 3.4 present the proposed distributed consensus design and stability analysis, respectively. The simulation examples are in Section 3.5 and Section 3.6 draws the conclusion.

3.1. Introduction

As we have discussed in Chapters 1 and 2, power-chained form systems are intrinsically challenging as feedback linearization and backstepping methods successfully developed for strict- and pure-feedback systems fail to work. Even the adding-one-power-integrator methodology, well explored for the single-agent power-chained form system, presents some complexity issues and is unsuited for distributed control (cf. the discussion in Section 2.2.2). In place of the standard backstepping, the adding-one-power-integrator technique was successfully proposed in [56] to handle power-chained form dynamics. Progress made for the single power-chained form case include relaxing the growth condition on the nonlinear functions [55, 83, 95] and employing neural network or fuzzy logic approximators to handle completely unknown nonlinearities [89, 112, 135,

136]. However, it has to be emphasized that a direct extension of the standard adding-one-power-integrator technique in a distributed sense is not meaningful due to some complex aspects of the procedure. At least the following two complex aspects are worth mentioning: (a) the high-power terms are separated from the control gain functions via *separation lemmas* that make the power of the virtual control gains grow exponentially with the order of the system; (b) the control gain of each virtual control is incorporated into the next virtual control law iteratively, thus increasing the control complexity at each step. Such issues result in high-complexity and high-gain designs which might be prohibitive for multi-agent systems with low computational power and limited actuation. Therefore, the crucial open question motivating this research is: *how can reduced-complexity distributed methodologies be designed for uncertain multi-agent systems in power-chained form systems?*

The main contribution of this chapter is to answer this question for a large class of uncertain multi-agent systems in power-chained form systems, which can exhibit heterogeneous nonlinearities. At the core of the proposed methodology is a newly proposed definition for separable functions and a new separation-based lemma to deal with the high-power terms. The lemma decreases the aforementioned complex aspects of the state of the art in a twofold direction:

- It avoids incorporating the control gain of each virtual control in the next virtual control law, thus significantly reducing the complexity of the control action.
- It allows the power of the virtual and actual control laws to increase only proportionally (rather than exponentially) with the order of the systems, thus dramatically reducing any high-gain issue (cf. the discussions in Remark 3.3 and 3.4).

3.2. Problem Formulation and Preliminaries

Consider a team of N ($N \geq 2$) undertain multi-agent systems whose dynamics are given by

$$\begin{cases} \dot{\chi}_{i,k} = \phi_{i,k}^{\sigma_i(t)}(\overline{\chi}_{i,k}) + \psi_{i,k}^{\sigma_i(t)}(\overline{\chi}_{i,k})\chi_{i,k+1}^{p_{i,k}}, \\ \dot{\chi}_{i,n_i} = \phi_{i,n_i}^{\sigma_i(t)}(\overline{\chi}_{i,n_i}) + \psi_{i,n_i}^{\sigma_i(t)}(\overline{\chi}_{i,n_i})u_i^{p_{i,n_i}}, \\ y_i = \chi_{i,1}, \end{cases} \tag{3.1}$$

with $1 \leq i \leq N$, $1 \leq k \leq n_i - 1$, $\overline{\chi}_{i,k} = [\chi_{i,1}, \ldots, \chi_{i,k}]^T \in \mathbb{R}^k$. The subscript i stands for follower, in order to distinguish them from the leader agent, as clarified later. In (3.1), $\sigma_i(\cdot) : [0, +\infty) \to \mathscr{M}_i = \{1, 2, \ldots, m_i\}$ is the switching signal for the ith follower, with $\mathscr{M}_i$ denoting the switching mode set and m_i denoting the number of modes for the ith follower; $p_{i,k} \in Q_{\text{odd}}$ are the high powers (positive-odd integers), and $u_i^j \in \mathbb{R}$ is the control input for the jth mode of the ith follower. For each mode $\sigma_i(t)$, the functions $\phi_{i,k}^{\sigma_i(t)}(\cdot)$ and $\psi_{i,k}^{\sigma_i(t)}(\cdot)$ are unknown continuous functions. The following remarks highlight the difference between (3.1) and other multi-agent system models considered in literature.

Remark 3.1 The multi-agent models in [16, 21, 24, 26, 35, 50, 69, 87, 88, 110, 111, 114, 119, 130, 140] are strict-feedback low-order, i.e. special cases of (3.1) when all the powers $p_{i,k}$ are equal to one. Apart from this, (3.1) also possesses several levels of heterogeneity because: each follower agent exhibits its own switching $\sigma_i(\cdot)$, leading to possibly

asynchronous switching among the N followers; the unknown switched nonlinearities $\phi_{i,k}^{\sigma_i(t)}(\cdot)$ and $\psi_{i,k}^{\sigma_i(t)}(\cdot)$ are possibly different for each follower. While similar levels of heterogeneity are considered in the pure-feedback multi-agent models in [70, 113, 127, 128], those multi-agent systems models are also homologous to the strict-feedback low-order case, i.e. they can be equivalently transformed into the strict-feedback low-order form using the mean-value theorem.

Assumption 3.1 [135] For each follower agent i, we assume the sign of $\psi_{i,k}^{j}$ is positive and there exist known real positive constants $\overline{\psi}_{i,k}^{j}$ and $\underline{\psi}_{i,k}^{j}$, $(1 \le k \le n_i,\ j \in \mathscr{M}_i)$ such that $\underline{\psi}_{i,k}^{j} \le \psi_{i,k}^{j}(\cdot) \le \overline{\psi}_{i,k}^{j}$.

3.2.1. Technical Lemmas

The following definition, lemma, and proposition are introduced to the purpose of reduced-complexity control, as it will be remarked later (cf. Remarks 3.3 and 3.4).

Definition 3.1 For any $x_1 \in \mathbb{R}$, $x_2 \in \mathbb{R}$, the continuous function $F(\cdot)\colon \mathbb{R} \to \mathbb{R}$ is said to be a *separable function* provided that the following is satisfied:

$$F(x_1 + x_2) = \ell(x_1, x_2)F(x_1) + \upsilon(x_1, x_2)F(x_2), \tag{3.2}$$

where $\ell(x_1, x_2) \in \left[\underline{\ell}_1, \overline{\ell}_1\right]$ with $\underline{\ell}_1 = 1-d$ and $\overline{\ell}_1 = 1+d$, with d an arbitrary constant taking value in $(0,1)$, $|\upsilon(x_1, x_2)| \le \overline{\upsilon}(d)$ with $\overline{\upsilon}(d)$ denoting a positive continuous function that is independent of x_1 and x_2. Moreover, for a given d, the value of $\overline{\upsilon}(d)$ is independent of x_1 and x_2.

It is trivial to verify that $F(z) = z$ is a separable function since (3.2) trivially holds with $\ell(\cdot,\cdot) = \upsilon(\cdot,\cdot) = 1$. However, for more general functions, the joint presence of x_1 and x_2 in $\ell(\cdot,\cdot)$ and $\upsilon(\cdot,\cdot)$ makes it difficult to directly use Definition 3.1 to determine which function possess such property. In view of this, we further provide a proposition that can be used for the positive odd power function $F(z) = z^r$ (with r being a positive odd integer).

Proposition 3.1 For any $x_1 \in \mathbb{R}$, $x_2 \in \mathbb{R}$, the continuous function $F(\cdot)$ is a separable function if the following hold:
(i) $F(x_1 x_2) = F(x_1)F(x_2)$
(ii) For $p \in \mathbb{R}$ and any constant d taking value in $(0,1)$, a positive continuous function $\overline{\upsilon}(d)$ exists satisfying $|F(\overline{p}) - 1| \le \overline{\upsilon}(d)|F(p)| + d$, where $\overline{p} = p + 1$.

Proof. When $x_1 \neq 0$, without losing generality, we let $x_2 = px_1$, $p \in \mathbb{R}$. Thus, using (ii) yields

$$|F(x_1)(F(\overline{p}) - 1)| \le \overline{\upsilon}(d)|F(p)| \cdot |F(x_1)| + |F(x_1)|d, \tag{3.3}$$

where $\overline{p} = p + 1$. Applying (i) on both sides of (3.3) gives

$$|F(x_1 + x_2) - F(x_1)| \le M + |F(x_1)|d, \tag{3.4}$$

where $M = \overline{\upsilon}(d)|F(x_2)|$. At this point, two situations are considered:
Situation 1: when $F(x_1) < 0$, it follows from (3.4) that

$$\overline{d}F(x_1) - M \le F(x_1 + x_2) \le \underline{d}F(x_1) + M, \tag{3.5}$$

where $\overline{d} = d + 1$ and $\underline{d} = 1 - d$.
Situation 2: when $F(x_1) \geq 0$, one has

$$\underline{d}F(x_1) - M \leq F(x_1 + x_2) \leq \overline{d}F(x_1) + M. \tag{3.6}$$

When $x_1 = 0$, (3.2) becomes

$$F(x_2) = \ell(x_1, x_2)F(0) + v(x_1, x_2)F(x_2), \tag{3.7}$$

which we have to prove. Using (i) we get $F(0) = F(0)F(x_2)$ and (3.7) becomes $F(x_2) = \big[\ell(0, x_2)F(0) + v(0, x_2)\big]F(x_2)$ which holds by taking $\ell(0, x_2) \equiv 0$ and $v(0, x_2) \equiv 1$. This completes the proof. ■

Again, the linear function $F(z) = z$ is a separable function since (i), (ii) hold with $\overline{v}(d) = 1$ and any $0 < d < 1$. The following lemma states that any positive odd power function is a separable function.

Lemma 3.1 A function $F(z) = z^r$ with r being a positive odd integer is a separable function. In particular, if we let $z = x_1 + x_2$, then it holds that $(x_1 + x_2)^r = \ell(x_1, x_2)x_1^r + v(x_1, x_2)x_2^r$, where $\ell(x_1, x_2) \in \big[\underline{\ell}_1, \overline{\ell}_1\big]$ with $\underline{\ell}_1 = 1 - d$ and $\overline{\ell}_1 = 1 + d$, where $d = \sum_{k=1}^{r} \frac{r!}{k!(r-k)!} \frac{r-k}{r} l^{\frac{r}{r-k}}$ is an arbitrary constant taking value in $(0, 1)$ for some appropriately small constant l, $|v(x_1, x_2)| \leq \overline{v}(d) = \sum_{k=1}^{r} \frac{r!}{k!(r-k)!} \frac{k}{r} l^{-\frac{r}{k}}$ with $\overline{v}(d)$ being a positive constant.

Proof. We will verify that condition (ii) in Lemma 3.1 holds (condition (i) is trivially satisfied). Using the binomial theorem [1, Sect. 3.1, page. 10] leads to

$$\overline{p}^r = 1 + \frac{p \cdot r!}{(r-1)!} + \cdots + \frac{p^{r-1} \cdot r!}{(r-1)!} + p^r, \tag{3.8}$$

which further results in

$$|\overline{p}^r - 1| \leq \sum_{k=1}^{r} \frac{r!}{k!(r-k)!} |p|^k. \tag{3.9}$$

At this point, note that for any positive constant d taking value in $(0, 1)$, we select an appropriately small constant $l > 0$ satisfying $d = \sum_{k=1}^{r} \frac{r!}{k!(r-k)!} \frac{r-k}{r} l^{\frac{r}{r-k}}$. In the meantime, if we choose $\overline{v}(d) = \sum_{k=1}^{r} \frac{r!}{k!(r-k)!} \frac{k}{r} l^{-\frac{r}{k}}$, then, it follows from Lemma 3.1 that $d + \overline{v}(d)|p^r| = \sum_{k=1}^{r} \left[\frac{r!}{k!(r-k)!} \frac{k}{r} l^{-\frac{r}{k}} |p|^r + \frac{r!}{k!(r-k)!} \frac{r-k}{r} l^{\frac{r}{r-k}} \right] \geq \sum_{k=1}^{r} \frac{r!}{k!(r-k)!} \times |p|^k$, which combined with (3.9) gives $|\overline{p}^r - 1| \leq d + \overline{v}(d)|p^r|$. Therefore, $F(z) = z^r$ is a separable function according to Proposition 3.1. This completes the proof. ■

Finally, the proof of Proposition 3.1 reveals that if we let $z = x_1 + x_2$, then it holds that $(x_1 + x_2)^r = \ell(x_1, x_2)x_1^r + v(x_1, x_2)x_2^r$, where $\ell(x_1, x_2) \in \big[\underline{\ell}_1, \overline{\ell}_1\big]$ with $\underline{\ell}_1 = 1 - d$ and $\overline{\ell}_1 = 1 + d$, and $|v(x_1, x_2)| \leq \overline{v}(d)$.

Remark 3.2 We provide an intuitive explanation of the requirements for the nonlinear function $F(\cdot)$ from a geometric perspective.

A nonlinear function $F(\cdot)$ is a separable function when it satisfies

$$F(x_1 + x_2) = \ell(x_1, x_2)F(x_1) + v(x_1, x_2)F(x_2), \tag{3.10}$$

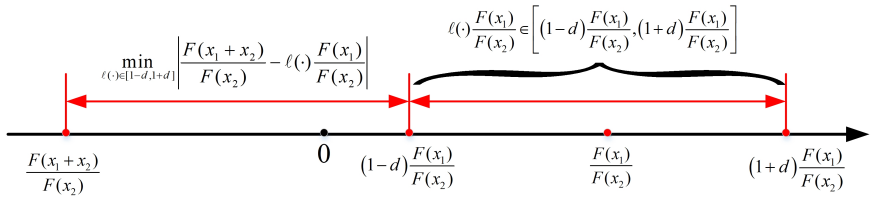

Figure 3.1: Distance between the point and interval

where $\ell(x_1,x_2)\in[\underline{\ell}_1,\overline{\ell}_1]$ with $\underline{\ell}_1=1-d$ and $\overline{\ell}_1=1+d$, with d an arbitrary constant taking value in $(0,1)$, $|v(x_1,x_2)|\le\overline{v}(d)$ with $\overline{v}(d)$ denoting a positive continuous function that is independent of x_1 and x_2. Namely, for a given d, $\overline{v}(d)$ is a positive constant.

By direct calculation, (3.10) is equivalent to

$$\left|\frac{F(x_1+x_2)}{F(x_2)}-\ell(\cdot)\frac{F(x_1)}{F(x_2)}\right|\le\overline{v}(d). \tag{3.11}$$

Since $\ell(\cdot)\in[1-d,1+d]$, the intuitive geometric meaning of (3.11) is that the distance between the point $\frac{F(x_1+x_2)}{F(x_2)}$ and the interval $\left[(1-d)\frac{F(x_1)}{F(x_2)},(1+d)\frac{F(x_1)}{F(x_2)}\right]$ is bounded by $\overline{v}(d)$ for any fixed constant $d\in(0,1)$, $\forall x_1,x_2\in\mathbb{R}$, as shown in the Fig. 3.1.

However, it is worth noticing that both the analytic expression (3.11) and the geometric description in Fig. 3.1 are hard to directly apply in practice due to the following two issues:

- There exist two arguments x_1 and x_2 simultaneously;
- The parameter $\ell(\cdot)$ is coupled with the arguments x_1 and x_2.

To address the first issue, a feasible solution is to impose an augmented condition on $F(\cdot)$ in the form of

$$F(x_1x_2)=F(x_1)F(x_2). \tag{3.12}$$

This gives the first condition $F(x_1x_2)=F(x_1)F(x_2)$. Based on $F(x_1x_2)=F(x_1)F(x_2)$, $F(0)=0$ and (3.10) is hence satisfied at $x_1=0$. When $x_1\neq0$, denote $x_2=px_1$, where $p\in\mathbb{R}$, the equation (3.11) is equivalent to

$$\left|F(p+1)-\ell(\cdot)\right|\le\overline{v}(d)|F(p)| \tag{3.13}$$

To address the second issue, an effective solution is transforming the distance between a point and an interval into the distance between two points. To be more specific and intuitive, we measure the distance between $F(p+1)$ and the middle point of the interval $[1-d,1+d]$, namely the point 1. To decouple $\ell(\cdot)$ and $F(p+1)$, we use the radius d of the interval to further build an equivalent representation of (3.12) (the intuitive meaning is parallel to that described in Fig. 3.1). That is,

$$\left|F(p+1)-1\right|\le d+\overline{v}(d)|F(p)| \tag{3.14}$$

which is exactly the second condition in Proposition 3.1.

3.2.2. Consensus Problem

Define the tracking error for the i-th follower as

$$s_{i,1} = \sum_{l\in\mathcal{N}_i} a_{il}(y_i - y_l) + \mu_i(y_i - y_r), \tag{3.15}$$

where $i = 1,\dots,N$. After defining $\boldsymbol{s}_1 = [s_{1,1},\dots,s_{N,1}]^T \in \mathbb{R}^N$, one has $\boldsymbol{s}_1 = (\overline{\mathscr{L}} + \mathscr{B})\boldsymbol{\delta}$ where $\boldsymbol{\delta} = \bar{\boldsymbol{y}} - \bar{\boldsymbol{y}}_r$ with $\bar{\boldsymbol{y}} = [y_1,\dots,y_N]^T$ and $\bar{\boldsymbol{y}}_r = [y_r,\dots,y_r]^T$. Due to the nonsingularity of $\overline{\mathscr{L}} + \mathscr{B}$, it holds that $\|\boldsymbol{\delta}\|_2 \le \frac{\|\boldsymbol{s}_1\|}{\underline{\sigma}_{\min}(\overline{\mathscr{L}}+\mathscr{B})}$ [132], with $\underline{\sigma}_{\min}$ the minimum singular value of $\overline{\mathscr{L}} + \mathscr{B}$.

3.3. Proposed Distributed Consensus Design

Let us define the following variables for the i-th follower:

$$s_{i,k} = \chi_{i,k} - \alpha_{i,k-1}, \quad k = 2,\dots,n_i, \tag{3.16}$$

and let us propose the following design:

$$\alpha_{i,1} = -s_{i,1}\underbrace{R_{i,1}^{\frac{1}{\overline{p}_{i,1}}}\left(c_{i,1} + \zeta_{i,1}^{\overline{p}_{i,1}}\widehat{\Xi}_{i,1}\Theta_{i,1}^{\overline{p}_{i,1}} + b_{i,1}^{\overline{p}_{i,1}}\right)^{\frac{1}{\overline{p}_{i,1}}}}_{\varsigma_{i,1}}, \tag{3.17}$$

$$R_{i,1} = \left[\underline{h}_{i,1}(d_i + \mu_i)(1-d)\right]^{-1}, \tag{3.18}$$

$$\alpha_{i,k} = -s_{i,k}\underbrace{R_{i,k}^{\frac{1}{\overline{p}_{i,k}}}\left(c_{i,k} + \zeta_{i,k}^{\overline{p}_{i,k}}\widehat{\Xi}_{i,k}\Theta_{i,k}^{\overline{p}_{i,k}} + b_{i,k}^{\overline{p}_{i,k}}\right)^{\frac{1}{\overline{p}_{i,k}}}}_{\varsigma_{i,k}}, \tag{3.19}$$

$$R_{i,k} = \left[\underline{h}_{i,k}(1-d)\right]^{-1}, \ (k = 2,\dots,n_i), \tag{3.20}$$

$$u_i \triangleq u_i^j = \alpha_{i,n_i}, \quad j \in \mathscr{M}_i, \tag{3.21}$$

where $p_i = \max\limits_{1\le k\le n_i}\{p_{i,k}\}$, $\overline{p}_{i,k} = \frac{p_i+1}{p_i - p_{i,k}+1}$, $\underline{p}_{i,k} = \frac{p_i+1}{p_{i,k}}$, $\underline{h}_{i,k} = \min\{\underline{h}_{i,k}^j, j\in\mathscr{M}_i\}$, $\zeta_{i,k} > 0$, $b_{i,k} > 0$ and $c_{i,k} > 0, (k = 1,\dots,n_i)$ are design constants.

Further, the parameters $\widehat{\Xi}_{i,k}$, $k = 1,...,n_i$, are adapted via the laws

$$\dot{\widehat{\Xi}}_{i,k} = \beta_{i,k}\zeta_{i,k}^{\overline{p}_{i,k}} s_{i,k}^{p_i+1}\Theta_{i,k}^{\overline{p}_{i,k}} - \beta_{i,k}\sigma_{i,k}\widehat{\Xi}_{i,k}, \tag{3.22}$$

where $\beta_{i,k} > 0$ denotes a tuning rate, $\sigma_{i,k} > 0$ stems from the leakage or σ-modification, well studied in robust adaptive control [39], and $\Theta_{i,k} > 0$ is a constant satisfying $\Theta_{i,k} \ge ||\boldsymbol{\varphi}_{i,k}||$ according to [89, Lemma 3] with $\boldsymbol{\varphi}_{i,k}$ being the activation functions coming from the use of RBF NN approximators [89, 135, 136]. The leakage or σ-modification is required to counteract the effect of disturbances or RBF NN approximation errors.

In the following, we describe the design steps leading to (3.17)-(3.22).

Step $i,1$ $(i = 1,\dots,N)$**:** The time derivative of $s_{i,1}$ along (3.1) and (3.16) is

$$\dot{s}_{i,1} = (d_i + \mu_i)\psi_{i,1}^j(\chi_{i,1})\chi_{i,2}^{p_{i,1}} + H_{i,1}^j, \tag{3.23}$$

where $H_{i,1}^{j}$ is a function defined as

$$H_{i,1}^{j} = (d_i + \mu_i)\phi_{i,1}^{j}(\chi_{i,1}) - \sum_{l\in\mathcal{N}_i} a_{il}\left(\phi_{l,1}^{j}(\chi_{l,1}) + \psi_{l,1}^{j}(\chi_{l,1})\chi_{l,2}^{p_{l,1}}\right) - \mu_i \dot{y}_{\mathrm{r}}(t). \tag{3.24}$$

From Assumptions 1.1 and 3.1, and along similar ideas to [40, 127, 135], one can conclude that there exist a continuous function $F_{i,1}(\cdot)$ and an RBF NN approximator $\widehat{F}_{i,1}(\cdot)$ such that, for any $j \in \mathcal{M}_i$,

$$\begin{aligned} s_{i,1}^{p_i-p_{i,1}+1} H_{i,1}^{j} &\le \left|s_{i,1}^{p_i-p_{i,1}+1}\right| F_{i,1}(\boldsymbol{Z}_{i,1}) + \epsilon_{i,1} \\ &= \left|s_{i,1}^{p_i-p_{i,1}+1}\right| \left[\widehat{F}_{i,1}\left(\boldsymbol{Z}_{i,1}\middle|\boldsymbol{W}_{i,1}^{*}\right) + \varepsilon_{i,1}(\boldsymbol{Z}_{i,1})\right] + \epsilon_{i,1} \\ &= \left|s_{i,1}^{p_i-p_{i,1}+1}\right| \left[\boldsymbol{W}_{i,1}^{*}\boldsymbol{\varphi}_{i,1}(\boldsymbol{Z}_{i,1}) + \varepsilon_{i,1}(\boldsymbol{Z}_{i,1})\right] + \epsilon_{i,1}, \end{aligned} \tag{3.25}$$

where $\boldsymbol{Z}_{i,1} = \left[x_{i,1}, x_{l,1,l\in\mathcal{N}_i}, x_{l,2,l\in\mathcal{N}_i}\right]^T$, $F_{i,1} = \max\left\{\left|H_{i,1}^{j}\right|, j \in \mathcal{M}_i\right\}$, $\epsilon_{i,1} > 0$ is a constant and $\varepsilon_{i,1}(\boldsymbol{Z}_{i,1})$ is the approximation error satisfying $\left|\varepsilon_{i,1}(\boldsymbol{Z}_{i,1})\right| \le \overline{\varepsilon}_{i,1}$ on a compact set $\Omega_{i,1}$, with $\boldsymbol{Z}_{i,1} \in \Omega_{i,1}$ and $\overline{\varepsilon}_{i,1} > 0$ being a constant. The weight $\boldsymbol{W}_{i,1}^{*}$ is the optimal weight vector such that $\boldsymbol{W}_{i,1}^{*} = \arg\min_{\widehat{\boldsymbol{W}}_{i,1}^{*}}\left\{\sup_{\Omega_{\boldsymbol{Z}_{i,1}}}\left|\widehat{F}_{i,1}\left(\boldsymbol{Z}_{i,1}\middle|\widehat{\boldsymbol{W}}_{i,1}^{*}\right) - F_{i,1}(\boldsymbol{Z}_{i,1})\right|\right\}$, with $\widehat{\boldsymbol{W}}_{i,1}^{*}$ being an estimate of $\boldsymbol{W}_{i,1}^{*}$. For subsequent analysis, let us define $\Xi_{i,1} = \left\|\boldsymbol{W}_{i,1}^{*}\right\|^{\overline{p}_{i,1}}$.

Consider the common Lyapunov function candidate

$$V_{i,1} = \frac{s_{i,1}^{p_i-p_{i,1}+2}}{p_i - p_{i,1} + 2} + \frac{1}{2\beta_{i,1}}\widetilde{\Xi}_{i,1}^{2}, \tag{3.26}$$

where $\widetilde{\Xi}_{i,1} = \Xi_{i,1} - \widehat{\Xi}_{i,1}$. Using Lemma 2.2 yields

$$\begin{aligned} &\left|s_{i,1}^{p_i-p_{i,1}+1}\right| F_{i,1} \le \left|s_{i,1}^{p_i-p_{i,1}+1}\right| \left(\left\|\boldsymbol{W}_{i,1}^{*}\right\| \left\|\boldsymbol{\varphi}_{i,1}\right\| + \overline{\varepsilon}_{i,1}\right) \\ &\le \frac{1}{\underline{p}_{i,1}}\zeta_{i,1}^{-\underline{p}_{i,1}} + \frac{1}{\overline{p}_{i,1}}\zeta_{i,1}^{\overline{p}_{i,1}} s_{i,1}^{p_i+1}\left(\left\|\boldsymbol{W}_{i,1}^{*}\right\| \left\|\boldsymbol{\varphi}_{i,1}\right\|\right)^{\overline{p}_{i,1}} \\ &\quad + \frac{1}{\overline{p}_{i,1}} b_{i,1}^{\overline{p}_{i,1}} s_{i,1}^{p_i+1} + \frac{1}{\underline{p}_{i,1}} b_{i,1}^{-\underline{p}_{i,1}} \overline{\varepsilon}_{i,1}^{\underline{p}_{i,1}} \\ &\le s_{i,1}^{p_i+1}\left(b_{i,1}^{\overline{p}_{i,1}} + \zeta_{i,1}^{\overline{p}_{i,1}} \Xi_{i,1} \Theta_{i,1}^{\overline{p}_{i,1}}\right) + \kappa_{i,1}, \end{aligned} \tag{3.27}$$

where the last inequality used the fact that $\frac{1}{\underline{p}_{i,1}} \le 1$ and $\|\boldsymbol{\varphi}_{i,1}\| \le \Theta_{i,1}$, $\kappa_{i,1} = \zeta_{i,1}^{-\underline{p}_{i,1}} + b_{i,1}^{-\underline{p}_{i,1}} \overline{\varepsilon}_{i,1}^{\underline{p}_{i,1}}$ with $\zeta_{i,1} > 0$ and $b_{i,1} > 0$ being design constants.

In light of (3.23), (3.24), and (3.26), the derivative of $V_{i,1}$ satisfies

$$\begin{aligned} \dot{V}_{i,1} \le &(d_i + \mu_i) s_{i,1}^{p_i-p_{i,1}+1} \psi_{i,1} \chi_{i,2}^{p_{i,1}} - \frac{\widetilde{\Xi}_{i,1}\dot{\widehat{\Xi}}_{i,1}}{\beta_{i,1}} \\ &+ s_{i,1}^{p_i+1}\left(b_{i,1}^{\overline{p}_{i,1}} + \zeta_{i,1}^{\overline{p}_{i,1}} \Xi_{i,1} \Theta_{i,1}^{\overline{p}_{i,1}}\right) + \hbar_{i,1}, \end{aligned} \tag{3.28}$$

where $\hbar_{i,1} = \kappa_{i,1} + \epsilon_{i,1}$. We are now in the position to handle the term $\chi_{i,2}^{p_{i,1}}$ in (3.28) through the proposed Lemma 3.1 as

$$\begin{aligned} s_{i,1}^{p_i-p_{i,1}+1}\chi_{i,2}^{p_{i,1}} &= s_{i,1}^{p_i-p_{i,1}+1}\left(s_{i,2}+\alpha_{i,1}\right)^{p_{i,1}} \\ &\leq \overline{v}_{i,1}\left|s_{i,1}^{p_i-p_{i,1}+1}s_{i,2}^{p_{i,1}}\right| + s_{i,1}^{p_i-p_{i,1}+1}\ell_{i,1}\alpha_{i,1}^{p_{i,1}}. \end{aligned} \tag{3.29}$$

Then, (3.28) can be rewritten as

$$\begin{aligned} \dot{V}_{i,1} \leq & (d_i+\mu_i)\overline{h}_{i,1}^{j}\overline{v}_{i,1}\left|s_{i,1}^{p_i-p_{i,1}+1}s_{i,2}^{p_{i,1}}\right| + (d_i+\mu_i) \\ & \times\left(h_{i,1}^{j}\ell_{i,1}s_{i,1}^{p_i-p_{i,1}+1}\alpha_{i,1}^{p_{i,1}}\right) - \frac{1}{\beta_{i,1}}\widetilde{\Xi}_{i,1}\dot{\widehat{\Xi}}_{i,1} \\ & + s_{i,1}^{p_i+1}\left(b_{i,1}^{\overline{p}_{i,1}} + \zeta_{i,1}^{\overline{p}_{i,1}}\Xi_{i,1}\Theta_{i,1}^{\overline{p}_{i,1}}\right) + \hbar_{i,1}. \end{aligned} \tag{3.30}$$

Substituting the virtual controller $\alpha_{i,1}$ (3.17) and the adaptation law $\dot{\widehat{\Xi}}_{i,1}$ (3.22) into (3.30), and using the fact that

$$\begin{aligned} &\overline{h}_{i,1}^{j}\overline{v}_{i,1}\left|s_{i,1}^{p_i-p_{i,1}+1}s_{i,2}^{p_{i,1}}\right| \leq \overline{\tau}_{i,1}\left(\frac{1}{\overline{p}_{i,1}}\rho_{i,1}^{\overline{p}_{i,1}}s_{i,1}^{p_i+1} + \frac{1}{\underline{p}_{i,1}}\varrho_{i,1}^{-\underline{p}_{i,1}}s_{i,2}^{p_i+1}\right) \\ &< \overline{\tau}_{i,1}\left(\rho_{i,1}^{\overline{p}_{i,1}}s_{i,1}^{p_i+1} + \varrho_{i,1}^{-\underline{p}_{i,1}}s_{i,2}^{p_i+1}\right), \end{aligned} \tag{3.31}$$

we can rewrite (3.30) as

$$\begin{aligned} \dot{V}_{i,1} \leq & -c_{i,1}s_{i,1}^{p_i+1} + (d_i+\mu_i)\overline{\tau}_{i,1}\rho_{i,1}^{\overline{p}_{i,1}}s_{i,1}^{p_i+1} + \hbar_{i,1} \\ & + (d_i+\mu_i)\overline{\tau}_{i,1}\varrho_{i,1}^{-\underline{p}_{i,1}}s_{i,2}^{p_i+1} + \frac{1}{2}\sigma_{i,1}\widetilde{\Xi}_{i,1}\widehat{\Xi}_{i,1} \\ \leq & -(c_{i,1}-\theta_{i,1})s_{i,1}^{p_i+1} + \vartheta_{i,1}s_{i,2}^{p_i+1} + \hbar_{i,1} \\ & + \frac{1}{2}\sigma_{i,1}\Xi_{i,1}^{2} - \frac{1}{2}\sigma_{i,1}\widetilde{\Xi}_{i,1}^{2}, \end{aligned} \tag{3.32}$$

where $\overline{\tau}_{i,1} = \overline{h}_{i,1}^{j}\overline{v}_{i,1}$, $\theta_{i,1} = (d_i+\mu_i)\overline{\tau}_{i,1}\rho_{i,1}^{\overline{p}_{i,1}}$ and $\vartheta_{i,1} = (d_i+\mu_i)\overline{\tau}_{i,1}\varrho_{i,1}^{-\underline{p}_{i,1}}$ with $\rho_{i,1} > 0$ and $\varrho_{i,1} > 0$ being design constants.

Step $i,2$ $(i = 1,\ldots,N)$ **:** Taking the derivative of $s_{i,2}$ yields

$$\dot{s}_{i,2} = \psi_{i,2}^{j}(\overline{\boldsymbol{\chi}}_{i,2})\chi_{i,3}^{p_{i,2}} + H_{i,2}^{j}, \tag{3.33}$$

where $H_{i,2}^{j}$ is a function defined as

$$\begin{aligned} H_{i,2}^{j} = & \phi_{i,2}^{j}(\overline{\boldsymbol{\chi}}_{i,2}) - \frac{\partial\alpha_{i,1}}{\partial\chi_{i,1}}\left(\phi_{i,1}^{j}(\chi_{i,1}) + \psi_{i,1}^{j}\chi_{i,2}^{p_{i,1}}\right) \\ & - \sum\nolimits_{l\in\mathcal{N}_i} a_{il}\frac{\partial\alpha_{i,1}}{\partial\chi_{l,1}}\left(\phi_{l,1}^{j}(\chi_{l,1}) + \psi_{l,1}^{j}\chi_{l,2}^{p_{l,1}}\right) \\ & - \frac{\partial\alpha_{i,1}}{\partial y_r}\dot{y}_r - \frac{\partial\alpha_{i,1}}{\partial\widehat{\Xi}_{i,1}}\dot{\widehat{\Xi}}_{i,1}, \end{aligned} \tag{3.34}$$

Proceeding similarly to Step $i,1$, there exist a continuous function $F_{i,2}(\cdot)$ and an RBF NN approximator $\widehat{F}_{i,2}(\cdot)$ such that, for any $j \in \mathscr{M}_i$,

$$\begin{aligned} s_{i,2}^{p_i-p_{i,2}+1} H_{i,2}^j &\le \left|s_{i,2}^{p_i-p_{i,2}+1}\right| F_{i,2}(\boldsymbol{Z}_{i,2}) + \epsilon_{i,2} \\ &= \left|s_{i,2}^{p_i-p_{i,2}+1}\right| \left[\widehat{F}_{i,2}\left(\boldsymbol{Z}_{i,2}\middle|\boldsymbol{W}_{i,2}^*\right) + \varepsilon_{i,2}(\boldsymbol{Z}_{i,2})\right] + \epsilon_{i,2} \\ &= \left|s_{i,2}^{p_i-p_{i,2}+1}\right| \left[\boldsymbol{W}_{i,2}^* \boldsymbol{\varphi}_{i,2}(\boldsymbol{Z}_{i,2}) + \varepsilon_{i,2}(\boldsymbol{Z}_{i,2})\right] + \epsilon_{i,2}, \end{aligned} \tag{3.35}$$

where $\boldsymbol{Z}_{i,2} = \left[\overline{\boldsymbol{\chi}}_{i,2}, \overline{\boldsymbol{\chi}}_{l,2,l\in\mathscr{N}_i}, \frac{\partial \alpha_{i,1}}{\partial \chi_{l,1}}, \frac{\partial \alpha_{i,1}}{\partial \chi_{i,1}}, \frac{\partial \alpha_{i,1}}{\partial y_r}, \frac{\partial \alpha_{i,1}}{\partial \widehat{\Xi}_{i,1}}, \widehat{\Xi}_{i,1}, y_r\right]^T$, $F_{i,2} = \max\left\{\left|H_{i,2}^j\right|,\ j \in \mathscr{M}_i\right\}$, $\epsilon_{i,2} > 0$ is a constant and $\left|\varepsilon_{i,2}(\boldsymbol{Z}_{i,2})\right| \le \overline{\varepsilon}_{i,2}$ with $\overline{\varepsilon}_{i,2} > 0$ being a constant. The optimal weight $\boldsymbol{W}_{i,2}^*$ and its estimate $\widehat{\boldsymbol{W}}_{i,2}^*$ are defined in a similar way as the previous step. Then, let us define $\Xi_{i,2} = \left\|\boldsymbol{W}_{i,2}^*\right\|^{\overline{p}_{i,2}}$.

Consider the common Lyapunov function candidate

$$V_{i,2} = V_{i,1} + \frac{s_{i,2}^{p_i-p_{i,2}+2}}{p_i - p_{i,2} + 2} + \frac{1}{2\beta_{i,2}} \widetilde{\Xi}_{i,2}^2, \tag{3.36}$$

where $\widetilde{\Xi}_{i,2} = \Xi_{i,2} - \widehat{\Xi}_{i,2}$. Along similar lines as (3.25), we obtain the following inequality:

$$\left|s_{i,2}^{p_i-p_{i,2}+1}\right| F_{i,2} \le s_{i,2}^{p_i+1}\left(b_{i,2}^{\overline{p}_{i,2}} + \zeta_{i,2}^{\overline{p}_{i,2}} \Xi_{i,2} \Theta_{i,2}^{\overline{p}_{i,2}}\right) + \kappa_{i,2}, \tag{3.37}$$

where $\Theta_{i,2} \ge ||\boldsymbol{\varphi}_{i,2}|| > 0$ is a constant, $\kappa_{i,2} = \zeta_{i,2}^{-p_{i,2}} + b_{i,2}^{-p_{i,2}} \overline{\varepsilon}_{i,2}^{p_{i,2}}$ with $\zeta_{i,2} > 0$ and $b_{i,2} > 0$ being design constants. Hence, the derivative of $V_{i,2}$ along (3.36) and (3.37) is

$$\begin{aligned} \dot{V}_{i,2} \le & -\left(c_{i,1} - \theta_{i,1}\right) s_{i,1}^{p_i+1} + \psi_{i,2}^j(\overline{\chi}_{i,2}) s_{i,2}^{p_i-p_{i,2}+1} \chi_{i,3}^{p_{i,2}} \\ & - \frac{1}{\beta_{i,2}} \widetilde{\Xi}_{i,2} \dot{\widehat{\Xi}}_{i,2} + s_{i,2}^{p_i+1}\left(b_{i,2}^{\overline{p}_{i,2}} + \zeta_{i,2}^{\overline{p}_{i,2}} \Xi_{i,2} \Theta_{i,2}^{\overline{p}_{i,2}}\right) \\ & + \frac{\sigma_{i,1}}{2}\left(\Xi_{i,1}^2 - \widetilde{\Xi}_{i,1}^2\right) + \vartheta_{i,1} s_{i,2}^{p_i+1} + \hbar_{i,1} + \hbar_{i,2}, \end{aligned} \tag{3.38}$$

where $\hbar_{i,2} = \kappa_{i,2} + \epsilon_{i,2}$. Similarly to (3.29), the use of the proposed Lemma 3.1 gives

$$\begin{aligned} & s_{i,2}^{p_i-p_{i,2}+1} \chi_{i,3}^{p_{i,2}} = s_{i,2}^{p_i-p_{i,2}+1}\left(s_{i,3} + \alpha_{i,2}\right)^{p_{i,2}} \\ & \le \overline{v}_{f,2}\left|s_{i,2}^{p_i-p_{i,2}+1} s_{i,3}^{p_{i,2}}\right| + s_{i,2}^{p_i-p_{i,2}+1} \ell_{i,2} \alpha_{i,2}^{p_{i,2}}. \end{aligned} \tag{3.39}$$

Remark 3.3 In order to highlight the distinguishing feature of the proposed design, let us recall the standard designs in [55, 83, 89, 112, 135, 136]. There, instead of (3.39), $\chi_{i,3}^{p_{i,2}}$ is tackled by subtracting and adding $\alpha_{i,2}^{p_{i,2}}$, namely,

$$s_{i,2}^{p_i-p_{i,2}+1} \chi_{i,3}^{p_{i,2}} = s_{i,2}^{p_i-p_{i,2}+1}\left[\left(\chi_{i,3}^{p_{i,2}} - \alpha_{i,2}^{p_{i,2}}\right) + \alpha_{i,2}^{p_{i,2}}\right].$$

Then, the use of Lemmas 2.2 and 2.3 yields

$$\begin{aligned} & s_{i,2}^{p_i-p_{i,2}+1}\left(\chi_{i,3}^{p_{i,2}}-\alpha_{i,2}^{p_{i,2}}\right) \\ & \leq p_{i,2}\left|s_{i,2}^{p_i-p_{i,2}+1}\right|\left|s_{i,3}\right|\Big[2^{p_{i,2}-2}\left(s_{i,3}^{p_{i,2}-1}+\alpha_{i,2}^{p_{i,2}-1}\right) \\ & \quad +\left(s_{i,2}\varsigma_{i,2}\right)^{p_{i,2}-1}\Big] \leq s_{i,2}^{p_i+1}+\overline{\varsigma}_{i,2}s_{i,3}^{p_i+1}, \end{aligned} \tag{3.40}$$

where $\overline{\varsigma}_{i,2}=\left(2^{p_{i,2}-2}p_{i,2}\right)^{\frac{p}{p_{i,2}}}+\left(2^{p_{i,2}-2}p_{i,2}\varsigma_{i,2}^{p_{i,2}-1}\right)^{p_i+1}$. However, for the methods in [55, 83, 89, 112, 135, 136] to work, $\overline{\varsigma}_{i,2}$ is incorporated into the virtual control law $\alpha_{i,3}$ to eliminate the extra term $\overline{\varsigma}_{i,2}s_{i,3}^{p_i+1}$ (e.g. [136, eq.(5)], [89, eq.(12)], [135, eq.(4)], [83, the equation after (3.11)]), [112, eq. (23)]: this inevitably increases the complexity of the controller structure. It is also worth remarking that the power of the control gain $\overline{\varsigma}_{i,k}$ in (3.40) grows dramatically (exponentially) as the order of the subsystems grows, leading to possibly high control gains. This is in contrast with the power of the control gain in (3.39) which is proportional to the power of the subsystems.

Remark 3.4 The benefits brought by the proposed Lemma 3.1 can be summarized as: (i) in the first line of (3.39), the virtual control $\alpha_{i,2}$ can be extracted from $\left(s_{i,3}+\alpha_{i,2}\right)^{p_{i,2}-1}$ directly without involving any inequalities scaling as in ([136, eq.(17)], [89, eq.(29)], [135, eq.(20)], [83, eq.(3.8)]), [112, eq. (20)] implying that the term $\overline{\varsigma}_{i,2}$ will not appear; (ii) the term $\upsilon_{i,2}$ in (3.39) is eventually upper bounded by a constant $\overline{\upsilon}_{i,2}$, which is independent of $s_{i,3}$ and $\alpha_{i,2}$ and can be easily handled as shown hereafter.

At this point, similarly to (3.31), we can bound one of the terms in (3.39) as

$$\begin{aligned} & \overline{\psi}_{i,2}^{j}\overline{\upsilon}_{i,2}\left|s_{i,2}^{p_i-p_{i,2}+1}\right|\left|s_{i,3}^{p_{i,2}}\right| = \overline{\tau}_{i,2}\left|s_{i,2}^{p_i-p_{i,2}+1}\right|\left|s_{i,3}^{p_{i,2}}\right| \\ & \leq \overline{\tau}_{i,2}\left(\rho_{i,2}^{\overline{p}_{i,2}}s_{i,2}^{p_i+1}+\varrho_{i,2}^{-\underline{p}_{i,2}}s_{i,3}^{p_i+1}\right), \end{aligned} \tag{3.41}$$

where $\overline{\tau}_{i,2}=\overline{h}_{i,2}^{j}\overline{\upsilon}_{i,2}$, $\rho_{i,2}>0$ and $\varrho_{i,2}>0$ are design constants.

Substituting the virtual controller $\alpha_{i,2}$ in (3.19) and the adaptation law $\dot{\hat{\Xi}}_{i,2}$ in (3.22) into the Lyapunov derivative (3.38) results in

$$\begin{aligned} \dot{V}_{i,2} \leq & -\left(c_{i,1}-\theta_{i,1}\right)s_{i,1}^{p_i+1}-\left(c_{i,2}-\vartheta_{i,1}-\theta_{i,2}\right)s_{i,2}^{p_i+1} \\ & +\vartheta_{i,2}s_{i,3}^{p_i+1}+\sum_{k=1}^{2}\left(\frac{\sigma_{i,k}}{2}\Xi_{i,k}^{2}-\frac{\sigma_{i,k}}{2}\widetilde{\Xi}_{i,k}^{2}+\hbar_{i,k}\right), \end{aligned}$$

where $\theta_{i,2}=\overline{\tau}_{i,2}\rho_{i,2}^{\overline{p}_{i,2}}$ and $\vartheta_{i,2}=\overline{\tau}_{i,2}\varrho_{i,2}^{-\underline{p}_{i,2}}$.

Step i,k $(i=1,\ldots,N,\ k=3,\ldots,n_i-1)$ **:** It follows from (3.1) and (3.15) that the derivative of $s_{i,k}$ is

$$\dot{s}_{i,k}=\psi_{i,k}^{j}(\overline{\boldsymbol{\chi}}_{i,k})\chi_{i,k+1}^{p_{i,k}}+H_{i,k}^{j}, \tag{3.42}$$

where $H_{i,k}^{j}$ is a function defined as

$$\begin{aligned} H_{i,k}^{j} =& \phi_{i,k}^{j}(\overline{\boldsymbol{\chi}}_{i,k}) - \sum_{l\in\mathscr{N}_i} \frac{\partial \alpha_{i,k-1}}{\partial \chi_{l,1}} \left(\phi_{l,1}^{j}(\chi_{l,1}) + \psi_{l,1}^{j} \chi_{l,2}^{p_{l,1}}\right) \\ & - \sum_{q=1}^{k-1} \frac{\partial \alpha_{i,k-1}}{\partial \chi_{i,q}} \left(\phi_{i,q}^{j}(\overline{\boldsymbol{\chi}}_{i,q}) + \psi_{i,q}^{j} \chi_{i,q+1}^{p_{i,q}}\right) \\ & - \sum_{q=1}^{k-1} \frac{\partial \alpha_{i,k-1}}{\partial \widehat{\Xi}_{i,q}} \dot{\widehat{\Xi}}_{i,q} - \frac{\partial \alpha_{i,k-1}}{\partial y_{\mathrm{r}}} \dot{y}_{\mathrm{r}}. \end{aligned} \tag{3.43}$$

Likewise, there exist a continuous function $F_{i,k}(\cdot)$ and an RBF NN approximator $\widehat{F}_{i,k}(\cdot)$ such that, for any $j \in \mathscr{M}_i$,

$$\begin{aligned} & s_{i,k}^{p_i - p_{i,k}+1} H_{i,k}^{j} \le \left| s_{i,k}^{p_i - p_{i,k}+1} \right| F_{i,k}(\boldsymbol{Z}_{i,k}) + \epsilon_{i,k} \\ &= \left| s_{i,k}^{p_i - p_{i,k}+1} \right| \left[\widehat{F}_{i,k}\left(\boldsymbol{Z}_{i,k} \middle| \boldsymbol{W}_{i,k}^{*}\right) + \varepsilon_{i,k}(\boldsymbol{Z}_{i,k}) \right] + \epsilon_{i,k} \\ &= \left| s_{i,k}^{p_i - p_{i,k}+1} \right| \left[\boldsymbol{W}_{i,k}^{*} \boldsymbol{\varphi}_{i,k}(\boldsymbol{Z}_{i,k}) + \varepsilon_{i,k}(\boldsymbol{Z}_{i,k}) \right] + \epsilon_{i,k}, \end{aligned} \tag{3.44}$$

where $\boldsymbol{Z}_{i,k} = \left[\overline{\boldsymbol{\chi}}_{i,k}, \overline{\boldsymbol{\chi}}_{l,2,l\in\mathscr{N}_i}, \frac{\partial \alpha_{i,k-1}}{\partial \chi_{l,1}}, \frac{\partial \alpha_{i,k-1}}{\partial \chi_{i,1}}, \ldots, \frac{\partial \alpha_{i,k-1}}{\partial \chi_{i,k-1}}, \frac{\partial \alpha_{i,k-1}}{\partial \widehat{\Xi}_{i,1}}, \ldots, \frac{\partial \alpha_{i,k-1}}{\partial \widehat{\Xi}_{i,k-1}}, \widehat{\Xi}_{i,1}, \ldots, \widehat{\Xi}_{i,k-1}, \frac{\partial \alpha_{i,k-1}}{\partial y_r}, y_r\right]^{T}$, $F_{i,k} = \max\left\{ \left| H_{i,k}^{j} \right|, j \in \mathscr{M}_i \right\}$, $\epsilon_{i,k} > 0$ is a constant and $\left|\varepsilon_{i,k}(\boldsymbol{Z}_{i,k})\right| \le \overline{\varepsilon}_{i,k}$ with $\overline{\varepsilon}_{i,k} > 0$ being a constant. The optimal weight $\boldsymbol{W}_{i,k}^{*}$ and its estimate $\widehat{\boldsymbol{W}}_{i,k}^{*}$ are defined in a similar way as the previous steps. Let us further define $\Xi_{i,k} = \left\| \boldsymbol{W}_{i,k}^{*} \right\|^{\overline{p}_{i,k}}$.

Consider the common Lyapunov function candidate

$$V_{i,k} = V_{i,k-1} + \frac{s_{i,k}^{p_i - p_{i,k}+2}}{p_i - p_{i,k} + 2} + \frac{1}{2\beta_{i,k}} \widetilde{\Xi}_{i,k}^{2}, \tag{3.45}$$

where $\widetilde{\Xi}_{i,k} = \Xi_{i,k} - \widehat{\Xi}_{i,k}$. Following similar lines as Step $i,1$ and Step $i,2$, it is possible to obtain the derivative of $V_{i,k}$ as

$$\begin{aligned} \dot{V}_{i,k} \le & - \sum_{m=1}^{k} \left(c_{i,m} - \theta_{i,m} - \vartheta_{i,m-1}\right) s_{i,m}^{p_i+1} + \vartheta_{i,k} s_{i,k+1}^{p_i+1} \\ & + \sum_{m=1}^{k} \left(\frac{\sigma_{i,m}}{2} \Xi_{i,m}^{2} - \frac{\sigma_{i,m}}{2} \widetilde{\Xi}_{i,m}^{2} + \hbar_{i,m} \right), \end{aligned} \tag{3.46}$$

where $\vartheta_{i,0} = 0$, $\theta_{i,1} = (d_i + \mu_i)\overline{\tau}_{i,1} \rho_{i,1}^{\overline{p}_{i,1}}$, $\vartheta_{i,1} = (d_i + \mu_i)\overline{\tau}_{i,1} \varrho_{i,1}^{-\underline{p}_{i,1}}$, $\theta_{i,m} = \overline{\tau}_{i,m} \rho_{i,m}^{\overline{p}_{i,m}}$ and $\vartheta_{i,m} = \overline{\tau}_{i,m} \varrho_{i,m}^{-\underline{p}_{i,m}} (m = 2, \ldots, k)$, $\overline{\tau}_{i,m} = \overline{h}_{i,m}^{j} \overline{v}_{i,m}$ with $\overline{v}_{i,m}$ being the upper bound of $v_{i,m}$ $(s_{i,m+1}, \alpha_{i,m})$, $\hbar_{i,m} = \kappa_{i,m} + \epsilon_{i,m}$, $\kappa_{i,m} = \zeta_{i,m}^{-\underline{p}_{i,m}} + b_{i,m}^{-\underline{p}_{i,m}} \overline{\varepsilon}_{i,m}^{\underline{p}_{i,m}}$, $\zeta_{i,m} > 0$, $b_{i,m} > 0$, $c_{i,m} > 0$, $\rho_{i,m} > 0$ and $\varrho_{i,m} > 0$ are design parameters.

Step i, n_i $(i = 1, \ldots, N)$**:** For the final step, the derivative of s_{i,n_i} along (3.1) and (3.16) is

$$\dot{s}_{i,n_i} = \psi_{i,n_i}^{j}(\overline{\boldsymbol{\chi}}_{i,n_i}) u_i^{p_{i,n_i}} + H_{i,n_i}^{j}, \tag{3.47}$$

where H_{i,n_i}^j is a function defined as

$$\begin{aligned} H_{i,n_i}^j =& \phi_{i,n_i}^j(\overline{\boldsymbol{\chi}}_{i,n_i}) - \sum_{l\in\mathcal{N}_f} \frac{\partial \alpha_{i,n_i-1}}{\partial \chi_{l,1}} \left(\phi_{l,1}^j(\chi_{l,1}) + \psi_{l,1}^j \chi_{l,2}^{p_{l,1}}\right) \\ & - \sum_{q=1}^{n_i-1} \frac{\partial \alpha_{i,n_i-1}}{\partial \chi_{i,q}} \left(\phi_{i,q}^j(\overline{\boldsymbol{\chi}}_{i,q}) + \psi_{i,q}^j \chi_{i,q+1}^{p_{i,q}}\right) \\ & - \sum_{q=1}^{n_i-1} \frac{\partial \alpha_{i,n_i-1}}{\partial \widehat{\Xi}_{i,q}} \dot{\widehat{\Xi}}_{i,q} - \frac{\partial \alpha_{i,n_i-1}}{\partial y_r} \dot{y}_r. \end{aligned} \tag{3.48}$$

Similarly to steps (3.25), (3.35) and (3.44), there exist a continuous function $F_{i,n_i}(\cdot)$ and an RBF NN approximator $\widehat{F}_{i,n_i}(\cdot)$ such that, for any $j \in \mathcal{M}_i$,

$$\begin{aligned} & s_{i,n_i}^{p_i-p_{i,n_i}+1} H_{i,n_i}^j \le \left| s_{i,n_i}^{p_i-p_{i,n_i}+1} \right| F_{i,n_i}(\boldsymbol{Z}_{i,n_i}) + \epsilon_{i,n_i} \\ & = \left| s_{i,n_i}^{p_i-p_{i,n_i}+1} \right| \left[\widehat{F}_{i,n_i}(\boldsymbol{Z}_{i,n_i} | \boldsymbol{W}_{i,n_i}^*) + \varepsilon_{i,n_i}(\boldsymbol{Z}_{i,n_i}) \right] + \epsilon_{i,n_i} \\ & = \left| s_{i,n_i}^{p_i-p_{i,n_i}+1} \right| \left[\boldsymbol{W}_{i,n_i}^* \boldsymbol{\varphi}_{i,n_i}(\boldsymbol{Z}_{i,n_i}) + \varepsilon_{i,n_i}(\boldsymbol{Z}_{i,n_i}) \right] + \epsilon_{i,n_i}, \end{aligned} \tag{3.49}$$

where $\boldsymbol{Z}_{i,n_i} = \left[\overline{\boldsymbol{\chi}}_{i,n_i}, \overline{\boldsymbol{\chi}}_{l,2,l\in\mathcal{N}_i}, \frac{\partial \alpha_{i,n_i-1}}{\partial \chi_{l,1}}, \frac{\partial \alpha_{i,n_i-1}}{\partial \chi_{i,1}}, \ldots, \frac{\partial \alpha_{i,n_i-1}}{\partial \chi_{i,n_i-1}}, \frac{\partial \alpha_{i,n_i-1}}{\partial \widehat{\Xi}_{i,1}}, \ldots, \frac{\partial \alpha_{i,n_i-1}}{\partial \widehat{\Xi}_{i,n_i-1}}, \widehat{\Xi}_{i,1}, \ldots, y_r, \right.$
$\left. \widehat{\Xi}_{i,n_i-1}, \frac{\partial \alpha_{i,n_i-1}}{\partial y_r} \right]^T$, $F_{i,n_i} = \max\left\{ \left| H_{i,n_i}^j \right|,\ j \in \mathcal{M}_i \right\}$, $\epsilon_{i,n_i} > 0$ is a constant and $\left| \varepsilon_{i,n_i}(\boldsymbol{Z}_{i,n_i}) \right| \le \overline{\varepsilon}_{i,n_i}$ with $\overline{\varepsilon}_{i,n_i} > 0$ being a constant. The optimal weight $\boldsymbol{W}_{i,n_i}^*$ and its estimate $\widehat{\boldsymbol{W}}_{i,n_i}^*$ are defined in a similar way as the previous steps. Let us further define $\Xi_{i,n_i} = \left\| \boldsymbol{W}_{i,n_i}^* \right\|^{\overline{p}_{i,n_i}}$.

Consider the common Lyapunov function candidate

$$V_{i,n_i} = V_{i,n_i-1} + \frac{s_{i,n_i}^{p_i-p_{i,n_i}+2}}{p_i - p_{i,n_i} + 2} + \frac{1}{2\beta_{i,n_i}} \widetilde{\Xi}_{i,n_i}^2, \tag{3.50}$$

where $\widetilde{\Xi}_{i,n_i} = \Xi_{i,n_i} - \widehat{\Xi}_{i,n_i}$.

Choosing the common actual controller $u_i \triangleq u_i^j$ for the ith follower as (3.21), one immediately gets from (3.46) that

$$\begin{aligned} \dot{V}_{i,n_i} \le & -\sum_{k=1}^{n_i} (c_{i,k} - \theta_{i,k} - \vartheta_{i,k-1}) \gamma_i^{\frac{p_{i,k}-1}{p_i+1}} s_{i,k}^{p_i-p_{i,k}+2} \\ & + \sum_{k=1}^{n_i} \left(\frac{1}{2}\sigma_{i,k}\Xi_{i,k}^2 - \frac{1}{2}\sigma_{i,k}\widetilde{\Xi}_{i,k}^2 + \hbar_{i,k} \right) \\ & + \sum_{k=1}^{n_i} \left(\gamma_i (c_{i,k} - \theta_{i,k} - \vartheta_{i,k-1}) \right), \end{aligned} \tag{3.51}$$

where above inequality holds due to $\vartheta_{i,0} = 0$, $s_{i,n_i+1} = 0$ and the fact that

$$\gamma_i^{(p_{i,n_i}-1)/(p_i+1)} s_{i,n_i}^{p_i-p_{i,n_i}+2} \le \gamma_i + s_{i,n_i}^{p_i+1}, \tag{3.52}$$

with $\gamma_i > 0$ a constant, according to Lemma 2.2.

3.4. Stability Analysis

To analyze the stability of the entire closed-loop system, consider the combined common Lyapunov function

$$V = \sum_{i=1}^{N} V_{i,n_i}. \tag{3.53}$$

The use of the common Lyapunov function (3.50) is possible because in (3.35), (3.44), and (3.49), the maximum value of the switching weights is estimated by the RBF NN approximators. A multiple Lyapunov function approach is in principle possible, but in this case the stability analysis requires to impose conditions on the switching signal [54]. With the common Lyapunov function (3.50), the following stability result holds for arbitrary switching $\sigma_i(\cdot)$.

Theorem 3.1 Under Assumptions 1.1 and 3.1, consider the closed-loop system composed by the power-chained form switched nonlinear multi-agent system (3.1), the distributed adaptive consensus controllers (3.17)-(3.21) and the parameter adaptation laws (3.22). For any $\varpi > 0$, and the initial conditions $\overline{\boldsymbol{\chi}}_{i,k}(0)$ and $\widehat{\overline{\Xi}}_{i,k}(0)$ for ($i = 1,\ldots,N$, $k = 1,\ldots,n_i$) satisfying $V\big(\overline{\boldsymbol{\chi}}_{i,k}(0), \widehat{\overline{\Xi}}_{i,k}(0)\big) < \varpi$, there exist positive design parameters $c_{i,k}$, $\beta_{i,k}$, $\sigma_{i,k}$, $\zeta_{i,k}$, $b_{i,k}$, γ_i, $\rho_{i,k}$, $\varrho_{i,k}$, and $\Theta_{i,k}$, $i = 1,\ldots,N$, $k = 1,\ldots,n_i$, such that

- The compact set $\Omega_0 = \Big\{\big(\overline{\boldsymbol{\chi}}_{i,k}, \widehat{\overline{\Xi}}_{i,k}\big) | V\big(\overline{\boldsymbol{\chi}}_{i,k}, \widehat{\overline{\Xi}}_{i,k}\big) \le \varpi, i = 1,\ldots,N, k = 1,\ldots,n_i\Big\}$ is an invariant set, namely, $V\big(\overline{\boldsymbol{\chi}}_{i,k}, \widehat{\overline{\Xi}}_{i,k}\big) \le \varpi$ holds for $\forall\, t \ge 0$, and hence all the closed-loop signals are bounded all the time;
- The consensus tracking error $\boldsymbol{\delta}$ converges to the following compact set:

$$\Omega_3 = \left\{ \lim_{t\to+\infty} \|\boldsymbol{\delta}\|_2 \le \sqrt{\frac{\sum_{i=1}^{N}\left[\frac{\chi}{\overline{\nu}}\overline{\psi}_i\right]^{\frac{2}{\underline{\psi}_i}}}{\sigma^2_{\min}\big(\overline{\mathscr{L}}+\mathscr{B}\big)}} \triangleq \Psi \right\}, \tag{3.54}$$

where $\overline{\psi}_i = \max\{p_i - p_{i,1} + 2, i \in \mathscr{M}_i\}$, $\underline{\psi}_i = \min\{p_i - p_{i,1} + 2, i \in \mathscr{M}_i\}$, $\overline{\nu}$ and χ are given in the proof.

Proof. It follows from (3.51) that

$$\dot{V}_{i,n_i} \le -\nu_i V_{i,n_i} + \Gamma_i,$$

where $\nu_i = \min\{(p_i - p_{i,k} + 2)\zeta_{i,k}, \beta_{i,k}\sigma_{i,k} : 1 \le k \le n_i\}$ with $\zeta_{i,k} = \gamma_i^{(p_{i,k}-1)/(p_i+1)}\big(c_{i,k} - \theta_{i,k} - \vartheta_{i,k-1}\big)$ and $\Gamma_i = \sum_{k=1}^{n_i}\Big[\frac{1}{2}\sigma_{i,k}\Xi_{i,k}^2 + \hbar_{i,k} + \gamma_i(c_{i,k} - \theta_{i,k} - \vartheta_{i,k-1})\Big]$. Therefore, the derivative of V can be obtained as

$$\dot{V} \le -\overline{\nu}V + \chi, \tag{3.55}$$

where $\overline{\nu} = \min_{1\le i\le N}\{\nu_i\}$ and $\chi = \sum_{i=1}^{N}\Gamma_i$. It can be concluded from (3.55) that $\frac{\chi}{\overline{\nu}}$ can be made arbitrarily small by increasing $c_{i,k}$, $\beta_{i,k}$, $\sigma_{i,k}$, $\rho_{i,k}$, and $\varrho_{i,k}$, and meanwhile decreasing $\zeta_{i,k}$, $b_{i,k}$, and γ_i for $i = 1,\ldots,N$, $k = 1,\ldots,n_i$. Namely, it is possible to make $\frac{\chi}{\overline{\nu}} \le \varpi$ by selecting the design parameters appropriately. Then, in light of (3.55), we have that $\dot{V} \le 0$ holds true for $V = \varpi$: consequently, the compact set Ω_0 is an invariant set and all closed-loop signals stay inside of the compact set Ω_0 all the time since $V(0) < \varpi$.

A bound on the tracking error can be obtained as follows: integrating $\dot{V}(\cdot)$ on $[0,t]$ gives

$$\int_0^\tau \mathrm{d}\big[\exp(\overline{\nu}\tau)V(\tau)\big] \le \int_0^\tau \chi\exp(\overline{\nu}\tau)\,\mathrm{d}\tau \tag{3.56}$$

which suggests that

$$V(t) \le \Big(V(0)-\frac{\chi}{\overline{\nu}}\Big)\exp(-\overline{\nu}t)+\frac{\chi}{\overline{\nu}} \le V(0)+\frac{\chi}{\overline{\nu}}. \tag{3.57}$$

Thus, invoking (3.26) yields that $\lim_{t\to+\infty}\frac{s_{i,1}^{p_i-p_{i,1}+2}}{p_i-p_{i,1}+2} \le \frac{\chi}{\overline{\nu}}$, which further leads to

$$\lim_{t\to+\infty}\|s_1\| \le \sqrt{\sum_{i=1}^N\left[\Big(\frac{\chi}{\overline{\nu}}\overline{\psi}_i\Big)^2\right]^{\frac{1}{\overline{\psi}_i}}}. \tag{3.58}$$

Then, from the inequalities below (3.15), one gets that $\lim_{t\to+\infty}\|\boldsymbol{\delta}\| \le \frac{\Gamma}{\underline{\sigma}_{\min}(\overline{\mathscr{L}}+\mathscr{B})}$. This concludes the proof. ■

In case the knowledge of $\underline{\sigma}_{\min}\big(\overline{\mathscr{L}}+\mathscr{B}\big)$ is not available, it was proposed to replace this terms in (3.54) with the more conservative bound $\frac{\overline{N}}{N^2+N-1}$ with $\overline{N}=\big(\frac{N-1}{N}\big)^{\frac{N-1}{2}}$ [34].

A design procedure for the proposed algorithm can be sketched as follows:

Step 1 : Specify a constant $\varpi>0$ and choose appropriate initial conditions $\chi_{i,k}(0)$ and $\widehat{\Xi}_{i,k}(0)\ge 0$ for $i=1,\dots,N$, $k=1,\dots,n_i$ to satisfy $V(0)<\varpi$;

Step 2 : Choose RBF NN approximators $\widehat{\boldsymbol{W}}_{i,k}\boldsymbol{\varphi}_{i,k}(\cdot)$ by appropriately selecting the number of network nodes, where $i=1,\dots,N$, $k=1,\dots,n_i$. Accordingly, calculate $\Theta_{i,k}$.

Step 3 : Assign specific values to the design parameters $c_{i,k}>0$, $\sigma_{i,k}>0$, $\beta_{i,k}>0$, $\zeta_{i,k}>0$, $\gamma_i>0$, $b_{i,k}>0$, $\rho_{i,k}>0$, and $\varrho_{i,k}>0$.

Step 4 : Determine the intermediate variables according to the following order: $s_{i,1}\to\widehat{\Xi}_{i,1}\to\alpha_{i,1}\to s_{i,2}\to\widehat{\Xi}_{i,2}\to\alpha_{i,2}\to\cdots s_{i,k}\to\widehat{\Xi}_{i,k}\to\alpha_{i,k}\to\cdots\to s_{i,n_i}\to\widehat{\Xi}_{i,n_i}\to u_i$ for $i=1,\dots,N$, $k=3,\dots,n_i-1$;

Remark 3.5 In line with [89], [135], and [136], Theorem 3.1 provides a practical consensus tracking result (i.e. convergence to a residual set). This is expected since [83] has proven that even for a single power-chained form system, asymptotic tracking is in general not possible (cf. Examples 2.1 and 2.2 of [83]).

Remark 3.6 The size of Ω_3 can be made small by increasing $c_{i,k}$, $\beta_{i,k}$, $\sigma_{i,k}$, $\rho_{i,k}$, and $\varrho_{i,k}$, and meanwhile decreasing $\zeta_{i,k}$, $b_{i,k}$, and γ_i for $i=1,\dots,N$, $k=1,\dots,n_i$. Then, the design parameters $c_{i,k}$, $\sigma_{i,k}$, $\beta_{i,k}$, $\zeta_{i,k}$, γ_i, $b_{i,k}$, and $\Theta_{i,k}$ can be adjusted so as to satisfy $\frac{\chi}{\overline{\nu}}\le\varpi$, namely, $V(t)\le\varpi$ holds for $\forall\, t\ge 0$ due to the fact that $V(0)<\varpi$ and $\dot{V}\le 0$ when $V=\varpi$.

Remark 3.7 Even though the exact bound of $||\boldsymbol{\delta}||_2$ cannot be obtained due to the unknown constant $\Xi_{i,k}$ coming from the optimal weight vector of approximator, one can follow similar ideas as [68, Sect. 2.2] and [73, Sect. IV] and give an estimate for the upper bound of $||\boldsymbol{\delta}||_2$ by assuming $\Xi_{i,k}$ to be bounded by a known constant. A similar approach is adopted in the simulations of Sect. 3.5.

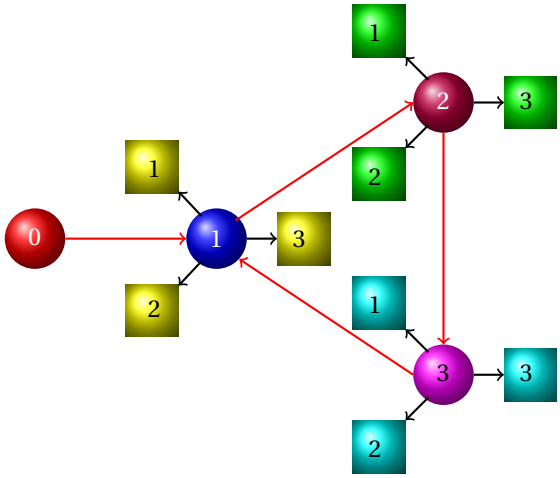

Figure 3.2: The communication graph between leader 0 and follower agents 1, 2 and 3. Each agent can switch among three dynamics, represented as three squares around each agent.

Remark 3.8 Note that the continuous function $F_{i,1}$ in (3.25) also embeds the effect of graph connectivity, since $F_{i,1}$ depends on the connectivity matrix $a_{i,j}$. At the same time, because the RBF NN activation functions depend on the neighboring states, one can rely on standard results [86] to get that any continuous function can be approximated by an RBF NN with desired accuracy over a compact set as long as we select enough neural network nodes. Similar idea is used in [127, eq. (18)], [70, eq. (12)], and [89, eq. (20)] to approximate unknown system nonlinearities over compact sets.

Remark 3.9 Because the universal approximation ability of RBF NNs is valid only for a compact set, Theorem 3.1 has used invariant set theory to prove that Ω_0 is an invariant set where all closed-loop signals are retained all the time. The effectiveness of the adopted approximators has also been validated in the simulation (cf. Sect. 3.5).

Remark 3.10 Despite the dimension of input variable $\boldsymbol{Z}_{i,k}$ in activation function $\boldsymbol{\varphi}_{i,k}(\cdot)$ inevitably grows as subsystem order k grows, there are two solutions to handle this issue: one is to use the fact $||\boldsymbol{\varphi}_{i,k}(\boldsymbol{Z}_{i,k})|| \leq ||\boldsymbol{\varphi}_{i,k}(\bar{\boldsymbol{Z}}_{i,k})||$ to reduce the dimension of $\boldsymbol{Z}_{i,k}$ during the control design and stability analysis as done in [70, Lemma 1 and eq. (13)] and [105, Lemma 4 and eq. (15)], where $\dim(\bar{\boldsymbol{Z}}_{i,k})<\dim(\boldsymbol{Z}_{i,k})$. Another one is to bound $||\boldsymbol{\varphi}_{i,k}(\boldsymbol{Z}_{i,k})||$ as $||\boldsymbol{\varphi}_{i,k}(\boldsymbol{Z}_{i,k})|| \leq \Theta_{i,k}$ as done in [89, Lemma 3], [135, Lemma 2] and in our paper (cf. (3.27)), where $\Theta_{i,k} > 0$ is an appropriately chosen constant.

3.5. Simulation Examples

3.5.1. Numerical Example

To validate the effectiveness of the proposed scheme, one leader (labeled by 0) with three follower agents are considered with the directed graph in Fig. 3.2. The odd powers are taken as $p_{1,1} = 3$, $p_{1,2} = 5$, $p_{2,1} = 3$, $p_{2,2} = 7$, $p_{3,1} = 5$, $p_{3,2} = 9$, $n_i = 2$, $i = 1,2,3$. For each follower, the switching signal is $\sigma_i(\cdot)$: $[0,\infty) \to \mathcal{M}_i = \{1,2,3\}$, which is shown in Fig. 3.3.

Note that each follower has its own switching signal, and thus can switch asynchronously with respect to the other followers. The unknown switched nonlinearities $\phi_{i,k}^{\sigma_i(t)}(\cdot)$ and $\psi_{i,k}^{\sigma_i(t)}(\cdot)$ are taken to be heterogeneous:

For follower agent 1, the three switching dynamics are:

$$\begin{aligned}
\phi_{1,1}^1 &= 1.3-\cos(\chi_{1,1}), & \psi_{1,1}^1 &= |\tanh(\chi_{1,1}^3)|+1.6,\\
\phi_{1,1}^2 &= 0.6+\exp(-\chi_{1,1}^2), & \psi_{1,1}^2 &= \cos(\chi_{1,1}^3)+2,\\
\phi_{1,1}^3 &= 0.8+0.2\cos(\chi_{1,1}^3), & \psi_{1,1}^3 &= 2\cos(\chi_{1,1}^2),\\
\phi_{1,2}^1 &= \chi_{1,2}\chi_{1,1}+0.75, & \psi_{1,2}^1 &= 2(|\cos(\chi_{1,2}^2)|+1.3),\\
\phi_{1,2}^2 &= 0.7+0.2\chi_{1,2}^2, & \psi_{1,2}^2 &= 3\sin(\chi_{1,2}^2)+4,\\
\phi_{1,2}^3 &= \cos(\chi_{1,2}^2)+0.3, & \psi_{1,2}^3 &= 5|\sin(0.1\chi_{1,2})|+1.5.
\end{aligned}$$

For follower agent 2, the three switching dynamics are:

$$\begin{aligned}
\phi_{2,1}^1 &= 1.1\chi_{2,1}+\chi_{2,1}^2, & \psi_{2,1}^1 &= 3\cos(\chi_{2,1}^2)+5,\\
\phi_{2,1}^2 &= \chi_{2,1}^2+0.5, & \psi_{2,1}^2 &= \sin(\chi_{2,1}^3)+3,\\
\phi_{2,1}^3 &= \chi_{2,1}^3+1.25, & \psi_{2,1}^3 &= \cos(\chi_{2,1}^2+\chi_{2,1}^3)+3,\\
\phi_{2,2}^1 &= 0.5\chi_{2,2}^2+0.75, & \psi_{2,2}^1 &= 3+2\cos(\chi_{2,1}^3\chi_{2,2}),\\
\phi_{2,2}^2 &= 1.3\chi_{2,1}^3+0.8\chi_{2,2}, & \psi_{2,2}^2 &= 2\cos(\chi_{2,1}^2)+4,\\
\phi_{2,2}^3 &= \cos(\chi_{2,1})\chi_{2,2}+0.25, & \psi_{2,2}^3 &= 3\cos(\chi_{2,2}^3)+5.
\end{aligned}$$

For follower agent 3, the three switching dynamics are:

$$\begin{aligned}
\phi_{3,1}^1 &= 1.5\sin(\chi_{3,1})+\chi_{3,1}^3, & \psi_{3,1}^1 &= |\sin(\chi_{3,1})|+6,\\
\phi_{3,1}^2 &= 0.3\chi_{3,1}^2+\sin(\chi_{3,1}), & \psi_{3,1}^2 &= |\sin(\chi_{3,1}^3)|+3,\\
\phi_{3,1}^3 &= \chi_{3,1}+0.2\cos(\chi_{3,1}), & \psi_{3,1}^3 &= \cos(\chi_{3,1}^2+\chi_{3,1}^3)+4.5,\\
\phi_{3,2}^1 &= 0.5\chi_{3,1}^2+0.5\chi_{3,2}, & \psi_{3,2}^1 &= \cos(\chi_{3,2}^2)+2,\\
\phi_{3,2}^2 &= \chi_{3,2}+0.8\sin(\chi_{3,1}), & \psi_{3,2}^2 &= 4\cos(\chi_{3,1})+5.5,\\
\phi_{3,2}^3 &= \cos(\chi_{3,2}^2)+0.7, & \psi_{3,2}^3 &= \cos(\chi_{3,2}^2)+3.5.
\end{aligned}$$

The leader output is $y_r(t)=2\sin(t)+2\sin(0.5t)$. For comparison purposes, three schemes are considered, the method proposed here and the two state-of-the-art methods of [89] and [135]. In our simulation, the centers and widths of RBF NNs are chosen on a regular lattice in the respective compact sets. In particular, the neural networks used to approximate $F_{1,1}(\cdot)$, $F_{2,1}(\cdot)$, and $F_{3,1}(\cdot)$ respectively contain 27 (Case I) or 3 (Case II) nodes with centers evenly spaced in the interval $[-2.5,2.5]\times[-2.5,2.5]\times[-2.5,2.5]$ and widths equal to two. The neural networks used to approximate $F_{1,2}(\cdot)$, $F_{2,2}(\cdot)$, and $F_{3,2}(\cdot)$ respectively contain 64 (Case I) or 6 (Case II) nodes with centers evenly spaced in the interval $[-4,4]\times[-4,4]\times[-4,4]\times[-4,4]\times[-4,4]\times[-4,4]\times[-4,4]\times[-4,4]$ and widths equal to two. The initial conditions for the follower agents are taken as: $\chi_{1,1}(0)=0.5$, $\chi_{2,1}(0)=0.55$, $\chi_{3,1}(0)=0.75$, $\chi_{1,2}(0)=0.25$, $\chi_{2,2}(0)=1.5$, $\chi_{3,2}(0)=-0.75$, $\widehat{\Xi}_{1,1}(0)=\widehat{\Xi}_{1,2}(0)=5$, $\widehat{\Xi}_{2,1}(0)=$

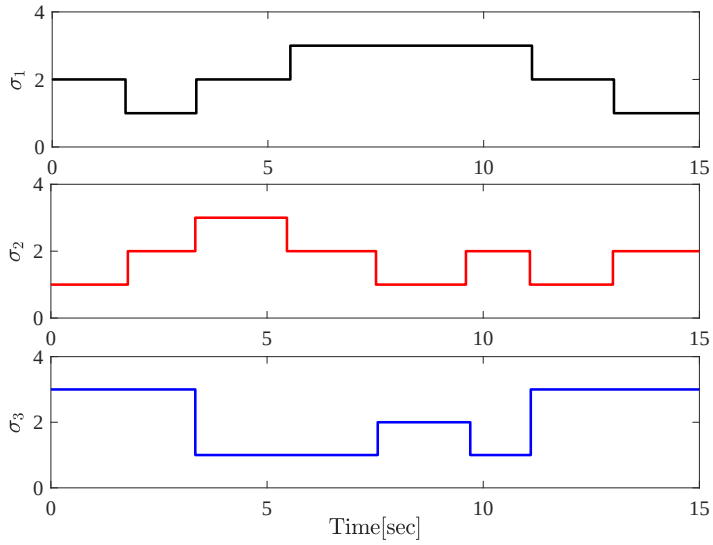

Figure 3.3: Switching signals $\sigma_i(\cdot)$ for the three followers. Note that the followers can switch asynchronously with each other.

$\widehat{\Xi}_{2,2}(0) = 7$ and $\widehat{\Xi}_{3,1}(0) = \widehat{\Xi}_{3,2}(0) = 10$. The design parameters are chosen to be: $c_{1,1} = 1.5$, $c_{2,1} = 2.5$, $c_{3,1} = 3$, $c_{1,2} = 1$, $c_{2,2} = 2$, $c_{3,2} = 1.5$, $\beta_{1,2} = \beta_{2,2} = \beta_{3,2} = 1$, $\beta_{1,1} = 7.5$, $\beta_{2,1} = 5$, $\beta_{3,1} = 15$, $\sigma_{1,1} = 0.25$, $\sigma_{2,1} = 0.75$, $\sigma_{3,1} = 0.5$, $\sigma_{1,2} = \sigma_{2,2} = \sigma_{3,2} = 1$, $\zeta_{1,1} = \zeta_{2,1} = \zeta_{3,1} = 0.5$, $\zeta_{1,2} = \zeta_{2,2} = \zeta_{3,2} = 0.75$, $b_{1,1} = b_{2,1} = b_{3,1} = 0.5$, $b_{1,2} = b_{2,2} = b_{3,2} = 1$, $\Theta_{1,1} = \Theta_{2,1} = \Theta_{3,1} = 5$, and $\Theta_{1,2} = \Theta_{2,2} = \Theta_{3,2} = 5\sqrt{5}$. The simulation results in Figs. 3.4-3.5 and in Tables 3.1 and 3.2 are carried out based on Case I. Tables 3.1 and 3.2 report the integral time absolute error ITAE=$\left[\int_0^T t|s_{i,1}(t)|dt\right]$, root mean square error RMSE=$\left[\frac{1}{T}\int_0^T s_{i,1}^2(t)dt\right]^{\frac{1}{2}}$, mean absolute error MAE=$\left[\frac{1}{T}|s_{i,1}(t)|dt\right]$, and mean absolute control actions MACA=$\left[\frac{1}{T}\int_0^T |u_i|dt\right]$ for $i = 1,2,3$, respectively. Fig. 3.3 reveals that the switching signals $\sigma_i(\cdot)$, $i = 1,2,3$, for three followers are asynchronous. It can be seen from Fig. 3.4 and Table 3.1 that the proposed method achieves smaller tracking errors $s_{1,1}$, $s_{2,1}$, and $s_{3,1}$ than that of [89] and [135]. From Fig. 3.3 and Table 3.2, one can conclude that the proposed method exhibits smaller control actions than that of [89] and [135]. Figs. 3.6-3.8 show that the RBF NN approximators can achieve satisfactory approximation performances as long as we choose a sufficiently large number of network nodes.

3.5.2. Practical Example

To further validate the developed method, a multi-agent version of the underactuated weakly coupled mechanical benchmark in [83] is considered, also shown in Fig. 1.3. The system includes a mass $m_{i,1}^{\sigma_i}$ on a horizontal smooth surface and an inverted pendulum $m_{i,2}^{\sigma_i}$ supported by a massless rod. The mass is connected to the wall surface by a linear spring and to the inverted pendulum by a nonlinear spring with a cubic force deforma-

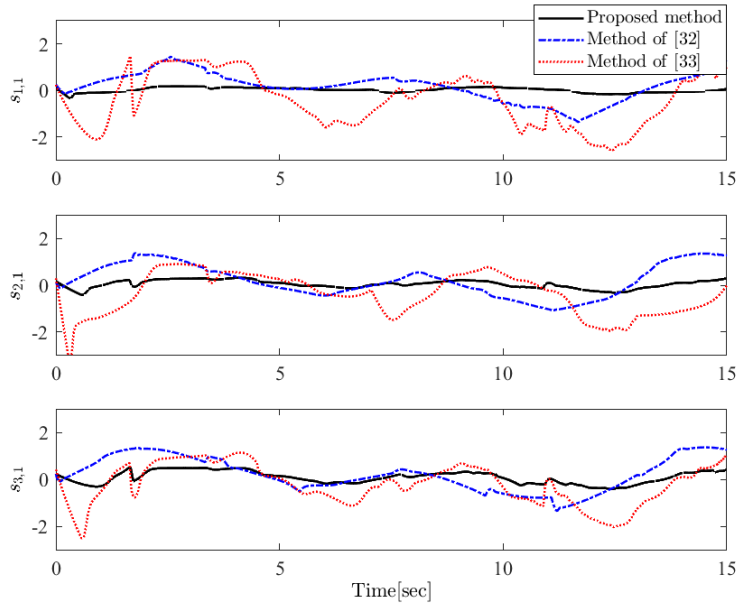

Figure 3.4: Tracking errors $s_{1,1}$, $s_{2,1}$, and $s_{3,1}$ under three schemes.

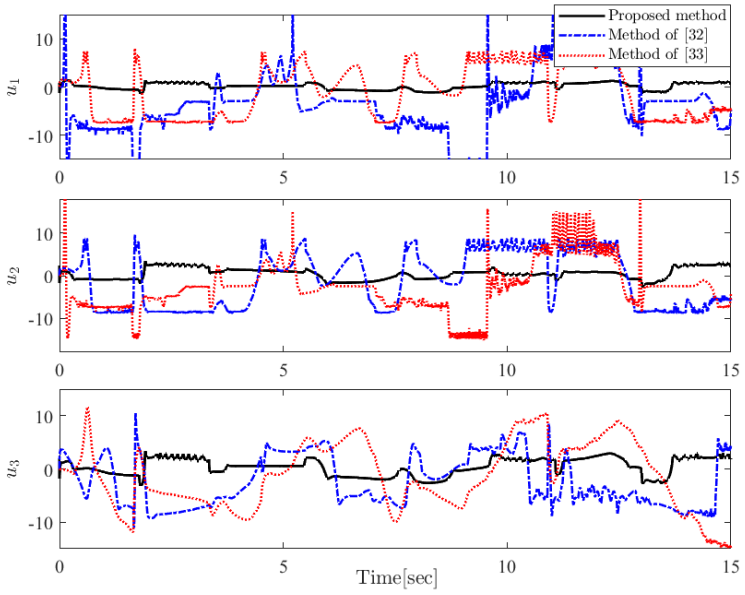

Figure 3.5: Control inputs u_1, u_2, and u_3 under three schemes. The proposed scheme avoids high control gains, as the result of the reduced-complexity design.

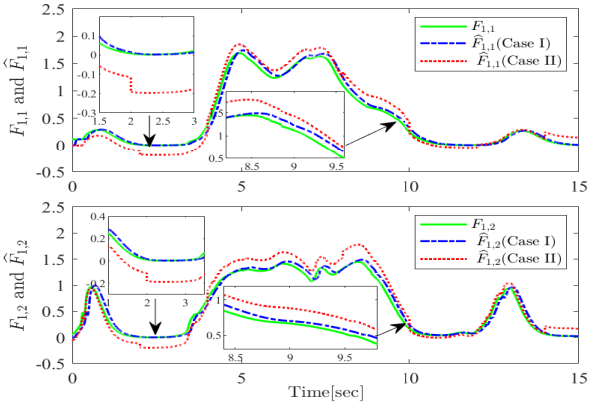

Figure 3.6: The true (unknown) $F_{1,1}$ and $F_{1,2}$ and their NN approximations $\widehat{F}_{1,1}$ and $\widehat{F}_{1,2}$.

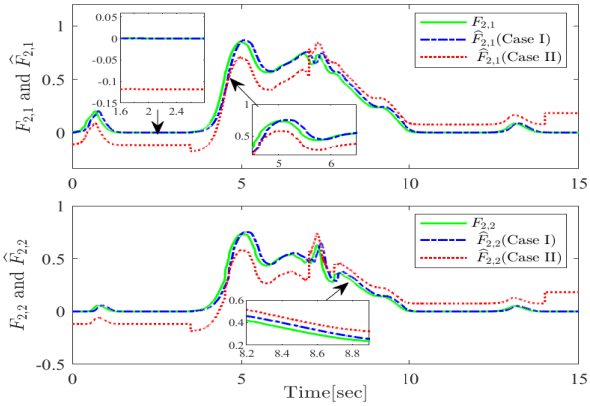

Figure 3.7: The true (unknown) $F_{2,1}$ and $F_{2,2}$ and their NN approximations $\widehat{F}_{2,1}$ and $\widehat{F}_{2,2}$.

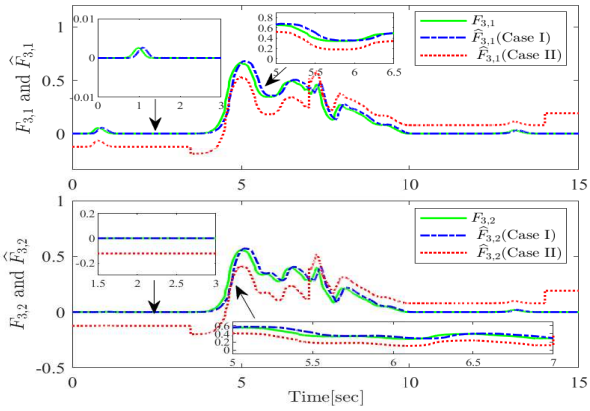

Figure 3.8: The true (unknown) $F_{3,1}$ and $F_{3,2}$ and their NN approximations $\widehat{F}_{3,1}$ and $\widehat{F}_{3,2}$.

Table 3.1: Performance indices for tracking errors $s_{1,1}$, $s_{2,1}$, and $s_{3,1}$ under three schemes.

Tracking Error	Index	Proposed Method	Method of [89]	Method of [135]
$s_{1,1}$	ITAE	3.268	12.693	15.226
	RMSE	0.213	0.876	0.926
	MAE	0.031	0.127	0.139
$s_{2,1}$	ITAE	3.747	13.214	14.944
	RMSE	0.237	0.914	0.954
	MAE	0.024	0.096	0.126
$s_{3,1}$	ITAE	3.994	13.693	15.696
	RMSE	0.264	0.887	0.969
	MAE	0.0289	0.133	0.152

Table 3.2: Performance indices for control inputs u_1, u_2, and u_3 under three schemes.

Control Input	Index	Proposed Method	Method of [89]	Method of [135]
u_1	MACA	2.113	11.021	6.564
u_2	MACA	2.457	8.689	8.012
u_3	MACA	2.754	7.254	8.367

tion relation. The dynamics of the ith agent can be represented by

$$\begin{cases} \ddot{\theta}_i = \dfrac{g\sin(\theta_i)}{l} + \dfrac{k_{i,2}^{\sigma_i(t)}}{m_{i,2}^{\sigma_i(t)} l}\big(x_i - l\sin(\theta_i)\big)^3\cos(\theta_i), \\ \ddot{x}_i = -\dfrac{k_{i,1}^{\sigma_i(t)}}{m_{i,1}^{\sigma_i(t)}}x_i - \dfrac{k_{i,2}^{\sigma_i(t)}}{m_{i,1}^{\sigma_i(t)}}\big(x_i - l\sin(\theta_i)\big)^3 + \dfrac{u_i}{m_{i,1}^{\sigma_i(t)}}, \end{cases} \tag{3.59}$$

for $i = 1,\ldots,10$, and $\sigma_i(\cdot) : [0,+\infty) \to \mathscr{M}_i = \{1,2,\ldots,10\}$, where $\theta_i \in (-\frac{\pi}{2}, \frac{\pi}{2})$, χ_i is the displacement of $m_{i,1}^{\sigma_i(t)}$, u_i is the control force acting on $m_{i,1}^{\sigma_i(t)}$. Moreover, $k_{i,2}^{\sigma_i(t)}$ and $k_{i,1}^{\sigma_i(t)}$ are spring coefficients, and l is the pendulum length. The specific values of $m_{i,1}^{\sigma_i(t)}$, $m_{i,2}^{\sigma_i(t)}$, $k_{i,2}^{\sigma_i(t)}$, and $k_{i,1}^{\sigma_i(t)}$, $i = 1,\ldots,10$, are given in the Table 3.3, and the switching signal is given in Fig. 3.9. The following change of coordinates:

$$\chi_{i,1} = \theta_i,\ \ \chi_{i,2} = \dot{\theta}_i,\ \ \chi_{i,3} = x_i,\ \ \chi_{i,4} = \dot{x}_i, \tag{3.60}$$

transforms (3.60) into

$$\begin{cases} \dot{\chi}_{i,1} = \chi_{i,2},\ \dot{\chi}_{i,2} = \phi_{i,2}^{\sigma_i(t)}(\bar{\boldsymbol{\chi}}_{i,2}) + \psi_{i,2}^{\sigma_i(t)}(\bar{\boldsymbol{\chi}}_{i,2})\chi_{i,3}^3, \\ \dot{\chi}_{i,3} = \chi_{i,4},\ \dot{\chi}_{i,4} = \phi_{i,4}^{\sigma_i(t)}(\bar{\boldsymbol{\chi}}_{i,4}) + \psi_{i,4}^{\sigma_i(t)}(\bar{\boldsymbol{\chi}}_{i,4})u_i, \end{cases} \tag{3.61}$$

where $\phi_{i,2}^{\sigma_i(t)}(\bar{\boldsymbol{\chi}}_{i,2}) = \frac{g}{l}\sin(\chi_{i,1}) + \frac{k_{i,2}^{\sigma_i(t)}}{m_{i,2}^{\sigma_i(t)} l}\cos(\chi_{i,1})\big[3\chi_{i,3} l^2 \times \sin^2(\chi_{i,1}) - 3\chi_{i,3}^2 l\sin(\chi_{i,1}) - l^3 \times \sin^3(\chi_{i,1})\big]$, $\phi_{i,4}(\bar{\boldsymbol{\chi}}_{i,4}) = -\frac{k_{i,1}^{\sigma_i(t)}}{m_{i,1}^{\sigma_i(t)}}\chi_{i,3} - \frac{k_{i,2}^{\sigma_i(t)}}{m_{i,1}^{\sigma_i(t)}}\big[\chi_{i,3}^3 - l^3\sin^3(\chi_{i,1}) - 3\chi_{i,3}^2 l\sin(\chi_{i,1}) + 3\chi_{i,3} l^2\sin^2(\chi_{i,1})\big]$, $\psi_{i,2}^{\sigma_i(t)}(\bar{\boldsymbol{\chi}}_{i,2}) = \frac{k_{i,2}^{\sigma_i(t)}}{m_{i,2}^{\sigma_i(t)} l}\cos(\chi_{i,1})$, and $\psi_{i,4}^{\sigma_i(t)}(\bar{\boldsymbol{\chi}}_{i,4}) = \frac{1}{m_{i,1}^{\sigma_i(t)}}$.

The leader signal is the same as previous numerical example. Due to space limits, we do not repeat all the state-of-the-art comparisons as in the previous example. The neural networks used to approximate $F_{i,1}(\cdot)$ and $F_{i,2}(\cdot)$ for $i = 1,\ldots,10$ contain 27 nodes with centers evenly spaced in the interval $[-2.5,2.5]\times[-2.5,2.5]\times[-2.5,2.5]$ and widths equal to two. The neural networks used to approximate $F_{i,3}(\cdot)$ and $F_{i,4}(\cdot)$ for $i = 1,\ldots,10$ contain 81 nodes with centers evenly spaced in the interval $[-4,4]\times[-4,4]\times[-4,4]\times[-4,4]\times[-4,4]\times[-4,4]\times[-4,4]\times[-4,4]\times[-4,4]$ and widths equal to two. The initial conditions for the follower agents are taken as: $\chi_{i,1}(0) = 0$ for $i = 1,\ldots,7$, $\chi_{i,1}(0) = 0.15$ for $i = 8,9,10$, $\chi_{i,2}(0) = 0.25$ for $i = 1,\ldots,5$, $\chi_{i,2}(0) = -0.5$ for $i = 6,\ldots,10$, $\chi_{i,3}(0) = 0$ for $i = 1,\ldots,10$, $\chi_{i,4}(0) = -0.75$ for $i = 1,\ldots,6$, $\chi_{i,4}(0) = 0.25$ for $i = 7,\ldots,10$, $\widehat{\Xi}_{i,1}(0) = \widehat{\Xi}_{i,2}(0) = 5$ for $i = 1,\ldots,5$, and $\widehat{\Xi}_{i,3}(0) = \widehat{\Xi}_{i,4}(0) = 7.5$ for $i = 6,\ldots,10$. The design parameters are chosen to be: $c_{i,1} = 1.5$ for $i = 1,\ldots,4$, $c_{i,1} = 2.5$ for $i = 5,\ldots,10$, $c_{i,2} = c_{i,3} = 2$ for $i = 1,\ldots,10$, $c_{i,4} = 3.5$ for $i = 1,\ldots,10$, $\beta_{i,1} = 5.5$ for $i = 1,\ldots,10$, $\beta_{i,2} = 7$ for $i = 1,\ldots,10$, $\beta_{i,3} = \beta_{i,4} = 3.5$ for $i = 1,\ldots,10$, $\sigma_{i,1} = \sigma_{i,2} = 0.5$ for $i = 1,\ldots,10$, $\sigma_{i,3} = \sigma_{i,4} = 0.75$ for $i = 1,\ldots,10$, $\zeta_{i,1} = \zeta_{i,3} = 0.25$ for $i = 1,\ldots,10$, $\zeta_{i,2} = \zeta_{i,4} = 0.5$ for $i = 1,\ldots,10$, $b_{i,1} = b_{i,2} = b_{i,3} = b_{i,4} = 1$ for $i = 1,\ldots,10$, $\Theta_{i,1} = 5$, and $\Theta_{i,2} = \Theta_{i,3} = \Theta_{i,4} = 7\sqrt{5}$ for $i = 1,\ldots,10$. Fig. 3.10-(a) shows that the 10 followers track the leader signal with bounded tracking errors. Fig. 3.10-(b) depicts the evolution of control inputs. Fig. 3.10-(c) draws the curves of $||\boldsymbol{\delta}||_2$ as well as its theoretical bound which is calculated assuming $\Xi_{i,k}$ to be bounded as $\Xi_{i,k} \le 7\sqrt{5}$ for $i = 1,\ldots,10$ and $k = 1,\ldots,4$.

3.6. Conclusions

This Chapter proposed a result about distributed consensus tracking for power-chained form nonlinear multi-agent systems with switched dynamics. The distinguishing feature of the proposed design is a new separation-based lemma that can simplify the control design in a twofold sense: the complexity of the virtual and actual control laws is significantly reduced; the power of the control gains does not increase exponentially with the order of the subsystems. An interesting point worth investigating in future research is to further simplify the design by avoiding the use of any RBF NN approximators.

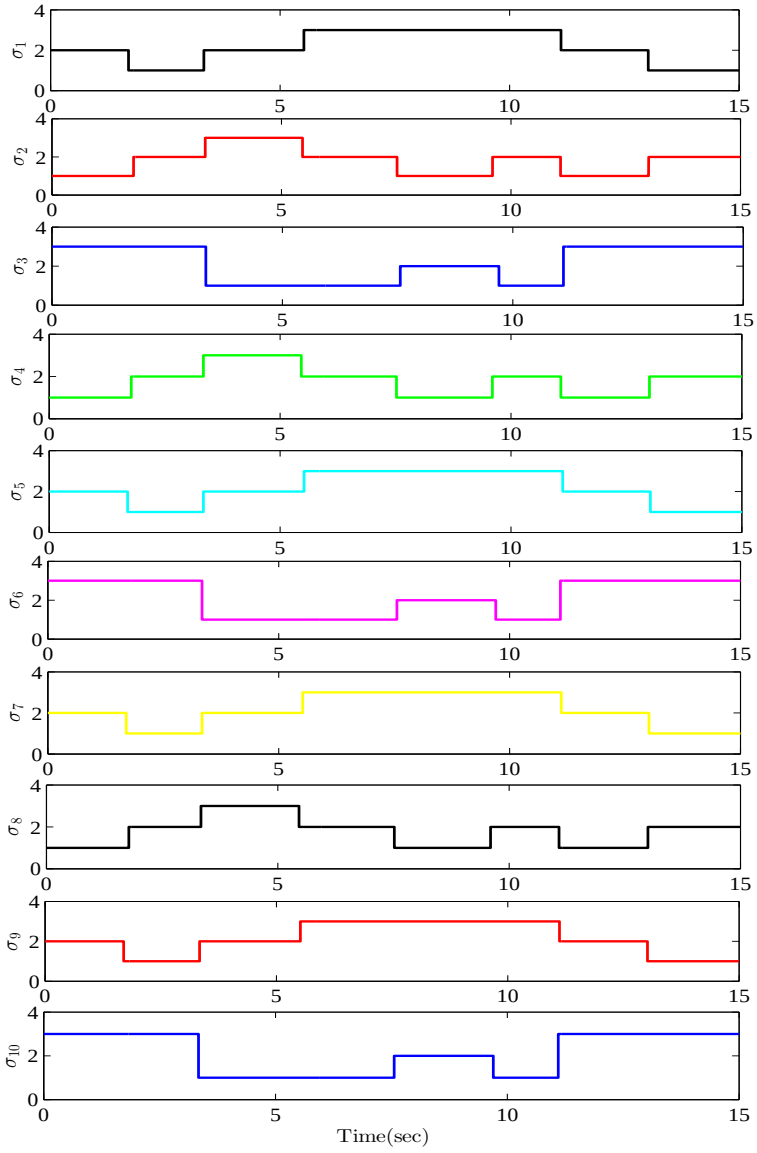

Figure 3.9: Asynchronous switching signal $\sigma_i(\cdot)$

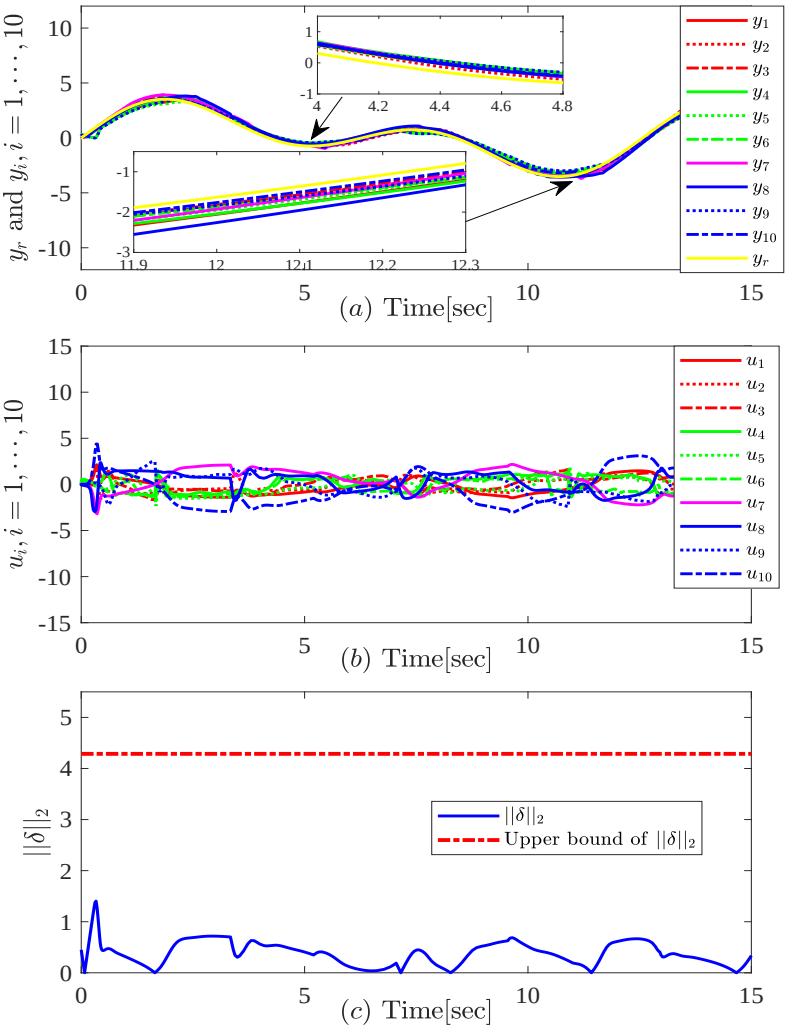

Figure 3.10: (a) Follower outputs y_i (i=1,...,10) and leader output y_r (b) control inputs (c) norm of consensus tracking error $||\delta||_2$ and its theoretic bound.

Table 3.3: The values of m_1, m_2, k_s, and k_ω of 10 followers.

Agents	Mode	m_1(kg)	m_2(kg)	k_2(N/m^3)	k_1(N/m)	Agents	Mode	m_1(kg)	m_2(kg)	k_2(N/m^3)	k_1(N/m)
Follower 1	①	1.25	1.50	75	70	Follower 6	①	1.75	2.50	65	57
	②	1.80	1.75	70	85		②	1.95	2.75	75	60
	③	2.25	3.50	45	50		③	2.80	3.75	80	75
Follower 2	①	2.50	4.50	55	60	Follower 7	①	2.95	3.75	55	67
	②	2.00	4.80	80	75		②	1.50	2.45	75	85
	③	1.85	2.75	45	50		③	2.25	1.85	55	60
Follower 3	①	1.50	2.35	45	55	Follower 8	①	2.85	3.75	60	75
	②	1.95	4.25	50	60		②	2.50	2.75	65	80
	③	2.25	3.50	70	55		③	1.85	2.55	70	65
Follower 4	①	2.75	3.50	75	70	Follower 9	①	2.25	3.75	65	70
	②	1.80	4.75	55	65		②	1.50	2.80	75	70
	③	2.65	4.50	80	75		③	2.25	3.65	80	75
Follower 5	①	3.25	2.75	75	55	Follower 10	①	1.75	2.85	65	55
	②	2.85	3.50	70	60		②	3.25	1.75	60	65
	③	3.50	4.00	65	70		③	1.85	3.50	65	75

4

CONSENSUS IN MULTI-AGENT SYSTEMS IN THE POWER-CHAINED FORM WITH MIXED UNKNOWN CONTROL DIRECTIONS

This chapter investigates the consensus tracking problem for uncertain multi-agent systems in the power-chained form systems with partially unknown control directions. The main challenge of solving such problem lies in the fact that the presence of mixed unknown control directions (some being known, some being unknown) requires a piecewise Nussbaum function that exploits the a priori knowledge of the known control directions. The introduction is given in Section 4.1. The problem formulation and preliminaries are provided in Section 4.2. Sections 4.3 and 4.4 present the proposed distributed consensus design and stability analysis, respectively. The simulation examples are in Section 4.5 and Section 4.6 draws the conclusion.

4.1. Introduction

In Chapter 3, we have proposed a reduced-complexity methodology for uncertain multi-agent systems in the power-chained form. However, the control design in Chapter 3 relies on the availability of control directions. In other words, the control directions are assumed to be known *a priori* for the purpose of facilitating control design. In this chapter, power-chained form dynamics is the object of the present work, which we study via the Nussbaum function method in the presence of multiple unknown control directions.

The Nussbaum function method to handle unknown control directions [14, 22, 23, 37, 75, 106, 122, 125] has not been explored in the distributed adding-one-power-integrator scenario, i.e. for coordination of multi-agent systems with power-chained form dynamics. The Nussbaum function method is challenging even for multi-agent systems controlled with the distributed adding-one-linear-integrator backstepping procedure [14,

17]: researchers have studied unknown but identical control directions [17], mixed unknown control directions (some directions being known, some being unknown) via a piecewise Nussbaum function that exploits the a priori knowledge of the known control directions [14], or multiple nonidentical unknown control directions with switching topologies [108, 109] and communication delays [81]. The piecewise Nussbaum function technique leaves the open problem: can the technique handle more than one control direction for each agent? In this chapter, we propose a hybrid Nussbaum technique that can handle uncertain agents with power-chained form dynamics, with non-smooth behaviors (switching and quantization), and with multiple unknown control directions for each agent. The main contribution of this chapter is to give positive answer to this question. In particular:

- The Nussbaum function techniques in [14, 22, 23, 75, 106, 122, 125] are designed to handle one unknown control direction for each agent, whereas the proposed technique uses hybrid Nussbaum gains that can handle multiple mixed unknown directions for each agent.

- The proposed technique can handle non-smooth behavior, i.e., switching dynamics and input quantization. The relevance of considering input quantization stems from works such as [47, 139], showing that appropriate designs must be proposed in the presence of input nonlinearities. Our proposed design relies on a variable-separable lemma to extract quantized control signal in a linear-like manner.

4.2. Problem Formulation and Preliminaries

Let us consider a multi-agent system composed of $N\,(N \geq 2)$ follower agents, under a directed communication topology described by $\mathcal{G} = (\mathcal{V}, \mathcal{E})$. Let the dynamics of the i-th follower agent, $i = 1, \ldots, N$, be represented by the power-chained form dynamics

$$\begin{cases} \dot{\chi}_{i,m} = \phi_{i,m}^{\sigma_i(t)}(\overline{\boldsymbol{\chi}}_{i,m}) + \psi_{i,m}^{\sigma_i(t)}(\overline{\boldsymbol{\chi}}_{i,m})\chi_{i,m+1}^{p_{i,m}}, \\ \dot{\chi}_{i,n_i} = \phi_{i,n_i}^{\sigma_i(t)}(\chi_i) + \psi_{i,n_i}^{\sigma_i(t)}(\boldsymbol{\chi}_i)(Q_i(u_i))^{p_{i,n_i}}, \\ \quad y_i = \chi_{i,1}, \end{cases} \tag{4.1}$$

where $1 \leq m \leq n_i - 1$, $\overline{\boldsymbol{\chi}}_{i,m} = [\chi_{i,1}, \chi_{i,2}, \ldots, \chi_{i,m}]^T \in \mathbb{R}^m$, $\boldsymbol{\chi}_i = [\chi_{i,1}, \chi_{i,2}, \ldots, \chi_{i,n_i}]^T \in \mathbb{R}^{n_i}$ and $y_i \in \mathbb{R}$ are the states and the output of the i-th follower agent, respectively. For $i = 1, \ldots, N$ and $m = 1, \ldots, n_i$, $\phi_{i,m}^{\sigma_i(t)}(\cdot)$ and $\psi_{i,m}^{\sigma_i(t)}(\cdot)$ are unknown continuous nonlinearities, and $p_{i,m}$ are positive odd integers. In (4.1), $\sigma_i(\cdot) : [0, +\infty) \to \mathcal{M}_i = \{1, 2, \ldots, m_i\}$ is a switching signal which selects at each time t the nonlinearities for agent i among m_i possibilities. The

control signal to be designed is u_i, with the quantized input $Q_i(u_i)$ being defined as

$$Q_i(u_i)=\begin{cases} u_{i,h}\mathrm{sgn}(u_i), & \text{if} \begin{cases} \frac{u_{i,h}}{1+\hbar_i}<|u_i|\le u_{i,h}, \dot{u}_i<0, \text{or}, \\ u_{i,h}<|u_i|\le \frac{u_{i,h}}{1-\hbar_i}, \dot{u}_i>0, \end{cases} \\ \overline{u}_{i,h}\mathrm{sgn}(u_i), & \text{if} \begin{cases} u_{i,h}<|u_i|\le \frac{u_{i,h}}{1-\hbar_i}, \dot{u}_i<0, \text{or}, \\ \frac{u_{i,h}}{1-\hbar_i}<|u_i|\le \frac{u_{i,h}(1+\hbar_i)}{1-\hbar_i}, \dot{u}_i>0, \end{cases} \\ 0, & \text{if} \begin{cases} 0\le|u_i|\le \frac{u_i^{\min}}{1+\hbar_i}, \dot{u}_i<0, \text{or}, \\ \frac{u_i^{\min}}{1+\hbar_i}<|u_i|\le u_i^{\min}, \dot{u}_i>0, \end{cases} \\ Q_i(u_i(t^-)), & \text{otherwise} \end{cases} \tag{4.2}$$

with $\overline{u}_{i,h}=u_{i,h}(1+\hbar_i)$, $u_{i,h}=\rho_i^{1-h}u_i^{\min}(h=1,2,\ldots)$ and $\hbar_i=\left[(1-\rho_i)/(1+\rho_i)\right]$ with $u_i^{\min}>0$ and $0<\rho_i<1$, and $u_i^{\min}$ and ρ_i represent the dead-zone range of $Q_i(u_i)$ and the measure of quantization density, respectively. Due to quantization, the continuous signal u_i is mapped into a discrete set $\mathscr{F}_i=\{0,\pm u_{i,h},\pm u_{i,h}(1+\hbar_i),h=1,2,\ldots\}$.

Remark 4.1 The quantizer parameter ρ_i, $f=1,\ldots,N$, is a measure of quantization density. The smaller ρ_i, the coarser the quantizer, i.e., $Q_i(u_i)$ will have less and less quantization levels [45, 47, 139].

Lemma 4.1 [45] The relation between the continuous input u_i and the quantized input $Q_i(u_i)$ can be described by

$$Q_i(u_i)=\kappa_i(u_i)u_i+\Delta_i(u_i), \tag{4.3}$$

where $\kappa_i(u_i)$ and $\Delta_i(u_i)$ satisfy $1-\hbar_i\le\kappa_i(u_i)\le 1+\hbar_i$, and $|\Delta_i(u_i)|\le u_i^{\min}$.

Assumption 4.1 [135] For each follower agent i, there exist known constants $\underline{\psi}_{i,m}>0$ and $\overline{\psi}_{i,m}>0,(1\le m\le n_i)$ such that

$$\underline{\psi}_{i,m}\le\left|\psi_{i,m}(\cdot)\right|\le\overline{\psi}_{i,m},\quad k\in\mathscr{M}_i.$$

Furthermore, some control directions of $\psi_{i,m}$ can be unknown.

Remark 4.2 The bounds $\underline{\psi}_{i,m}$ and $\overline{\psi}_{i,m}$ ensure controllability of each agent, but instead of assuming known sign of $\psi_{i,m}^k$ as in [112, 135, 136], Assumption 4.1 allows some signs to be unknown.

Problem 4.1 The goal is consensus tracking, i.e. to design u_i such that the output of each agent can track the leader agent's signal while respecting the communication topology defined by the graph $\overline{\mathscr{G}}$. Practical consensus tracking will be sought, due to the fact that asymptotic tracking cannot be realized in general for power-chained form systems [55, 56, 83].

It is worth mentioning that the problem of unknown control directions for the dynamics (4.1) is open and requires a new design that is not available in literature.

4.2.1. Newly Proposed Nussbaum Functions-based Technical Tool

In this section, we give the main result concerning hybrid Nussbaum-based control. To counteract the lack of a priori knowledge of control directions, we define the Nussbaum function as [14]:

$$\mathcal{N}_R(\nu) = \begin{cases} \mathcal{N}_R^{\overline{1}}(\nu), \text{ if the control direction is unknown,} \\ \mathcal{N}_R^{\overline{2}}(\nu), \text{ if the control direction is known,} \end{cases} \tag{4.4}$$

where $N_R^{\overline{1}}(\nu) = -\mu \exp\left(\frac{\nu^2}{2}\right)\left(\nu^2+2\right)\sin(\nu)$, and $N_R^{\overline{2}}(\nu) = -\exp\left(\frac{\nu^2}{2}\right)\nu$ with ν being a real variable and μ being a positive constant.

Remark 4.3 To explain the meaning of (4.4), note that in the mixed situation in which some control directions are known and some are unknown, it is not appropriate to adopt the standard Nussbaum function for every agent. This is because, differently from the hybrid Nussbaum function in (4.4), a standard Nussbaum function typically does not guarantee a boundedness of the summation of multiple Nussbaum integral terms [37, 125].

The following result is proposed to establish boundedness of a Lyapunov function when a hybrid Nussbaum function as in (4.4) is adopted.

Lemma 4.2 Let $V_i(\cdot)$ be a smooth positive definite function with bounded initial value $V_i(0)$. Let $\xi_{i,n}(t)$ for $n = 1,2,\ldots,n_i$, be smooth and increasing functions with their initial values $\xi_{i,n}(0)$ bounded. Furthermore, let $\psi_{i,n}(\cdot)$ be a time-varying gain, nonzero in the closed interval $\left[\underline{\psi}_{i,n}, \overline{\psi}_{i,n}\right]$ for $i = 1,2,\ldots,N$. If the following inequality holds:

$$\begin{aligned} V_i(t) \leq & \sum_{n=1}^{n_i} \int_0^t \psi_{i,n}(\nu)\theta_{i,n}\mathcal{N}_R\left(\xi_{i,n}(\nu)\right)\dot{\xi}_{i,n}(\nu) \\ & + \sum_{n=1}^{n_i} \int_0^t \iota_i \dot{\xi}_{i,n}(\nu)\, d\nu + \varpi_i, \end{aligned} \tag{4.5}$$

where ι_i and ϖ_i are constants, $\theta_{i,n}$ is a positive and bounded function, and $\mathcal{N}_R(\cdot)$ as in (4.4), then $\xi_{i,n}(\cdot)$, $V_i(\cdot)$, and $\sum_{n=1}^{n_i}\int_0^t\left(\psi_{i,n}(\nu)\theta_{i,n}\mathcal{N}_R\left(\xi_{i,n}(\nu)\right)+\iota_i\right)\dot{\xi}_{i,n}(\nu)\, d\nu$ are bounded on the time interval $[0, t_\nu)$ for $i = 1,2,\ldots,N$.

Proof. The main idea is to prove the boundedness of ξ_n on $[0, t_\nu)$ through seeking a contradiction.

For simplicity, the index i is removed in the following analysis. Without loss of generality, let us assume $\xi_1(\cdot), \ldots, \xi_\lambda(\cdot)$ are unbounded and $\xi_{\lambda+1}(\cdot), \ldots, \xi_{n_i}(\cdot)$ are bounded for $1 \leq \lambda \leq n_i$. We first rewrite (4.5) as

$$\begin{aligned} V\left(\xi_i,\xi_j\right) = & \sum_{n=1}^{l}\left\{\int_{\xi_i}^{\xi_j} \mathcal{N}_R^{\overline{1}}(\xi_n(\nu))\theta_n\psi_n(\nu)d\xi_n(\nu)\right\} + \sum_{n=1}^{n_i}\int_{\xi_i}^{\xi_j}\iota_n d\xi_n(\nu) \\ & + \sum_{n=l+1}^{n_i}\left\{\int_{\xi_i}^{\xi_j}\theta_n\mathcal{N}_R^{\overline{2}}(\xi_n(\nu))\psi_n(\nu)d\xi_n(\nu)\right\}, \end{aligned} \tag{4.6}$$

where we have used the following notation for compactness: $V(\xi_i,\xi_j) = V(\xi(t_i),\xi(t_j)) = V(t_i,t_j)$. At this point, two situations should be taken into account: the first one is when

$\xi_n(\cdot)$ has no upper bound on $[0, t_v)$; the second one is when $\xi_n(\cdot)$ has no lower bound on $[0, t_v)$.

1) *Situation 1:* $\xi_n(\cdot)$ has no upper bound on $[0, t_v)$ for $1 \le n \le \lambda$. Let us first consider the case $\psi_n(t) > 0$. Following the method in [14], we construct three increasing time sequences $\{t_\varrho\}$, $\{t'_\varrho\}$, and $\{t''_\varrho\}$ defined by $t_\varrho = \min_{1\le n\le\lambda}\{t : \xi_n(t) = (2\varrho+1)\pi\}$, $t'_\varrho = \min_{1\le n\le\lambda}\{t : \xi_n(t) = (2\varrho-1)\pi\}$ and $t''_\varrho = \min_{1\le n\le\lambda}\{t : \xi_n(t) = 2\varrho\pi\}$. It follows from above definitions that there exists a set $\Omega_\varrho = \{\omega_\varrho\} \subset \mathscr{R}^{\omega_\varrho}$ satisfying $\xi_n(t_\varrho) = (2n+1)\pi$ for $\omega_\varrho \in [1, \lambda]$. To facilitate later analysis, we define sets $\Omega'_\varrho \subset \mathscr{R}^{\omega'_\varrho}$ and $\Omega''_\varrho \subset \mathscr{R}^{\omega_\varrho - \omega'_\varrho}$, where $\omega'_\varrho \in [0, \omega_\varrho]$. Furthermore, the bound $\xi_n(t_\varrho) \le (2\varrho+1)\pi$ holds if n is not from Ω_ϱ. The following steps are standard in Nussbaum-based control literature [14] and we shall provide only the main steps for compactness. Using above definitions, (4.6) can be expressed by

$$\begin{aligned} V\big(\xi_n(t_\varrho)\big) \le & \sum_{n=1, n\notin\Omega_\varrho}^{\lambda}\left\{\int_0^{\xi_n(t_\varrho)} \psi_n(\nu)\theta_n \mathscr{N}_R(\xi_n(\nu))d\xi_n(\nu)\right\} + \sum_{n=0}^{\lambda}\xi_n(t_\varrho)\iota_n \\ & + \sum_{k=0, k\in\Omega'_{\varrho'}}^{\omega'_\varrho}\left\{\int_0^{\xi_k(t_\varrho)} \psi_k(\nu)\theta_k \mathscr{N}_R^{\bar{1}}(\xi_k(\nu))d\xi_k(\nu)\right\} + \Sigma \\ & + \sum_{k=0, k\in\Omega''_\varrho}^{\omega''_\varrho}\int_0^{\xi_k(t_\varrho)}\left\{\mathscr{N}_R^{\bar{2}}(\xi_k(\nu))\psi_k(\nu)\theta_k d\xi_k(\nu)\right\}, \end{aligned} \tag{4.7}$$

where $\Sigma = \sum_{n=\lambda+1}^{n_i}\int_0^{\xi_n(t_\varrho)}\psi_n(\nu)\mathscr{N}_R(\xi_n(\nu))d\xi_n(\nu) + \sum_{n=\lambda+1}^{n_i}(\xi_n(t_\varrho))\iota_n$ and $\xi_n(0) = 0$. The function $V(\xi_n(\cdot))$ can be further bounded as

$$\begin{aligned} V\big(\xi_n(t_\varrho)\big) \le & \sum_{n=1}^{\lambda}\left\{\int_0^{\xi_n(t'_\varrho)} \psi_n(\nu)\theta_n \mathscr{N}_R(\xi_n(\nu))d\xi_n(\nu)\right\} + \sum_{n=0}^{\lambda}\xi_n(t_\varrho)\iota_n \\ & + \sum_{n=1, k\notin\Omega_{\varrho''}}^{\lambda}\left\{\int_{2\varrho\pi-\pi}^{2\varrho\pi} \overline{\phi}^\star |\mathscr{N}_R^{\bar{1}}(\nu)|d\nu\right\} + \Sigma \\ & + \sum_{k=1, k\in\Omega_\varrho}^{\omega_\varrho}\int_{2\varrho\pi}^{2\varrho\pi+\pi} \underline{\phi}^\star \mathscr{N}_R(\nu)d\nu, \end{aligned} \tag{4.8}$$

where $\overline{\phi}^\star = \overline{\psi}_n\overline{\theta}_n$ and $\underline{\phi}^\star = \underline{\psi}_n\underline{\theta}_n$ with $\overline{\theta}_n > 0$ and $\underline{\theta}_n > 0$ being the upper and lower bounds of θ_n for $1 \le n \le n_i$, respectively. Note that the integral value of $\mathscr{N}_R(\nu)$ (represented by $\mathscr{N}_T(\nu)$) on $[0, t_v)$ is

$$\mathscr{N}_T(\nu) = \begin{cases} -\mu\big(1+\exp(\frac{\nu^2}{2})(\nu\sin(\nu)-\cos(\nu))\big), & \text{if the control direction is unknown} \\ 1-\exp(\frac{\nu^2}{2}), & \text{otherwise.} \end{cases} \tag{4.9}$$

Substituting (4.9) into (4.8) and after arrangements gives

$$\begin{aligned} V\big(\xi_n(t_\varrho)\big) = & \sum_{n=1}^{\lambda}\left\{\int_0^{\xi_n(t'_\varrho)} \psi_n(\nu)\theta_n \mathscr{N}_R(\xi_n(\nu))d\xi_n(\nu)\right\} + (2\varrho+1)\pi\lambda\iota_{\max} \\ & \times\left\{\Im^\star\exp\Big(\frac{(4\varrho+1)\pi^2}{2}\Big) - \epsilon^\star\overline{\phi}^\star\mu\right\} - \exp\Big(\frac{4\varrho^2\pi^2}{2}\Big) \\ & - \exp\Big(\frac{(2\varrho-1)^2\pi^2}{2}\Big)\left\{\Im^\star\exp\Big(\frac{(4\varrho-1)\pi^2}{2}\Big) - \epsilon^\star\overline{\phi}^\star\right\} + \Sigma, \end{aligned} \tag{4.10}$$

where $\Im^\star = \omega_\varrho' \exp(-t^\star\mu^\star)\mu + (\omega_\varrho - \omega_\varrho')\phi^\star \exp(-t^\star\mu^\star)$ with $t^\star = t_\varrho - t_\varrho''$, $\epsilon^\star = \lambda + \omega_\varrho' - \omega_\varrho$ and $\iota_{\max} = \max_{1\le n\le n_i}\{\iota_n\}$. Apparently, the terms on the right hand of (4.10) (except the first term) approach to negative infinity as $\varrho \to +\infty$. For the first term in (4.10), we define three sequences $\{t_\varrho^{2\pi}\}$, $\{t_\varrho^{4\pi}\}$, and $\{t_\varrho^{(2\varrho-4)\pi}\}$ defined by $t_\varrho^{2\pi} = \min_{1\le n\le\lambda}\{t : \xi_n(t) = 2\pi\}$, $t_\varrho^{4\pi} = \min_{1\le n\le\lambda}\{t : \xi_n(t) = 4\pi\}$ and $t_\varrho^{(2\varrho-4)\pi} = \min_{1\le n\le\lambda}\{t : \xi_n(t) = (2\varrho-4)\pi\}$. Then, it can be deduced that the value of the first term approaches to zero as $\varrho \to +\infty$. To this end, one can conclude that

$$V\big(\xi_n(t_\varrho)\big) \longrightarrow -\infty \quad \text{as} \quad \varrho \longrightarrow +\infty \tag{4.11}$$

which leads to a contradiction with the fact that $V(\cdot)$ is predesigned to be non-negative. As a result, $\xi_n(t)$, $1 \le n \le n_i$, are upper bounded.

2) *Situation 2:* $\xi_n(\cdot)$ has no lower bound on $[0, t_v)$ for $1 \le n \le \lambda$. The proof is similar to Situation 1 and thus it is omitted. ■

Remark 4.4 Similarly to the lemmas in [14, 17, 29, 31, 53, 127], the proposed Lemma 4.2 holds over a finite time interval. Extending such lemmas to the whole time domain is not trivial, as discussed in [37]. Nevertheless, works such as [81] have shown that boundedness on the entire time domain can be obtained during stability analysis, by using continuation of the maximal solution of the closed-loop system. In this work we will adopt a similar argument to obtain stability (cf. proof of Theorem 4.1).

4.3. Proposed Distributed Consensus Design

To start the design, let us define $p_i = \max_{1\le m\le n_i}\{p_{i,m}\}$ and let us define the following changes of coordinates

$$\begin{cases} s_{i,1} = \sum_{l\in\bar{\mathcal{N}}_i} a_{il}(y_i - y_l) + \mu_i(y_i - y_r), \\ s_{i,m} = \chi_{i,m} - \alpha_{i,m}, \quad m = 2,3,\ldots,n_i, \end{cases} \tag{4.12}$$

where $\alpha_{i,m}$ represents the virtual control law which will be specified later. After defining $s_1 = \big[s_{1,1}, s_{2,1}, \ldots, s_{N,1}\big]^T \in \mathbb{R}^N$, one has $s_1 = (\overline{\mathscr{L}} + \mathscr{B})\delta$ where $\delta = \overline{y} - \overline{y}_r$ with $\overline{y} = \big[y_1, y_2, \ldots, y_N\big]^T$ and $\overline{y}_r = \big[y_r, y_r, \ldots, y_r\big]^T$. Due to the nonsingularity of $\overline{\mathscr{L}} + \mathscr{B}$, it holds that $\|\delta\| \le \frac{\|s_1\|}{\sigma_{\min}(\overline{\mathscr{L}}+\mathscr{B})}$, where $\sigma_{\min}(\overline{\mathscr{L}} + \mathscr{B})$ is the minimum singular value of $\overline{\mathscr{L}} + \mathscr{B}$.

The design proceeds iteratively along the following steps.

Step 1 for the i-th agent ($i \in \{1,\ldots,N\}$): Using (4.1) and (4.12), we obtain the time derivative of $s_{i,1}$ as

$$\dot{s}_{i,1} = \big(d_i + \mu_i\big)\psi_{i,1}^k(\chi_{i,1})\chi_{i,2}^{p_{i,1}} + F_{i,1}^k(\boldsymbol{Z}_{i,1}),\ k \in \mathscr{M}_i, \tag{4.13}$$

where $\boldsymbol{Z}_{i,1} = [\chi_{i,1}, \chi_{l,1}, \chi_{l,2}]^T (l \in \bar{\mathcal{N}}_i)$ and

$$\begin{aligned} F_{i,1}^k(\boldsymbol{Z}_{i,1}) = &-\sum_{l\in\bar{\mathcal{N}}_i} a_{il}(\psi_{l,1}^k(\chi_{l,1})\chi_{l,2}^{p_{l,1}} + \phi_{l,1}^k(\chi_{l,1})) \\ &+ (d_i + \mu_i)\phi_{i,1}^k(\chi_{l,1}) - \mu_i\dot{y}_r. \end{aligned} \tag{4.14}$$

From Lemma 2.2.1, it follows that the unknown continuous function $F_{i,1}^k(\cdot)$ can be approximated by an RBF NN as

$$F_{i,1}^k(\boldsymbol{Z}_{i,1})=\boldsymbol{W}_{i,1}^{k*T}\boldsymbol{\varphi}_{i,1}^k(\boldsymbol{Z}_{i,1})+\varepsilon_{i,1}^k(\boldsymbol{Z}_{i,1}),$$

where $\left|\varepsilon_{i,1}^k(\boldsymbol{Z}_{i,1})\right|\leq\bar{\varepsilon}_{i,1}^k$ includes both the bounded approximation error and the bounded $\dot{y}_r$.

According to Lemma 2.2, it holds that

$$\begin{aligned}s_{i,1}^{p_i-p_{i,1}+3}F_{i,1}^k\leq&\frac{p_i-p_{i,1}+3}{p_i+3}\nu_{i,1}^{\frac{p_i+3}{p_i-p_{i,1}+3}}s_{i,1}^{p_i+3}\left\|\boldsymbol{W}_{i,1}^{k*}\right\|^{\frac{p_i+3}{p_i-p_{i,1}+3}}\left\|\boldsymbol{\varphi}_{i,1}^k\right\|^{\frac{p_i+3}{p_i-p_{i,1}+3}}\\&+\frac{p_{i,1}}{p_i+3}\varsigma_{i,1}^{-\frac{p_i+3}{p_{i,1}}}\bar{\varepsilon}_{i,1}^{k\frac{p_i+3}{p_{i,1}}}+\frac{p_{i,1}}{p_i+3}\ell_{i,1}^{-\frac{p_i+3}{p_{i,1}}}+\frac{p_i-p_{i,1}+3}{p_i+3}\varsigma_{i,1}^{\frac{p_i+3}{p_i-p_{i,1}+3}}s_{i,1}^{p_i+3}\\\leq&s_{i,1}^{p_i+3}\left(\ell_{i,1}^{\frac{p_i+3}{p_i-p_{i,1}+3}}\beta_{i,1}\left\|\boldsymbol{\varphi}_{i,1}\right\|^{\frac{p_i+3}{p_i-p_{i,1}+3}}+\varsigma_{i,1}^{\frac{p_i+3}{p_i-p_{i,1}+3}}\right)+\lambda_{i,1},\end{aligned}\tag{4.15}$$

where $\beta_{i,1}=\max\{\beta_{i,1}^k,k\in\mathscr{M}_i\}$, $\boldsymbol{\varphi}_{i,1}=\max\{\boldsymbol{\varphi}_{i,1}^k,k\in\mathscr{M}_i\}$, $\beta_{i,1}^k=\left\|\boldsymbol{W}_{i,1}^{k*}\right\|^{\frac{p_i+3}{p_i-p_{i,1}+3}}$, $\bar{\varepsilon}_{i,1}=\max\{\bar{\varepsilon}_{i,1}^k,k\in\mathscr{M}_i\}$ and $\lambda_{i,1}=\ell_{i,1}^{-\frac{p_i+3}{p_{i,1}}}+\varsigma_{i,1}^{-\frac{p_i+3}{p_{i,1}}}\bar{\varepsilon}_{i,1}^{\frac{p_i+3}{p_{i,1}}}$.

Let us start constructing the Lyapunov function as

$$V_{i,1}=\frac{s_{i,1}^{p_i-p_{i,1}+4}}{p_i-p_{i,1}+4}+\frac{1}{2\vartheta_{i,1}}\tilde{\beta}_{i,1}^2,\tag{4.16}$$

where $\tilde{\beta}_{i,1}=\beta_{i,1}-\hat{\beta}_{i,1}$ and $\vartheta_{i,1}>0$ is a design parameter.

It follows from (4.13), (4.15) and (4.16) that the time derivative of $V_{i,1}$ is

$$\begin{aligned}\dot{V}_{i,1}\leq&s_{i,1}^{p_i-p_{i,1}+3}\left(d_i+\mu_i\right)\left(\psi_{i,1}^k(\chi_{i,1})\alpha_{i,2}^{p_{i,1}}+s_{i,1}^{p_{i,1}}\tau_{i,1}\right)-s_{i,1}^{p_i+3}\left(d_i+\mu_i\right)\tau_{i,1}\\&-\frac{\tilde{\beta}_{i,1}\dot{\hat{\beta}}_{i,1}}{\vartheta_{i,1}}+s_{i,1}^{p_i+3}\ell_{i,1}^{\frac{p_i+1}{p_i-p_{i,1}+3}}\beta_{i,1}\left\|\boldsymbol{\varphi}_{i,1}\right\|^{\frac{p_i+3}{p_i-p_{i,1}+3}}+s_{i,1}^{p_i+3}\varsigma_{i,1}^{\frac{p_i+3}{p_i-p_{i,1}+3}}+\lambda_{i,1}\\&+s_{i,1}^{p_i-p_{i,1}+3}\left(d_i+\mu_i\right)\psi_{i,1}^k(\chi_{i,1})\left(\chi_{i,2}^{p_{i,1}}-\alpha_{i,2}^{p_{i,1}}\right).\end{aligned}\tag{4.17}$$

Design the virtual controllers $\alpha_{i,2}$ and adaptive laws $\hat{\beta}_{i,1}$ as

$$\alpha_{i,2}=\mathscr{N}_R^{\frac{1}{p_{i,1}}}(\xi_{i,1})\tau_{i,1}^{\frac{1}{p_{i,1}}}s_{i,1},\tag{4.18}$$

$$\tau_{i,1}=\left(d_i+\mu_i\right)^{-1}\left(\ell_{i,1}^{\frac{p_i+3}{p_i-p_{i,1}+3}}\hat{\beta}_{i,1}\left\|\boldsymbol{\varphi}_{i,1}\right\|^{\frac{p_i+3}{p_i-p_{i,1}+3}}+c_{i,1}+\varsigma_{i,1}^{\frac{p_i+3}{p_i-p_{i,1}+3}}\right),\tag{4.19}$$

$$\dot{\xi}_{i,1}=s_{i,1}^{p_i+3}\left(d_i+\mu_i\right)\tau_{i,1},\tag{4.20}$$

$$\dot{\hat{\beta}}_{i,1}=\vartheta_{i,1}\ell_{i,1}^{\frac{p_i+3}{p_i-p_{i,1}+3}}s_{i,1}^{p_i+3}\left\|\boldsymbol{\varphi}_{i,1}\right\|^{\frac{p_i+3}{p_i-p_{i,1}+3}}-\gamma_{i,1}\hat{\beta}_{i,1},\tag{4.21}$$

where $\ell_{i,1}$, $c_{i,1}$, $\gamma_{i,1}$, and $\varsigma_{i,1}$ are positive design parameters.

Substituting(4.18), (4.19), (4.20), and (4.21) into (4.17) yields

$$\begin{aligned}\dot{V}_{i,1} \leq & s_{i,1}^{p_i-p_{i,1}+3}\left(d_i+\mu_i\right)\psi_{i,1}(\chi_{i,1})\left(\chi_{i,2}^{p_{i,1}}-\alpha_{i,2}^{p_{i,1}}\right)+\frac{1}{\vartheta_{i,1}}\gamma_{i,1}\tilde{\beta}_{i,1}\hat{\beta}_{i,1}\\ & +\dot{\xi}_{i,1}\left(\psi_{i,1}(\chi_{i,1})\mathcal{N}_R(\xi_{i,1})+1\right)+\lambda_{i,1}-c_{i,1}s_{i,1}^{p_i+3}.\end{aligned} \tag{4.22}$$

By using Lemmas (2.3) and (2.2), we have that

$$\begin{aligned}\left|s_{i,1}^{p_i-p_{i,1}+3}\psi_{i,1}(\chi_{i,1})\left(\chi_{i,2}^{p_{i,1}}-\alpha_{i,2}^{p_{i,1}}\right)\right| \leq & \frac{\eta_{i,1}^{-p_i}s_{i,2}^{p_i+3}}{p_i+3}\left(p_{i,1}\overline{\phi}_{i,1}\mathcal{N}_R^{\frac{1}{p_{i,1}}}(\xi_{i,1})\tau_{i,1}^{\frac{p_{i,1}-1}{p_{i,1}}}\right)^{p_i+3}\\ & +\frac{p_{i,1}s_{i,2}^{p_i+3}}{p_i+3}\eta_{i,1}^{-\frac{p_i-p_{i,1}+3}{p_{i,1}}}\left(2^{p_{i,1}-2}p_{i,1}\overline{\phi}_{i,1}\right)^{\frac{p_i+3}{p_{i,1}}}\\ & +\frac{\eta_{i,1}^{-p_i}s_{i,2}^{p_i+3}}{p_i+3}\left(2^{p_{i,1}-2}p_{i,1}\overline{\phi}_{i,1}\tau_{i,1}^{p_{i,1}-1}\right)^{p_i+3}\\ & +\frac{p_i-p_{i,1}+7}{p_i+3}\eta_{i,1}s_{i,1}^{p_i+1}+\frac{2p_i\eta_{i,1}s_{i,1}^{p_i+1}}{p_i+3}\\ \leq & s_{i,1}^{p_i+3}+\left(d_i+\mu_i\right)^{-1}s_{i,2}^{p_i+3}\Theta_{i,1}\end{aligned} \tag{4.23}$$

with $\eta_{i,1}=\frac{p_i+3}{3p_i-p_{i,1}+7}$ and $\Theta_{i,1}$ a function given by

$$\begin{aligned}\Theta_{i,1}=\left(d_i+\mu_i\right)\Big[& \frac{p_{i,1}}{p_i+3}\eta_{i,1}^{-\frac{p_i-p_{i,1}+3}{p_{i,1}}}\left(2^{p_{i,1}-2}p_{i,1}\overline{\phi}_{i,1}\right)^{\frac{p_i+3}{p_{i,1}}}\\ & +\frac{1}{p_i+3}\eta_{i,1}^{-p_i}\left(p_{i,1}\overline{\phi}_{i,1}\mathcal{N}_R^{\frac{1}{p_{i,1}}}(\xi_{i,1})\tau_{i,1}^{\frac{p_{i,1}-1}{p_{i,1}}}\right)^{p_i+3}\\ & +\frac{1}{p_i+3}\eta_{i,1}^{-p_i}\left(2^{p_{i,1}-2}p_{i,1}\overline{\phi}_{i,1}\tau_{i,1}^{p_{i,1}-1}\right)^{p_i+3}\Big].\end{aligned}$$

From (4.23), the time derivative of $V_{i,1}$ can be rewritten as

$$\begin{aligned}\dot{V}_{i,1} \leq & \frac{\gamma_{i,1}}{\vartheta_{i,1}}\tilde{\beta}_{i,1}\hat{\beta}_{i,1}-\left(c_{i,1}-\left(d_i+\mu_i\right)\right)s_{i,1}^{p_i+3}+s_{i,2}^{p_i+3}\Theta_{i,1}\\ & +\dot{\xi}_{i,1}\left(\psi_{i,1}(\chi_{i,1})\mathcal{N}_R(\xi_{i,1})+1\right)+\lambda_{i,1}.\end{aligned} \tag{4.24}$$

Defining $\psi_{i,1}=\max\{\psi_{i,1}^k, k\in\mathcal{M}_i\}$ and using Young's inequality

$$\tilde{\beta}_{i,1}\hat{\beta}_{i,1}=\left(\tilde{\beta}_{i,1}\beta_{i,1}-\tilde{\beta}_{i,1}^2\right)\leq\frac{1}{2}\left(\beta_{i,1}^2-\tilde{\beta}_{i,1}^2\right) \tag{4.25}$$

it can be obtained that $\dot{V}_{i,1}$ satisfies

$$\begin{aligned}\dot{V}_{i,1} \leq & \dot{\xi}_{i,1}\left(\psi_{i,1}(\chi_{i,1})\mathcal{N}_R(\xi_{i,1})+1\right)+s_{i,2}^{p_i+3}\Theta_{i,1}+\frac{\gamma_{i,1}}{2\vartheta_{i,1}}\left(\beta_{i,1}^2-\tilde{\beta}_{i,1}^2\right)\\ & -\left(c_{i,1}-\left(d_i+\mu_i\right)\right)s_{i,1}^{p_i+3}+\lambda_{i,1}.\end{aligned} \tag{4.26}$$

Step m for the i-th agent $\left(i \in \{1,\ldots,N\},\ m \in \{2,\ldots,n_i-1\}\right)$: From (4.1) and (4.12), the time derivative of $s_{i,m}$ is given by

$$\dot{s}_{i,m} = \psi_{i,m}^{k}(\overline{\boldsymbol{\chi}}_{i,m})\chi_{i,m+1}^{p_{i,m}} + F_{i,m}^{k}(\boldsymbol{Z}_{i,m}),\ k \in \mathscr{M}_i, \tag{4.27}$$

where $\boldsymbol{Z}_{i,m} = [\overline{\boldsymbol{\chi}}_{i,m}^{T}, \overline{\boldsymbol{\chi}}_{l,m}^{T}, \overline{\hat{\beta}}_{i,m-1}, \overline{\xi}_{i,m-1}, y_r]^{T}\left(l \in \mathscr{N}_i\right)$, $\overline{\hat{\beta}}_{i,m-1} = [\hat{\beta}_{i,1}, \hat{\beta}_{i,2}, \ldots, \hat{\beta}_{i,m-1}]$, $\overline{\xi}_{i,m-1} = [\xi_{i,1}, \xi_{i,2}, \ldots, \xi_{i,m-1}]$ and

$$\begin{aligned} F_{i,m}^{k}(\boldsymbol{Z}_{i,m}) = &-\sum_{n=1}^{m-1}\sum_{l\in\mathscr{N}_i}\frac{\partial\alpha_{i,m}}{\partial\chi_{l,n}}\left(\psi_{l,n}^{k}(\overline{\boldsymbol{\chi}}_{l,n})\chi_{l,n+1}^{p_{l,n}} + \phi_{l,n}^{k}(\overline{\boldsymbol{\chi}}_{l,n})\right) \\ &-\sum_{n=1}^{m-1}\frac{\partial\alpha_{i,m}}{\partial\chi_{i,n}}\left(\psi_{i,n}^{k}(\overline{\boldsymbol{\chi}}_{i,n})\chi_{i,n+1}^{p_{i,n}} + \phi_{i,n}^{k}(\overline{\boldsymbol{\chi}}_{i,n})\right) \\ &-\frac{\partial\alpha_{i,m}}{\partial y_r}\dot{y}_r - \sum_{n=1}^{m-1}\frac{\partial\alpha_{i,m}}{\partial\hat{\beta}_{i,n}}\dot{\hat{\beta}}_{i,n} \\ &-\sum_{n=1}^{m-1}\frac{\partial\alpha_{i,m}}{\partial\xi_{i,n}}\dot{\xi}_{i,n} + \phi_{i,m}^{k}(\overline{\boldsymbol{\chi}}_{i,m}) \end{aligned} \tag{4.28}$$

Along similar lines as Step 1, the following inequality holds:

$$\begin{aligned} &s_{i,m}^{p_i-p_{i,m}+3}F_{i,m}^{k}(\boldsymbol{Z}_{i,m}) \le s_{i,m}^{p_i+3}\varsigma_{i,m}^{\frac{p_i+3}{p_i-p_{i,m}+3}} + \lambda_{i,m} \\ &+ s_{i,m}^{p_i+3}\ell_{i,m}^{\frac{p_i+3}{p_i-p_{i,m}+3}}\beta_{i,m}\left\|\boldsymbol{\varphi}_{i,m}\right\|^{\frac{p_i+3}{p_i-p_{i,m}+3}}, \end{aligned} \tag{4.29}$$

where $\beta_{i,m}^{k} = \left\|\boldsymbol{W}_{i,m}^{k*}\right\|^{\frac{p_i+3}{p_i-p_{i,m}+3}}$, $\beta_{i,m} = \max\{\beta_{i,m}^{k}, k \in \mathscr{M}_i\}$, $\boldsymbol{\varphi}_{i,m} = \max\{\boldsymbol{\varphi}_{i,m}^{k}, k \in \mathscr{M}_i\}$, $\overline{\varepsilon}_{i,m} = \max\{\overline{\varepsilon}_{i,m}^{k}, k \in \mathscr{M}_i\}$, and $\lambda_{i,m} = \ell_{i,m}^{-\frac{(p_i+3)}{p_{i,m}}} + \varsigma_{i,m}^{-\frac{(p_i+3)}{p_{i,m}}}\overline{\varepsilon}_{i,m}^{\frac{(p_i+3)}{p_{i,m}}}$.

Starting from (4.16), the Lyapunov function is constructed iteratively as

$$V_{i,m} = V_{i,m-1} + \frac{s_{i,m}^{p_i-p_{i,m}+4}}{p_i-p_{i,m}+4} + \frac{1}{2\vartheta_{i,m}}\tilde{\beta}_{i,m}^{2}, \tag{4.30}$$

where $\tilde{\beta}_{i,m} = \beta_{i,m} - \hat{\beta}_{i,m}$ and $\vartheta_{i,m} > 0$ is a design constant.

Combining (4.26), (4.27), (4.29) with (4.30), the time derivative of $V_{i,m}$ is written as

$$\begin{aligned} \dot{V}_{i,m} \le &s_{i,m}^{p_i+3}\Theta_{i,m-1} - s_{i,m}^{p_i-p_{i,m}+3}\psi_{i,m}^{k}(\overline{\boldsymbol{\chi}}_{i,m})\alpha_{i,m+1}^{p_{i,m}} + \sum_{n=1}^{m-1}\left(\frac{\gamma_{i,n}}{2\vartheta_{i,n}}(\beta_{i,n}^{2} - \tilde{\beta}_{i,n}^{2})\right) \\ &+ s_{i,m}^{p_i-p_{i,m}+3}\psi_{i,m}(\overline{\boldsymbol{\chi}}_{i,m})\left(\chi_{i,m+1}^{p_{i,m}} - \alpha_{i,m+1}^{p_{i,m}}\right) - \frac{\tilde{\beta}_{i,m}\dot{\hat{\beta}}_{i,m}}{\vartheta_{i,m}} + s_{i,m}^{p_i+3}\varsigma_{i,m}^{\frac{p_i+3}{p_i-p_{i,m}+3}} \\ &+ s_{i,m}^{p_i+3}\ell_{i,m}^{\frac{p_i+3}{p_i-p_{i,m}+3}}\beta_{i,m}\left\|\boldsymbol{\varphi}_{i,m}\right\|^{\frac{p_i+3}{p_i-p_{i,m}+3}} + \sum_{n=1}^{m-1}\dot{\xi}_{i,n}\left(\psi_{i,n}(\overline{\boldsymbol{\chi}}_{i,n})\mathscr{N}_R(\xi_{i,n}) + 1\right) \\ &+ \sum_{n=1}^{m}\lambda_{i,n} - (c_{i,1} - (d_i+\mu_i))s_{i,1}^{p_i+3} - \sum_{n=2}^{m-1}(c_{i,n}-1)s_{i,n}^{p_i+3}. \end{aligned} \tag{4.31}$$

Design the virtual controllers $\alpha_{i,m+1}$ and adaptive laws $\hat{\beta}_{i,m}$ as

$$\alpha_{i,m+1} = \mathscr{N}_R^{\frac{1}{p_{i,m}}}(\xi_{i,m})s_{i,m}\tau_{i,m}^{\frac{1}{p_{i,m}}}, \tag{4.32}$$

$$\tau_{i,m}=c_{i,m}+\ell_{i,m}^{\frac{p_i+3}{p_i-p_{i,m}+3}}\hat{\beta}_{i,m}\|\boldsymbol{\varphi}_{i,m}\|^{\frac{p_i+3}{p_i-p_{i,m}+3}}+\Theta_{i,m-1}+\varsigma_{i,m}^{\frac{p_i+3}{p_i-p_{i,m}+3}},$$

$$\dot{\xi}_{i,m}=s_{i,m}^{p_i+3}\tau_{i,m}, \tag{4.33}$$

$$\dot{\hat{\beta}}_{i,m}=\vartheta_{i,m}\ell_{i,m}^{\frac{p_i+3}{p_i-p_{i,m}+3}}s_{i,m}^{p_i+3}\|\boldsymbol{\varphi}_{i,m}\|^{\frac{p_i+3}{p_i-p_{i,m}+3}}-\gamma_{i,m}\hat{\beta}_{i,m}, \tag{4.34}$$

where $\ell_{i,m}$, $c_{i,m}$, $\gamma_{i,m}$, and $\varsigma_{i,m}$ are positive design parameters.

Substituting (4.32), (4.33), and (4.34) into (4.31) and along similar lines as (4.23)-(4.25), we can obtain the time derivative of $V_{i,m}$ as

$$\begin{aligned}\dot{V}_{i,m}\leq{}&s_{i,m+1}^{p_i+3}\Theta_{i,m}-\big(c_{i,1}-(d_i+\mu_i)\big)s_{i,1}^{p_i+3}+\sum_{n=1}^{m}\left(\frac{\gamma_{i,n}}{2\vartheta_{i,n}}\Big(\beta_{i,n}^2-\tilde{\beta}_{i,n}^2\Big)\right)\\&+\sum_{n=1}^{m}\lambda_{i,n}-\sum_{n=2}^{m}(c_{i,n}-1)s_{i,n}^{p_i+3}+\sum_{n=1}^{m}\dot{\xi}_{i,n}\big(\psi_{i,n}(\overline{\boldsymbol{\chi}}_{i,n})\mathcal{N}_R(\xi_{i,n})+1\big).\end{aligned} \tag{4.35}$$

where $\psi_{i,m}=\max\left\{\psi_{i,m}^k,k\in\mathcal{M}_i\right\}$.

Step n_i for the i-th agent ($i\in\{1,\ldots,N\}$): In view of Lemma 3.1 and using (4.1), (4.3), and (4.12), the time derivative of s_{i,n_i} can be written as

$$\dot{s}_{i,n_i}\leq\psi_{i,n_i}^k(\chi_i)\zeta_{1,f}\kappa_i^{p_{i,n_i}}u_i^{p_{i,n_i}}+F_{i,n_i}^k(\boldsymbol{Z}_{i,n_i}),\ k\in\mathcal{M}_i, \tag{4.36}$$

where $\boldsymbol{Z}_{i,n_i}=\big[\chi_i^T,\chi_l^T,\overline{\hat{\beta}}_{i,n_i-1},\overline{\xi}_{i,n_i-1},y_r\big]^T\big(l\in\bar{\mathcal{N}}_i\big)$, $\overline{\hat{\beta}}_{i,n_i-1}=\big[\hat{\beta}_{i,1},\hat{\beta}_{i,2},\ldots,\hat{\beta}_{i,n_i-1}\big]$, $\overline{\xi}_{i,n_i-1}=\big[\xi_{i,1},\xi_{i,2},\ldots,\xi_{i,n_i-1}\big]$ and

$$\begin{aligned}F_{i,n_i}^k(\boldsymbol{Z}_{i,n_i})=&-\sum_{n=1}^{n_i-1}\sum_{l\in\bar{\mathcal{N}}_i}\frac{\partial\alpha_{i,n_i}}{\partial\chi_{l,n}}\Big(\psi_{l,n}^k(\overline{\boldsymbol{\chi}}_{l,n})\chi_{l,n+1}^{p_{l,n}}+\phi_{l,n}^k(\chi_l)\Big)\\&-\sum_{n=1}^{n_i-1}\frac{\partial\alpha_{i,n_i}}{\partial\chi_{i,n}}\Big(\psi_{i,n}^k(\overline{\boldsymbol{\chi}}_{i,n})\chi_{i,n+1}^{p_{i,n}}+\phi_{i,n}^k(\chi_i)\Big)\\&-\sum_{n=1}^{n_i-1}\frac{\partial\alpha_{i,n_i}}{\partial\hat{\beta}_{i,n}}\dot{\hat{\beta}}_{i,n}-\frac{\partial\alpha_{i,m}}{\partial y_r}\dot{y}_r+\phi_{i,n_i}^k(\chi_i)\\&-\sum_{n=1}^{n_i-1}\frac{\partial\alpha_{i,n_i}}{\partial\xi_{i,n}}\dot{\xi}_{i,n}+\psi_{i,n_i}^k(\chi_i)\zeta_{2,f}\Delta_i(t)^{p_{i,n_i}}.\end{aligned} \tag{4.37}$$

Similar to Step f,m, it can be obtained that

$$\begin{aligned}&s_{i,n_i}^{p_i-p_{i,n_i}+3}F_{i,n_i}^k(\boldsymbol{Z}_{i,n_i})\\&\leq s_{i,n_i}^{p_i+3}\varsigma_{i,n_i}^{\frac{p_i+3}{p_i-p_{i,n_i}+3}}+\lambda_{i,n_i}+s_{i,n_i}^{p_i+3}\ell_{i,n_i}^{\frac{p_i+3}{p_i-p_{i,n_i}+3}}\beta_{i,n_i}\|\boldsymbol{\varphi}_{i,n_i}\|^{\frac{p_i+3}{p_i-p_{i,n_i}+3}},\end{aligned} \tag{4.38}$$

where $\beta_{i,n_i}^k=\|\boldsymbol{W}_{i,n_i}^{k*}\|^{\frac{p_i+3}{p_i-p_{i,n_i}+3}}$, $\beta_{i,n_i}=\max\{\beta_{i,n_i}^k,k\in\mathcal{M}_i\}$, $\boldsymbol{\varphi}_{i,n_i}=\max\{\boldsymbol{\varphi}_{i,n_i}^k,k\in\mathcal{M}_i\}$, $\overline{\varepsilon}_{i,n_i}=\max\{\overline{\varepsilon}_{i,n_i}^k,k\in\mathcal{M}_i\}$ and $\lambda_{i,n_i}=\ell_{i,n_i}^{-\frac{p_i+3}{p_{i,n_i}}}+\varsigma_{i,n_i}^{-\frac{p_i+3}{p_{i,n_i}}}\overline{\varepsilon}_{i,n_i}^{\frac{p_i+3}{p_{i,n_i}}}$.

The last step in the construction of the Lyapunov function for agent i is

$$V_{i,n_i} = V_{i,n_i-1} + \frac{s_{i,n_i}^{p_i-p_{i,n_i}+4}}{p_i-p_{i,n_i}+4} + \frac{1}{2\vartheta_{i,n_i}}\tilde{\beta}_{i,n_i}^2, \tag{4.39}$$

where $\tilde{\beta}_{i,n_i} = \beta_{i,n_i} - \hat{\beta}_{i,n_i}$ and $\vartheta_{i,n_i} > 0$ is a design parameter.

The derivative of V_{i,n_i} along (4.35)-(4.39) is given by

$$\begin{aligned}
\dot{V}_{i,n_i} \leq & \sum_{n=1}^{n_i}\lambda_{i,n} + \sum_{n=1}^{n_i-1}\dot{\xi}_{i,n}\left(\psi_{i,n}(\overline{\boldsymbol{\chi}}_{i,n})\mathcal{N}_R(\xi_{i,n})+1\right) + s_{i,n_i}^{p_i+3}\varsigma_{i,n_i}^{\frac{p_i+3}{p_i-p_{i,n_i}+3}} \\
& - \sum_{n=2}^{n_i-1}(c_{i,n}-1)s_{i,n}^{p_i+3} - \left(c_{i,1}-(d_i+\mu_i)\right)s_{i,1}^{p_i+3} + \Theta_{i,n_i-1}s_{i,n_i}^{p_i+3} \\
& + \sum_{n=1}^{n_i-1}\left(\frac{\gamma_{i,n}}{2\vartheta_{i,n}}\left(\beta_{i,n}^2-\tilde{\beta}_{i,n}^2\right)\right) - \frac{\tilde{\beta}_{i,n_i}\dot{\hat{\beta}}_{i,n_i}}{\vartheta_{i,n_i}} \\
& + s_{i,n_i}^{p_i+3}\ell_{i,n_i}^{\frac{p_i+3}{p_i-p_{i,n_i}+3}}\beta_{i,n_i}\left\|\boldsymbol{\varphi}_{i,n_i}\right\|^{\frac{p_i+3}{p_i-p_{i,n_i}+3}} \\
& + s_{i,n_i}^{p_i-p_{i,n_i}+3}\psi_{i,n_i}^k(\chi_i)\zeta_{1,f}\kappa_i^{p_{i,n_i}}u_i^{p_{i,n_i}}.
\end{aligned} \tag{4.40}$$

Let us design the actual controller u_i and parameters adaption laws $\hat{\beta}_{i,n_i}$ as follows:

$$u_i = \mathcal{N}_R^{\frac{1}{p_{i,n_i}}}(\xi_{i,n_i})\tau_{i,n_i}^{\frac{1}{p_{i,n_i}}}s_{i,n_i}, \tag{4.41}$$

$$\tau_{i,n_i} = c_{i,n_i} + \ell_{i,n_i}^{\frac{p_i+3}{p_i-p_{i,n_i}+3}}\hat{\beta}_{i,n_i}\left\|\boldsymbol{\varphi}_{i,n_i}\right\|^{\frac{p_i+3}{p_i-p_{i,n_i}+3}} + \Theta_{i,n_i-1} + \varsigma_{i,n_i}^{\frac{p_i+3}{p_i-p_{i,n_i}+3}}, \tag{4.42}$$

$$\dot{\xi}_{i,n_i} = s_{i,n_i}^{p_i+3}\tau_{i,n_i}, \tag{4.43}$$

$$\dot{\hat{\beta}}_{i,n_i} = \vartheta_{i,n_i}\ell_{i,n_i}^{\frac{p_i+3}{p_i-p_{i,n_i}+3}}s_{i,n_i}^{p_i+3}\left\|\boldsymbol{\varphi}_{i,n_i}\right\|^{\frac{p_i+3}{p_i-p_{i,n_i}+3}} - \gamma_{i,n_i}\hat{\beta}_{i,n_i}, \tag{4.44}$$

where ℓ_{i,n_i}, c_{i,n_i}, λ_{i,n_i} and ς_{i,n_i} are positive design parameters.

Substituting (4.41)-(4.44) into (4.40) results in

$$\begin{aligned}
\dot{V}_{i,n_i} \leq & \sum_{n=1}^{n_i}\lambda_{i,n} + \sum_{n=1}^{n_i}\frac{\gamma_{i,n}}{2\vartheta_{i,n}}\beta_{i,n}^2 - \sum_{n=2}^{n_i}(c_{i,n}-1)s_{i,n}^{p_i+3} \\
& - \sum_{n=1}^{n_i}\frac{\gamma_{i,n}}{2\vartheta_{i,n}}\tilde{\beta}_{i,n}^2 - \left(c_{i,1}-(d_i+\mu_i)\right)s_{i,1}^{p_i+3} \\
& + \sum_{n=1}^{n_i}\dot{\xi}_{i,n}\left(\psi_{i,n}(\overline{\boldsymbol{\chi}}_{i,n})\theta_{i,n}\mathcal{N}_R(\xi_{i,n})+1\right),
\end{aligned} \tag{4.45}$$

where $\psi_{i,n_i} = \max\{\psi_{i,n_i}^k, k \in \mathcal{M}_i\}$, and when $1 \leq n \leq n_i - 1$, let $\theta_{i,n} = 1$, when $n = n_i$, let $\theta_{i,n} = \zeta_{1,f}\kappa_i^{p_{i,n_i}}$.

4.4. Stability Analysis

We are now at the position to present the main results of the proposed method in the following theorem.

Theorem 4.1 Under Assumption 4.1, consider the closed-loop multi-agent system composed by the switched power-chained form dynamics (4.1), the virtual control laws (4.18) and (4.32), the actual control law (4.41) and the parameter adaptation laws (4.21), (4.34), and (4.44). Then, it holds that: i) all signals of the closed-loop multi-agent system remain bounded; ii) the tracking error δ converges to the compact set Ω_e defined by

$$\Omega_e = \left\{ \|\delta\| \leq \sqrt{\frac{N^{N-1}\left(N^2+N-1\right)^2 \sum_{i=1}^{N} \Upsilon_i^2}{(N-1)^{N-1}}} \right\},$$

where $\Upsilon_i = \left((\Pi_i + P_i)\left(p_i - p_{i,1} + 4\right)\right)^{\frac{1}{p_i - p_{i,1}+4}}$. The constants Π_i and P_i are not given here for compactness, but they are derived during the proof.

Proof. Consider the total Lyapunov function

$$V = \sum_{i=1}^{N} V_{i,n_i} = \sum_{i=1}^{N} \sum_{m=1}^{n_i} \left(\frac{s_{i,m}^{p_i - p_{i,m}+4}}{p_i - p_{i,m}+4} + \frac{1}{2\vartheta_{i,m}} \tilde{\beta}_{i,m}^2 \right). \tag{4.46}$$

Applying Lemma 2.3 to the term $\hbar_i^{\frac{p_{i,n}-1}{p_i+3}} s_{i,n}^{p_i - p_{i,n}+4}$ with $\hbar_i > 0$ being a constant, the following inequality holds:

$$\hbar_i^{\frac{p_{i,n}-1}{p_i+3}} s_{i,n}^{p_i - p_{i,n}+4} \leq \hbar_i + s_{i,n}^{p_i+3}, (n = 1,2,\ldots,n_i). \tag{4.47}$$

Substituting (4.47) into (4.46) and synthesising previous analysis, it is possible to obtain

$$\begin{aligned} \dot{V}_{n_i} \leq & \sum_{n=1}^{n_i} \frac{\gamma_{i,n}}{2\vartheta_{i,n}} \beta_{i,n}^2 - \sum_{n=1}^{n_i} \left(c_{i,n} - \bar{\lambda}_{i,n}\right) \hbar_i^{\frac{p_{i,n}-1}{p_i+3}} s_{i,n}^{p_i - p_{i,n}+4} \\ & + \sum_{n=1}^{n_i} \lambda_{i,n} + \sum_{n=1}^{n_i} \left(c_{i,n} - \bar{\lambda}_{i,n}\right) \hbar_i - \sum_{n=1}^{n_i} \frac{\gamma_{i,n}}{2\vartheta_{i,n}} \tilde{\beta}_{i,n}^2 \\ & + \sum_{n=1}^{n_i} \dot{\xi}_{i,n} \left(\psi_{i,n}(\overline{\chi}_{i,n}) \theta_{i,n} \mathcal{N}_R(\xi_{i,n}) + 1\right), \end{aligned} \tag{4.48}$$

where $\bar{\lambda}_{i,1} = \left(d_i + \mu_i\right)$ and $\bar{\lambda}_{i,n} = 1\,(n = 2,\ldots,n_i)$.

Then, (4.48) can be further written as

$$\dot{V}_i \leq \sum_{n=1}^{n_i} \dot{\xi}_{i,n} \left(\psi_{i,n}(\overline{\chi}_{i,n}) \theta_{i,n} \mathcal{N}_R(\xi_{i,n}) + 1\right) - \mu_i V_{i,n_i} + \varrho_i, \tag{4.49}$$

where $\mu_i = \min\limits_{1 \leq n \leq n_i} \left\{ \left(p_i - p_{i,n}+4\right)\left(c_{i,n} - \bar{\lambda}_{i,n}\right) \hbar_i^{\frac{p_{i,n}-1}{p_i+3}}, \gamma_{i,n} \right\}$ and $\varrho_i = \sum\limits_{n=1}^{n_i} \left(\hbar_i \left(c_{i,n} - \bar{\lambda}_{i,n}\right) + \lambda_{i,n}\right) + \sum_{n=1}^{n_i} \frac{\gamma_{i,n}}{2\vartheta_{i,n}} \beta_{i,n}^2$.

Multiplying both sides of (4.49) by $\exp(\mu_i t)$, integrating it over $[0,t]$ and multiplying both sides by $\exp(-\mu_i t)$ yields

$$V_{i,n_i}(t) \leq \sum_{n=1}^{n_i} \int_0^t \psi_{i,n}(\overline{\chi}_{i,n}) \theta_{i,n} \mathcal{N}_R(\xi_{i,n}) \dot{\xi}_{i,n} d\nu + \sum_{n=1}^{n_i} \int_0^t \dot{\xi}_{i,n} d\nu + \Pi_i, \tag{4.50}$$

where $\Pi_i = V_{i,n_i}(0) + \sum_{n=1}^{n_i} \left(\hbar_i \left(c_{i,n} - \bar{\lambda}_{i,n}\right) + \lambda_{i,n}\right) + \sum_{n=1}^{n_i} \frac{\gamma_{i,n}}{2\vartheta_{i,n}} \beta_{i,n}^2$ is a positive constant.

At this point, we aim to extend the boundedness of Lemma 4.2 from a finite interval to the entire time domain. Along similar lines as [81], for the i-th agent, we consider an augmented state vector $x_{\text{ag}} \triangleq [\chi_{i,1}, \ldots, \chi_{i,n_i}, \xi_{i,1}, \ldots, \xi_{i,n_i}, \widehat{\beta}_{i,1}, \ldots, \widehat{\beta}_{i,n_i}, \alpha_{i,1}, \ldots, u_i]^T$ so that they can describe the closed-loop dynamic system as $\dot{x}_{\text{ag}}(t) = F_{\text{ag}}(t, x_{\text{ag}}(t))$ for $t \in [0, t_i)$. We start from $t = 0$; since $F_{\text{ag}}(\cdot) : \mathbb{R}^+ \times \mathbb{R}^{4\times n_i} \to \mathbb{R}$ is a locally Lipschitz map with respect to $x_{\text{ag}}(t)$, a solution exists on the time interval $[0, t_v)$ with $t_v \leq t_i$ (where the strict inequality holds if there is finite-time escape phenomenon [33]). It follows from (4.50) and Lemma 4.2 that $\xi_{i,n}(\cdot)$, $V_i(\cdot)$, and $\sum_{n=1}^{n_i} \int_0^t \left(\psi_{i,n}(\nu) \theta_{i,n} \mathcal{N}_R\left(\xi_{i,n}(\nu)\right) + \iota_i\right) \dot{\xi}_{i,n}(\nu) d\nu$ are bounded on the time interval $[0, t_v)$ for $n = 1, \ldots, n_i$, which implies $\chi_{i,1}, \ldots, \chi_{i,n_i}$, $\widehat{\beta}_{i,1}, \ldots, \widehat{\beta}_{i,n_i}$, and $\alpha_{i,1}, \ldots, u_i$ remain bounded on $[0, t_v)$. Hence, the whole solution x_{ag} is bounded on $[0, t_v)$. In accordance with [33, Chap. 8, Sect. 5], the solution of the closed-loop system $\dot{x}_{\text{ag}}(t) = F_{\text{ag}}(t, x_{\text{ag}}(t))$ can be extended to t_i. Repeating the above analysis on the continuation of the solution of the closed-loop system and invoking [33, pp. 476, Theorem 54] we conclude that there is no finite-time escape phenomenon that will occur and the solution of the closed-loop system exists on the entire time domain $[0, \infty)$ and that $\xi_{i,n}(\cdot)$, $\widehat{\beta}_{i,n}(\cdot)$, $\alpha_{i,n}(\cdot)$, $V_i(\cdot)$, $\chi_{i,n}$ for $n = 1, \ldots, n_i$ are bounded on the entire time domain.

Let P_i be the upper bound of the integral term $\sum_{n=1}^{n_i} \int_0^t \psi_{i,n}(\overline{\chi}_{i,n}) \theta_{i,n} \mathcal{N}_R\left(\xi_{i,n}\right) \dot{\xi}_{i,n} d\nu + \sum_{n=1}^{n_i} \int_0^t \dot{\xi}_{i,n} d\nu$.

Considering (4.16) and (4.50), the following inequality holds:

$$\frac{s_{i,1}^{p_i - p_{i,1} + 4}}{p_i - p_{i,1} + 4} \leq \Pi_i + P_i. \tag{4.51}$$

Noting (4.51), we know that $V_i(t) \leq \Pi_i + P_i$, and the following inequality holds:

$$|s_{i,1}| \leq \Upsilon_i, \tag{4.52}$$

where $\Upsilon_i = \left((\Pi_i + P_i)\left(p_i - p_{i,1} + 4\right)\right)^{\frac{1}{p_i - p_{i,1} + 4}}$.

From (4.52), we can obtain

$$\|s_1\| \leq \sqrt{\sum_{i=1}^{N} |s_{i,1}|^2} \leq \sqrt{\sum_{i=1}^{N} \Upsilon_i^2}. \tag{4.53}$$

Consequently, we can obtain that $\|\delta\| \leq \frac{\sqrt{\sum_{i=1}^{N} \Upsilon_i^2}}{\sigma_{\min}\left(\overline{\mathscr{L}} + \mathscr{B}\right)}$. It is known that $\sigma_{\min}\left(\overline{\mathscr{L}} + \mathscr{B}\right)$ can be replaced by a more conservative bound $\frac{\bar{N}}{N^2 + N - 1}$ with $\bar{N} = \left(\frac{N-1}{N}\right)^{\frac{N-1}{2}}$ [34] that does not involve global information $\sigma_{\min}\left(\overline{\mathscr{L}} + \mathscr{B}\right)$. This completes the proof. ■

Remark 4.5 Consensus tracking is solved in Theorem 4.1 via a common Lyapunov function, by estimating the maximum value of the switching weights in the linear-in-the-parameter approximator. A multiple Lyapunov function approach is in principle possible by estimating different switching weights for different subsystems. However, in this case the stability analysis becomes more challenging because it requires to impose conditions at switching instants, whereas a common Lyapunov function can guarantee stability under arbitrary switching.

Remark 4.6 Some guidelines for selecting appropriate design parameters are: (i) Choosing small positive constants $\gamma_{i,m}$ and increasing $\vartheta_{i,m}$ results in a faster convergence rate of adaptation parameters $\widehat{\beta}_{i,m}$; (ii) Decreasing $c_{i,m}$, $\lambda_{i,m}$, $\gamma_{i,m}$, while increasing $\vartheta_{i,m}$ helps to reduce ϱ_i, and thus to reduce the size of Ω_e; (iii) Enhancing the connectivity of the communication link $\overline{\mathscr{L}}+\mathscr{B}$ also contributes to reducing the size of Ω_e.

4

Remark 4.7 To clarify the importance of Lemma 4.2 and Theorem 4.1, consider that [37] has shown that the summation of conditional inequality may be bounded even when each term approaches infinity individually, but with opposite signs. To avoid this problem, [37] proposed new Nussbaum functions having the same signs on some periods of time. The results in [14] proposed conditional inequalities where no sign assumption is necessary: however, these results are applied to systems with one single control direction. Lemma 4.2 and Theorem 4.1 solved the open problem of handling multiple mixed unknown control directions with multiple hybrid Nussbaum functions.

4.5. Simulation Examples

In this section, we provide one numerical and one practical examples to validate the effectiveness of the proposed scheme.

4.5.1. Numerical Example

One leader (labeled by 0) with three (switched) follower agents are considered by the directed graph as in Fig. 3.2. From Fig. 3.2, it can be seen that the signal of leader is accessible to follower 1 only. The leader output is $y_{\mathrm{r}}(t)=5\sin(t)+10\sin(0.5t)$. The follower agents are described by the following dynamics:

$$\begin{cases} \dot{\chi}_{1,1} = \phi_{1,1}^{\sigma_i(t)}(\chi_{1,1}) + \psi_{1,1}^{\sigma_i(t)}(\chi_{1,1})\chi_{1,2}^3, \\ \dot{\chi}_{1,2} = \phi_{1,2}^{\sigma_i(t)}(\chi_1) + \psi_{1,2}^{\sigma_i(t)}(\chi_1)(Q_1(u_1))^3, \\ \dot{\chi}_{2,1} = \phi_{2,1}^{\sigma_i(t)}(\chi_{2,1}) + \psi_{2,1}^{\sigma_i(t)}(\chi_{2,1})\chi_{2,2}^3, \\ \dot{\chi}_{2,2} = \phi_{2,2}^{\sigma_i(t)}(\chi_2) + \psi_{2,2}^{\sigma_i(t)}(\chi_2)(Q_2(u_2))^5, \\ \dot{\chi}_{3,1} = \phi_{3,1}^{\sigma_i(t)}(\chi_{3,1}) + \psi_{3,1}^{\sigma_i(t)}(\chi_{3,1})\chi_{3,2}^5, \\ \dot{\chi}_{3,2} = \phi_{3,2}^{\sigma_i(t)}(\chi_3) + \psi_{3,2}^{\sigma_i(t)}(\chi_3)(Q_3(u_3))^5, \\ y_i = \chi_{i,1}, f = 1,2,3, \end{cases} \tag{4.54}$$

where $\sigma_i(\cdot):[0,+\infty)\to\mathscr{M}_i=\{1,2,3\}$: note that each follower has its own switching signal, and thus can switch asynchronously with respect to the other followers (cf. Fig. 4.1).

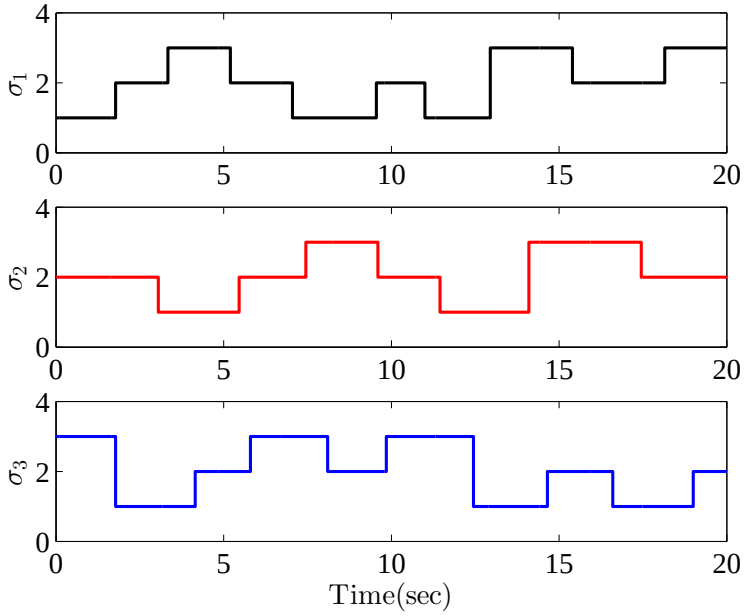

Figure 4.1: Asynchronous switching signals $\sigma_i(\cdot)$.

For follower agent 1, the three switching dynamics are:

$$\phi^1_{1,1} = 1.3 - \cos(\chi_{1,1}), \qquad \psi^1_{1,1} = |\tanh(\chi^3_{1,2})| + 1.6,$$
$$\phi^2_{1,1} = 0.6 + \exp(-\chi^2_{1,2}), \qquad \psi^2_{1,1} = \cos(\chi^3_{1,1}) + 2,$$
$$\phi^3_{1,1} = 0.8 + 0.2\cos(\chi_{1,1}), \qquad \psi^3_{1,1} = 2\cos(\chi_{1,2})^2,$$
$$\phi^1_{1,2} = \chi_{1,2}\chi_{1,1} + 0.8, \qquad \psi^1_{1,2} = 2(|\cos(\chi^2_{1,1})| + 1.3),$$
$$\phi^2_{1,2} = 0.7 + 0.2\chi^2_{1,2}, \qquad \psi^2_{1,2} = 3\sin(\chi_{1,2})^2 + 4,$$
$$\phi^3_{1,2} = \cos(\chi^2_{1,2}) + 0.3, \qquad \psi^3_{1,2} = 5|\sin(0.1\chi_{1,1})| + 1.5.$$

For follower agent 2, the three switching dynamics are:

$$\phi^1_{2,1} = 1.1\chi_{2,1} + \chi_{2,2}, \qquad \psi^1_{2,1} = 1.5\sin(\chi^2_{2,1} + \chi^2_{2,2}),$$
$$\phi^2_{2,1} = \chi^2_{2,1}\chi_{2,2}, \qquad \psi^2_{2,1} = \sin(\chi_{2,2}\chi^2_{2,1}) + 2.5,$$
$$\phi^3_{2,1} = \chi_{2,1}\chi^2_{2,2} + 1.2, \qquad \psi^3_{2,1} = \cos(\chi^2_{2,2}\chi^3_{2,1}) + 3,$$
$$\phi^1_{2,2} = \chi_{2,1}\chi^2_{2,2} + 0.5, \qquad \psi^1_{2,2} = 3 + 2\cos(\chi^3_{2,1}\chi_{2,2}),$$
$$\phi^2_{2,2} = 1.3\chi^3_{2,2} + 0.8\chi_{2,1}, \qquad \psi^2_{2,2} = 2\cos(\chi^2_{2,1}) + 4,$$
$$\phi^3_{2,2} = \cos(\chi_{2,1})\chi_{2,2}, \qquad \psi^3_{2,2} = 5 + 3\sin(\chi_{2,2}\chi^2_{2,1}).$$

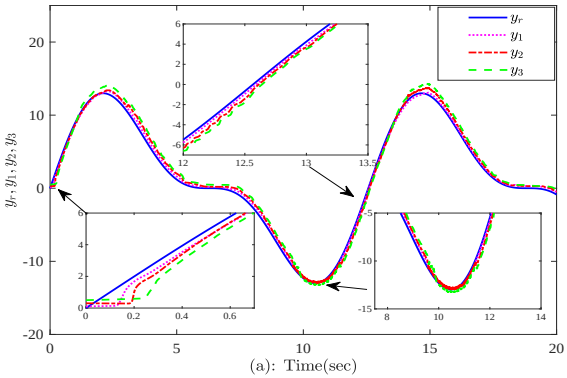

Figure 4.2: Evolutions of y_r, y_1, y_2, and y_3.

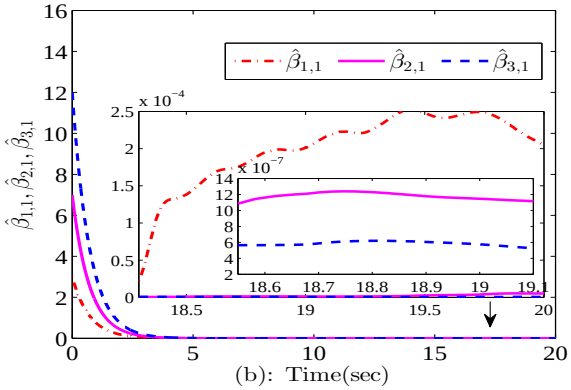

Figure 4.3: Evolutions of $\hat{\beta}_{1,1}$, $\hat{\beta}_{2,1}$, and $\hat{\beta}_{3,1}$.

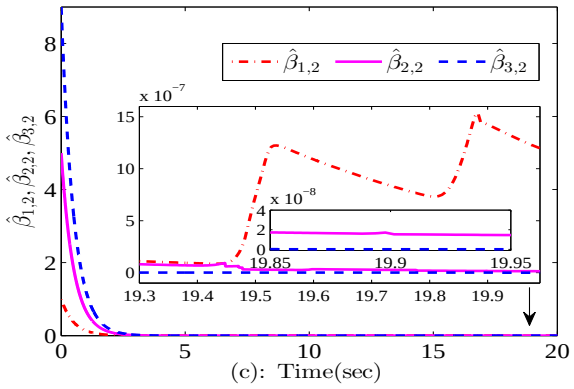

Figure 4.4: Evolutions of $\hat{\beta}_{1,2}$, $\hat{\beta}_{2,2}$, and $\hat{\beta}_{3,2}$.

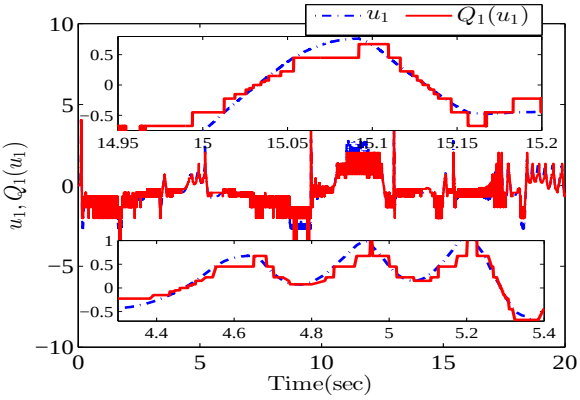

Figure 4.5: Trajectories of u_1 and $Q_1(u_1)$.

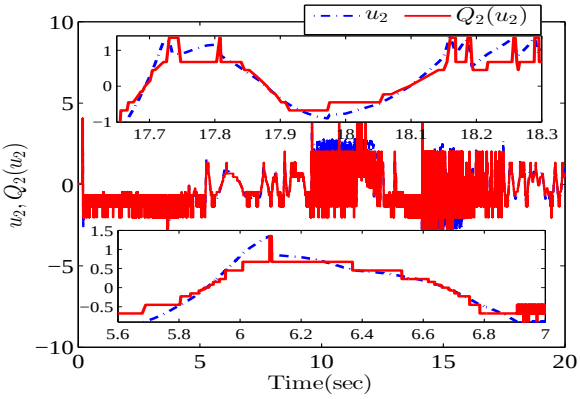

Figure 4.6: Trajectories of u_2 and $Q_2(u_2)$.

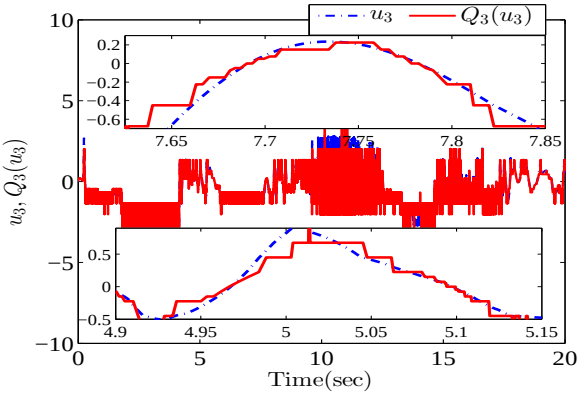

Figure 4.7: Trajectories of u_3 and $Q_3(u_3)$.

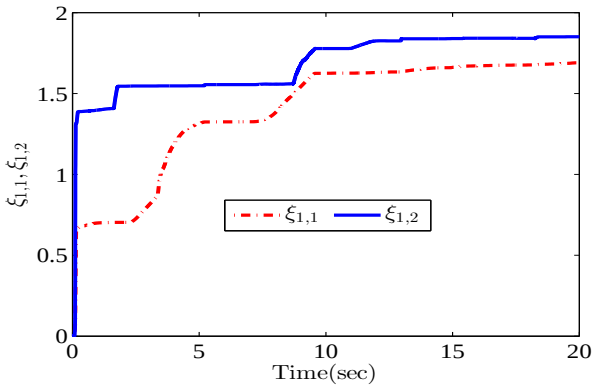

Figure 4.8: Trajectories of $\xi_{1,1}$ and $\xi_{1,2}$.

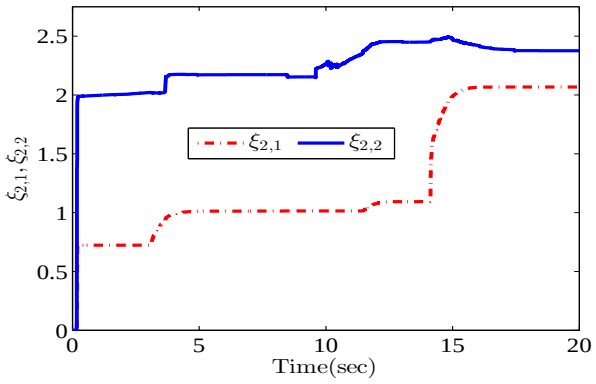

Figure 4.9: Trajectories of $\xi_{2,1}$ and $\xi_{2,2}$.

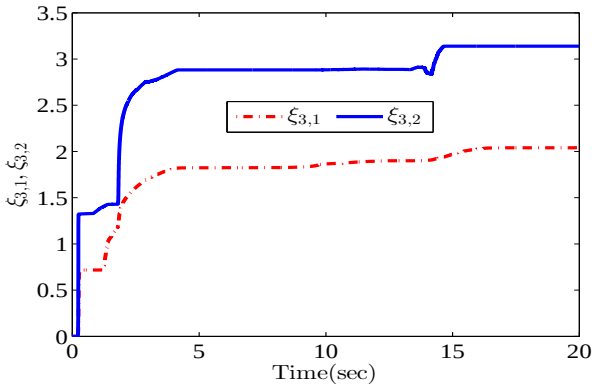

Figure 4.10: Trajectories of $\xi_{3,1}$ and $\xi_{3,2}$.

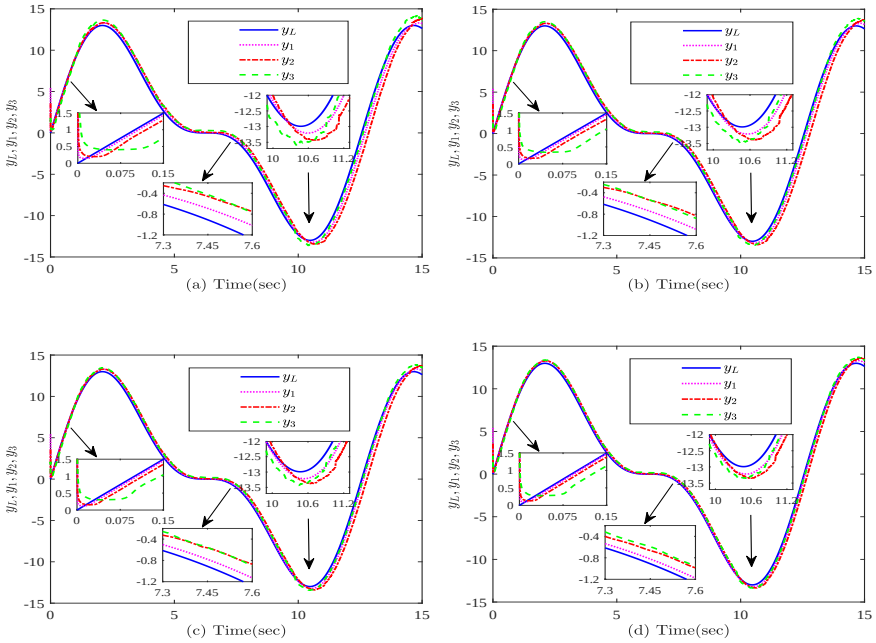

Figure 4.11: Evolutions of y_r, y_1, y_2, and y_3 under four cases: (a) $\overline{\rho} = 0.02$; (b) $\overline{\rho} = 0.03$; (c) $\overline{\rho} = 0.05$; (d) $\overline{\rho} = 0.08$.

For follower agent 3, the three switching dynamics are:

$$\phi_{3,1}^1 = 1.5\sin(\chi_{3,2}) + \chi_{3,1}, \qquad \psi_{3,1}^1 = |\sin(\chi_{3,1})| + 6,$$
$$\phi_{3,1}^2 = 0.3\chi_{3,1}^2 + \sin(\chi_{3,2}), \qquad \psi_{3,1}^2 = |\sin(\chi_{3,2}^3)| + 3,$$
$$\phi_{3,1}^3 = \chi_{3,1} + 0.2\chi_{3,2}, \qquad \psi_{3,1}^3 = \cos(\chi_{3,2}^2\chi_{3,1}^3) + 4.5,$$
$$\phi_{3,2}^1 = 0.5\chi_{3,1}^2 + \chi_{3,2}, \qquad \psi_{3,2}^1 = \cos(\chi_{3,2}^2) + 2,$$
$$\phi_{3,2}^2 = \chi_{3,2} + 0.8\sin(\chi_{3,1}), \qquad \psi_{3,2}^2 = 4\cos(\chi_{3,1}) + 5.5,$$
$$\phi_{3,2}^3 = \cos(\chi_{3,2})^2 + 0.7, \qquad \psi_{3,2}^3 = \cos(\chi_{3,2})^3 + 3.5.$$

While conducting the simulation, the control directions of $\psi_{i,1}^{\sigma_i}$, $\sigma_i = 1,2,3$, $f = 1,2,3$, are assumed known and the control directions of $\psi_{i,2}^{\sigma_i}$, $\sigma_i = 1,2,3$, $f = 1,2,3$, are assumed unknown. The initial conditions are: $\chi_1(0) = [0.1,-0.1]^T$, $\chi_2(0) = [0.3,-0.3]^T$, $\chi_3(0) = [0.5,-0.5]^T$, $\hat{\beta}_{1,1}(0) = 3$, $\hat{\beta}_{1,2}(0) = 1$, $\hat{\beta}_{2,1}(0) = 7$, $\hat{\beta}_{2,2}(0) = 5$, $\hat{\beta}_{3,1}(0) = 12$, $\hat{\beta}_{3,2}(0) = 9$, $\xi_{1,1}(0) = \xi_{1,2}(0) = \xi_{2,1}(0) = \xi_{2,2}(0) = \xi_{3,1}(0) = \xi_{3,2}(0) = 0$. The design parameters are chosen to be: $c_{1,1} = c_{2,1} = c_{3,1} = 10$, $c_{1,2} = c_{2,2} = c_{3,2} = 15$, $\varsigma_{1,1} = \varsigma_{2,1} = \varsigma_{3,1} = 0.8$, $\varsigma_{1,2} = \varsigma_{2,2} = \varsigma_{3,2} = 1$, $\ell_{1,1} = \ell_{2,1} = \ell_{3,1} = 0.5$, $\ell_{1,2} = \ell_{2,2} = \ell_{3,2} = 0.75$, $\vartheta_{1,1} = \vartheta_{2,1} = \vartheta_{3,1} = 1$, $\vartheta_{1,2} = \vartheta_{2,2} = \vartheta_{3,2} = 2$, $\gamma_{1,1} = \gamma_{2,1} = \gamma_{3,1} = 1.4$, $\gamma_{1,2} = \gamma_{2,2} = \gamma_{3,2} = 2$, $u_1^{\min} = u_2^{\min} = u_3^{\min} = 0.05$, $\rho_1 = 0.02$, $\rho_2 = 0.025$ and $\rho_3 = 0.015$. The simulation results are shown in Figs. 4.2-4.10. Fig. 4.2 shows that the three followers track the leader output signal with bounded consensus

Table 4.1: Performance indices for four different sets of quantizer parameters $\overline{\rho}$.

Indices	$\overline{\rho}=0.02$	$\overline{\rho}=0.03$	$\overline{\rho}=0.05$	$\overline{\rho}=0.08$
ITAE	1.7281	1.5982	1.4443	1.2796
RMSE	0.2163	0.1857	0.1448	0.0958
MACA	8.6374	9.0853	10.7742	11.6563

tracking errors. Figs. 4.3-4.4 depict the boundedness of $\widehat{\beta}_{1,1}$, $\widehat{\beta}_{2,1}$, and $\widehat{\beta}_{3,1}$, and of $\widehat{\beta}_{1,2}$, $\widehat{\beta}_{2,2}$, and $\widehat{\beta}_{3,2}$, respectively. Figs. 4.5-4.7 reveal the trajectories of the actual control signals u_i and quantized control $Q_i(u_i)$, $i=1,2,3$. Figs. 4.8-4.10 provide the evolutions of the adaptation parameters $\xi_{1,1}$, $\xi_{1,2}$, $\xi_{2,1}$, $\xi_{2,2}$, $\xi_{3,1}$, and $\xi_{3,2}$.

4

4.5.2. Practical Example

To further validate the developed control method, a multi-agent version of the underactuated weakly coupled mechanical benchmark in [83] is considered, also shown in Fig. 1.3. The dynamics of the ith agent remain the same as (3.59). The system parameters of the three follower agents are the exactly ones of the first three follower agents of Table 3.3. While carrying out the simulation, the control directions of $\psi_{i,2}^{\sigma_i(t)}$, $f=1,2,3$, are assumed unknown and the other control directions are assumed known. The switching signal is as in Fig. 4.1. Let the initial conditions be $\chi_{1,1}(0)=5.5$, $\chi_{1,2}(0)=0.25$, $\chi_{1,3}(0)=0.75$, $\chi_{1,4}(0)=-0.5$, $\chi_{2,1}(0)=3.7$, $\chi_{2,2}(0)=0.2$, $\chi_{2,3}(0)=0.35$, $\chi_{2,4}(0)=0.25$, $\chi_{3,1}(0)=1.5$, $\chi_{3,2}(0)=-0.75$, $\chi_{3,3}(0)=0.5$, $\chi_{3,4}(0)=-0.75$, $\hat{\beta}_{1,1}(0)=3$, $\hat{\beta}_{1,3}(0)=1$, $\hat{\beta}_{1,4}(0)=5$, $\hat{\beta}_{2,1}(0)=7$, $\hat{\beta}_{2,2}(0)=5$, $\hat{\beta}_{2,3}(0)=3.5$, $\hat{\beta}_{2,4}(0)=2.5$, $\hat{\beta}_{3,1}(0)=12$, $\hat{\beta}_{3,2}(0)=9$, $\hat{\beta}_{3,1}(0)=\hat{\beta}_{3,2}(0)=9$, $\hat{\beta}_{3,3}(0)=\hat{\beta}_{3,4}(0)=5.5$, $\xi_{1,1}(0)=\xi_{1,2}(0)=\xi_{1,3}(0)=\xi_{1,4}(0)=\xi_{2,1}(0)=\xi_{2,2}(0)=\xi_{2,3}(0)=\xi_{2,4}(0)=\xi_{3,1}(0)=\xi_{3,2}(0)=\xi_{3,3}(0)=\xi_{3,4}(0)=0$. The design parameters are chosen to be: $c_{1,1}=c_{2,1}=c_{3,1}=7.5$, $c_{1,2}=c_{2,2}=c_{3,2}=10$, $c_{1,3}=c_{2,3}=c_{3,3}=5$, $c_{1,4}=c_{2,4}=c_{3,4}=5$, $\varsigma_{1,1}=\varsigma_{2,1}=\varsigma_{3,1}=0.8$, $\varsigma_{1,2}=\varsigma_{2,2}=\varsigma_{3,2}=1$, $\varsigma_{1,3}=\varsigma_{2,3}=\varsigma_{3,3}=0.25$, $\varsigma_{1,4}=\varsigma_{2,4}=\varsigma_{3,4}=1.5$, $\ell_{1,1}=\ell_{2,1}=\ell_{3,1}=0.5$, $\ell_{1,2}=\ell_{2,2}=\ell_{3,2}=0.75$, $\ell_{1,3}=\ell_{2,3}=\ell_{3,3}=0.35$, $\ell_{1,4}=\ell_{2,4}=\ell_{3,4}=0.5$, $\vartheta_{1,1}=\vartheta_{2,1}=\vartheta_{3,1}=1$, $\vartheta_{1,2}=\vartheta_{2,2}=\vartheta_{3,2}=2$, $\vartheta_{1,3}=\vartheta_{2,3}=\vartheta_{3,3}=2.75$, $\vartheta_{1,4}=\vartheta_{2,4}=\vartheta_{3,4}=1.5$, $\gamma_{1,1}=\gamma_{2,1}=\gamma_{3,1}=1.4$, $\gamma_{1,2}=\gamma_{2,2}=\gamma_{3,2}=2$, $\gamma_{1,3}=\gamma_{2,3}=\gamma_{3,3}=2.5$, $\gamma_{1,4}=\gamma_{2,4}=\gamma_{3,4}=3.5$, $u_1^{\min}=u_2^{\min}=u_3^{\min}=0.05$. Let $\overline{\rho}=\rho_1=\rho_2=\rho_3$. To investigate the effects of quantizer parameter ρ_i, $f=1,2,3$, on system performances, several performance indices are used: integral time absolute error (ITAE) $\left[\frac{1}{3}\int_0^T t|\sum_{i=1}^3 s_{i,1}(t)|dt\right]$, root mean square error (RMSE) $\left[\frac{1}{3T}\int_0^T|\sum_{i=1}^3 s_{i,1}^2(t)|dt\right]^{\frac{1}{2}}$, mean absolute control action (MACA) $\left[\frac{1}{3T}\int_0^T|\sum_{i=1}^3 u_i|dt\right]$. The simulation results are given in Fig. 4.11 and the calculation results are summarized in Table 4.1. It can be seen from Table 4.1 that the tracking accuracy improves as ρ_i increases, while larger control effort is required: that is, a finer quantizer leads to improved precision, which might require larger controls.

4.6. Conclusions

This chapter investigated a Nussbaum function approach in the distributed adding-one-power-integrator scenario. The distributed control challenges lie in the power-chained

form nonlinear dynamics, in the switching behavior, in the input quantization and, most importantly, in the partially unknown control directions. A new lemma involving multiple Nussbaum functions and quantization decomposition parameter was constructed to handle these challenges.

5

Logic-based Distributed Switching Control for Agents in the Power-Chained Form with Unknown Control Directions

This chapter studies logic-based distributed switching control for nonlinear agents in power-chained form systems, where logic-based (switching) control arises from the online estimation of the control directions assumed to be unknown for all agents. The introduction is given in Section 5.1. The problem formulation and preliminaries are provided in Section 5.2. Sections 5.3 and 5.4 present the proposed distributed consensus design and stability analysis, respectively. The simulation examples are in Section 5.5 and Section 5.6 draws the conclusion.

5.1. Introduction

In Chapter 4, we have proposed a hybrid Nussbaum function-based methodology to consensus tracking of power-chained form systems subject to multiple unknown control directions. At the same time, because it is well-recognized that Nussbaum-based methods require additional complexity in the control design and continuous parameter adaptation may lead to large learning transients, several researchers have been engaged in the problem of overcoming continuous parameter adaptation by means of logic-based control [32, 54]. Notable settings where logic-based control was employed include overcoming conventional continuous tuning of control parameters [2, 27, 123, 124] and overcoming the conventional Nussbaum approach for strict-feedback dynamics [36, 115].

It is important to notice that the state-of-the-art logic-based mechanisms in [36,

115] for strict-feedback systems rely on monitor functions that monitor whether asymptotic tracking can be achieved (resulting in bounded energy of the tracking error) [36] or whether finite-time stabilization (i.e. the tracking error converges to zero in finite time) can be achieved [115]. Unfortunately, the same mechanism and monitor functions cannot be adopted for agents in power-chained form systems due to the aforementioned structural difficulty in achieving asymptotic tracking, see also [83, Examples 2.1 and 2.2]. Therefore, a different logic-based mechanism must be sought for distributed control of power chained dynamics. This motivates the research question in this chapter: *is it possible to design a new logic-based mechanism for multi-agent systems in power-chained form systems with multiple unknown control directions even when asymptotic tracking cannot be structurally obtained?*

This chapter provides a positive answer to this question with the following contributions:

- To overcome the difficulty that no asymptotic tracking can be achieved for the power-chained form systems, we propose a new dynamic boundary function, which is decreasing in-between switching instants and possibly increasing at the switching instants of logic-based control (cf. Fig. 5.1);
- We formally exclude any chattering phenomenon by proposing a new dynamic threshold condition at the switching instants of logic-based control. It is worth noticing that state-of-the-art switching mechanisms cannot formally exclude chattering (cf. the discussion in our Remark 5.1);
- To overcome the challenge that the exact value of the Lyapunov function is unavailable for logic-based control, we propose a new Lyapunov-like function (cf. the discussion in our Remark 5.2).

5.2. Problem Formulation and Preliminaries

Consider a multi-agent system whose agents have the following nonlinear dynamics:

$$\begin{cases} \dot{\chi}_{i,m} = \phi_{i,m}(\overline{\chi}_{i,m}) + \psi_{i,m}(\overline{\chi}_{i,m})\chi_{i,m+1}^{p_{i,m}}, \\ \dot{\chi}_{i,n_i} = \phi_{i,n_i}(\overline{\chi}_{i,n_i}) + \psi_{i,n_i}(\overline{\chi}_{i,n_i})u_i^{p_{i,n_i}}, \\ y_i = \chi_{i,1}, \end{cases} \tag{5.1}$$

for $i = 1,\dots,N$, $m = 1,\dots,n_i-1$, where n_i is the dimension of system state $\overline{\chi}_{i,n_i} = [\chi_{i,1},\dots,\chi_{i,n_i}]^T \in \mathbb{R}^{n_i}$ and $\overline{\chi}_{i,m} = [\chi_{i,1},\dots,\chi_{i,m}]^T \in \mathbb{R}^m$. In (5.1), $p_{i,m} \in \mathbb{N}_{\text{odd}}$ are positive odd powers, and $u_i \in \mathbb{R}$ is the agent control input to be designed. The functions $\phi_{i,m}(\cdot)$ and $\psi_{i,m}(\cdot)$ are unknown locally Lipschitz continuous nonlinearities. The following assumptions are considered.

Assumption 5.1 [135] For each follower i, the signs of $\psi_{i,m}(\cdot)$, called the *control directions*, are unknown and there exist known positive constants $\overline{\psi}_{i,m}$ and $\underline{\psi}_{i,m}$ such that

$$\underline{\psi}_{i,m} \le |\psi_{i,m}(\cdot)| \le \overline{\psi}_{i,m} \tag{5.2}$$

for $i = 1,\dots,N$, $m = 1,\dots,n_i$.

Define the consensus tracking error for the i-th follower as

$$\xi_{i,1} = \sum_{j\in\mathcal{N}_i} a_{ij}(y_i - y_j) + b_i(y_i - y_r), \tag{5.3}$$

for $i = 1,\dots,N$. After collecting $\boldsymbol{\xi}_1 = [\xi_{1,1},\dots,\xi_{N,1}]^T \in \mathbb{R}^N$, one has $\boldsymbol{\xi}_1 = (\overline{\mathscr{L}} + \mathscr{B})\boldsymbol{\delta}$, where $\boldsymbol{\delta} = \overline{\boldsymbol{y}} - \overline{\boldsymbol{y}}_r$ with $\overline{\boldsymbol{y}} = [y_1,\dots,y_N]^T$ and $\overline{\boldsymbol{y}}_r = [y_r,\dots,y_r]^T$. Due to the nonsingularity of $\overline{\mathscr{L}} + \mathscr{B}$, it holds that $\|\boldsymbol{\delta}\| \le \frac{\|\boldsymbol{\xi}_1\|}{\sigma_{\min}(\overline{\mathscr{L}}+\mathscr{B})}$, where $\sigma_{\min}(\overline{\mathscr{L}} + \mathscr{B})$ is the minimum singular value of $\overline{\mathscr{L}} + \mathscr{B}$. We impose a prescribed performance [6] on the consensus tracking error $\xi_{i,1}$ as $\underline{\xi}_{i,1}(t) \le \xi_{i,1}(t) \le \overline{\xi}_{i,1}(t)$ for $t \ge 0$, where $\overline{\xi}_{i,1}(t) = (\overline{\rho}_{i,1} - \rho_{i,\infty})\exp(-\overline{l}_{i,1}t) + \rho_{i,\infty}$ and $\underline{\xi}_{i,1}(t) = (\underline{\rho}_{i,1} + \rho_{i,\infty})\exp(-\underline{l}_{i,1}t) - \rho_{i,\infty}$ are the so-called performance functions [6], where $\overline{l}_{i,1} > 0$ and $\underline{l}_{i,1} > 0$ denote the minimum admissible convergence rates, $\rho_{i,\infty} > 0$ is the maximum allowable tracking error at steady state, $\overline{\rho}_{i,1} > \rho_{i,\infty} > 0$ and $\underline{\rho}_{i,1} < -\rho_{i,\infty} < 0$ respectively represent the maximum and minimum bounds for $\xi_{i,1}(0)$. The following transformed consensus tracking error is then used for feedback:

$$s_{i,1}(t) = \ln\left(\frac{\xi_{i,1}(t) - \underline{\xi}_{i,1}(t)}{\overline{\xi}_{i,1}(t) - \xi_{i,1}(t)}\right). \tag{5.4}$$

Note that $s_{i,1}$ is monotonically increasing w.r.t. $\xi_{i,1}$ and that (5.4) implies that the consensus tracking error $\xi_{i,1}$ is within its imposed bounds provided $s_{i,1}$ is bounded [6].

Problem 5.1 The goal is consensus tracking, i.e. to design u_i such that the output of each agent can track the leader agent's signal y_r in spite of completely multiple unknown control directions, while guaranteeing the boundedness of closed-loop signals.

Practical tracking [83, eq. (2.10)] (i.e. the tracking error converges to a residual set) will be sought, due to the fact that asymptotic tracking cannot be realized in general for dynamics (5.1) [83].

5.3. Proposed Distributed Consensus Design

5.3.1. Adaptive Switching Consensus Protocol

The control design solving the consensus tracking problem comprises a *continuous* input (i.e. acting in-between two consecutive switching instants) and a *switching* mechanism (acting at the switching instants) to tune online some parameters of the continuous input. In this section, we focus on the continuous input, the design of which is well-established in literature under the assumption that the control directions are known [89, 135]. Therefore, this section is kept short so as to give more space to the novel switching mechanism in Sect. 5.3.2.

After defining $s_{i,1}$ as in (5.4), and state errors

$$s_{i,m} = \chi_{i,m} - \alpha_{i,m-1}, \quad m = 2,\dots,n_i, \tag{5.5}$$

the continuous control input comprises the so-called virtual laws $\alpha_{i,m}$ and the actual control u_i, designed as

$$\alpha_{i,1} = -h_{i,1} R_{i,1}^{\frac{1}{\overline{p}_{i,1}}} \left(k_{i,1} + \epsilon_{i,1}^{\overline{p}_{i,1}} \widehat{\Theta}_{i,1} \Gamma_{i,1}^{\overline{p}_{i,1}} + \varrho_{i,1}^{\overline{p}_{i,1}} \right)^{\frac{1}{\overline{p}_{i,1}}}, \tag{5.6}$$

$$R_{i,1} = s_{i,1}^{p_{i,1}} \left[\ell_{i,1} \underline{\psi}_{i,1} (d_i + b_i)(1 - \pi_{i,1}) \right]^{-1},$$

$$\alpha_{i,m} = -h_{i,m} R_{i,m}^{\frac{1}{\overline{p}_{i,m}}} \left(k_{i,m} + \epsilon_{i,m}^{\overline{p}_{i,m}} \widehat{\Theta}_{i,m} \Gamma_{i,m}^{\overline{p}_{i,m}} + \varrho_{i,m}^{\overline{p}_{i,m}} \right)^{\frac{1}{\overline{p}_{i,m}}}, \tag{5.7}$$

$$R_{i,m} = s_{i,m}^{p_{i,m}} \left[\underline{\psi}_{i,m} (1 - \pi_{i,m}) \right]^{-1}, (m = 1, \ldots, n_i)$$

$$u_i = \alpha_{i,n_i},\ \pi_{i,n_i} = 0, \tag{5.8}$$

$$\dot{\widehat{\Theta}}_{i,m} = \gamma_{i,m} \left[\epsilon_{i,m}^{\overline{p}_{i,m}} s_{i,m}^{p_i+3} \Gamma_{i,m}^{\overline{p}_{i,m}} - \beta_{i,m} \widehat{\Theta}_{i,m} \right], \tag{5.9}$$

with $\overline{p}_{i,m} = \frac{p_i+3}{p_i - p_{i,m}+3}$, $\underline{p}_{i,m} = \frac{p_i+3}{p_{i,m}}$, $p_i = \max\limits_{m=1,\ldots,n_i} \{p_{i,m}\}$, and where $0 < \pi_{i,m} < 1$, $\varrho_{i,m} > 0$, $\epsilon_{i,m} > 0$, $\gamma_{i,m} > 0$ and $\beta_{i,m} > 0, (m = 1, \ldots, n_i)$ are design parameters. In (5.9), $\widehat{\Theta}_{i,m}$ is the estimate of $\Theta_{i,m} = \|\boldsymbol{W}_{i,m}^*\|^{\overline{p}_{i,m}}$ and $\Gamma_{i,m} = \|\boldsymbol{\varphi}_{i,m}\|$, which comes from appropriately designed function approximators (as detailed later on). Notice that the control design (5.6)-(5.9) is not complete, since the terms $k_{i,m}$ and $h_{i,m}$ are to be designed: these terms are necessary to tackle the multiple unknown control directions, and their design will be addressed in Sect. 5.3.2 via a switching mechanism. The rationale for the design (5.6)-(5.9) is given in the following steps.

Step $i, 1$ $(i = 1, \ldots, N)$**:** The time derivative of $s_{i,1}$ along (5.1), (5.3), and (5.4) is

$$\dot{\vartheta}_{i,1} = l_{i,1} \dot{\xi}_{i,1} + H_{i,1} = l_{i,1}(d_i + \mu_i) \psi_{i,1} \chi_{i,2}^{p_{i,1}} + E_{i,1}, \tag{5.10}$$

where $l_{i,1} = \partial s_{i,1} / \partial \xi_{i,1} > 0$, $H_{i,1} = \left(\partial s_{i,1} / \partial \overline{\xi}_{i,1} \right) \dot{\overline{\xi}}_{i,1} + \left(\partial s_{i,1} / \partial \underline{\xi}_{i,1} \right) \dot{\underline{\xi}}_{i,1}$, and $E_{i,1} = l_{i,1}(d_i + \mu_i)\phi_{i,1} - l_{i,1} \sum_{j \in \mathcal{N}_i} a_{ij} (\phi_{i,1} + \psi_{i,1} \chi_{i,2}^{p_{i,1}}) - \mu_i \dot{y}_r + H_{i,1}$. Along the same veins as [126], there exist some optimal weights $\boldsymbol{W}_{i,1}^*$, and a linear-in-the-parameter approximator $\boldsymbol{W}_{i,1}^* \boldsymbol{\varphi}_{i,1}(\boldsymbol{Z}_{i,1})$ for $|E_{i,1}|$ such that

$$\begin{aligned} s_{i,1}^{p_i - p_{i,1}+3} E_{i,1} &\leq \left| s_{i,1}^{p_i - p_{i,1}+3} \right| \left[\boldsymbol{W}_{i,1}^* \boldsymbol{\varphi}_{i,1}(\boldsymbol{Z}_{i,1}) + \varepsilon_{i,1}(\boldsymbol{Z}_{i,1}) \right] \\ &\leq s_{i,1}^{p_i+3} \left(\varrho_{i,1}^{\overline{p}_{i,1}} + \epsilon_{i,1}^{\overline{p}_{i,1}} \Theta_{i,1} \Gamma_{i,1}^{\overline{p}_{i,1}} \right) + \hbar_{i,1}, \end{aligned}$$

where the last inequality uses Lemma 3.1. Furthermore, $\hbar_{i,1} = \epsilon_{i,1}^{-\underline{p}_{i,1}} + \varrho_{i,1}^{-\underline{p}_{i,1}} \overline{\varepsilon}_{i,1}^{\underline{p}_{i,1}}$ with $\epsilon_{i,1} > 0$ and $\varrho_{i,1} > 0$ being design constants, $\varepsilon_{i,1}(\boldsymbol{Z}_{i,1})$ is the approximation error satisfying $\left| \varepsilon_{i,1}(\boldsymbol{Z}_{i,1}) \right| \leq \overline{\varepsilon}_{i,1}$ on a compact set $\Omega_{i,1}$, $\boldsymbol{Z}_{i,1} = \left[\chi_{i,1}, \chi_{j,1,j \in \mathcal{N}_i}, \chi_{j,2,j \in \mathcal{N}_i}, b_i y_r, b_i \dot{y}_r \right]^T \in \Omega_{i,1}$, and $\overline{\varepsilon}_{i,1} > 0$ a constant.

Consider the Lyapunov function candidate

$$V_{i,1} = \frac{s_{i,1}^{p_i - p_{i,1}+4}}{p_i - p_{i,1} + 4} + \frac{1}{2\gamma_{i,1}} \widetilde{\Theta}_{i,1}^2 \tag{5.11}$$

where $\widetilde{\Theta}_{i,1} = \Theta_{i,1} - \widehat{\Theta}_{i,1}$. According to Lemma 3.1, it holds that

$$\begin{aligned} s_{i,1}^{p_i-p_{i,1}+3}\chi_{i,2}^{p_{i,1}} &= \ell_{i,1}s_{i,1}^{p_i-p_{i,1}+3}s_{i,2}^{p_{i,1}} + \upsilon_{i,1}s_{i,1}^{p_i-p_{i,1}+3}\alpha_{i,1}^{p_{i,1}} \\ &< |\ell_{i,1}|\left(s_{i,1}^{p_i+3} + s_{i,2}^{p_i+3}\right) + \upsilon_{i,1}s_{i,1}^{p_i-p_{i,1}+3}\alpha_{i,1}^{p_{i,1}}. \end{aligned} \tag{5.12}$$

Then, it follows from (5.10)-(5.12) that the derivative of $V_{i,1}$ with respect to time satisfies

$$\begin{aligned} \dot{V}_{i,1} <& l_{i,1}(d_i+b_i)s_{i,1}^{p_i-p_{i,1}+3}\alpha_{i,1}^{p_{i,1}}h_{i,1}\upsilon_{i,1}|\psi_{i,1}| - \frac{\widetilde{\Theta}_{i,1}\dot{\widehat{\Theta}}_{i,1}}{\gamma_{i,1}} \\ &+ s_{i,1}^{p_i+3}\left(\varrho_{i,1}^{\overline{p}_{i,1}} + \epsilon_{i,1}^{\overline{p}_{i,1}}\Theta_{i,1}\Gamma_{i,1}^{\overline{p}_{i,1}}\right) + \Pi_{i,1} + \hbar_{i,1} \\ &+ \varpi_{i,1}\left(s_{i,1}^{p_i+3} + s_{i,2}^{p_i+3}\right), \end{aligned} \tag{5.13}$$

where $\Pi_{i,1} = l_{i,1}(d_i+b_i)\upsilon_{i,1}s_{i,1}^{p_i-p_{i,1}+3}\alpha_{i,1}^{p_{i,1}}(\mathrm{sign}(\psi_{i,1})-h_{i,1})|\psi_{i,1}|$, $\varpi_{i,1} = (d_i+b_i)l_{i,1}\overline{\psi}_{i,1}\overline{\ell}_{i,1}$, and we used the fact that $\psi_{i,1} = \mathrm{sign}(\psi_{i,1})|\psi_{i,1}|$. Substituting the virtual control $\alpha_{i,1}$ (5.6) into (5.13) gives

$$\begin{aligned} \dot{V}_{i,1} <& -(k_{i,1}-\varpi_{i,1})s_{i,1}^{p_i+3} + s_{i,1}^{p_i+3}\epsilon_{i,1}^{\overline{p}_{i,1}}\widetilde{\Theta}_{i,1}\Gamma_{i,1}^{\overline{p}_{i,1}} \\ &- \frac{\widetilde{\Theta}_{i,1}\dot{\widehat{\Theta}}_{i,1}}{\gamma_{i,1}} + \varpi_{i,1}s_{i,2}^{p_i+3} + \Pi_{i,1} + \hbar_{i,1}. \end{aligned} \tag{5.14}$$

Substituting the adaptive law $\dot{\widehat{\Theta}}_{i,1}$ (5.9) into (5.14) yields

$$\dot{V}_{i,1} < -c_{i,1}s_{i,1}^{p_i+3} + \varpi_{i,1}s_{i,2}^{p_i+3} + \beta_{i,1}\widetilde{\Theta}_{i,1}\widehat{\Theta}_{i,1} + \Pi_{i,1} + \hbar_{i,1},$$

where $c_{i,1} = k_{i,1} - \varpi_{i,1}$.

Step i, m $(i = 1,\ldots,N,\ m = 2,\ldots,n_i-1)$**:** It follows from (5.1), (5.5), and (5.7) that the derivative of $s_{i,m}$ is

$$\dot{s}_{i,m} = \psi_{i,m}\chi_{i,m+1}^{p_{i,m}} + E_{i,m}, \tag{5.15}$$

where $E_{i,m} = \phi_{i,m} - \sum_{q=1}^{m-1}\frac{\partial\alpha_{i,m-1}}{\partial\chi_{i,q}}\left(\phi_{i,q}+\psi_{i,q}\chi_{i,q+1}^{p_{i,q}}\right) - \frac{\partial\alpha_{i,m-1}}{\partial y_{\mathrm{r}}}\dot{y}_{\mathrm{r}} - \sum_{q=1}^{m-1}\frac{\partial\alpha_{i,m-1}}{\partial\widehat{\Theta}_{i,q}}\dot{\widehat{\Theta}}_{i,q} - \sum_{j\in\mathcal{N}_i}a_{ij}\frac{\partial\alpha_{i,m-1}}{\partial\chi_{j,1}}\left(\phi_{j,1}+\psi_{j,2}\chi_{j,2}^{p_{j,1}}\right)$. Referring to Step $i,1$, there exist some optimal weights $\boldsymbol{W}_{i,m}^*$, and a linear-in-the-parameter approximator $\boldsymbol{W}_{i,m}^*\boldsymbol{\varphi}_{i,m}(\boldsymbol{Z}_{i,m})$ for $|E_{i,m}|$ such that

$$\begin{aligned} s_{i,m}^{p_i-p_{i,m}+3}E_{i,m} \le& \left|s_{i,m}^{p_i-p_{i,m}+3}\right|\left|\boldsymbol{W}_{i,m}^*\boldsymbol{\varphi}_{i,m}(\boldsymbol{Z}_{i,m}) + \varepsilon_{i,m}(\boldsymbol{Z}_{i,m})\right| \\ \le& s_{i,m}^{p_i+3}\left(\varrho_{i,m}^{\overline{p}_{i,m}} + \epsilon_{i,m}^{\overline{p}_{i,m}}\Theta_{i,m}\Gamma_{i,m}^{\overline{p}_{i,m}}\right) + \hbar_{i,m}, \end{aligned}$$

where $\hbar_{i,m} = \epsilon_{i,m}^{-\underline{p}_{i,m}} + \varrho_{i,m}^{-\underline{p}_{i,m}}\overline{\varepsilon}_{i,m}^{\underline{p}_{i,m}}$ with $\epsilon_{i,m} > 0$ and $\varrho_{i,m} > 0$ design constants, $\varepsilon_{i,m}(\boldsymbol{Z}_{i,m})$ is the approximation error satisfying $\left|\varepsilon_{i,m}(\boldsymbol{Z}_{i,m})\right| \le \overline{\varepsilon}_{i,m}$ on a compact set $\Omega_{i,m}$, with $\boldsymbol{Z}_{i,m} = \left[\overline{\boldsymbol{\chi}}_{i,m}, \overline{\boldsymbol{\chi}}_{j,m,}, \frac{\partial\alpha_{i,m-1}}{\partial\chi_{j,1}}, \frac{\partial\alpha_{i,m-1}}{\partial\chi_{i,1}}, \ldots, \frac{\partial\alpha_{i,m-1}}{\partial\chi_{i,m-1}}, \frac{\partial\alpha_{i,m-1}}{\partial\widehat{\Theta}_{i,1}}, \ldots, \frac{\partial\alpha_{i,m-1}}{\partial\widehat{\Theta}_{i,m-1}}, \widehat{\Theta}_{i,1}, \ldots, \widehat{\Theta}_{i,m-1}, \frac{\partial\alpha_{i,m-1}}{\partial y_{\mathrm{r}}}, b_i y_{\mathrm{r}}\right]_{j\in\mathcal{N}_i}^T \in \Omega_{i,m}$ and $\overline{\varepsilon}_{i,m} > 0$ a constant. Consider the Lyapunov function candidate

$$V_{i,m} = V_{i,m-1} + \frac{s_{i,m}^{p_i-p_{i,m}+4}}{p_i-p_{i,m}+4} + \frac{1}{2\gamma_{i,m}}\widetilde{\Theta}_{i,m}^2, \tag{5.16}$$

where $\widetilde{\Theta}_{i,m} = \Theta_{i,m} - \widehat{\Theta}_{i,m}$. Following similar derivations as in Step $i,1$, the derivative of $V_{i,m}$ with respect to time is

$$\dot{V}_{i,m} < -\sum_{q=1}^{m} c_{i,q} s_{i,q}^{p_i+3} + \varpi_{i,m} s_{i,m+1}^{p_i+3} + \sum_{q=1}^{m} \Pi_{i,q} + \sum_{q=1}^{m} \left(\frac{\beta_{i,q}}{2} \left(\Theta_{i,q}^2 - \widetilde{\Theta}_{i,q}^2 \right) + h_{i,q} \right), \tag{5.17}$$

where $c_{i,m} = k_{i,m} - \varpi_{i,m} - \varpi_{i,m-1}$, $\varpi_{i,m} = \overline{\psi}_{i,m} \overline{\ell}_{i,m}$, and $\Pi_{i,m} = s_{i,m}^{p_i - p_{i,m}+3} \alpha_{i,m}^{p_{i,m}} (\text{sign}(\psi_{i,m}) - h_{i,m}) v_{i,m} |\psi_{i,m}|$, $(m = 2, \ldots, n_i - 1)$.

Step $i, n_i (i = 1, \ldots, N)$ **:** For the last step, consider the Lyapunov function candidate

$$V_{i,n_i} = V_{i,n_i-1} + \frac{s_{i,n_i}^{p_i - p_{i,n_i}+4}}{p_i - p_{i,n_i} + 4} + \frac{1}{2\gamma_{i,n_i}} \widetilde{\Theta}_{i,n_i}^2, \tag{5.18}$$

where $\widetilde{\Theta}_{i,n_i} = \Theta_{i,n_i} - \widehat{\Theta}_{i,n_i}$. Along similar lines as the previous steps, it is possible to conclude that

$$\dot{V}_{i,n_i} < -\sum_{q=1}^{n_i} c_{i,q} s_{i,q}^{p_i+3} + \sum_{q=1}^{n_i} \left(\frac{\beta_{i,q}}{2} \left(\Theta_{i,q}^2 - \widetilde{\Theta}_{i,q}^2 \right) \right) + \sum_{q=1}^{n_i} h_{i,q} + \sum_{q=1}^{n_i} \Pi_{i,q}, \tag{5.19}$$

with $c_{i,n_i} = k_{i,n_i} - \varpi_{i,n_i-1}$ and $\Pi_{i,n_i} = s_{i,n_i}^{p_i - p_{i,n_i}+3} u_i^{p_{i,n_i}} (\text{sign}(\psi_{i,n_i}) - h_{i,n_i}) |\psi_{i,n_i}|$. For any constant $\eta_i > 0$, in light of Lemma 2.2, we have $\eta_i + s_{i,q}^{p_i+3} \geq \eta_i^{\frac{p_{i,q}-1}{p_i+3}} s_{i,q}^{p_i - p_{i,q}+4}$. Thus, (5.19) can be upper bounded as

$$\dot{V}_{i,n_i} < -\varsigma_i V_{i,n_i} + \Xi_i + \sum_{q=1}^{n_i} \Pi_{i,q}, \tag{5.20}$$

where $\varsigma_i = \min \{ \gamma_{i,q} \beta_{i,q}, (p_i - p_{i,q} + 4) c_{i,q} \eta_i^{\frac{p_{i,q}-1}{p_i+3}}, i = 1, \ldots, N, q = 1, \ldots, n_i \}$, $\Xi_i = \sum_{q=1}^{n_i} (c_{i,q} \eta_i + \mu_{i,q}) + \sum_{q=1}^{n_i} \frac{1}{2} \beta_{i,q} \Theta_{i,q}^2$.

The remaining problem is now the one of handling the term $\sum_{q=1}^{n_i} \Pi_{i,q}$ in (5.20) containing the signs of the control directions, which are unknown in view of Assumption 5.1. To tackle this term, a logic-based switching mechanism is proposed in the next section to adapt online the estimates $h_{i,m}$ of the multiple control directions.

5.3.2. Proposed Logic-based Design

Logic-based control has been proposed in the literature for different classes of systems [36, 77, 115]. Because logic-based loops are switched systems [9, 54, 134], the concept of solution is intended in the sense of Carathéodory [54, Sect. 1.2.1]. Also, the subsequent switching mechanism is designed in such a way that chattering is avoided and the switching stops in finite time. Therefore, phenomena such as sliding mode or Zeno behavior, which are often a concern in switched systems, are avoided.

We adopt a similar notation to [36], where the vectors $\boldsymbol{d}_{i,\sigma} \in \mathbb{R}^{n_i}$, whose elements are either 1 or -1, are used to represent all possible combinations of n_i control directions for

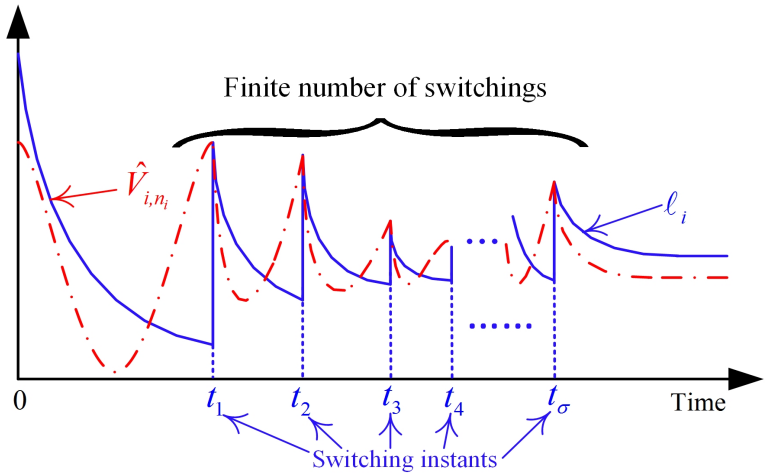

Figure 5.1: The sketch of the proposed switching mechanism.

each agent i. Accordingly, the switching sequence $\sigma(\cdot)$, taking values in $0,1,\ldots,2^{n_i}-1$, is a piecewise right-continuous function [54, Chap.1], and goes through all such possible combinations. For example, if $n_i = 2$, we have four possible combinations: $\boldsymbol{d}_{i,0} = [-1,-1]^T$, $\boldsymbol{d}_{i,1} = [-1,1]^T$, $\boldsymbol{d}_{i,2} = [1,1]^T$, $\boldsymbol{d}_{i,3} = [1,-1]^T$. The order according to which the combinations are listed can be arbitrary, provided that all combinations are listed without repetitions. The reader can refer to [36] for more details on $\boldsymbol{d}_{i,\sigma}$. Please notice that each agent i can exhibit its own switching sequence $\sigma_i(\cdot)$: however, in the following we will simply use $\sigma(\cdot)$ to avoid complicating the notation. Define $\boldsymbol{h}_i(t) = [h_{i,1},\ldots,h_{i,n_i}]^T$ with $h_{i,m} \in \{-1,1\}$, $m = 1,\ldots,n_i$. Let us now define

$$\overline{V}_i(t) = \max\left\{\ell_i(t_\sigma,t),\ \widehat{V}_{i,n_i}(t)\right\}, \tag{5.21}$$

$$\mathscr{L}_i(t_\sigma,t) = \ell_i(t_\sigma,t) - \overline{V}_i(t), \tag{5.22}$$

with

$$\widehat{V}_{i,n_i} = \sum_{m=1}^{n_i}\left\{\frac{s_{i,m}^{p_i-p_{i,m}+4}}{p_i-p_{i,m}+4} + \frac{1}{2\gamma_{i,m}}\widehat{\Theta}_{i,m}^2\right\} \tag{5.23}$$

and $\ell_i(\cdot,\cdot)$ a dynamic boundary function designed as

$$\ell_i(t_\sigma,t) = \left(\overline{V}_i(t_\sigma) - \ell_{i,\infty}(t_\sigma)\right)\exp\left(-\theta_i(t-t_\sigma)\right) + \ell_{i,\infty}(t_\sigma),$$

where $\theta_i > 0$ is a design parameter. Let

$$\mathscr{M}_i(t_\sigma,t) = \mathscr{L}_i(t_\sigma,t) + \kappa_i \tag{5.24}$$

where $\kappa_i > 0$ is a preselected constant.

We are now at the position to present the logic-based mechanism for updating $\boldsymbol{h}_i(t)$, $\sigma(t)$, $k_{i,m}(t)$, $m = 1,\cdots,n_i$, and $\ell_{i,\infty}(t)$. After an initialization phase, the mechanism

comprises a hold phase (i.e. σ is kept constant) and an update phase (i.e. σ is switched to a new value).

Initialization: $t_0 \leftarrow 0, \sigma \leftarrow 0, \boldsymbol{h}_i(t_0) \leftarrow \boldsymbol{d}_{i,0}, \overline{V}_i(t_0) \geq \ell_{i,\infty}(t_0) > 0$ and $\overline{V}_i(t_0) \geq \widehat{V}_{i,n_i}(t_0)$.

Hold phase: Phase in-between consecutive switching instants:

$$\begin{aligned}
&\text{while} && \mathscr{M}_i(t_\sigma, t) \geq 0, && (5.25)\\
&\quad \text{do} && \boldsymbol{h}_i(t) \leftarrow \boldsymbol{d}_{i,\sigma}; && (5.26)\\
& && \ell_{i,\infty}(t) \leftarrow \ell_{i,\infty}(t_\sigma); && (5.27)\\
& && k_{i,m}(t) \leftarrow k_{i,m}(t_\sigma); && (5.28)\\
&\text{end while}
\end{aligned}$$

Update phase: Phase at the switching instant:

$$\begin{aligned}
&\text{if} && \mathscr{M}_i(t_\sigma, t) < 0, && (5.29)\\
&\text{then} && \sigma \leftarrow \sigma + 1; && (5.30)\\
&\quad \text{if} && \sigma \text{ is equal to } 2^{n_i}, \\
&\quad \text{then} && \sigma \leftarrow 0; && (5.31)\\
&\quad \text{end if} \\
& && t_\sigma \leftarrow t; && (5.32)\\
& && \overline{V}_i(t_\sigma) \leftarrow \max\left\{\widehat{V}_{i,n_i}(t_\sigma^-), \widehat{V}_{i,n_i}(t_\sigma)\right\}; && (5.33)\\
& && \boldsymbol{h}_i(t) \leftarrow \boldsymbol{d}_{i,\sigma}; && (5.34)\\
& && \ell_{i,\infty}(t_\sigma) \leftarrow \ell_{i,\infty}(t_{\sigma-1}) + \zeta_{\ell_{i,\infty}}; && (5.35)\\
& && \ell_{i,\infty}(t) \leftarrow \ell_{i,\infty}(t_\sigma); && (5.36)\\
& && k_{i,m}(t_\sigma) \leftarrow k_{i,m}(t_{\sigma-1}) + \zeta_{k_{i,m}}; && (5.37)\\
& && k_{i,m}(t) \leftarrow k_{i,m}(t_\sigma); && (5.38)\\
&\text{end if}
\end{aligned}$$

with $\zeta_{\ell_{i,\infty}} > 0$ and $\zeta_{k_{i,m}} > 0$ design constants, $m = 1,\ldots,n_i$, $\sigma = 1,2,\ldots$, and where t_σ^- denotes the value of t_σ when (5.29) is satisfied but $\boldsymbol{h}_i(t_\sigma)$, $\ell_{i,\infty}(t_\sigma)$, and $k_{i,m}(t_\sigma)$ have not been updated yet, and t_σ represents the time instant when (5.29) holds, and in the meantime, $\boldsymbol{h}_i(t_\sigma)$, $\ell_{i,\infty}(t_\sigma)$, and $k_{i,m}(t_\sigma)$ also have been updated according to (5.34)-(5.38).

The rationale for the proposed mechanism is as follows: the switching instants t_σ, $\sigma = 0,1,...$, occur whenever condition (5.29) is satisfied. The reset condition in (5.31) is necessary when all combinations in $\boldsymbol{d}_{i,\sigma}$ have been visited and thus it is necessary to start from the first one. The logic condition (5.33) circumvents the chattering phenomenon at the switching instants t_σ, as elaborated in Remark 5.3.

Remark 5.1 Inequality (5.29) guarantees that a new switching instant cannot occur immediately after the previous one, i.e., there always exists a positive dwell time between two consecutive switchings. This is due to the fact that $\mathscr{M}_i(t_\sigma, t_\sigma)$ is strictly positive in view of $\mathscr{M}_i(t_\sigma, t_\sigma) = \kappa_i > 0$ since $\ell_i(t_\sigma, t_\sigma) = \overline{V}_i(t_\sigma)$. This eventually implies $t_\sigma \neq t_{\sigma+1}$.

Algorithm 1 Logic-Based Distributed Switching Control Mechanism for the ith Follower Agent

Initialize: Set $t_0 \leftarrow 0$, $\sigma \leftarrow 0$, $\boldsymbol{h}_i(t_0) \leftarrow \boldsymbol{d}_{i,0}$, $\overline{V}_i(t_0) \geq \ell_{i,\infty}(t_0) > 0$ and
  $\overline{V}_i(t_0) \geq \widehat{V}_{i,n_i}(t_0)$. Select positive design parameters $\zeta_{\ell_{i,\infty}}$
  and $\zeta_{k_{i,m}}$, $i = 1,\ldots,N$, $m = 1,\ldots,n_i$.
For every time t, for every agent i, calculate $\widehat{V}_{i,n_i}(t)$, $\ell_i(t_\sigma, t)$, $\overline{V}_i(t)$,
  $\mathscr{L}_i(t_\sigma, t)$, and $\mathscr{M}_i(t_\sigma, t)$.
while $\big(\mathscr{M}_i(t_\sigma, t) \geq 0\big)$, **do**
  Implement virtual control law (5.7), actual control
  law (5.8), and parameter adaptation law (5.9).
  $\boldsymbol{h}_i(t) \leftarrow \boldsymbol{d}_{i,\sigma}$;
  $\ell_{i,\infty}(t) \leftarrow \ell_{i,\infty}(t_\sigma)$;
  $k_{i,m}(t) \leftarrow k_{i,m}(t_\sigma)$;
else
  $\sigma \leftarrow \sigma + 1$;
    if σ is equal to 2^{n_i};
    then $\sigma \leftarrow 0$;
    end if
  $t_\sigma \leftarrow t$;
  $\overline{V}_i(t_\sigma) \leftarrow \max\Big\{\widehat{V}_{i,n_i}(t_\sigma^-),\ \widehat{V}_{i,n_i}(t_\sigma)\Big\}$;
  $\boldsymbol{h}_i(t) \leftarrow \boldsymbol{d}_{i,\sigma}$;
  $\ell_{i,\infty}(t_\sigma) \leftarrow \ell_{i,\infty}(t_{\sigma-1}) + \zeta_{\ell_{i,\infty}}$;
  $\ell_{i,\infty}(t) \leftarrow \ell_{i,\infty}(t_\sigma)$;
  $k_{i,m}(t_\sigma) \leftarrow k_{i,m}(t_{\sigma-1}) + \zeta_{k_{i,m}}$;
  $k_{i,m}(t) \leftarrow k_{i,m}(t_\sigma)$.
end while

The unique challenges of using logic-based mechanisms to handle multiple unknown control directions for power-chained form systems are elaborated in the following remarks:

Remark 5.2 A crucial challenge of the proposed logic-based switching is that the exact value of the Lyapunov function $V_{i,m}$ (5.16) is unavailable (as it contains the unknown constants $\Theta_{i,m}$ in $\widetilde{\Theta}_{i,m} = \Theta_{i,m} - \widehat{\Theta}_{i,m}$). Therefore, the unavailable Lyapunov function must be replaced by some estimate.

Remark 5.3 State-of-the-art logic-based mechanisms [36, 115] cannot formally exclude any chattering phenomenon. This is because these mechanisms adopt $\ell_i(t_\sigma, t_\sigma) = \widehat{V}_{i,n_i}(t_\sigma) = \widehat{V}_{i,n_i}(t_\sigma^-)$. In view of the discussions in [124, Remark 2 and the analysis after eq. (35)], it is theoretically possible for such mechanisms to yield an increase $\widehat{V}_{i,n_i}(t_\sigma) = \overline{V}_i(t_\sigma) > \widehat{V}_{i,n_i}(t_\sigma^-) + \kappa_i = \ell_i(t_\sigma, t_\sigma) + \kappa_i$, which indicates that $\mathscr{M}_i(t_\sigma, t) < 0$, leading to a new switching instant immediately after the previous one. This is because updating $\boldsymbol{h}_i(t)$ and $k_{i,m}$ may result in instantaneous changes in the tracking errors $s_{i,m}$, according to (5.5)-(5.8), which may lead to an increase of Lyapunov functions (5.11), (5.16) and (5.18). This would make the inequality (5.29) hold once more immediately after the previous time instant.

Remark 5.4 State-of-the-art logic-based designs for strict-feedback systems [36, 115] rely on the fact that asymptotic tracking can be obtained for this class of systems: there exists at least one $\boldsymbol{d}_{i,\sigma}$, $\sigma \in \{0, 1, \ldots, 2^{n_i} - 1\}$, that leads to a vanishing tracking error. Unfortunately, it is well known in the literature that asymptotic tracking is impossible in general for the class of nonlinear systems (5.1) [83]. Therefore, the switching logic cannot rely on vanishing tracking errors.

5.4. Stability Analysis

To analyze the stability of the closed-loop system, we consider the global Lyapunov function

$$V = \sum_{i=1}^{N} V_{i,n_i}. \tag{5.39}$$

Theorem 5.1 Under Assumption 5.1 and given bounded initial conditions $\widehat{\Theta}_{i,m}(0) \geq 0$, $i = 1, \ldots, N$, $m = 1, \ldots, n_i$, consider the closed-loop system consisting of the nonlinear multi-agent dynamics (5.1) in power-chained form systems and the logic-based switching control mechanism in Algorithm 1. Then, it holds that:

- All closed-loop signals are semi-globally ultimately uniformly bounded, while the prescribed performances of $\xi_{i,1}(t)$ $\left(i.e.\ \underline{\xi}_{i,1}(t) \leq \xi_{i,1}(t) \leq \overline{\xi}_{i,1}(t)\right)$, $i = 1, \ldots, N$, are ensured.
- Switching stops in finite time and $\delta(t)$ converges to the compact set

$$\Omega^\star = \left\{ \delta(t) \middle| \|\delta(t)\|_{t\to+\infty} \leq \sqrt{\frac{(N^2+N-1)^2 \sum_{i=1}^{N} \frac{\rho_{i,\infty}^2 [(\exp(\overline{s}_{i,1})-1)]^2}{[1+\exp(\overline{s}_{i,1})]^2}}{N^{1-N}(N-1)^{N-1}}} \right\}$$

where $\overline{s}_{i,1} = \left[\left(p_i - p_{i,1} + 4\right)\left(\ell_{i,\infty}(t_{\sigma_s}) + \kappa_i\right)\right]^{\frac{1}{p_i - p_{i,1}+4}}$ with σ_s a sufficiently large integer.

Proof. We provide the proof through two stages. At stage 1, we show that the control goals of Theorem 5.1 are guaranteed on the interval $[0, +\infty)$ provided that the switching stops in finite time. At stage 2, we show by contradiction that indeed the switching stops in finite time.

Stage 1: Let $[0, t_s)$ be the maximum interval of the existence of the closed-loop solution, σ_s be the final switching index, and $t_{\sigma_s} < t_s$ be the time instant when the final switching occurs. Combining (5.21), (5.24), (5.25) and the fact that there is only a finite number of switchings, one can conclude that after the final switching (i.e. for $t > t_{\sigma_s}$), it holds that $\mathscr{L}_i(t_{\sigma_s}, t) + \kappa_i \geq 0$, $t \in [t_{\sigma_s}, t_s)$, which indicates that

$$\widehat{V}_{i,n_i}(t) \leq \ell_i(t_{\sigma_s}, t) + \kappa_i, \ t \in [t_{\sigma_s}, t_s). \tag{5.40}$$

Thus, $\widehat{V}_{i,n_i}(t)$, $s_{i,m}$ and $\widehat{\Theta}_{i,m}(t)$, $i = 1, \ldots, N$, $m = 1, \ldots, n_i$, are bounded due to the boundedness of $\ell_i(\cdot)$ and κ_i on the interval $[t_{\sigma_s}, t_s)$. Furthermore, the virtual control laws $\alpha_{i,m}$, $m = 1, \ldots, n_i - 1$, $i = 1, \ldots, N$ and the actual control law u_i, $i = 1, \ldots, N$ are bounded on $[t_{\sigma_s}, t_s)$ according to (5.6)-(5.8). Thus, $\chi_{i,m}$, $\widetilde{\Theta}_{i,m}$, $m = 1, \ldots, n_i$, $i = 1, \ldots, N$, are bounded on $[t_{\sigma_s}, t_s)$ arising from the fact that $y_r(\cdot)$, $\Theta_{i,m}$ and $\widehat{\Theta}_{i,m}(\cdot)$ are bounded on $[t_{\sigma_s}, t_s)$. According to [91, Theorem 54, page. 476], no finite-time escape phenomenon occurs, and thus $t_s = +\infty$. As a result, one concludes that all closed-loop signals are bounded on the interval $[0, +\infty)$. Then, invoking (5.23) yields

$$\begin{aligned}\lim_{t \to +\infty} |s_{i,1}| &\leq \left[\left(p_i - p_{i,1} + 4\right)\left(\ell_{i,\infty}(t_{\sigma_s}) + \kappa_i\right)\right]^{\frac{1}{p_i - p_{i,1}+4}} \\ &\triangleq \overline{s}_{i,1}\end{aligned}$$

which, in combination with the definition of $s_{i,1}$, gives

$$\lim_{t \to +\infty} \xi_{i,1}(t) \leq \frac{\rho_{i,\infty} \exp(\overline{s}_{i,1}) - \rho_{i,\infty}}{1 + \exp(\overline{s}_{i,1})}$$

After using a lower bound $\frac{\bar{N}}{N^2+N-1}$ [34] with $\bar{N} = \left(\frac{N-1}{N}\right)^{\frac{N-1}{2}}$ for $\sigma_{\min}\left(\overline{\mathscr{L}} + \mathscr{B}\right)$, it follows that

$$\lim_{t \to +\infty} \|\delta(t)\| \leq \sqrt{\frac{(N^2+N-1)^2 \sum_{i=1}^{N} \frac{\rho_{i,\infty}^2 [(\exp(\overline{s}_{i,1})-1)]^2}{[1+\exp(\overline{s}_{i,1})]^2}}{N^{1-N}(N-1)^{N-1}}}.$$

We are now in a position to discuss the existence of a compact set that makes the universal approximation ability valid, provided that the switching stops in finite time.

Consider the initial conditions $\overline{\chi}_{i,m}(0)$ and $\widehat{\Theta}_{i,m}(0) \geq 0$, for $i = 1, \ldots, N$, $m = 1, \ldots, n_i$, satisfying $\widehat{V}\left(\overline{\chi}_{i,m}(0), \widehat{\Theta}_{i,m}(0)\right) < \Upsilon_0$ with $\Upsilon_0 = \sum_{i=1}^{N} \hbar_i$ with $\hbar_i \triangleq \max_{\sigma \in \{0,1,\ldots,\sigma_s\}} \ell_i(t_\sigma, t_\sigma)$ and consider the compact set

$$\Omega_0 = \left\{\left(\overline{\chi}_{i,m}(t), \widehat{\Theta}_{i,m}(t)\right) \middle| \widehat{V}\left(\overline{\chi}_{i,m}, \widehat{\Theta}_{i,m}\right) \leq \Upsilon, \ t \geq 0\right\} \tag{5.41}$$

where $\Upsilon = \Upsilon_0 + \sum_{i=1}^{N} \kappa_i$. According to Algorithm 1, (5.39), and (5.40), $\hbar_i$ is bounded provided that the switching stops in finite time, and that the inequality

$$\widehat{V}\left(\overline{\chi}_{i,m}(t), \widehat{\Theta}_{i,m}(t)\right) < \Upsilon, \tag{5.42}$$

5

holds true for all $t \geq 0$ provided that $\widehat{V}\big(\overline{\boldsymbol{\chi}}_{i,m}(0), \widehat{\Theta}_{i,m}(0)\big) < \Upsilon_0$ holds true. Therefore, the existence of the compact set Ω_0 makes the universal approximation ability of the linear-in-the-parameter approximation valid since all state variables involved are retained in Ω_0 all the time.

Stage 2: At this stage, by seeking a contradiction, we prove that there indeed exist a finite number of switchings. Let us first suppose that there exist an infinite number of switchings. Therefore, there surely exists a sufficiently large t_{σ_s} such that $\gamma_{i,q}\beta_{i,q} \leq (p_i - p_{i,q} + 4)c_{i,q}\eta_i^{\frac{p_{i,q}-1}{p_i+3}}$, $i = 1,\ldots,N, q = 1,\ldots,n_i$, and such that

$$\boldsymbol{h}_i(t) = \boldsymbol{d}_{i,\sigma_s} = [\text{sign}(\psi_{i,1}),\ldots,\text{sign}(\psi_{i,n_i})]^T \tag{5.43}$$

on $[t_{\sigma_s}, t_{\sigma_s+1})$. Thus, $\varsigma_i = \gamma_{i,q}\beta_{i,q}, q = 1,\ldots,n_i, i = 1,\ldots,N$. It follows from (5.40) that (5.43) becomes

$$\dot{V}_{i,n_i} < -\varsigma_i V_{i,n_i} + \Xi_i \ \text{ as } \ \sum_{q=1}^{n_i}\Pi_{i,q} = 0, \tag{5.44}$$

which, combined with (20) and the Gronwall inequality [83], implies that

$$\begin{aligned}
\big|\widehat{\Theta}_{i,m}\big| &< \sqrt{2\gamma_{i,m}\big(V_{i,n_i}(0) + \Xi_i/\varsigma_i\big)} + \Theta_{i,m} \triangleq \bar{\Lambda}_{i,m} \\
s_{i,m}^{p_i+3} &< \Big[(p_i - p_{i,m} + 4)\big(V_{i,n_i}(0) + \Xi_i/\varsigma_i\big)\Big]^{\frac{p_i+3}{p_i-p_{i,m}+4}} \\
&\triangleq \Psi_{i,m}
\end{aligned} \tag{5.45}$$

holds on $[t_{\sigma_s}, t_{\sigma_s+1})$ for $i = 1,\ldots,N$, $m = 1,\ldots,n_i$. Thus, it follows from (5.9) that

$$\big|\dot{\widehat{\Theta}}_{i,m}\big| < \gamma_{i,m}\epsilon_{i,m}^{\overline{p}_{i,m}}\Psi_{i,m}\overline{\Gamma}_{i,m} + \gamma_{i,m}\beta_{i,m}\bar{\Lambda}_{i,m} \triangleq \Upsilon_{i,m} \tag{5.46}$$

holds on $[t_{\sigma_s}, t_{\sigma_s+1})$, where $\overline{\Gamma}_{i,m}$ is the upper bound of $\Gamma_{i,m}^{\overline{p}_{i,m}}$ according to [135, Lemma 2], for $i = 1,\ldots,N$, $m = 1,\ldots,n_i$.

Recalling (5.18), (5.23), (5.44)-(5.46), we can obtain that

$$\begin{aligned}
\dot{\widehat{V}}_{i,n_i}(t) &< -\varsigma_i V_{i,n_i} + \Xi_i + \sum_{m=1}^{n_i}\frac{\Theta_{i,m}\dot{\widehat{\Theta}}_{i,m}}{\gamma_{i,m}} \\
&< -\varsigma_i \widehat{V}_{i,n_i} + \Xi_i + \sum_{m=1}^{n_i}\frac{\Theta_{i,m}\dot{\widehat{\Theta}}_{i,m}}{\gamma_{i,m}} - \sum_{m=1}^{n_i}\frac{\varsigma_i\Theta_{i,m}^2}{2\gamma_{i,m}} \\
&\quad + \sum_{m=1}^{n_i}\frac{\varsigma_i\Theta_{i,m}\widehat{\Theta}_{i,m}}{\gamma_{i,m}} < -\varsigma_i\widehat{V}_{i,n_i} + \widehat{\Xi}_i,
\end{aligned} \tag{5.47}$$

where $\widehat{\Xi}_i = \Xi_i + \sum_{m=1}^{n_i}\frac{\Theta_{i,m}\Upsilon_{i,m}}{\gamma_{i,m}} + \sum_{m=1}^{n_i}\frac{\varsigma_i\Theta_{i,m}\bar{\Lambda}_{i,m}}{\gamma_{i,m}}$ is an unknown positive constant. Hence, we have $\widehat{V}_{i,n_i}(t) \leq \frac{\widehat{\Xi}_i}{\varsigma_i}$, on $[t^*, t_{\sigma_s+1})$, where t^* is the first time instant satisfying $\widehat{V}_{i,n_i}(t^*) = \frac{\widehat{\Xi}_i}{\varsigma_i}$. Then, one has that $\dot{\widehat{V}}_{i,n_i} < 0$ holds when $\widehat{V}_{i,n_i} \geq \frac{\widehat{\Xi}_i}{\varsigma_i}$. The fact that $\widehat{V}_{i,n_i}(\cdot)$ strictly decreases on the time interval $[t_{\sigma_s}, t^*)$ implies that no new switching occurs on $[t_{\sigma_s}, t^*)$ and that $t^* < t_{\sigma_s+1}$.

When $t \in [t_{\sigma_s}, t^*)$, we can guarantee $0 < \theta_i \le \varsigma_i$ by choosing proper $\gamma_{i,q}$, and $\beta_{i,q}$, $q = 1,\ldots,n_i$, according to $\varsigma_i = \gamma_{i,q}\beta_{i,q}, q = 1,\ldots,n_i, i = 1,\ldots,N$, which implies that $\widehat{V}_{i,n_i}(t) \le \ell_i(t)$, on $[t_{\sigma_s}, t^*)$. When $t \in [t^*, t_{\sigma_s+1})$, the condition $\ell_{i,\infty}(t) \ge \frac{\widehat{\Xi}_i}{\varsigma_i}$ can be satisfied via a sufficiently large σ_s in view of (5.27) and (5.28). Hence, it holds that $\widehat{V}_{i,n_i}(t) \le \ell_i(t_{\sigma_s}, t)$, $\forall\, t \in [t^*, t_{\sigma_s+1})$.

To summarize, we have that $\widehat{V}_{i,n_i}(t) < \ell_i(t_{\sigma_s}, t) < \ell_i(t_{\sigma_s}, t) + \kappa_i$, on $[t_{\sigma_s}, t_{\sigma_s+1})$, which means that switching condition (5.29) can never be satisfied on the time interval $[t_{\sigma_s}, t_{\sigma_s+1})$. This contradicts the assumption made in the beginning of stage 2. Thus, the proof is completed. ■

5.5. Simulation Example

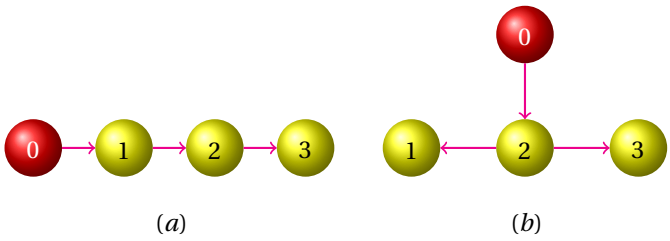

Figure 5.2: Two different communication topologies

To validate the effectiveness of the proposed control method, two sorts of communication topologies including one leader (labeled by 0) with three follower agents are considered as represented by the directed graph of Fig. 5.2. From Fig. 5.2-(a) and 5.2-(b), it can be seen that the signal of the leader is only accessible to follower 1 and follower 2, respectively. The following parameter settings are kept the same for both topologies. The leader output is $y_r = 6\sin(0.5t) + 6\sin(t)$ and the three follower agents are described by the following dynamics:

$$\text{Agent 1} \begin{cases} \dot{\chi}_{1,1} = 1.5\cos(\chi_{1,1})\chi_{1,1} + 0.8\chi_{1,2}^3, \\ \dot{\chi}_{1,2} = \chi_{1,1}\sin(\chi_{1,2}) + \big(\tanh(\chi_{1,1}) + 1.2\big)u_1^5. \end{cases}$$

$$\text{Agent 2} \begin{cases} \dot{\chi}_{2,1} = 1.25\chi_{2,1} + 0.5\chi_{2,1}^3 + 1.5\chi_{2,2}^3, \\ \dot{\chi}_{2,2} = 0.75\chi_{2,2}\chi_{2,1}^2 + \big(\sin(\chi_{2,1})^2 + 0.75\big)u_2^5. \end{cases}$$

$$\text{Agent 3} \begin{cases} \dot{\chi}_{3,1} = 0.5\big(\cos(\chi_{3,1}) + \chi_{3,1}^2\big) + 1.2\chi_{3,2}^3, \\ \dot{\chi}_{3,2} = \chi_{3,1}\sin(\chi_{3,2}) + \big(|\cos(\chi_{3,1})| + 0.2\big)u_3^5. \end{cases}$$

In our simulation, RBF neural networks (NNs) are used as linear-in-the-parameter approximators to approximate $|E_{i,j}(\boldsymbol{Z}_{i,j})|$, $i = 1,2,3$, $j = 1,2$, employing 64 nodes with centers evenly spaced in the interval $[-1.5,1.5] \times [-1.5,1.5] \times [-1.5,1.5] \times [-1.5,1.5] \times [-1.5,1.5] \times [-1.5,1.5] \times [-1.5,1.5] \times [-1.5,1.5]$ and widths equal to two. The initial conditions are selected as: $\chi_{1,1}(0) = 0.75$, $\chi_{1,2}(0) = -1.75$, $\chi_{2,1}(0) = 1.5$, $\chi_{2,2}(0) = -1.5$, $\chi_{3,1}(0) = 1.75$, $\chi_{3,2}(0) = -1.2$, $\widehat{\Theta}_{1,1}(0) = 6.5$, $\widehat{\Theta}_{1,2}(0) = 7.5$, $\widehat{\Theta}_{2,1}(0) = 4$, $\widehat{\Theta}_{2,2}(0) = 3$,

$\widehat{\Theta}_{3,1}(0) = 6.5$, $\widehat{\Theta}_{3,2}(0) = 4.75$, $\ell_{1,\infty}(0) = \ell_{2,\infty}(0) = \ell_{3,\infty}(0) = 0.5$, $k_{1,1}(0) = k_{2,1}(0) = k_{3,1}(0) = 6$, $k_{1,2}(0) = k_{2,2}(0) = k_{3,2}(0) = 8$. The design parameters are chosen as: $\zeta_{k_{1,1}} = \zeta_{k_{1,2}} = 1$, $\zeta_{k_{2,1}} = \zeta_{k_{2,2}} = \zeta_{k_{3,1}} = \zeta_{k_{3,2}} = 1.5$, $\epsilon_{1,1} = \epsilon_{1,2} = \epsilon_{2,1} = \epsilon_{2,2} = \epsilon_{3,1} = \epsilon_{3,2} = 1$, $\varrho_{1,1} = \varrho_{1,2} = \varrho_{2,1} = \varrho_{2,2} = \varrho_{3,1} = \varrho_{3,2} = 1$, $\gamma_{1,1} = \gamma_{2,1} = \gamma_{3,1} = 1$, $\gamma_{1,2} = \gamma_{2,2} = \gamma_{3,2} = 0.4$, $\beta_{1,1} = \beta_{2,1} = \beta_{3,1} = 0.8$, $\beta_{1,2} = \beta_{2,2} = \beta_{3,2} = 6.25$, $\pi_{1,1} = \pi_{2,1} = \pi_{3,1} = 0.25$, $\kappa_1 = \kappa_2 = \kappa_3 = 0.3$, $\theta_1 = 1.8$, $\theta_2 = 1.25$, $\theta_3 = 0.75$, $\zeta_{\ell_{1,\infty}} = \zeta_{\ell_{2,\infty}} = \zeta_{\ell_{3,\infty}} = 0.5$, $\underline{\rho}_{1,1} = \underline{\rho}_{2,1} = \underline{\rho}_{3,1} = -6$, $\overline{\rho}_{1,1} = \overline{\rho}_{2,1} = \overline{\rho}_{3,1} = 8$, $\underline{l}_{1,1} = \underline{l}_{2,1} = \underline{l}_{3,1} = 3$, $\overline{l}_{1,1} = \overline{l}_{2,1} = \overline{l}_{3,1} = 4$, and $\rho_{1,\infty} = \rho_{2,\infty} = \rho_{3,\infty} = 0.95$.

The simulation results are shown in Figs. 5.3-5.18. Fig. 5.3 and Fig. 5.4 reveal that the tracking errors $\xi_{i,1}$, $i = 1,2,3$, under two topologies evolve within their respective bounds. Figs. 5.5-5.7 and Figs. 5.8-5.10 show that the functions $\widehat{V}_{i,n_i}$, $i = 1,2,3$, under both topologies are upper bounded by ℓ_i, $i = 1,2,3$, respectively. It can be seen from Figs. 5.11-5.13 and 5.14-5.16 that switching for both topologies stops in finite time and that the parameters $k_{i,j}$, $i = 1,2,3$, $j = 1,2$, are updated synchronously with the control directions $h_{i,j}$, $i = 1,2,3$, $j = 1,2$. Figs. 5.17-5.18 show that the NN approximators can achieve satisfactory approximation.

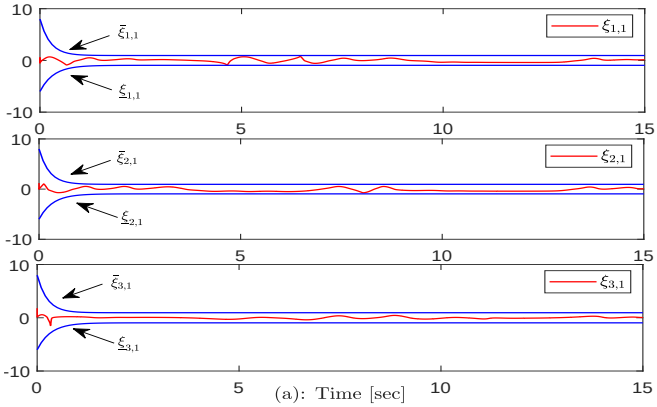

Figure 5.3: Trajectories of the consensus tracking errors $\xi_{1,1}$, $\xi_{2,1}$, and $\xi_{3,1}$.

5.6. Conclusions

This chapter has proposed a logic-based switching mechanism for distributed switching tracking control for nonlinear multi-agent systems in power-chained form systems and with multiple unknown control directions. A novel dynamic boundary function that is decreasing in-between switching instants and possibly increasing at the switching instants has been devised to tackle the issue that asymptotic tracking cannot be achieved for such challenging nonlinear systems. An interesting problem to be investigated in the future is to combine logic-based updates of the control directions with logic-based updates of the parameters.

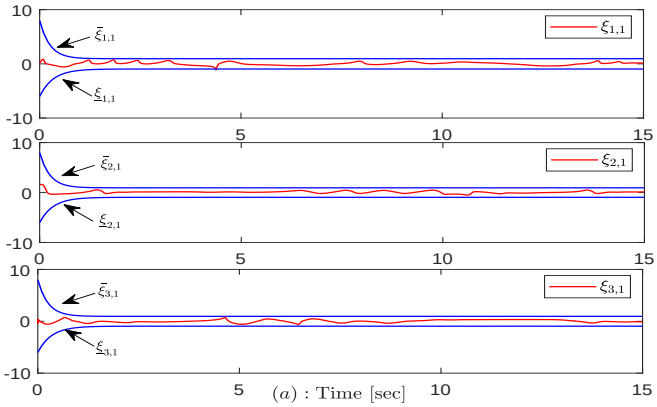

Figure 5.4: Topology in Fig. 2-(b): trajectories of the consensus tracking errors $\xi_{1,1}$, $\xi_{2,1}$, and $\xi_{3,1}$.

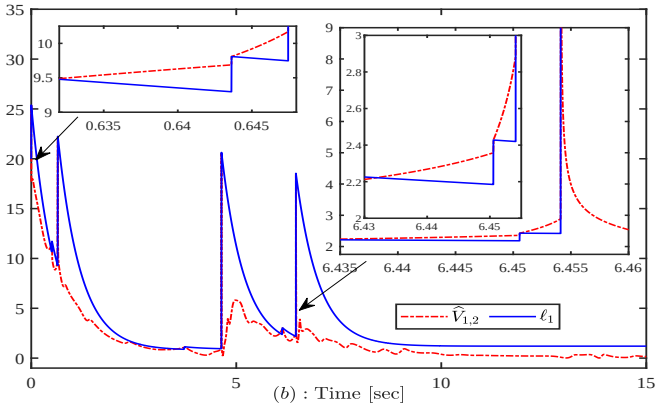

Figure 5.5: Topology in Fig. 2-(a): trajectories of $\widehat{V}_{1,2}$ and ℓ_1 .

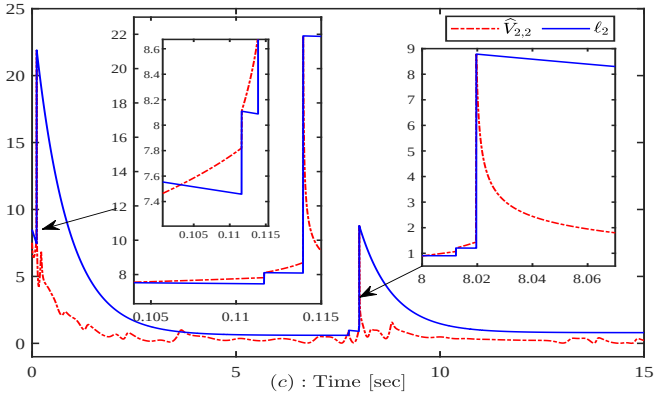

Figure 5.6: Topology in Fig. 2-(a): trajectories of $\widehat{V}_{2,2}$ and ℓ_2.

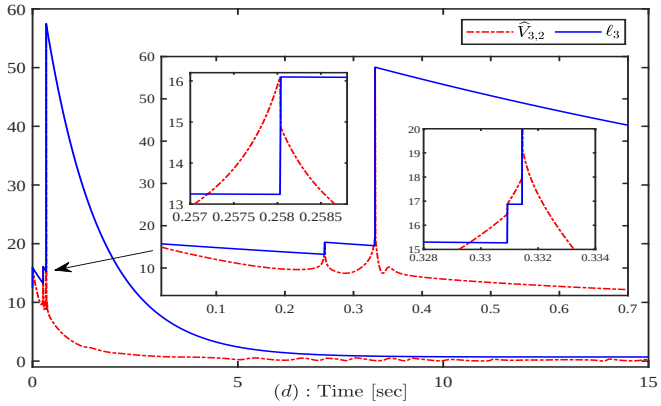

Figure 5.7: Topology in Fig. 2-(a): trajectories of $\widehat{V}_{3,2}$ and ℓ_3.

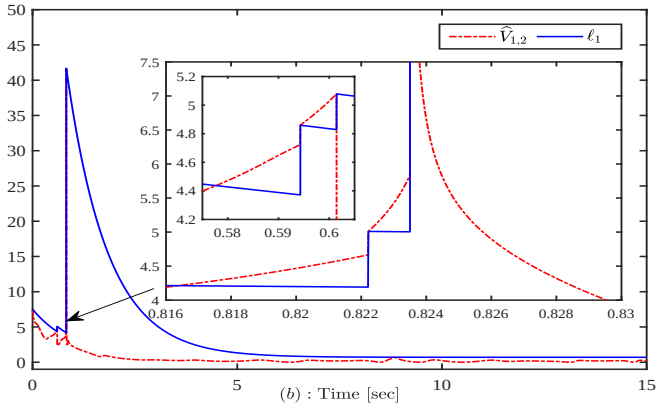

Figure 5.8: Topology in Fig. 2-(b): trajectories of $\widehat{V}_{1,2}$ and ℓ_1 .

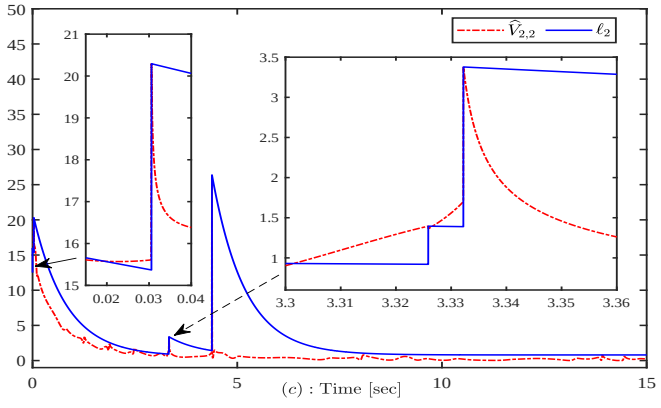

Figure 5.9: Topology in Fig. 2-(b): trajectories of $\widehat{V}_{2,2}$ and ℓ_2.

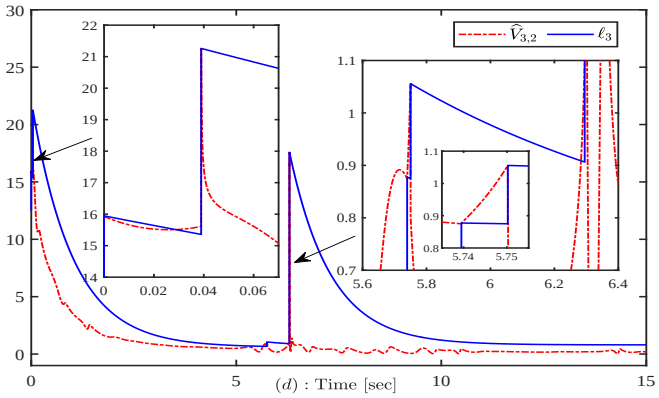

Figure 5.10: Topology in Fig. 2-(b): trajectories of $\widehat{V}_{3,2}$ and ℓ_3.

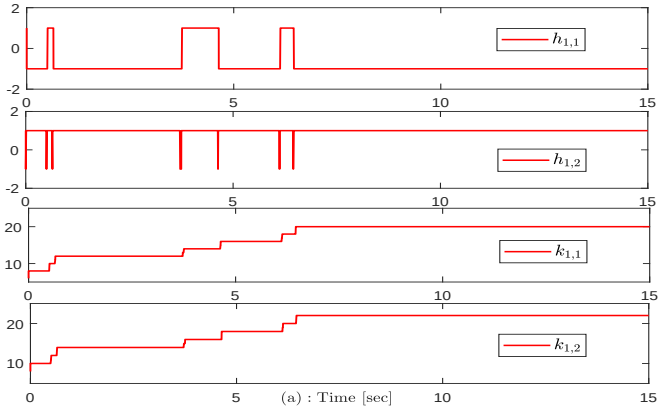

Figure 5.11: Topology in Fig. 2-(a): evolution of $h_{1,1}$, $h_{1,2}$, $k_{1,1}$, and $k_{1,2}$.

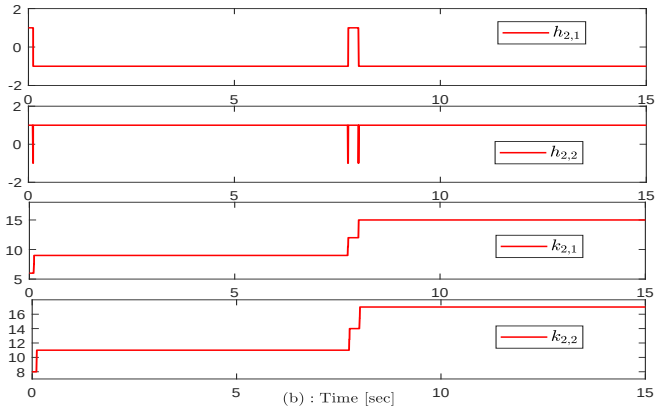

Figure 5.12: Topology in Fig. 2-(a): evolution of $h_{2,1}$, $h_{2,2}$, $k_{2,1}$ and $k_{2,2}$.

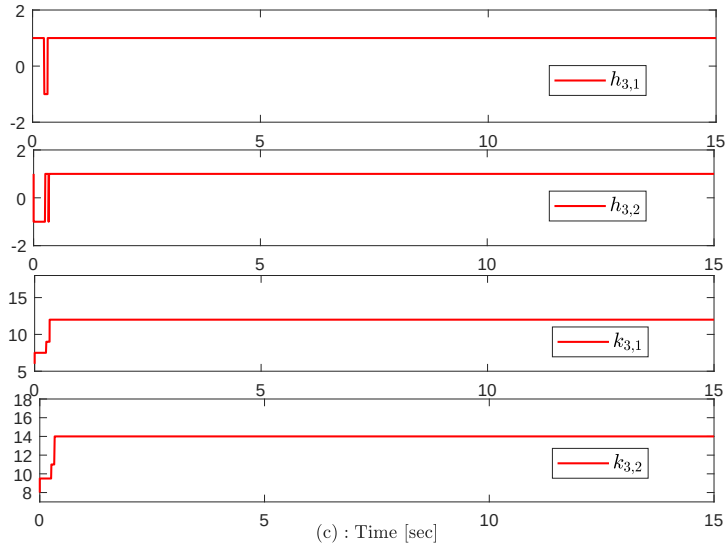

Figure 5.13: Topology in Fig. 2-(a): evolution of $h_{3,1}$, $h_{3,2}$, $k_{3,1}$, and $k_{3,2}$.

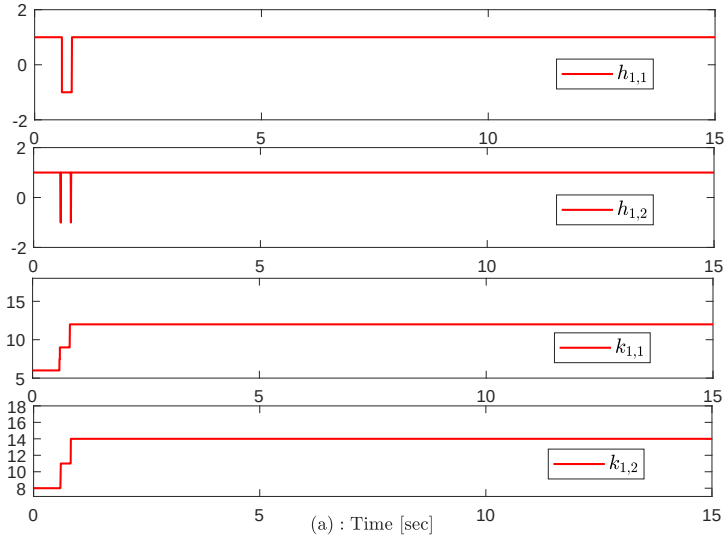

Figure 5.14: Topology in Fig. 2-(b): evolution of $h_{1,1}$, $h_{1,2}$, $k_{1,1}$, and $k_{1,2}$.

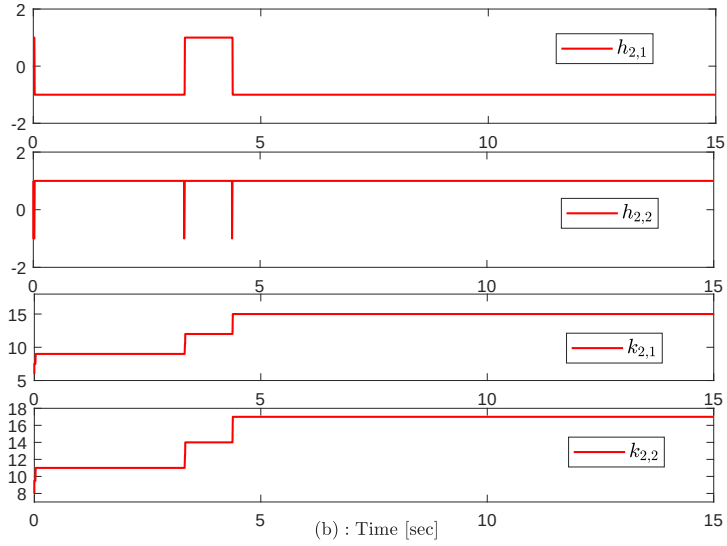

Figure 5.15: Topology in Fig. 2-(b): evolution of $h_{2,1}$, $h_{2,2}$, $k_{2,1}$, and $k_{2,2}$.

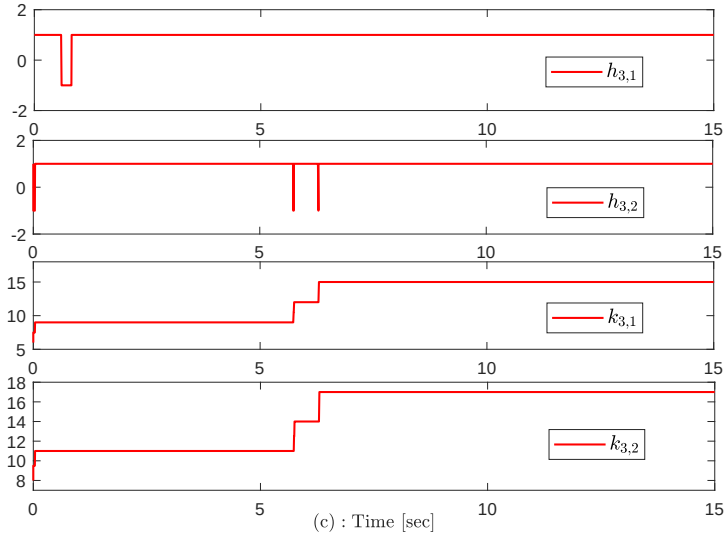

Figure 5.16: Topology in Fig. 2-(b): evolution of $h_{3,1}$, $h_{3,2}$, $k_{3,1}$, and $k_{3,2}$.

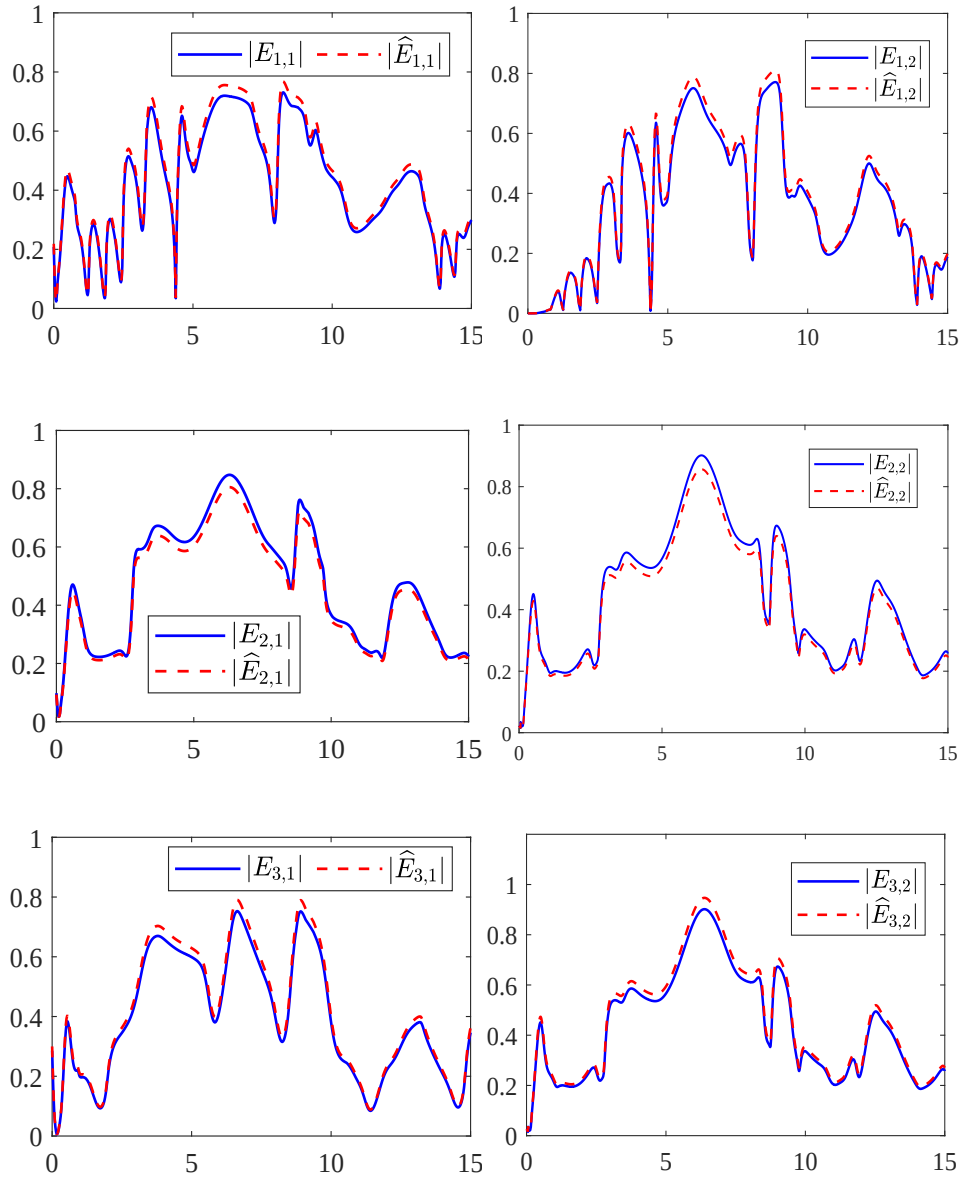

Figure 5.17: Topology in Fig. 2-(a): evolution of $|E_{1,1}|$, $|E_{1,2}|$, $|E_{2,1}|$, $|E_{2,2}|$, $|E_{3,1}|$, $|E_{3,2}|$, and their NN approximations $|\widehat{E}_{1,1}|$, $|\widehat{E}_{1,2}|$, $|\widehat{E}_{2,1}|$, $|\widehat{E}_{2,2}|$, $|\widehat{E}_{3,1}|$, $|\widehat{E}_{3,2}|$.

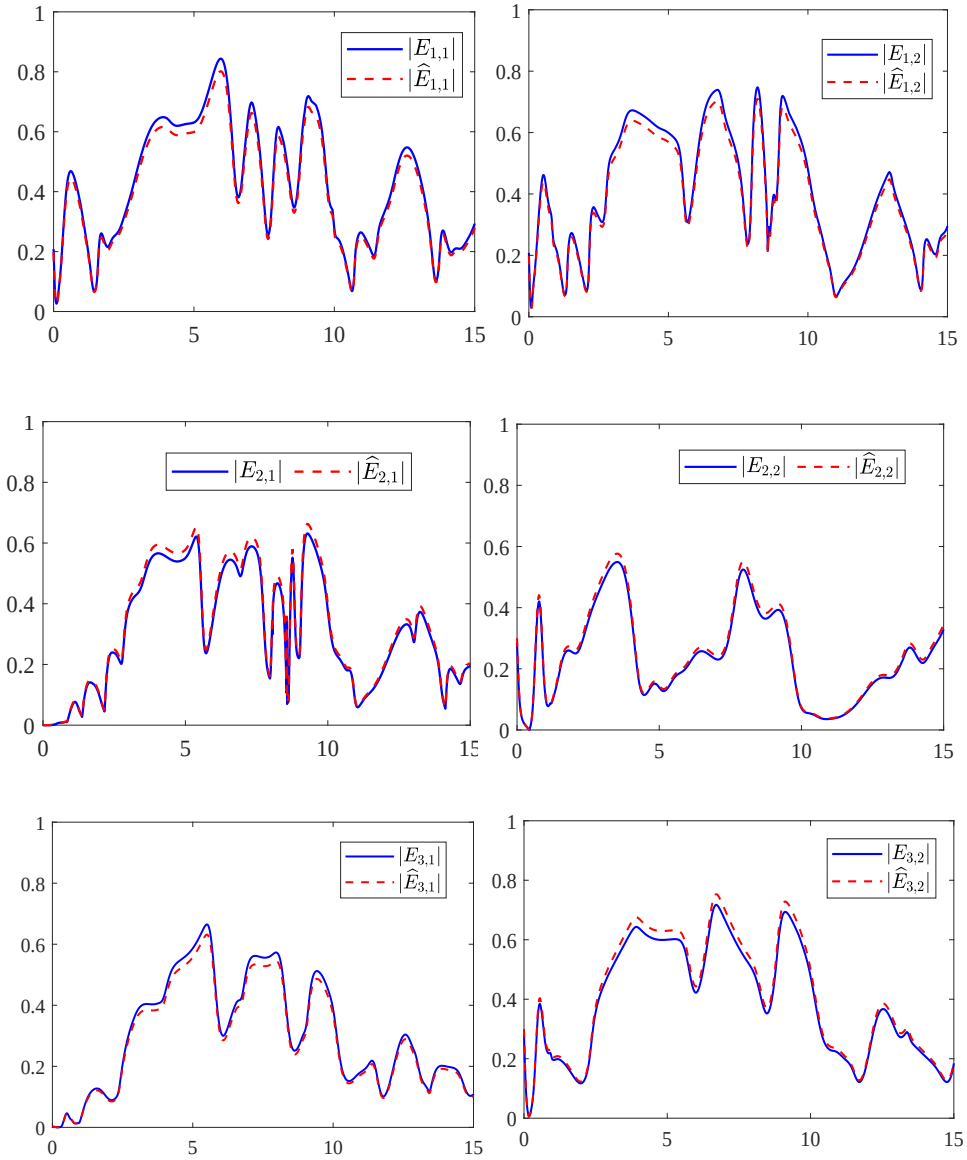

Figure 5.18: Topology in Fig. 2-(b): evolution of $|E_{1,1}|$, $|E_{1,2}|$, $|E_{2,1}|$, $|E_{2,2}|$, $|E_{3,1}|$, $|E_{3,2}|$, and their NN approximations $|\widehat{E}_{1,1}|$, $|\widehat{E}_{1,2}|$, $|\widehat{E}_{2,1}|$, $|\widehat{E}_{2,2}|$, $|\widehat{E}_{3,1}|$, $|\widehat{E}_{3,2}|$.

6

Approximation-Free Prescribed-Performance Tracking for Power-Chained Form Systems with Time-Varying Unknown Control Coefficients

Approximation-free prescribed-performance control (PPC) for power-chained form systems with time-varying unknown control coefficients requires to address two open problems: a) given a Nussbaum function, which properties hold for the power of the Nussbaum function? b) to avoid high gains, how to design a switching gain that increases only when the tracking error is close to violating the performance bounds? To address the first problem, we show with a counterexample and a positive example that only some Nussbaum functions are suited to handle time-varying unknown control coefficients for power-chained form systems. To address the second problem, we propose a new switching conditional inequality. The introduction is given in Section 6.1. The problem formulation and preliminaries are provided in Section 6.2. Sections 6.3 and 6.4 present the proposed distributed consensus design and stability analysis, respectively. The simulation examples are in Section 6.5 and Section 6.6 draws the conclusion.

6.1. Introduction

In Chapters 4-5, the adding-one-power-integrator technique has been successfully combined with Nussbaum functions and logic-based adaptation method to tackle multiple unknown control directions, respectively. However, it should be noted that a universal

approximator (i.e. RBF NN) has been involved in the design therein to approximate unknown system nonlinearities. Such a fact unavoidably increases the complexity of the control schemes since additional adaptation parameters are required to be updated online (i.e. additional nonlinear differential equations must be solved numerically) and additional calculations must be performed to generate control signal [12]. Approximation-free PPC is a control methodology whose strongest feature is its structural simplicity: uncertainty can be handled without unknown parameter estimators nor approximation structures (neural networks, fuzzy logic, etc.) being involved in the control design, while at the same time guaranteeing some prescribed specifications (e.g. maximum overshoot, minimum convergence rate, and maximum steady-state error).

With respect to handling unknown signs of control coefficients, the Nussbaum function invented in [75] has been extensively used for tackling such issue. A fundamental tool to prove closed-loop stability is the so-called conditional inequality, which consists in guaranteeing the boundedness of a Lyapunov-like function when its derivative along the system trajectories is upper bounded by an appropriate expression depending on the Nussbaum function. As the control coefficients can be constants or time-varying functions, three representative conditional inequalities have been proposed so far [18, 29, 125] to handle these cases. The first conditional inequality was formulated in [125] to handle unknown signs of constant control coefficients. The second conditional inequality in [29] (see also discussions in [81]) is given in integral form to handle unknown signs of time-varying control coefficients. Recently, [18] categorized the Nussbaum functions according to some special properties. This categorization led to type A and type B Nussbaum functions where the former can handle constant control coefficients, but only the latter can handle time-varying control coefficients. Unfortunately, the capability to handle time-varying control coefficients was shown in [18] only for strict-feedback and pure-feedback systems, and handling power-chained form nonlinear systems is an open question due to the presence of positive odd-integer-power in their dynamics.

The main challenge of incorporating Nussbaum functions into approximation-free PPC is to avoid high-gain issues, since the current results are based on a continuous and monotonic increase of the gain of the Nussbaum function [133]. With these problems in mind, realizing Nussbaum adaptive PPC for power-chained form nonlinear dynamics with time-varying control coefficients of unknown signs requires to answer two open questions: *(i) whether a positive odd-integer power of a type B Nussbaum function is still a type B Nussbaum function and why? (ii) is it possible to design a switching conditional inequality (replacing standard non-switching conditional inequalities) that avoids monotonically increasing high-gain issues?*

This chapter gives positive answers to above-mentioned questions and its main contributions are listed below:

- A counterexample and a positive example are given to show two crucial points: a positive odd-integer power of a type B Nussbaum function might not be a type B Nussbaum function; only some particular type B Nussbaum functions keep their property even when elevated to a positive odd-integer power. These latter functions can be used for handling time-varying unknown control coefficients.

- A new switching conditional inequality is proposed. This inequality encompasses existing ones as special cases: instead of always increasing the Nussbaum gain, its design is based on increasing the Nussbaum gain only when the tracking error is close to violating the performance bounds.

6.2. Problem Formulation and Preliminaries

This chapter considers the power-chained form nonlinear systems [55, 56, 83]:

$$\begin{cases} \dot{\chi}_i = \phi_i(\overline{\boldsymbol{\chi}}_i) + \psi_i(\overline{\boldsymbol{\chi}}_i)\chi_{i+1}^{p_i}, \ i = 1,\ldots,n-1, \\ \dot{\chi}_n = \phi_n(\overline{\boldsymbol{\chi}}_n) + \psi_n(\overline{\boldsymbol{\chi}}_n)u^{p_n}, \\ y = \chi_1, \end{cases} \tag{6.1}$$

where $\overline{\boldsymbol{\chi}}_i = [\chi_1,\ldots,\chi_i]^T \in \mathbb{R}^i$, p_i, $i = 1,\ldots,n$, are positive odd integers, and $u \in \mathbb{R}$ is the control input to be designed. The unknown continuous nonlinear functions $\phi_i(\cdot) : \mathbb{R}^i \to \mathbb{R}$ (referred to as drift coefficients) and $\psi_i(\cdot) : \mathbb{R}^i \to \mathbb{R}$, $i = 1,\ldots,n$, (referred to as control coefficients) satisfy the following standard assumption.

Assumption 6.1 [133] There exist unknown, continuous, and positive functions $\overline{\phi}_i(\cdot) : \mathbb{R}^i \to \mathbb{R}^+$, $\underline{\psi}_i(\cdot)$, and $\overline{\psi}_i(\cdot) : \mathbb{R}^i \to \mathbb{R}^+$, $i = 1,\ldots,n$, such that

$$|\phi_i(\overline{\boldsymbol{\chi}}_i)| \le \overline{\phi}_i(\overline{\boldsymbol{\chi}}_i), \text{ and } \underline{\psi}_i(\overline{\boldsymbol{\chi}}_i) \le |\psi_i(\overline{\boldsymbol{\chi}}_i)| \le \overline{\psi}_i(\overline{\boldsymbol{\chi}}_i). \tag{6.2}$$

Note that Assumption 6.1 does not require the knowledge of the signs of the control coefficients. Nussbaum functions [75] are standard tools to address unknown signs of the control coefficients.

Definition 6.1 [18, Definition 3.1], [75] A continuous function $\mathcal{N}(\cdot) : [0,+\infty) \to (-\infty,+\infty)$ is called a *type A Nussbaum function* if it satisfies

$$\lim_{y\to+\infty} \sup \frac{\int_0^y \mathcal{N}(s)ds}{y} = +\infty, \lim_{y\to+\infty} \inf \frac{\int_0^y \mathcal{N}(s)ds}{y} = -\infty.$$

Definition 6.2 [18, Definition 4.3] A continuous function $\mathcal{N}(\cdot) : [0,+\infty) \to (-\infty,+\infty)$ is called a *type B Nussbaum function* if it satisfies

$$\lim_{y\to+\infty} \frac{\int_0^y \mathcal{N}_+(s)ds}{y} = +\infty, \lim_{y\to+\infty} \sup \frac{\int_0^y \mathcal{N}_-(s)ds}{\int_0^y \mathcal{N}_+(s)ds} = +\infty,$$

$$\lim_{y\to+\infty} \frac{\int_0^y \mathcal{N}_-(s)ds}{y} = +\infty, \lim_{y\to+\infty} \sup \frac{\int_0^y \mathcal{N}_+(s)ds}{\int_0^y \mathcal{N}_-(s)ds} = +\infty,$$

where $\mathcal{N}_+(s) = \max\{0, \mathcal{N}(s)\}$ and $\mathcal{N}_-(s) = \max\{0, -\mathcal{N}(s)\}$ are the positive and negative truncated functions of $\mathcal{N}(s)$.

Remark 6.1 Note that type B Nussbaum functions are a special class of type A Nussbaum functions [18]. It was shown in [18] that type A Nussbaum functions can handle unknown signs of constant control coefficients, but may fail to handle unknown signs of time-varying control coefficients. Accordingly, type B Nussbaum functions were proposed to tackle the time-varying scenarios.

The main problem studied in this chapter is stated below.

Prescribed-performance control (PPC) problem: Consider a bounded reference signal $y_r(t)$ with bounded derivative and a performance function $\rho_1(t) = (\rho_{1,0} - \rho_{1,\infty}) \times \exp(-\kappa_1 t)$
$+ \rho_{1,\infty}$ for positive constants $\rho_{1,0} > \rho_{1,\infty}$ and κ_1. The PPC problem aims to design a controller for the system (6.1) such that the closed-loop system satisfies the following two properties:

(P1) The output tracking error $e_1(t) = y(t) - y_r(t)$ evolves in the prescribed set $\Omega = \{e_1(t) \in \mathbb{R} \,|\, |e_1(t)| < \rho_1(t)\}$ for $t \geq 0$; and

(P2) The closed-loop signals are bounded on the entire time domain $[0, +\infty)$.

The PPC problem has been well formulated in literature. However, this problem remains unsolved for the class of dynamics (6.1) and even the stability analysis recently proposed in [18] does not apply. Solving this problem requires to address two open issues: given a Nussbaum function, which properties hold for the power of the Nussbaum function? To avoid high gains, how to design a switching gain that increases only when the tracking error is close to violating the performance bounds? These two problems are addressed by the technical results in the next section.

To handle the power-chained form systems nonlinearities in (6.1) with unknown control coefficients, it is required that the positive odd-integer power of a Nussbaum function, denoted by $\mathscr{N}^p(\cdot)$, is still a Nussbaum function. However, we show that the positive odd-integer-power of a type B Nussbaum function may not always result in a type B Nussbaum function. A counterexample and a positive example are given in the following two propositions, respectively, with the proofs given in Appendix.

Proposition 6.1 (Counterexample) Consider the function defined by

$$\mathscr{N}(s) = \sum_{\lambda \in \mathbb{N}^+} \mathscr{N}_\lambda(s + 2 - 2^\lambda), \tag{6.3}$$

where $\mathbb{N}^+$ is the set of positive integers and

$$\mathscr{N}_\lambda(s) = \begin{cases} 2^{(\lambda^3+\frac{1}{3})\lambda} \sin(s\pi), & \text{if } s \in [0,1) \\ -2^{\lambda^4} \sin\left(\dfrac{s-1}{2^\lambda - 1}\pi\right), & \text{if } s \in [1, 2^\lambda) \\ 0, & \text{otherwise} \end{cases}. \tag{6.4}$$

Then, $\mathscr{N}(\cdot)$ is a type B Nussbaum function, but $\mathscr{N}^p(\cdot)$ with $p \geq 3$ a positive odd integer is *not* a type B Nussbaum function.

Proof. We first define some quantities as follows:

$$\begin{aligned} \varsigma_{\lambda,p} &= \int_0^1 \left[2^{(\lambda^3+\frac{1}{3})\lambda} \sin(s\pi)\right]^p ds \\ &= 2^{p(\lambda^3+\frac{1}{3})\lambda} \int_0^1 \sin^p(s\pi) ds = 2^{p(\lambda^4+\frac{1}{3}\lambda)} \alpha_p \end{aligned}$$

and

$$q_{\lambda,p} = \int_1^{2^\lambda} \left[2^{\lambda^4} \sin\left(\frac{s-1}{2^\lambda-1}\pi\right)\right]^p ds = 2^{p\lambda^4} \int_1^{2^\lambda} \sin^p\left(\frac{s-1}{2^\lambda-1}\pi\right) ds$$
$$= 2^{p\lambda^4}(2^\lambda-1)\int_0^1 \sin^p(s\pi)\, ds = 2^{p\lambda^4}(2^\lambda-1)\alpha_p$$

for $\alpha_p = \int_0^1 \sin^p(s\pi) ds$. In accordance with Definition 6.2, the proof is divided into three parts.

(i) For any $y \geq 0$, there exists $\lambda \in \mathbb{N}^+$ such that $y \in [2^\lambda - 2, 2^{\lambda+1} - 2)$. As a result, it holds that

$$\frac{1}{y}\int_0^y \mathscr{N}_-(s)ds \geq \frac{1}{2^{\lambda+1}-2}\int_0^{2^\lambda-1} \mathscr{N}_-(s)ds$$
$$= \frac{\sum_{k=1}^{\lambda-1} q_{k,1}}{2^{\lambda+1}-2} = \frac{\sum_{k=1}^{\lambda-1} 2^{k^4}(2^k-1)\alpha_p}{2^{\lambda+1}-2} \geq 2^\lambda \alpha_p$$

for $\lambda \geq 3$. The fact that $\lambda \to +\infty$ as $y \to +\infty$ implies $\lim_{y\to+\infty} \frac{1}{y}\int_0^y \mathscr{N}_-(s)ds = +\infty$.

(ii) Note the following calculation, with $y = 2^\lambda - 1$:

$$\frac{\int_0^y \mathscr{N}_+(s)ds}{\int_0^y \mathscr{N}_-(s)ds} = \frac{\sum_{k=1}^{\lambda} \varsigma_{k,1}}{\sum_{k=1}^{\lambda-1} q_{k,1}} = \frac{\sum_{k=1}^{\lambda} 2^{k^4+\frac{1}{3}k}}{\sum_{k=1}^{\lambda-1} 2^{k^4}(2^k-1)}. \tag{6.5}$$

It follows from the Stolz-Cesaro Theorem [72, Sect. 3.17, pp. 85, Theorem 1.22] that

$$\lim_{\lambda\to+\infty} \frac{\sum_{k=1}^{\lambda} 2^{k^4+\frac{1}{3}k}}{\sum_{k=1}^{\lambda-1} 2^{k^4}(2^k-1)} = \lim_{\lambda\to+\infty} \frac{2^{\lambda^4+\frac{1}{3}\lambda}}{2^{(\lambda-1)^4+\lambda-1}} = +\infty$$

which, together with (6.5), implies $\lim\limits_{y\to+\infty} \sup \frac{\int_0^y \mathscr{N}_+(s)ds}{\int_0^y \mathscr{N}_-(s)ds} = +\infty$.

The results $\lim\limits_{y\to+\infty} \frac{1}{y}\int_0^y \mathscr{N}_+(s)ds = +\infty$ and $\lim\limits_{y\to+\infty} \sup \frac{\int_0^y \mathscr{N}_-(s)ds}{\int_0^y \mathscr{N}_+(s)ds} = +\infty$ can be proved in a similar way and are omitted. According to Definition 6.2, $\mathscr{N}(\cdot)$ is a type B Nussbaum function.

(iii) For any $y \geq 0$, there exists $\lambda \in \mathbb{N}^+$ such that $y \in [2^\lambda - 2, 2^{\lambda+1} - 2)$. According to the definition of $\mathscr{N}^p$, we have

$$\frac{\int_0^y \mathscr{N}_-^p(s)ds}{\int_0^y \mathscr{N}_+^p(s)ds} \leq \frac{\int_0^{2^\lambda-2} \mathscr{N}_-^p(s)ds}{\int_0^{2^\lambda-2} \mathscr{N}_+^p(s)ds} \text{ or } \frac{\int_0^{2^{\lambda+1}-2} \mathscr{N}_-^p(s)ds}{\int_0^{2^{\lambda+1}-2} \mathscr{N}_+^p(s)ds}.$$

The following calculation:

$$\lim_{y\to+\infty}\sup\frac{\int_0^y \mathscr{N}_-^p(s)ds}{\int_0^y \mathscr{N}_+^p(s)ds}\le\lim_{\lambda\to+\infty}\frac{\int_0^{2^{\lambda+1}-2}\mathscr{N}_-^p(s)ds}{\int_0^{2^{\lambda+1}-2}\mathscr{N}_+^p(s)ds}=$$
$$\le\lim_{\lambda\to+\infty}\frac{\sum_{k=1}^{\lambda}q_{k,p}}{\sum_{k=1}^{\lambda-1}\varsigma_{k,p}}=\lim_{\lambda\to+\infty}\frac{\sum_{k=1}^{\lambda}2^{pk^4}\left(2^k-1\right)}{\sum_{k=1}^{\lambda}2^{p\left(k^4+\frac{1}{3}k\right)}}$$
$$=\lim_{\lambda\to+\infty}\left(2^{\lambda-\frac{p\lambda}{3}}-2^{-\frac{p\lambda}{3}}\right)=\begin{cases}+\infty, & p=1;\\ 1, & p=3;\\ 0, & p>3.\end{cases}$$

shows the violation of Definition 6.2. Thus, one can conclude that $\mathscr{N}^p(\cdot)$ is not a type B Nussbaum function. This completes the proof. ■

Proposition 6.2 (Positive example) Consider the function

$$\mathscr{N}(s)=\exp(\mu s^2)\cos\left(\frac{\pi s}{2}\right),\ \mu>0. \tag{6.6}$$

Then, $\mathscr{N}^p(\cdot)$ is a type B Nussbaum function for any positive odd integer $p\ge1$.

Proof. According to [18], $\mathscr{N}^p(\cdot)$ is a type B Nussbaum function for $p=1$. So the remaining task is to show that statement still holds for $p\ge3$. By the Darboux-Stieltjes integral property [72, Sect. 6.12, pp. 257, Theorem 1.7, (h)], for any $a\ge0$, it holds that

$$\exp\left(p\mu a^2\right)\alpha_p\le\int_a^{a+1}\exp\left(p\mu s^2\right)\left|\cos^p\left(\frac{\pi s}{2}\right)\right|ds$$
$$=\exp\left(p\mu\bar{s}^2\right)\int_a^{a+1}\left|\cos^p\left(\frac{\pi s}{2}\right)\right|ds\le\exp\left(p\mu(a+1)^2\right)\bar{\alpha}_p \tag{6.7}$$

for some $\bar{s}\in(a,a+1)$ and $\bar{\alpha}_p=\int_0^1\cos^p\left(\frac{\pi s}{2}\right)ds$, which is used in the remainder of the proof. In accordance with Definition 6.2, the proof is divided into two parts.

(i) For any $y\ge0$, there exists $\lambda\in\mathbb{N}$ such that $y\in[4\lambda-3,4\lambda+1)$, where $\mathbb{N}$ is the set of integers. As a result, one has

$$\frac{1}{y}\int_0^y\mathscr{N}_+^p(s)ds>\frac{1}{4\lambda+1}\int_0^{4\lambda-1}\mathscr{N}_+^p(s)ds$$
$$>\frac{1}{4\lambda+1}\sum_{k=1}^{\lambda-1}\int_{4k-1}^{4k+1}\exp\left(p\mu s^2\right)\cos^p\left(\frac{\pi s}{2}\right)ds.$$

By (6.7), we can arrive at

$$\int_{4k-1}^{4k+1}\exp\left(p\mu s^2\right)\cos^p\left(\frac{\pi s}{2}\right)ds\ge2\bar{\alpha}_p\exp\left(p\mu(4k-1)^2\right)$$

and hence

$$\lim_{y\to+\infty}\frac{1}{y}\int_0^y \mathscr{N}_+^p(s)ds \geq \lim_{\lambda\to+\infty}\frac{2\bar{\alpha}_p\sum_{k=1}^{\lambda-1}\exp\left(p\mu(4k-1)^2\right)}{4\lambda+1}=+\infty.$$

(ii) Note the following calculation, with $y=4\lambda+3$:

$$\begin{aligned}\frac{\int_0^y \mathscr{N}_-^p(s)ds}{\int_0^y \mathscr{N}_+^p(s)ds} &= \frac{\int_0^{4\lambda+3} \mathscr{N}_-^p(s)ds}{\int_0^{4\lambda+3} \mathscr{N}_+^p(s)ds}\\ &> \frac{\sum_{k=0}^{\lambda}\int_{4k+1}^{4k+3}\exp\left(p\mu s^2\right)\left|\cos^p\left(\frac{\pi s}{2}\right)\right|ds}{\sum_{k=0}^{\lambda}\int_{4k-1}^{4k+1}\exp\left(p\mu s^2\right)\cos^p\left(\frac{\pi s}{2}\right)ds}\\ &\geq \frac{\sum_{k=0}^{\lambda}\left[\exp\left(p\mu(4k+1)^2\right)+\exp\left(p\mu(4k+2)^2\right)\right]\bar{\alpha}_p}{\sum_{k=0}^{\lambda}\left[\exp\left(p\mu(4k)^2\right)+\exp\left(p\mu(4k+1)^2\right)\right]\bar{\alpha}_p}.\end{aligned}$$

It follows from Stolz-Cesaro Theorem [72] that

$$\lim_{\lambda\to+\infty}\frac{\int_0^{4\lambda+3} \mathscr{N}_-^p(s)ds}{\int_0^{4\lambda+3} \mathscr{N}_+^p(s)ds} \geq \lim_{\lambda\to+\infty}\frac{\exp\left(p\mu(4\lambda+2)^2\right)}{\exp\left(p\mu(4\lambda+1)^2\right)}=+\infty,$$

which implies $\lim_{y\to+\infty}\sup\frac{\int_0^y \mathscr{N}_-^p(s)ds}{\int_0^y \mathscr{N}_+^p(s)ds}=+\infty$.

The results $\lim_{y\to+\infty}\frac{1}{y}\int_0^y \mathscr{N}_-^p(s)ds=+\infty$ and $\lim_{y\to+\infty}\sup\frac{\int_0^y \mathscr{N}_+^p(s)ds}{\int_0^y \mathscr{N}_-^p(s)ds}=+\infty$ can be proved similarly. According to Definition 6.2, $\mathscr{N}^p(\cdot)$ is a type B Nussbaum function. ■

The following lemma is instrumental to constructing a Nussbaum gain that increases only when the tracking error is close to violate the performance bounds.

Lemma 6.1 (Switching conditional inequality) Let $\mathscr{N}(\cdot)$ be a type B Nussbaum function. Consider two continuous and piecewise differentiable functions $V(\cdot)$ and $s(\cdot)$ such that

$$\dot{V}(t)\leq\left[\psi(t)\mathscr{N}(s(t))+\beta\right]\dot{s}(t), \tag{6.8}$$

$$\dot{s}(t)\begin{cases}\geq 0, & \text{if } V(t)\geq\phi,\\ =0, & \text{if } V(t)<\phi,\end{cases} \tag{6.9}$$

where ϕ and β are positive constants, $V(0)<\phi$, $s(0)=0$, and $\psi(\cdot)$ is a time-varying unknown function satisfying $\psi(t)\in[l_1,l_2]$, $\forall t\geq 0$ with either $0>l_2>l_1$ or $l_2>l_1>0$. Then, $V(\cdot)$ and $s(\cdot)$ are bounded on the entire time domain $[0,+\infty)$.

Remark 6.2 For better comprehension, a sketch of the idea behind (6.8) is shown in Fig. 6.1. In the figure and in the following proof, let $0=t_0<t_1\leq t_2\leq t_3\leq\ldots$ be the time sequence satisfying $V(t_j)=\phi$, $V(t)<\phi$, $\forall t\in(t_{2j-2},t_{2j-1})$, and $V(t)\geq\phi$, $\forall t\in[t_{2j-1},t_{2j}]$, for $j=1,2,\ldots$

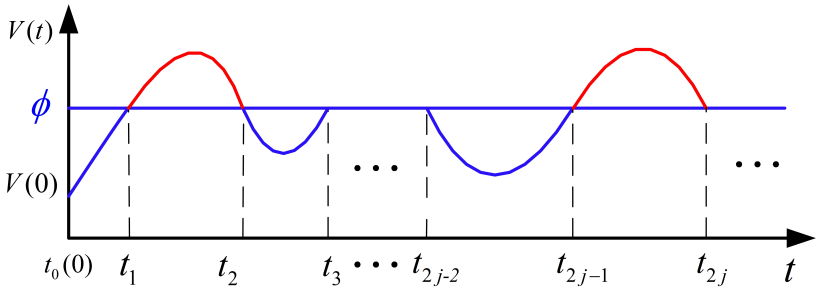

Figure 6.1: Illustration of evolution of $V(\cdot)$.

Proof. According to the time sequence in Remark 6.2, we consider the case of $t \in [t_{2m-1}, t_{2m}]$ for $m \in \mathbb{N}^+$. Integrating $\dot{V}(\cdot)$ over the time intervals $[t_0, t_1)$, $[t_1, t_2)$, ..., $[t_{2m-2}, t_{2m-1})$, $[t_{2m-1}, t]$ results in

$$\begin{aligned} V(t) \leq & \sum_{j=1}^{m-1} \int_{t_{2j-1}}^{t_{2j}} \left[\psi(t)\mathcal{N}(s(t)) + \beta\right] \dot{s}(t)dt + \sum_{i=1}^{m} \int_{t_{2j-2}}^{t_{2j-1}} \dot{V}(t)dt \\ & + \phi + \int_{t_{2m-1}}^{t} \left[\psi(t)\mathcal{N}(s(t)) + \beta\right] \dot{s}(t)dt \\ \leq & \phi + \sum_{j=1}^{m-1} \int_{t_{2j-1}}^{t_{2j}} \left[\psi(t)\mathcal{N}(s(t)) + \beta\right] \dot{s}(t)dt \\ & + \int_{t_{2m-1}}^{t} \left[\psi(t)\mathcal{N}(s(t)) + \beta\right] \dot{s}(t)dt, \end{aligned}$$

where the integral over $t \in [t_{2j-2}, t_{2j-1})$ has been removed by observing that $V(t_{2j-1}) = V(t_{2j-2}) = \phi$. Then, it follows that

$$\begin{aligned} V(t) \leq & \phi + \sum_{j=1}^{m-1} \int_{t_{2j-1}}^{t_{2j}} \left[\psi(t)\mathcal{N}(s(t)) + \beta\right] \dot{s}(t)dt \\ & + \underbrace{\sum_{j=1}^{m-1} \int_{t_{2j-2}}^{t_{2j-1}} \left[\psi(t)\mathcal{N}(s(t)) + \beta\right] \dot{s}(t)dt}_{\Theta(s(t))} \\ & + \int_{t_{2m-1}}^{t} \left[\psi(t)\mathcal{N}(s(t)) + \beta\right] \dot{s}(t)dt \\ \leq & \phi + \int_{0}^{t} \left[\psi(t)\mathcal{N}(s(t)) + \beta\right] \dot{s}(t)dt \\ \leq & \phi + \beta s(t) + \underbrace{l_2 \int_{0}^{s(t)} \mathcal{N}_+(\tau)d\tau - l_1 \int_{0}^{s(t)} \mathcal{N}_-(\tau)d\tau}_{\Xi(s(t))}, \end{aligned} \tag{6.10}$$

by noting the facts that $\Theta(s(t)) \equiv 0$ due to $\dot{s}(t) = 0$ for $t \in [t_{2j-2}, t_{2j-1}]$, $s(0) = 0$, and $\mathcal{N}(s) = \mathcal{N}_+(s) - \mathcal{N}_-(s)$. When $s(t) = 0$, $\forall t$, the boundedness of $s(t)$ and $V(t)$ can be trivially obtained according to (6.10).

When $s(t) \neq 0$, it is obtained from (6.10) that

$$0 \leq \frac{V(t)}{s(t)} \leq \underbrace{\overbrace{\left[\frac{\Xi\big(s(t)\big)}{s(t)}\right]}^{\Delta(s(t))} + \frac{\phi}{s(t)} + \beta}_{\Upsilon(s(t))}. \tag{6.11}$$

In the following, we aim to prove boundedness of $s(\cdot)$ on $[0,+\infty)$ by contradiction. If $s(\cdot)$ is unbounded, one can calculate the limit behavior of $\Delta(s)$ in (6.11) as $s \to +\infty$, using the Definition 6.2. In particular, for the case of $0 > l_2 > l_1$,

$$\begin{aligned}
&\lim_{s\to+\infty} \inf \Delta(s) \\
&= \lim_{s\to+\infty} \overbrace{\frac{1}{s}\int_0^s \mathscr{N}_-(\tau)d\tau}^{\to+\infty} \overbrace{\left[-l_1 + \underbrace{l_2 \sup \frac{\int_0^s \mathscr{N}_+(\tau)d\tau}{\int_0^s \mathscr{N}_-(\tau)d\tau}}_{\to-\infty}\right]}^{\to-\infty} \\
&= -\infty,
\end{aligned} \tag{6.12}$$

and similarly, for the case of $l_2 > l_1 > 0$,

$$\begin{aligned}
&\lim_{s\to+\infty} \inf \Delta(s) \\
&= \lim_{s\to+\infty} \overbrace{\frac{1}{s}\int_0^s \mathscr{N}_+(\tau)d\tau}^{\to+\infty} \overbrace{\left[l_2 - \underbrace{l_1 \sup \frac{\int_0^s \mathscr{N}_-(\tau)d\tau}{\int_0^s \mathscr{N}_+(\tau)d\tau}}_{\to-\infty}\right]}^{\to-\infty} \\
&= -\infty.
\end{aligned} \tag{6.13}$$

Note that 'inf' in (6.12) and (6.13) becomes 'sup' due to $l_2 < 0$ and $l_1 > 0$, respectively. The relations above indicate that an unbounded s leads to a negative unbounded $\Delta(s)$. Independently of whether the unboundedness of $\Delta(s)$ occurs in finite time or at infinity (this depends on the behavior of $s(\cdot)$), the consequence would be that there exists a time $\bar{t} > 0$ such that

$$\Upsilon\big(s(\bar{t})\big) \leq -\varepsilon$$

for some positive ε, which contradicts (6.11). It concludes that $s(\cdot)$ is bounded over the entire time domain $[0,+\infty)$, so are $\Xi(s(\cdot))$ and hence $V(\cdot)$ from (6.10).

Finally, let us now consider the case of $t \in (t_{2m}, t_{2m+1})$. The boundedness of $s(\cdot)$ and $V(\cdot)$ is guaranteed by the above argument for $t = t_{2m}$ and the facts that $V(t) < \phi$ and $\dot{s}(t) = 0$ for $t \in (t_{2m}, t_{2m+1})$. ■

Remark 6.3 Lemma 6.1 encompasses [18, Lemma 4.3] as special case when $\dot{s}(t) = 0$ in (6.9) is never active (e.g. when ϕ is sufficiently small). Also, while existing conditional inequalities [29, Lemma 2], [60, Lemma 1], [46, Lemma 1], and [31, Lemma 2] guarantee boundedness on a finite time interval $[0, t_\delta)$ with $t_\delta < +\infty$ (cf. discussion in [81, Remark 1]), the proposed Lemma 6.1 can ensure boundedness on the entire time domain $[0,+\infty)$. This is essentially due to the properties of type B Nussbaum functions used in the proof by contradiction (cf. (6.12)-(6.13)).

6.3. Nussbaum Gain Adaptive Prescribed Performance Control Design

The development of this section starts with performance functions $\rho_i(t) = (\rho_{i,0} - \rho_{i,\infty})\exp(-\kappa_i t) + \rho_{i,\infty}$ for positive constants $\rho_{i,0} > \rho_{i,\infty}$ and κ_i, $i = 1,\ldots,n$. Let $\alpha_1(t) = y_r(t)$, $\alpha_{i+1}(t)$, $i = 1,\ldots,n$, be the virtual control laws to be designed, and the real control law $u(t) = \alpha_{n+1}(t)$.

Next, we introduce the virtual tracking error $e_i(t) = \chi_i(t) - \alpha_i(t)$ and the error transformation

$$\mathcal{T}_i(t) = \frac{\tan\left(\frac{\pi}{2}\frac{e_i(t)}{\rho_i(t)}\right)}{\cos^2\left(\frac{\pi}{2}\frac{e_i(t)}{\rho_i(t)}\right)},\ i = 1,\ldots,n. \tag{6.14}$$

As a result, the virtual control functions are devised as follows,

$$\alpha_{i+1}(t) = \varrho_i \mathcal{N}\big(s_i(t)\big)\mathcal{T}_i(t),\ i = 1,\ldots,n, \tag{6.15}$$

where $\varrho_i > 0$ is a design parameter and $\mathcal{N}^p(\cdot)$ is a type B Nussbaum function for any positive odd integer $p \geq 1$. An adaptation law for $s_i(t)$ is constructed as

$$\dot{s}_i(t) = \begin{cases} \mathcal{T}_i^{p_i+1}(t), & \text{if } |e_i(t)| \geq \delta_i\rho_i(t) \\ 0, & \text{if } |e_i(t)| < \delta_i\rho_i(t) \end{cases} \tag{6.16}$$

for a constant $\delta_i \in (0,1)$. Similarly to [133, eq. (8)], equation (6.16) is devised to avoid high-gain because it increases only when tracking error is close to violating the performance bound: however, the stability analysis in [133] is for strict-feedback dynamics and cannot be used to prove stability here. The way to prove the stability of this mechanism relies on the proposed Lemma 6.1. Before moving on, we first give a technical lemma that is similar to [133, Lemma 3] and the proof is thus omitted. Then, the main result is stated in the following theorem below.

Lemma 6.2 If $\overline{\chi}_i(\cdot)$, $\dot{\alpha}_i(\cdot)$, $s_i(\cdot)$, $\mathcal{T}_i(\cdot)$, and $e_{i+1}(\cdot)$ are bounded on a time interval $[0, t_\delta)$, then $\dot{\alpha}_{i+1}(\cdot)$ is bounded on $[0, t_\delta)$ for $i = 1,\ldots,n$.

6.4. Stability Analysis

Theorem 6.1 Under Assumption 6.1, consider the closed-loop system composed of (6.1), the control laws (6.14) and (6.15), and the adaptation law (6.16). In particular, $\mathcal{N}^p(\cdot)$ is a type B Nussbaum function for any positive odd integer $p \geq 1$. For any initial conditions $|e_i(0)| < \rho_i(0)$, $i = 1,\ldots,n$, the PPC problem is solved in the sense of P1 and P2.

Proof. (Time dependence of the functions e_i, α_i, $\dot{\alpha}_i$, and $\mathcal{N}(\cdot)$ will be omitted whenever unambiguous). Taking the time derivative of e_i along (6.1), (6.14) and (6.15) yields

$$\begin{aligned} \dot{e}_i(t) &= \dot{\chi}_i - \dot{\alpha}_i = \phi_i(\overline{\chi}_i) + \psi_i(\overline{\chi}_i)(e_{i+1} + \alpha_{i+1})^{p_i} - \dot{\alpha}_i \\ &= \phi_i(\overline{\chi}_i) + \psi_i(\overline{\chi}_i)\vartheta_i(e_{i+1}, \alpha_{i+1})e_{i+1}^{p_i} - \dot{\alpha}_i \\ &\quad + \psi_i(\overline{\chi}_i)\gamma_i(e_{i+1}, \alpha_{i+1})\alpha_{i+1}^{p_i} \\ &= F_i(t) + \gamma_i(e_{i+1}, \alpha_{i+1})\psi_i(\overline{\chi}_i)\varrho_i^{p_i}\mathcal{N}^{p_i}(s_i)\mathcal{T}_i^{p_i}(t), \\ \dot{e}_n(t) &= F_n(t) + \psi_n(\overline{\chi}_n)\varrho_n^{p_n}\mathcal{N}^{p_n}(s_n)\mathcal{T}_n^{p_n}(t), \end{aligned} \tag{6.17}$$

where the second equality used the separation lemma 2 of [62], $|\vartheta_i(e_{i+1},\alpha_{i+1})| \le \bar{\vartheta}_i$ with $\bar{\vartheta}_i$ a positive constant, $\gamma_i(e_{i+1},\alpha_{i+1}) \in [1-\bar{\epsilon}_i, 1+\bar{\epsilon}_i]$ with an arbitrary constant $\bar{\epsilon}_i \in (0,1)$, $F_i(t) = \phi_i(\overline{\chi}_i) + \psi_i(\overline{\chi}_i)\vartheta_i(e_{i+1},\alpha_{i+1})e_{i+1}^{p_i} - \dot{\alpha}_i$, $i = 1,\ldots,n-1$, and $F_n(t) = \phi_n(\overline{\chi}_n) - \dot{\alpha}_n$.

In what follows, we will prove that $|e_i(t)| < \rho_i(t)$, $i = 1,\ldots,n$, holds for $t \ge 0$ using a contradiction. Suppose there exists an error e_m such that

$$|e_m(t_m)| \ge \rho_m(t_m), \quad \forall m \in \{1,\ldots,n\}. \tag{6.18}$$

Let $t_\delta = \min\{t_m\}$ be the time instant when (6.18) is violated for the first time. Then, due to the continuity of e_i and the fact that $|e_i(0)| < \rho_i(0)$, $i = 1,\ldots,n$, it follows that

$$|e_i(t)| < \rho_i(t), \quad \forall t \in [0, t_\delta), \tag{6.19}$$

and that there exists an error e_δ satisfying

$$\lim_{t\to t_\delta^-} |e_\delta(t)| = \lim_{t\to t_\delta^-} |\rho_\delta(t)|, \quad \delta \in \{1,\ldots,n\}, \tag{6.20}$$

where t_δ^- denotes the left limit of t_δ.

To seek a contradiction, the analysis given below is conducted on a finite time interval $[0, t_\delta)$.

Step 1: Consider the Lyapunov function candidate

$$V_1(t) = \frac{1}{2}\tan^2\left(\frac{\pi}{2}\frac{e_1(t)}{\rho_1(t)}\right), \quad \forall t \in [0, t_\delta). \tag{6.21}$$

When $|e_1(t)| < \delta_1\rho_1(t)$, it immediately follows that

$$V_1(t) < \frac{1}{2}\tan^2\left(\frac{\pi\delta_1}{2}\right) \triangleq \overline{\omega}_1. \tag{6.22}$$

From (6.16), we further have

$$\dot{s}_1(t) = 0, \quad \text{when } V_1(t) < \overline{\omega}_1. \tag{6.23}$$

When $|e_1(t)| \ge \delta_1\rho_1(t)$, $V_1(t) \ge \overline{\omega}_1$ holds. Taking the time derivative of $V_1(t)$ along (6.17) yields

$$\begin{aligned}\dot{V}_1(t) &= \frac{\pi}{2}\frac{\mathcal{T}_1(t)}{\rho_1^2(t)}\left[\dot{e}_1(t)\rho_1(t) - e_1(t)\dot{\rho}_1(t)\right] \\ &= \mathcal{T}_1(t)F_{1f}(t) + g_{1f}(t)\mathcal{N}^{p_1}(s_1)\mathcal{T}_1^{p_1+1}(t),\end{aligned} \tag{6.24}$$

where

$$\begin{aligned}F_{1f}(t) &= \frac{\pi}{2}\left(\frac{F_1(t)}{\rho_1(t)} - \frac{e_1(t)\dot{\rho}_1(t)}{\rho_1^2(t)}\right), \\ g_{1f}(t) &= \frac{\pi}{2}\frac{1}{\rho_1(t)}\gamma_1(e_2,\alpha_2)\psi_1(t,\chi_1)\varrho_1^{p_1}.\end{aligned}$$

According to the boundedness of y_r and its derivative, α_1 and $\dot{\alpha}_1$ are bounded on $[0, t_\delta)$, which, together with (6.19), yields the boundedness of χ_1 on $[0, t_\delta)$. By Assumption 6.1, the boundedness of χ_1 and $\dot{\alpha}_1$ results in that of $F_1(t)$ and hence $F_{1f}(t)$ on $[0, t_\delta)$. Invoking the boundedness of $\gamma_1(e_2, \alpha_2)$, $\rho_1(t)$, and $\psi_1(t, \chi_1)$ leads to that of $g_{1f}(t)$ on $[0, t_\delta)$. Then, it follows from the Extreme Value Theorem that there exist positive constants $\bar{F}_{1f}$, $\underline{g}_{1f}$, and $\bar{g}_{1f}$ such that

$$|F_{1f}(t)| \le \bar{F}_{1f},\ g_{1f}(t) \in [\underline{g}_{1f}, \bar{g}_{1f}],\ 0 \notin [\underline{g}_{1f}, \bar{g}_{1f}]. \tag{6.25}$$

Substituting $|e_1(t)| \ge \delta_1 \rho_1(t)$ into (6.14) gives

$$\left|\mathcal{T}_1^{p_1}(t)\right| \ge \frac{\tan^{p_1}\left(\frac{\pi}{2}\delta_1\right)}{\cos^{2r_1}\left(\frac{\pi}{2}\delta_1\right)} \ge \tan^{p_1}\left(\frac{\pi}{2}\delta_1\right). \tag{6.26}$$

Synthesizing (6.24)-(6.26) results in

$$\begin{aligned}\dot{V}_1(t) &\le \frac{|F_{1f}(t)|}{|\mathcal{T}_1^{p_1}(t)|}\mathcal{T}_1^{p_1+1}(t) + g_{1f}(t)\mathcal{N}^{p_1}(s_1)\mathcal{T}_1^{p_1+1}(t) \\ &\le \left[\frac{\bar{F}_{1f}}{\tan^{p_1}\left(\frac{\pi}{2}\delta_1\right)} + g_{1f}(t)\mathcal{N}^{p_1}(s_1)\right]\dot{s}_1(t).\end{aligned} \tag{6.27}$$

It is noted from Proposition 6.2 that $\mathcal{N}^{p_1}(\cdot)$ is a type B Nussbaum function. So, we can apply Lemma 6.1 to prove that $V_1(\cdot)$ and $s_1(\cdot)$ are bounded on $[0, t_\delta)$. In view of (6.21), we can claim that there exists a constant $\bar{\sigma}_1 > 0$ such that $|e_1(t)| \le \rho_1(t) - \bar{\sigma}_1 < \rho_1(t)$ on $[0, t_\delta)$ (equivalently to the boundedness of $\mathcal{T}_1(t)$ on $[0, t_\delta)$). This, together with (6.14) and the boundedness of $\mathcal{N}(s_1)$, gives the boundedness of α_2 and $\overline{\chi}_2$ on $[0, t_\delta)$ due to $\chi_i = e_i + \alpha_i$, $i = 1, 2$. By Lemma 6.2, $\dot{\alpha}_2$ is bounded on $[0, t_\delta)$.

Step i**(**$i = 2, \ldots, n$**):** Boundedness of $\overline{\chi}_i$ and $\dot{\alpha}_i$ on $[0, t_\delta)$ was obtained from step $i-1$. Consider the Lyapunov function candidate

$$V_i(t) = \frac{1}{2}\tan^2\left(\frac{\pi}{2}\frac{e_i(t)}{\rho_i(t)}\right),\ \ \forall t \in [0, t_\delta). \tag{6.28}$$

When $|e_i(t)| < \delta_i \rho_i(t)$, it follows that

$$V_i(t) < \frac{1}{2}\tan^2\left(\frac{\pi\delta_i}{2}\right) \triangleq \overline{\omega}_i. \tag{6.29}$$

From (6.16) one has

$$\dot{s}_i(t) = 0,\ \text{ when } V_i(t) < \overline{\omega}_i. \tag{6.30}$$

When $|e_i(t)| \ge \delta_i \rho_i(t)$, it holds that $V_i(t) \ge \overline{\omega}_i$. Taking the time derivative of $V_i(t)$ along (6.16) gives

$$\begin{aligned}\dot{V}_i(t) &= \frac{\pi}{2}\frac{\mathcal{T}_i(t)}{\rho_i^2(t)}\left[\dot{e}_i(t)\rho_i(t) - e_i(t)\dot{\rho}_i(t)\right] \\ &= \mathcal{T}_i(t)F_{if}(t) + g_{if}(t)\mathcal{N}^{p_i}(s_i)\mathcal{T}_i^{p_i+1}(t),\end{aligned} \tag{6.31}$$

where

$$F_{if}(t)=\frac{\pi}{2}\left(\frac{F_i(t)}{\rho_i(t)}-\frac{e_i(t)\dot{\rho}_i(t)}{\rho_i^2(t)}\right),$$
$$g_{if}(t)=\frac{\pi}{2}\frac{1}{\rho_i(t)}\gamma_i(e_{i+1},\alpha_{i+1})\psi_i(\overline{\chi}_i)\varrho_i^{p_i}.$$

In light of Assumption 6.1 and the boundedness of $\overline{\chi}_i$, $\dot{\alpha}_i$ and e_{i+1} on $[0,t_\delta)$, $F_i(t)$ is bounded on $[0,t_\delta)$, which further ensures the boundedness of $F_{if}(t)$ on $[0,t_\delta)$. Recalling Assumption 6.1 and the boundedness of $\gamma_i(e_{i+1},\alpha_{i+1})$ leads to that of $g_{if}(t)$ on $[0,t_\delta)$. Similar to Step 1, one can conclude there exist positive constants $\bar{F}_{if}$, $\underline{g}_{if}$, and $\bar{g}_{if}$ such that

$$|F_{if}(t)|\le\bar{F}_{if},\ g_{if}(t)\in[\underline{g}_{if},\bar{g}_{if}],\ 0\notin[\underline{g}_{if},\bar{g}_{if}]. \tag{6.32}$$

Substituting $|e_i(t)|\ge\delta_i\rho_i(t)$ into (6.14) results in

$$\left|\mathscr{T}_i^{p_i}(t)\right|\ge\frac{\tan^{p_i}\left(\frac{\pi}{2}\delta_i\right)}{\cos^{2p_i}\left(\frac{\pi}{2}\delta_i\right)}\ge\tan^{p_i}\left(\frac{\pi}{2}\delta_i\right). \tag{6.33}$$

Summarizing (6.31)-(6.33) leads to

$$\begin{aligned}\dot{V}_i(t)&\le\frac{|F_{if}(t)|}{|\mathscr{T}_i^{p_i}(t)|}\mathscr{T}_i^{p_i+1}(t)+g_{if}(t)\mathscr{N}^{p_i}(s_i)\mathscr{T}_i^{p_i+1}(t)\\&\le\left[\frac{\bar{F}_{if}}{\tan^{p_i}\left(\frac{\pi}{2}\delta_i\right)}+g_{if}(t)\mathscr{N}^{p_i}(s_i)\right]\dot{s}_i(t).\end{aligned} \tag{6.34}$$

Likewise, $\mathscr{N}^{p_i}(\cdot)$ is a type B Nussbaum function, so we apply Lemma 6.1 to prove that $V_i(\cdot)$ and $s_i(\cdot)$ are bounded on $[0,t_\delta)$. According to (6.28), there exists a constant $\bar{\sigma}_i>0$ such that $|e_i(t)|\le\rho_i(t)-\bar{\sigma}_i<\rho_i(t)$ on $[0,t_\delta)$, which, combined with (6.15) and the boundedness of $\mathscr{N}(s_i)$, yields the boundedness of α_{i+1} and $\overline{\chi}_{i+1}$ on $[0,t_\delta)$ owing to $\chi_{i+1}=e_{i+1}+\alpha_{i+1}$. Therefore, $\dot{\alpha}_{i+1}$ is bounded on $[0,t_\delta)$ according to Lemma 6.2.

In summary, we have proved that $|e_i(t)|\le\rho_i(t)-\bar{\sigma}_i<\rho_i(t)$, $i=1,\ldots,n$, for $t\in[0,t_\delta)$. However, this contradicts the assumption made in (6.20) and implies that t_δ should be extended to $+\infty$. As a result, $|e_i(t)|<\rho_i(t)$, $i=1,\ldots,n$, holds for $t\in[0,+\infty)$. Given that Lemma 6.1 holds true on $[0,+\infty)$, the boundedness of closed-loop signals is guaranteed on $[0,+\infty)$. This completes the proof. ■

6.5. Simulation Example

To validate the proposed method, a two-degree-of-freedom wing section with leading-edge (LE) and trailing-edge (TE) control surfaces as shown in Fig. 6.2 is considered. The dynamic of this aeroelastic system can be described by [28, 43]:

$$\begin{aligned}&\begin{bmatrix}I_\alpha & m_w x_\alpha b\\ m_w x_\alpha b & m_t\end{bmatrix}\begin{bmatrix}\ddot{\alpha}\\ \ddot{h}\end{bmatrix}+\begin{bmatrix}c_h & 0\\ 0 & c_\alpha(\dot{\alpha})\end{bmatrix}\begin{bmatrix}\dot{\alpha}\\ \dot{h}\end{bmatrix}\\&+\begin{bmatrix}k_\alpha(\alpha) & 0\\ 0 & k_h(h)\end{bmatrix}\begin{bmatrix}\alpha\\ h\end{bmatrix}=\begin{bmatrix}M\\ -L\end{bmatrix}\end{aligned} \tag{6.35}$$

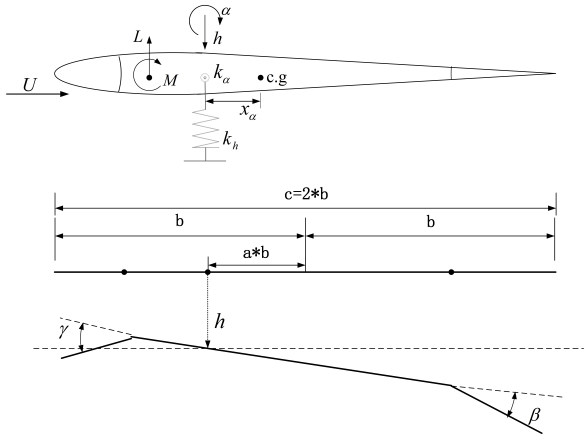

Figure 6.2: Wing section with leading-edge (LE) and trailing-edge (TE) control surfaces.

where α and h denote the pitch angle and the plunge displacement, respectively; I_α is the moment of inertia; $m_w = m_t + m_l$ is the sum of wing section mass m_t and load section mass m_l; x_α is the distance between the center of mass and the elastic axis; b is the semi-chord of the wing; c_h is the plunge damping coefficient. The pitch damping $c_\alpha(\dot{\alpha})$, the pitch stiffness $k_\alpha(\alpha)$, and the plunge stiffness $k_h(h)$ are expressed as $c_\alpha(\dot{\alpha}) = \sum_{j=0}^{2} c_{\alpha j}\dot{\alpha}^j$, $k_\alpha(\alpha) = \sum_{j=0}^{2} k_{\alpha j}\alpha^j$, and $k_h(h) = \sum_{j=0}^{2} k_{hj}h^j$, where $c_{\alpha j}$, $k_{\alpha j}$, and k_{hj} are unknown non-zero constants and cannot be used in control design. In (6.35), M and L represent the aerodynamic moment and lift expressed by

$$\begin{cases} M=\rho U^2 b^2 s_p\left\{\bar{c}_{l_\alpha}\left(\alpha+\dfrac{\dot{h}}{U}+(0.5-a)\,b\dfrac{\dot{\alpha}}{U}\right)+\bar{c}_{l_\beta}\beta+\bar{c}_{l_\gamma}\gamma\right\} \\ L=\rho U^2 b s_p\left\{c_{l_\alpha}\left(\alpha+\dfrac{\dot{h}}{U}+(0.5-a)\,b\dfrac{\dot{\alpha}}{U}\right)+c_{l_\beta}\beta+c_{l_\gamma}\gamma\right\} \end{cases} \tag{6.36}$$

where $\bar{c}_{l_\alpha} = \left(\frac{1}{2}+a\right)c_{l_\alpha} + 2c_{m_\alpha}$, $\bar{c}_{l_\beta} = \left(\frac{1}{2}+a\right)c_{l_\beta} + 2c_{m_\beta}$, $\bar{c}_{l_\gamma} = \left(\frac{1}{2}+a\right)c_{l_\gamma} + 2c_{m_\gamma}$, and ρ is the air density; U denotes the freestream velocity; c_{l_α}, c_{l_β} and c_{l_γ} are the lift derivatives; c_{m_α}, c_{m_β} and c_{m_γ} are the moment derivatives; s_p is the span; a is the nondimensional distance from midchord to the elastic axis; β and γ are the TE and LE control surface deflections, respectively. With the change of coordinates $\chi_1 = \alpha$, $\chi_2 = \dot{\alpha}$, $\chi_3 = h$, $\chi_4 = \dot{h}$, and $u = \beta + \gamma$, we can rewrite (6.35) as

$$\dot{\chi}_1 = \chi_2, \quad \dot{\chi}_2 = \phi_2\left(\bar{\chi}_2\right) + \ell_2\left(\bar{\chi}_2\right)\chi_3^3, \quad \dot{\chi}_3 = \chi_4, \quad \dot{\chi}_4 = \phi_4\left(\bar{\chi}_4\right) + u, \tag{6.37}$$

where $\phi_2(\chi) = c_{\bar{\alpha}_1}\chi_1 + c_{\alpha_{11}}\chi_1^3 + c_{\dot{\alpha}_1}\chi_2 + c_{\dot{\alpha}_{11}}\chi_2^3 + c_{\dot{h}_1}\chi_2 + c_{\beta_1}\beta + c_{\gamma_1}\gamma$, $\phi_4(\chi) = c_{\alpha_2}\chi_1 + c_{\alpha_{21}}\chi_1^3 + c_{\dot{\alpha}_2}\chi_2 + c_{\dot{\alpha}_{21}}\chi_2^3 + c_{h_{21}}\chi_3^3 + c_{\dot{h}_2}\chi_4$, and $\ell_2(\bar{\chi}_2) = m_w x_\alpha b k_{h2}$ with $c_{\bar{\alpha}_1} = c_2 m_t c_{m\alpha} + c_1 m_t x_\alpha b c_{l\alpha}$, $c_{\alpha_{11}} = -m_t k_{\alpha_2}$, $c_{\dot{\alpha}_1} = c_2 m_t c_{m\alpha}(0.5-a)\frac{b}{U} - c_{\alpha 0} m_t + c_1 m_t x_\alpha b c_{l\alpha}(0.5-a)\frac{b}{U}$, $c_{\dot{\alpha}_{11}} = -m_t c_{\alpha 2}$, $c_{\dot{h}_1} = c_2 m_t c_{m\alpha}\frac{1}{U} + c_1 m_t x_\alpha b c_{l\alpha}\frac{1}{U} - c_h m_t x_\alpha b$, $c_{\beta_1} = c_2 m_t c_{m\beta} + c_1 m_t x_\alpha b c_{l\beta}$, $c_{\gamma_1} = c_1 m_t x_\alpha b c_{l\gamma} + c_2 m_t c_{m\gamma}$, $c_{\alpha_2} = -c_2 m_t x_\alpha b c_{m\alpha} - c_1 I_\alpha c_{l\alpha}$, $c_{\alpha_{21}} = m_t x_\alpha b k_{\alpha_2}$, $c_{\dot{\alpha}_2} = -c_2 m_t x_\alpha b c_{m\alpha}(0.5-a)\frac{b}{U} - c_1 I_\alpha c_{l\alpha}(0.5-a)\frac{b}{U} + c_{\alpha 0} m_t x_\alpha b$, $c_{\dot{\alpha}_{21}} = m_t x_\alpha b c_{\alpha 2}$, $c_{h_{21}} = -k_{h2} I_\alpha$, $c_{\dot{h}_2} = -c_2 m_t x_\alpha c_{m\alpha}\frac{b}{U} -$

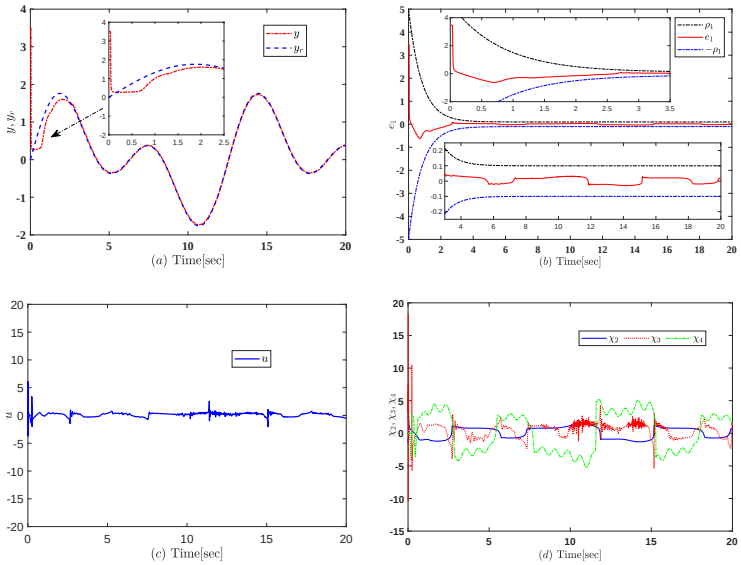

Figure 6.3: (a): Evolution of y and y_r; (b): Evolution of the tracking error e_1; (c): Evolution of the control input signal u; (d): Evolution of the state variables χ_2, χ_3, and χ_4.

$c_h I_\alpha - c_1 I_\alpha c_{l\alpha} \frac{1}{U}$, $c_{\beta_2} = -c_2 m_t x_\alpha b c_{m\beta} - c_1 I_\alpha c_{l\beta}$, $c_{\gamma_2} = -c_2 m_t x_\alpha b c_{m\gamma} - c_1 I_\alpha c_{l\gamma}$, $c_1 = \rho U^2 b s_p$, and $c_2 = \rho U^2 b^2 s_p$.

Since the sign of k_{h2} is unknown, the sign of control coefficient $\ell_2(\cdot)$ is unknown and cannot be used in the control design. Taking the same structural parameters as [43] gives the values of model parameters used for simulation in Table I. Let the reference signal be $y_r(t) = \sin(0.5t) + \sin(t)$. The initial state values are chosen as $\chi_1(0) = 3.5$, $\chi_2(0) = -1.5$, $\chi_3(0) = -2.5$ and $\chi_4(0) = -1.5$. The design parameters are chosen to be: $\varrho_1 = 1.25$, $\varrho_2 = 1.75$, $\varrho_3 = \varrho_4 = 5$, $\delta_1 = 0.5$, $\delta_2 = 0.75$, $\delta_3 = 0.35$, $\delta_4 = 0.9$, $\rho_{1,0} = \rho_{2,0} = \rho_{3,0} = \rho_{4,0} = 5$, $\rho_{1,\infty} = 0.1$, $\rho_{2,\infty} = 0.85$, $\rho_{3,\infty} = 0.5$, $\rho_{4,\infty} = 0.75$, $\kappa_1 = 1.25$, $\kappa_2 = 0.75$, $\kappa_3 = \kappa_4 = 0.5$. The parameters and initial conditions of Nussbaum functions are $\mu = 0.25$ and $s_1(0) = s_2(0) = s_3(0) = s_4(0) = 0$, respectively. The simulation results are shown in Figs. 6.3 and 6.4. In

Table 6.1: The values of model parameters

Coefficient	Value	Coefficient	Value	Coefficient	Value
$c_{\bar{\alpha}_1}$	0.7835	$c_{\alpha_{11}}$	−1.5616	k_{α_1}	-0.9475
$c_{\dot{\alpha}_{11}}$	−7.6423	$c_{\dot{h}_1}$	2.6583	k_{α_2}	4.7562
c_{γ_1}	0.7256	c_{α_2}	−5.8731	k_{h_2}	3.6937
$c_{\dot{\alpha}_2}$	−3.2567	$c_{\dot{\alpha}_{21}}$	1.2548	k_{α_0}	−2.0593
$c_{\dot{h}_2}$	−8.2431	c_{α_1}	0.5717	k_{h_0}	2.3985
$c_{\dot{\alpha}_1}$	4.9527	c_{β_1}	0.5394	k_{h_1}	−4.7592

particular, Fig. 6.3 (a) and (b) show that system output y tracks the reference signal y_r with bounded tracking error and that the output tracking error e_1 evolves within the prescribed bounds $(-\rho_1, \rho_1)$ in spite of unknown control coefficient $\ell_2(\cdot)$. Fig. 6.3 (c) and (d) indicate the boundedness of control signal u and state variables χ_2, χ_3, and χ_4. Fig. 6.4 (a) and (b) show the boundedness of s_1, s_2, s_3, s_4,$\mathcal{N}(s_1)$, $\mathcal{N}(s_2)$, $\mathcal{N}(s_3)$,and $\mathcal{N}(s_4)$.

To investigate the influence of parameter δ_i, $i = 1,\ldots,4$, on the closed-loop response, we carry out the simulation based on three different sets of δ_i: Case 1: $\delta_1 = 0.15$, $\delta_2 = 0.2$, $\delta_3 = 0.25$, $\delta_4 = 0.3$; Case 2: $\delta_1 = 0.25$, $\delta_2 = 0.3$, $\delta_3 = 0.35$, $\delta_4 = 0.4$; Case 3: $\delta_1 = 0.35$, $\delta_2 = 0.45$, $\delta_3 = 0.55$, $\delta_4 = 0.6$. The trajectories of adaptation parameters s_i are depicted in Fig. 6.5, which validate the boundedness of s_i for different δ_i, $i = 1,\ldots,4$.

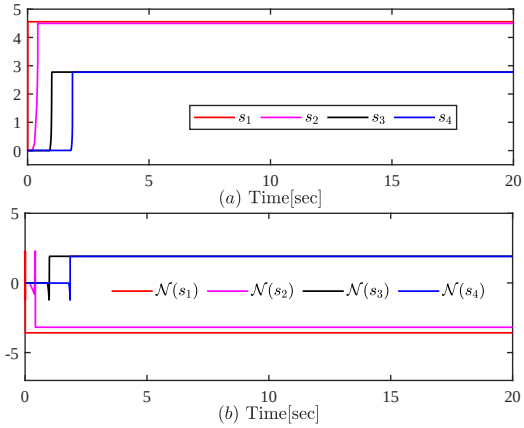

Figure 6.4: (a): Evolution of s_1, s_2, s_3, and s_4; (b): Evolution of $\mathcal{N}(s_1)$, $\mathcal{N}(s_2)$, $\mathcal{N}(s_3)$, and $\mathcal{N}(s_4)$.

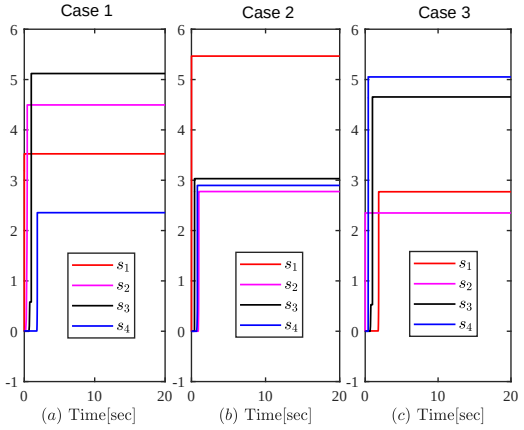

Figure 6.5: Evolution of s_1, s_2, s_3, and s_4 under three cases.

6.6. Conclusions

In the context of prescribed performance control for power-chained form systems with time-varying unknown control coefficients, this chapter has studied the properties associated to the power of Nussbaum functions, and the design of a novel switching Nussbaum conditional inequality. An interesting open problem deserving future investigation is PPC with time-varying unknown control coefficients and positive-odd rational powers, which contains positive-odd integer powers as a special case.

7

CONCLUSIONS AND RECOMMENDATIONS

In this thesis, we have investigated the consensus tracking problem for power-chained form systems in several scenarios, such as having (partially) completely unknown control directions, guaranteed transient and steady-state performance, and switching dynamics. In this final chapter, the main results of this thesis and some recommendations for future research are presented.

7.1. Conclusions

The main results of this thesis are summarized below.

- **Separation-based adaptive consensus tracking control of multi-agent nonlinear systems in power-chained form systems**

  We have proposed a new separation-based lemma for the purpose of handling high-power terms during the control design and stability analysis. With this new tool, we were capable of extracting virtual control variables in a "linear-like" fashion. Thus, the complexity was reduced by avoiding incorporating the control gain of each virtual control in the next virtual control law, and by allowing the power of the virtual and actual control laws to increase proportionally with the order of the systems.

- **Consensus tracking of power-chained form systems with mixed unknown control directions via hybrid Nussbaum-based control**

  A novel conditional inequality including a hybrid Nussbaum function was proposed to deal with mixed unknown control directions (some being known and some being unknown) for power-chained form systems subject to switching dynamics and input quantization. The distinguishing feature of the newly proposed conditional inequality consists in ensuring the boundedness of multiple Nussbaum integral terms.

- **Logic-based switching control of power-chained form systems with multiple unknown control directions**

  A novel logic-based switching mechanism was designed to online estimate multiple control directions assumed to be unknown *a priori*. Specifically, a new dynamic boundary function that is decreasing in-between switching instants and monotonically increasing at the switching instants is proposed to address the challenge that asymptotic tracking was impossible in general for power-chained form systems. Apart from this, a dynamic threshold was delicately devised in such a way that chattering is fully excluded by choosing the maximum values of an appropriately designed Lyapunov like function before and after switching.

- **Prescribed performance tracking control of power-chained form systems with time-varying unknown control coefficients**

  We have shown with a counterexample and a positive example that only partial type B Nussbaum functions whose positive odd-integer powers are still type B Nussbaum functions can be incorporated into a Nussbaum function-based approach to tackle time-varying unknown control coefficients. To avoid high-gain issues, a new switching conditional inequality was designed based on increasing the Nussbaum gain only when the tracking error is close to violating the performance bounds instead of always increasing the Nussbaum gain.

7.2. Impact of this Research on Society

Despite the theoretical nature of this work, the control methodologies proposed in this thesis fit the recent progress in autonomous and unmanned systems, a crucial research field in a modern technological society. In particular

- **Unmanned and/or autonomous vehicles** have been recently studied by several researchers, such as hypersonic flight vehicles [10, 11, 118], tailless flight vehicles [137], ship maneuvering systems [127, 138], and so on. With respect to these researches, the method proposed in Chapters 5 and 6 fit the need of tackling the inevitable uncertainty that these systems exhibit during their operation. In fact, our methodologies need neither some accurate modelling information (e.g. a priori knowledge of the control directions), nor universal approximators (e.g. neural networks and fuzzy logic systems) to handle the completely known model dynamics. Besides, the fact that prescribed specifications (e.g. maximum overshoot, minimum convergence rate, and maximum steady-state error) can be guaranteed, means that prescribed performance over the operating region can be guaranteed despite the presence of uncertainty.

- **Smart grids and smart energy systems** are other fields where the proposed methods can have an important impact. Currently, power-chained form dynamics similar to the ones in this thesis have been adopted for the boiler-turbine units [15] and hydraulic dynamics [66], which are fundamental parts of many power plants. The method proposed in Chapters 3 and 4 provides a more practical way to control these systems: first, we solve the high-gain issues of the methods of [15, 66],

which implies that less energy can be required to operate such power plants; second, we provide a better tracking performance, which implies that the power grids potentially connected to such power plants can be operated in a more accurate way.

7.3. Recommendations for Future Research

In this section, some potential topics based on the research of this thesis are introduced.

- **Adaptive output-feedback control of power-chained form systems**

  The developed adaptive controllers in Chapters 3-6 rely on the availability of system states. Such prerequisite in many cases cannot be satisfied arising from the fact that the measurements of system states are uneconomical or even technically impossible. In this sense, designing adaptive controllers on the basis of output measurements is relevant and deserves further investigations. It seems feasible that the output-feedback designs developed in [48, 49] can be extended to control power-chained form systems.

- **Adaptive tracking control of power-chained form systems with finite-time (fixed-time) convergence guarantee**

  The adaptive controllers proposed in Chapters 3-6 can only obtain bounded stability (i.e. the tracking error converges to a residual set around zero). In some practical engineering scenarios, finite-time (fixed-time) stability might be required, and currently this is not guaranteed by the proposed designs. The finite-time (fixed-time) stability results proposed in [8, 142] may provide a possible solution to this issue.

- **Event-triggered adaptive tracking control of power-chained form systems**

  If the proposed methods had to be implemented in a digital controller, one could select a fixed sample time with equal time intervals between any two consecutive time steps. However, in event-triggered control approaches the time instants of updating control signals are not fixed *a priori*, but can change to reduce the signal transmission burden, and to save on system resources. It is an open problem to implement the proposed control design in such an event-triggered framework. Following similar event-triggered designs as in [116, 117] probably can solve this problem.

- **Adaptive consensus tracking control for multi-agent in power-chained form systems with undesired communication conditions**

  In this thesis, we have assumed that there exist ideal communication channels among different agents in the sense that there is not any time delay and packet loss in the communication process. However, further research in the presence of undesired communication conditions can be worth of consideration. The methods of [38, 102] dealing with similar challenges might be helpful for resolving this issue.

- **Adaptive constrained tracking control of power-chained from systems with state constraints**

  In practical engineering systems, the states variables can be required to satisfy various constraints and the violation of these constraints may deteriorate system performance. It is worth investigating whether Barrier Lyapunov functions proposed in [51, 58, 59, 99, 100, 129] can be embedded into the proposed methodologies to ensure state constraint satisfaction.

References

[1] M. Abramowitz and I. A. Stegun. *Handbook of Mathematical Functions with Formulas, Graphs, and Mathematical Tables, 9th printing*. New York Dover, 1972.

[2] D. Angeli and E. Mosca. Adaptive switching supervisory control of nonlinear systems with no prior knowledge of noise bounds. *Automatica*, 40(3):449–457, 2004.

[3] K. Aryankia and R. R. Selmic. Neuro-adaptive formation control and target tracking for nonlinear multi-agent systems with time-delay. *IEEE Control Systems Letters*, 5(3):791–796, 2021.

[4] A. Astolfi, H. Liu, M. S. Netto, and R. Ortega. Two solutions to the adaptive visual servoing problem. *IEEE Transactions on Robotics and Automation*, 18(3):387–392, 2002.

[5] C. P. Bechlioulis and G. A. Rovithakis. Robust adaptive control of feedback linearizable MIMO nonlinear systems with prescribed performance. *IEEE Transactions on Automatic Control*, 53(9):2090–2099, 2008.

[6] C. P. Bechlioulis and G. A. Rovithakis. A low-complexity global approximation-free control scheme with prescribed performance for unknown pure feedback systems. *Automatica*, 50:1217–1226, 2014.

[7] C. P. Bechlioulis and G. A. Rovithakis. Decentralized robust synchronization of unknown high order nonlinear multi-agent systems with prescribed transient and steady state performance. *IEEE Transactions on Automatic Control*, 62(1):123–134, 2017.

[8] S. P. Bhat and D. S. Bernstein. Finite-time stability of continuous autonomous systems. *SIAM Journal on Control and Optimization*, 38(3):751–766, 2000.

[9] M. S. Branicky. Multiple Lyapunov functions and other analysis tools for switched and hybrid systems. *IEEE Transactions on Automatic Control*, 43(3):475–482, 1998.

[10] X. Bu. Air-breathing hypersonic vehicles funnel control using neural approximation of non-affine dynamic. *IEEE/ASME Transactions on Mechatronics*, 23(5):2099–2108, 2018.

[11] X. Bu, Y. Xiao, and H. Lei. An adaptive critic design-based fuzzy neural controller for hypersonic vehicles: predefined behavioral nonaffine contro. *IEEE/ASME Transactions on Mechatronics*, 24(4):1871–1881, 2019.

[12] X. Cai, C. Wang, Y. Li, L. Xu, and Z. Zhang. Distributed low-complexity output feedback tracking control for nonlinear multi-agent systems with unmodeled dynamics and prescribed performance. *International Journal of Systems Science*, 50 (6):1229–1243, 2019.

[13] C. Chen, Z. Liu, Y. Zhang, C. L. P. Chen, and S. Xie. Saturated nussbaum function based approach for robotic systems with unknown actuator dynamics. *IEEE Transactions on Cybernetics*, 46(10):2311–2322, 2015.

[14] C. Chen, C. Wen, Z. Liu, K. Xie, Y. Zhang, and C. L. P. Chen. Adaptive consensus of nonlinear multi-agent systems with non-identical partially unknown control directions and bounded modelling errors. *IEEE Transactions on Automatic Control*, 62(9):4654–4659, 2017.

[15] C. C. Chen and G. S. Chen. A new approach to stabilization of high-order nonlinear systems with an asymmetric output constraint. *International Journal of Robust and Nonlinear Control*, 30(2):756–775, 2020.

[16] C. L. Philip Chen, G. Wen, Y. Liu, and F. Wang. Adaptive consensus control for a class of nonlinear multiagent time-delay systems using neural networks. *IEEE Transactions on Neural Networks and Learning Systems*, 25(6):1217–1226, 2014.

[17] W. Chen, X. Li, W. Ren, and C. Wen. Adaptive consensus of multi-agent systems with unknown identical control directions based on a novel Nussbaum-type function. *IEEE Transactions on Automatic Control*, 59(7):1887–1892, 2014.

[18] Z. Y. Chen. Nussbaum functions in adaptive control with time-varying unknown control coefficients. *Automatica*, 102(1):72–79, 2019.

[19] N. Chopra. Output synchronization on strongly connected graphs. *IEEE Transactions on Automatic Control*, 57(11):2896–2901, 2012.

[20] D. Chowdhury and H. K. Khalil. Practical synchronization in networks of nonlinear heterogeneous agents with application to power systems. *IEEE Transactions on Automatic Control*, 66(1):184–198, 2021.

[21] A. Das and F. Lewis. Distributed adaptive control for synchronization of unknown nonlinear networked systems. *Automatica*, 46:2014–2021, 2010.

[22] Z. Ding. Adaptive consensus output regulation of a class of nonlinear systems with unknown high-frequency gain. *Automatica*, 51:348–355, 2015.

[23] Z. Ding and X. Ye. A flat-zone modification for robust adaptive control of nonlinear output feedback systems with unknown high-frequency gains. *IEEE Transactions on Automatic Control*, 47(2):358–363, 2002.

[24] G. Dong, H. Li, H. Ma, and R. Lu. Finite-time consensus tracking neural network FTC of multi-agent systems. *IEEE Transactions on Neural Networks and Learning Systems*, 32(2):653–662, 2021.

[25] B. Fan, Q. Yang, S. Jagannathan, and Y. Sun. Output-constrained control of non-affine multi-agent systems with partially unknown control directions. *IEEE Transactions on Automatic Control*, 64(9):3936–3942, 2019.

[26] S. Ferik, A. Qureshi, and F. Lewis. Neuro-adaptive cooperative tracking control of unknown higher-order affine nonlinear systems. *Automatica*, 50:798–808, 2014.

[27] L. B. Freidovich and H. K. Khalil. Lyapunov-based switching control of nonlinear systems using high-gain observers. *Automatica*, 43(1):150–157, 2007.

[28] Y. C. Fung. *An Introduction to the Theory of Aeroelasticity*. Wiley, 1955.

[29] S. S. Ge and J. Wang. Robust adaptive tracking for time-varying uncertain nonlinear systems with unknown control coefficients. *IEEE Transactions on Automatic Control*, 48(8):1463–1469, 2003.

[30] S. S. Ge, C. C. Hang, T. H. Lee, and T. Zhang. *Stable Adaptive Neural Network Control*. Springer, 2002.

[31] S. S. Ge, H. Fan, and T. H. Lee. Adaptive neural control of nonlinear time-delay systems with unknown virtual control coefficients. *IEEE Transactions on Systems, Man, and Cybernetics, Part B (Cybernetics)*, 34(1):499–516, 2004.

[32] J. P. Hespanhaa, D. Liberzon, and A. S. Morse. Overcoming the limitations of adaptive control by means of logic-based switching. *Systems & Control Letters*, 49(1): 49–65, 2003.

[33] M. Hirsch and S. Smale. *Differential Equations, Dynamical Systems and Linear Algebra*. New York, NY, USA: Academic, 1973.

[34] Y. Hong and C. Pan. A lower bound for the smallest singular value. *Linear Algebra and its Applications*, 172:27–32, 1992.

[35] C. Hua, X. You, and X. Guan. Leader-following consensus for a class of high-order nonlinear multi-agent systems. *Automatica*, 73:138–144, 2016.

[36] C. Huang and C. Yu. Tuning function design for nonlinear adaptive control systems with multiple unknown control directions. *Automatica*, 89:259–265, 2018.

[37] J. Huang, W. Wang, C. Wen, and J. Zhou. Adaptive control of a class of strict-feedback time-varying nonlinear systems with unknown control coefficients. *Automatica*, 93:98–105, 2018.

[38] X. Huang and Y. Tian. Asynchronous distributed localization in networks with communication delays and packet losses. *Automatica*, 96:134–140, 2018.

[39] P. Ioannou and J. Sun. *Robust Adaptive Control*. Dover Publications, 2012.

[40] B. Jiang, Q. Shen, and P. Shi. Neural-networked adaptive tracking control for switched nonlinear pure-feedback systems under arbitrary switching. *Automatica*, 61:119–125, 2015.

[41] H. K. Khalil. *Nonlinear Systems (3rd Edition)*. Pearson, 2001.

[42] H. Kim, H. Shim, J. Back, and J. H. Seo. Consensus of output-coupled linear multi-agent systems under fast switching network: averaging approach. *Automatica*, 49: 267–272, 2013.

[43] J. Ko, A. Kurdila, and T. Strganac. Nonlinear control of a prototypical wing section with torsional nonlinearity. *Journal of Guidance, Control, and Dynamics*, 20(6): 1181–1189, 1997.

[44] M. Krstic, I. Kanellakopoulos, and P. Kokotovic. *Nonlinear and Adaptive Control Design*. New York, NY, USA : Wiley, 1995.

[45] G. Lai, Z. Liu, C. L. P. Chen, and Y. Zhang. Adaptive asymptotic tracking control of uncertain nonlinear system with input quantization. *Systems and Control Letters*, 96(8):23–29, 2016.

[46] D. J. Li and D. P. Li. Adaptive tracking control for nonlinear time-varying delay systems with full state constraints and unknown control coefficients. *Automatica*, 93:444–453, 2018.

[47] Y. Li and G. Yang. Adaptive asymptotic tracking control of uncertain nonlinear systems with input quantization and actuator faults. *Automatica*, 72:177–185, 2016.

[48] Y. Li, S. Tong, L. Liu, and G. Feng. Adaptive output-feedback control design with prescribed performance for switched nonlinear systems. *Automatica*, 80:225–231, 2017.

[49] Y. Li, L. Liu, and G. Feng. Robust adaptive output feedback control to a class of non-triangular stochastic nonlinear systems. *Automatica*, 89:325–332, 2018.

[50] Y. Li, F. Qu, and S. Tong. Observer-based fuzzy adaptive finite-time containment control of nonlinear multiagent systems with input delay. *IEEE Transactions on Cybernetics*, 51(1):126–137, 2021.

[51] Y. X. Li. Barrier lyapunov function-based adaptive asymptotic tracking of nonlinear systems with unknown virtual control coefficients. *Automatica*, 121:109181, 2020.

[52] Y. X. Li and G. H. Yang. Adaptive asymptotic tracking control of uncertain nonlinear systems with input quantization and actuator faults. *Automatica*, 72:177–185, 2016.

[53] H. Liang, Y. Zhang, T. Huang, and H. Ma. Prescribed performance cooperative control for multi-agent systems with input quantization. *IEEE Transactions on Cybernetics*, 50(2):1810–1819, 2020.

[54] D. Liberzon. *Switching in Systems and Control*. Boston: Birkhauser, 2003.

[55] W. Lin and R. Pongvuthithum. Adaptive output tracking of inherently nonlinear systems with nonlinear parameterization. *IEEE Transactions on Automatic Control*, 48(10):1737–1745, 2003.

[56] W. Lin and C. Qian. Adding one power integrator: a tool for global stabilization of high-order lower-triangular systems. *Systems & Control Letters*, 39:339–351, 2000.

[57] W. Lin, R. Pongvuthithum, and C. Qian. Control of high-order nonholonomic systems in power chained form using discontinuous feedback. *IEEE Transactions on Automatic Control*, 47(1):108–115, 2002.

[58] Y. Liu and S. Tong. Barrier lyapunov functions for nussbaum gain adaptive control of full state constrained nonlinear systems. *Automatica*, 76:143–152, 2017.

[59] Y. Liu, S. Lu, S. Tong, X. Chen, C. L. P. Chen, and D. Li. Adaptive control-based Barrier Lyapunov Functions for a class of stochastic nonlinear systems with full state constraints. *Automatica*, 87:83–93, 2018.

[60] Y. J. Liu and S. C. Tong. Barrier Lyapunov functions for Nussbaum gain adaptive control of full state constrained nonlinear systems. *Automatica*, 76:143–152, 2017.

[61] M. Lv, W. Yu, J. Cao, and S. Baldi. Consensus in high-power multiagent systems with mixed unknown control directions via hybrid nussbaum-based control. *IEEE Transactions on Cybernetics*, DOI: 10.1109/TCYB.2020.3028171.

[62] M. Lv, W. Yu, J. Cao, and S. Baldi. A separation-based methodology to consensus tracking of switched high-order nonlinear multi-agent systems. *IEEE Transactions on Neural Networks and Learning Systems*, DOI:10.1109/TNNLS.2021.3070824.

[63] M. Lv, B. De Schutter, C. Shi, and S. Baldi. Logic-based distributed switching control for agents inpower chained form with multiple unknown control directions. *Automatica*, Second Review.

[64] M. Lv, Z. Chen, B. De Schutter, and S. Baldi. Prescribed performance tracking for high-power nonlinear dynamics with time-varying unknown control coencients. *Automatica*, Under Review.

[65] Y. Man and Y. Liu. Global adaptive stabilization and practical tracking for nonlinear systems with unknown powers. *Automatica*, 100:171–181, 2018.

[66] N. D. Manring and R. C. Fales. *Hydraulic Control Systems*. New York, USA: John Wiley, 2019.

[67] U. Münz, A. Papachristodoulou, and F. Allgöwer. Robust consensus controller design for nonlinear relative degree two multi-agent systems with communication constraints. *IEEE Transactions on Automatic Control*, 56(1):145–161, 2011.

[68] W. Meng, Q. Yang, S. Jagannathan, and Y. Sun. Adaptive neural control of high-order uncertain nonaffine systems: A transformation to affine systems approach. *Automatica*, 50:1473–1480, 2014.

[69] W. Meng, Q. Yang, S. Jagannathan, and Y. Sun. Distributed control of high-order nonlinear input constrained multiagent systems using a backstepping-free method. *IEEE Transactions on Cybernetics*, 49(11):3923–3933, 2019.

[70] W. Meng, X. Liu, Q. Yang, and Y. Sun. Distributed synchronization control of non-affine multiagent systems with guaranteed performance. *IEEE Transactions on Neural Networks and Learning Systems*, 31(5):1571–1580, 2020.

[71] K. H. Movric and F. L. Lewis. Cooperative optimal control for multi-agent systems on directed graph topologies. *IEEE Transactions on Automatic Control*, 59(3):769–774, 2014.

[72] M. Muresan. *A Concrete Approach to Classical Analysis*. Springer, 2008.

[73] J. Na, X. Ren, and D. Zheng. Adaptive control for nonlinear pure-feedback systems with high-order sliding mode observer. *IEEE Transactions on Neural Networks and Learning Systems*, 24(3):370–382, 2013.

[74] D. H. Nguyen. Minimum-rank dynamic output consensus design for heterogeneous nonlinear multi-agent systems. *IEEE Transactions on Control of Network Systems*, 5(1):105–115, 2018.

[75] R. D. Nussbaum. Some remarks on a conjecture in parameter adaptive control. *Systems & Control Letters*, 3(5):243–246, 1983.

[76] K. K. Oh, M. C. Park, and H. S. Ahn. A survey of multi-agent formation control. *Automatica*, 53:424–440, 2015.

[77] T. R. Oliveria, A. J. Peixoto, and H. Liu. Sliding mode control of uncertain multivariable nonlinear systems with unknown control directions via switching and monitoring function. *IEEE Transactions on Automatic Control*, 55(4):1028–1034, 2010.

[78] H. P. Ouyang and Y. Lin. Adaptive fault-tolerant control for actuator failures: A switching strategy. *Automatica*, 81:87–95, 2017.

[79] F. D. Priscoli, A. Isidori, L. Marconi, and A. Pietrabissa. Leader following coordination of nonlinear agents under time-varying communication topologies. *IEEE Transactions on Control of Network Systems*, 2(4):393–405, 2015.

[80] H. E. Psillakis. Further results on the use of nussbaum gains in adaptive neural network control. *IEEE Transactions on Automatic Control*, 55(12):2841–2846, 2010.

[81] H. E. Psillakis. Adaptive NN cooperative control of unknown nonlinear multiagent systems with communication delays. *IEEE Transactions on Systems, Man, and Cybernetics: Systems*, DOI: 10.1109/TSMC.2019.2950114.

[82] C. Qian and W. Lin. Output feedback control of a class of nonlinear systems: A nonseparation principle paradigm. *IEEE Transactions on Automatic Control*, 47 (10):1710–1715, 2002.

[83] C. Qian and W. Lin. Practical output tracking of nonlinear systems with uncontrollable unstable linearization. *IEEE Transactions on Automatic Control*, 47(1):21–35, 2002.

[84] W. Ren and Y. Cao. *Distributed Coordination of Multi-Agent Networks: Emergent Problems, Models, and Issues*. London: Springer-Verlag, 2010.

[85] R. O. Saber and R. M. Murray. Consensus problems in networks of agents with switching topology and time-delays. *IEEE Transactions on Automatic Control*, 49 (9):1520–1533, 2004.

[86] R. M. Sanner and J. E. Slotine. Gaussian networks for direct adaptive control. *IEEE Transactions on Neural Networks*, 3(6):837–863, 1992.

[87] Q. Shen and P. Shi. Distributed command filtered backstepping consensus tracking control of nonlinear multiple-agent systems in strict-feedback form. *Automatica*, 53:120–124, 2015.

[88] Q. Shen, P. Shi, J. Zhu, S. Wang, and Y. Shi. Neural networks-based distributed adaptive control of nonlinear multiagent systems. *IEEE Transactions on Neural Networks and Learning Systems*, 31(3):1010–1021, 2020.

[89] C. Shi, Z. Liu, X. Dong, and Y. Chen. A novel error-compensation control for a class of high-order nonlinear systems with input delay. *IEEE Transactions on Neural Networks and Learning Systems*, 29(9):4077–4087, 2018.

[90] Y. Song and Y. Wang. *Cooperative Control of Nonlinear Networked Systems: Infinite-time and Finite-time Design Methods*. Springer, 2019.

[91] E. D. Sontag. *Mathematical Control Theory*. London, U.K.: Springer, 1998.

[92] W. Sun, S. F. Su, Y. Q. Wu, J. W. Xia, and V. T. Nguyen. Adaptive fuzzy control with high-order barrier Lyapunov functions for high-order uncertain nonlinear systems with full-state constraints. *IEEE Transactions on Cybernetics*, 50(8):3424–3432, 2020.

[93] W. Sun, Y. Q. Wu, and Z. Y. Sun. Command filter-based finite-time adaptive fuzzy control for uncertain nonlinear systems with prescribed performance. *IEEE Transactions on Fuzzy Systems*, 28(12):3167–3170, 2020.

[94] W. Sun, S. F. Su, Y. Q. Wu, and J. W. Xia. Adaptive fuzzy event-triggered control for high-order nonlinear systems with prescribed performance. *IEEE Transactions on Cybernetics*, DOI: 10.1109/TCYB.2020.3025829.

[95] Z. Sun, X. Zhang, and X. Xie. Global continuous output-feedback stabilization for a class of high-order nonlinear systems with multiple time delays. *Journal of the Franklin Institute*, 351(8):4344–4356, 2014.

[96] Z. Sun, L. Xue, and K. Zhang. A new approach to finite-time adaptive stabilization of high-order uncertain nonlinear system. *Automatica*, 58:60–66, 2015.

[97] Z. Sun, T. Li, and S. Yang. A unified time-varying feedback approach and its applications in adaptive stabilization of high-order uncertain nonlinear systems. *Automatica*, 70:249–257, 2016.

[98] Z. Y. Sun and Y. G. Liu. Adaptive state-feedback stabilization for a class of high-order nonlinear uncertain systems. *Automatica*, 43:1772–1783, 2007.

[99] K. Tee, S. Ge, and E. Tay. Barrier lyapunov Functions for the control of output-constrained nonlinear systems. *Automatica*, 45:918–927, 2009.

[100] K. Tee, B. Ren, and S. Ge. Control of nonlinear systems with time-varying output constraints. *Automatica*, 47:2511–2516, 2011.

[101] A. Theodorakopoulos and G. A. Rovithakis. Guaranteeing preselected tracking quality for uncertain strict-feedback systems with deadzone input nonlinearity and disturbances via low-complexity control. *Automatica*, 54:135–145, 2015.

[102] Y. Tian and Y. Zhang. High-order consensus of heterogeneous multi-agent systems with unknown communication delays. *Automatica*, 48:1205–1212, 2012.

[103] C. Wang and D. J. Hill. *Deterministic Learning Theory for Identification, Recognition, and Control*. Taylor & Francis Group, 2009.

[104] C. Wang, G. Chen, and S. Ge. Smart neural control of uncertain nonlinear systems. *International Journal of Adaptive Control and Signal Processing*, 17:467–488, 2003.

[105] F. Wang, B. Chen, C. Lin, and X. Li. Distributed adaptive neural control for stochastic nonlinear multiagent systems. *IEEE Transactions on Cybernetics*, 47(7):1795–1803, 2017.

[106] G. Wang. Distributed control of higher-order nonlinear multi-agent systems with unknown non-identical control directions under general directed graphs. *Automatica*, 110:108559, 2019.

[107] N. Wang, G. Wen, Y. Wang, F. Zhang, and A. Zemouche. Fuzzy adaptive cooperative consensus tracking of high-order nonlinear multiagent networks with guaranteed performances. *IEEE Transactions on Cybernetics*, DOI: 10.1109/TCYB.2021.3051002.

[108] Q. Wang, H. E. Psillakis, and C. Sun. Adaptive cooperative control with guaranteed convergence in time-varying networks of nonlinear dynamical systems. *IEEE Transactions on Cybernetics*, 50(12):5035–5046, 2020.

[109] Q. Wang, H. E. Psillakis, and C. Sun. Cooperative control of multiple high-order agents with nonidentical unknown control directions under fixed and time-varying topologies. *IEEE Transactions on Systems, Man, and Cybernetics: Systems*, 51(4):2582–2591, 2021.

[110] W. Wang and S. Tong. Adaptive fuzzy bounded control for consensus of multiple strict-feedback nonlinear systems. *IEEE Transactions on Cybernetics*, 48(2):522–531, 2018.

[111] W. Wang, C. Wen, and J. Huang. Distributed adaptive asymptotically consensus tracking control of nonlinear multi-agent systems with unknown parameters and uncertain disturbances. *Automatica*, 77:133–142, 2017.

[112] X. Wang, H. Li, G. Zong, and X. Zhao. Adaptive fuzzy tracking control for a class of high-order switched uncertain nonlinear systems. *Journal of the Franklin Institute*, 354(4):6567–6587, 2017.

[113] Y. Wang and Y. Song. Fraction dynamic-surface-based neuroadaptive finite-time containment control of multiagent systems in nonaffine pure-feedback form. *IEEE Transactions on Neural Networks and Learning Systems*, 28(3):678–689, 2017.

[114] Y. Wang and Y. Song. Leader-following control of high-order multi-agent systems under directed graphs: pre-specified finite time approach. *Automatica*, 87:113–120, 2018.

[115] J. Wu, W. Chen, and J. Li. Global finite-time adaptive stabilization for nonlinear systems with multiple unknown control directions. *Automatica*, 69:298–307, 2016.

[116] L. Xing, C. Wen, Z. Liu, H. Su, and J. Cai. Event-triggered adaptive control for a class of uncertain nonlinear systems. *IEEE Transactions on Automatic Control*, 62 (4):2071–2076, 2017.

[117] L. Xing, C. Wen, Z. Liu, H. Su, and J. Cai. Event-triggered output feedback control for a class of uncertain nonlinear systems. *IEEE Transactions on Automatic Control*, 64(1):290–297, 2019.

[118] B. Xu, C. Yang, and Y. Pan. Global neural dynamic surface tracking control of strict-feedback systems with application to hypersonic flight vehicl. *IEEE Transactions on Neural Networks and Learning Systems*, 26(10):2563–2575, 2015.

[119] J. Xu. Fault tolerant finite-time leader follower formation control for autonomous surface vessels with LOS range and angle constraints. *Automatica*, 68:228–236, 2016.

[120] J. Xu. Adaptive iterative learning control for high-order nonlinear multi-agent systems consensus tracking. *Systems & Control Letters*, 89:16–23, 2016.

[121] J. Xu. Nonrepetitive leader follower formation tracking for multiagent systems with LOS range and angle constraints using iterative learning control. *IEEE Transactions on Cybernetics*, 49(5):1748–1758, 2019.

[122] X. Ye. Adaptive nonlinear output-feedback control with unknown high-frequency gain sign. *IEEE Transactions on Automatic Control*, 46(1):112–115, 2001.

[123] X. Ye. Global adaptive control of nonlinearly parametrized systems. *IEEE Transactions on Automatic Control*, 48(1):169–173, 2003.

[124] X. Ye. Switching adaptive output-feedback control of nonlinearly parametrized systems. *Automatica*, 41:983–989, 2005.

[125] X. Ye and J. Jiang. Adaptive nonlinear design without a priori knowledge of control directions. *IEEE Transactions on Automatic Control*, 43(11):1617–1621, 1998.

[126] S. Yoo. Distributed consensus tracking for multiple uncertain nonlinear strict-feedback systems under a directed graph. *IEEE Transactions on Neural Networks and Learning Systems*, 24(4):666–672, 2013.

[127] S. Yoo. Distributed consensus tracking of a class of asynchronously switched nonlinear multi-agent systems. *Automatica*, 87:421–427, 2018.

[128] S. Yoo. Distributed low-complexity fault-tolerant consensus tracking of switched nonlinear pure-feedback multi-agent systems under asynchronous switching. *Nonlinear Analysis: Hybrid Systems*, 32:239–253, 2019.

[129] J. Yu, L. Zhao, H. Yu, and C. Lin. Barrier lyapunov functions-based command filtered output feedback control for full-state constrained nonlinear systems. *Automatica*, 105:71–79, 2019.

[130] W. Yu, W. Ren, W. Zheng, G. Chen, and J. Lü. Distributed control gains design for consensus in multi-agent systems with second-order nonlinear dynamics. *Automatica*, 49(7):2107–2115, 2013.

[131] W. Yu, G. Wen, G. Chen, and J. Cao. *Distributed Cooperative Control of Multi-agent Systems, 1st Edition*. Wiley, 2017.

[132] H. Zhang and F. L. Lewis. Adaptive cooperative tracking control of higher-order nonlinear systems with unknown dynamics. *Automatica*, 48:1432–1439, 2012.

[133] J. X. Zhang and G. H. Yang. Prescribed performance fault-tolerant control of uncertain nonlinear systems with unknown control directions. *IEEE Transactions on Automatic Control*, 62(12):6529–6535, 2017.

[134] W. Zhang, M. S. Branicky, and S. M. Phillips. Stability of networked control systems. *IEEE Control Systems Magazine*, 21(1):84–99, 2001.

[135] X. Zhao, P. Shi, X. Zheng, and J. Zhang. Intelligent tracking control for a class of uncertain high-order nonlinear systems. *IEEE Transactions on Neural Networks and Learning Systems*, 27(9):1976–1982, 2016.

[136] X. Zhao, X. Wang, G. Zong, and X. Zheng. Adaptive neural tracking control for switched high-order stochastic nonlinear systems. *IEEE Transactions on Cybernetics*, 47(10):3088–3099, 2017.

[137] S. Zheng and Q. Meng. Ananti-windup INDI fault-tolerant control scheme for flying wing aircraft with actuator faults. *ISA Transactions*, 93:172–179, 2019.

[138] X. Zheng, X. Zhao, R. Li, and Y. Yin. Adaptive neural tracking control for a class of switched uncertain nonlinear systems. *Neurocomputing*, 168(30):320–326, 2015.

[139] J. Zhou, C. Wen, and G. Yang. Adaptive backstepping stabilization of nonlinear uncertain systems with quantized input signal. *IEEE Transactions on Automatic Control*, 59(2):460–464, 2014.

[140] W. Zou, P. Shi, Z. Xiang, and Y. Shi. Consensus tracking control of switched stochastic nonlinear multiagent systems via event-triggered strategy. *IEEE Transactions on Neural Networks and Learning Systems*, 31(3):1036–1045, 2020.

[141] W. Zou, P. Shi, Z. Xiang, and Y. Shi. Finite-time consensus of second-order switched nonlinear multi-agent systems. *IEEE Transactions on Neural Networks and Learning Systems*, 31(5):1757–1762, 2020.

[142] Z. Y. Zuo. Nonsingular fixed-time consensus tracking for second-order multi-agent networks. *Automatica*, 54(54):305–309, 2015.

CURRICULUM VITÆ

The photo was shot in November 2017, at Terracotta Warriors, Xi'an, China.

Maolong Lv (left in the picture) was born on November 18th 1991, Mianyang, Sichuan Province, China. He obtained his BSc degree and MSc degree both from China. In January 2018, he became a Ph.D. candidate at the Delft Center for Systems and Control, Delft University of Technology, in Delft, The Netherlands. In his Ph.D. project, he worked on adaptive distributed control of uncertain multi-agent systems in power-chained form systems under the supervision of Dr. Simone Baldi (right in the picture) and Prof. dr. ir. Bart De Schutter.

Mr. Lv was awarded a Descartes Excellence Fellowship from the Institut Francais des Pays-Bas in 2018, which allowed him a research visit and cooperation with the University of Grenoble on the topic of adaptive networked systems with emphasis on ring stability analysis for mixed traffic with human driven and autonomous vehicles from September 2018 to January 2019.

The focus of his PhD was on distributed control for multi-agent nonlinear systems in power-chained form with emphasis on (partially) unknown control directions. His research interests include distributed control, reinforcement learning control, ADP, swarm control and switched systems with applications in multi-agent systems and unmanned and/or autonomous systems.

List of Publications

Journal Articles

12. **M. Lv**, B. De Schutter, C. Shi, and S. Baldi, “Logic-based Distributed Switching Control for Agents in Power-Chained Form with Multiple Unknown Control Directions", *Automatica*. Conditionally accepted.

11. **M. Lv**, W. Yu, J. Cao, and S. Baldi, “A Separation-based Methodology to Consensus Tracking of Switched High-Order Nonlinear Multi-Agent Systems", *IEEE Transactions on Neural Network and Learning Systems*. 2021. DOI:10. 1109/TNNLS.2021. 3070824.

10. **M. Lv**, B. De Schutter, W. Yu, W. Zhang, and S. Baldi, “Nonlinear Systems with Uncertain Periodically Disturbed Control Gain Functions: Adaptive Fuzzy Control with Invariance Properties", *IEEE Transactions on Fuzzy Systems*, vol. 28, no. 4, pp. 746-757, 2020.

9. **M. Lv**, Y. Li, W. Pan, and S. Baldi, “Finite-Time Fuzzy Adaptive Constrained Tracking Control for Hypersonic Flight Vehicles with Singularity-Free Switching", *IEEE/ASME Transactions on Mechatronics*, 2021. doi:10.1109/TMECH.2021.3090509.

8. **M. Lv**, B. De Schutter, W. Yu, and S. Baldi, “Adaptive Asymptotic Tracking for a Class of Uncertain Switched Positive Compartmental Models with Application to Anesthesia", *IEEE Transactions on Systems, Man, and Cybernetics: Systems*, vol. 51, no. 8, pp. 4936-4942, 2021.

7. **M. Lv**, W. Yu, J. Cao, and S. Baldi, “Consensus in High-Power Multiagent Systems With Mixed Unknown Control Directions via Hybrid Nussbaum-Based Control", *IEEE Transactions on Cybernetics*. 2020. DOI: 10.1109/TCYB. 2020.3028171.

6. **M. Lv**, W. Yu, and S. Baldi, “The Set-Invariance Paradigm in Fuzzy Adaptive DSC Design of Large-Scale Nonlinear Input-Constrained Systems", *IEEE Transactions on Systems, Man, and Cybernetics: Systems*, vol. 51, no. 2, pp. 1035-1045, 2021.

5. **M. Lv**, S. Baldi, and Z. C. Liu, “The Non-Smoothness Problem in Disturbance Observer Design: A Set-Invariance-Based Adaptive Fuzzy Control Method", *IEEE Transactions on Fuzzy Systems*, vol. 27, no. 3, pp. 598-604, 2019.

4. **M. Lv**, B. De Schutter, J. Cao, and S. Baldi, “Adaptive Prescribed Performance Asymptotic Tracking for High-Order Odd-Rational-Power Nonlinear Systems", *IEEE Transactions on Automatic Control*. Third round review.

3. **M. Lv**, Z. Chen, B. De Schutter, and S. Baldi, “Prescribed Performance Tracking for High-Power Nonlinear Dynamics with Time-Varying Unknown Control Coefficients", *Automatica*. Under review.

2. **M. Lv**, B. De Schutter, and S. Baldi, “Non-Recursive Control for Formation Containment of HFV Swarms with Dynamic Event-Triggered Communication", *IEEE Transactions on Industrial Informatics*. Under review.

1. S. Yuan, **M. Lv**, S. Baldi, and L. Zhang “Lyapunov-Equation-based Stability Analysis for Switched Linear Systems and Its Application to Switched Adaptive Control", *IEEE Transactions on Automatic Control*. DOI: 10.1109/TAC.2020.3003647.

Conference Proceedings

5. **M. Lv**, W. Yu, and S. Baldi, “Fuzzy Adaptive Tracking Control of High-order Nonlinear Dynamics with Mixed Control Directions", *the 39th Chinese Control Conference (CCC)*, July 27th-29th, Shenyang, China, 2020.

4. **M. Lv**, W. Yu, S. Baldi, and F. Zhang, “Model Reference Switched Adaptive Control with Nonnegative Orthant State Constraints", *the 38th Chinese Control Conference (CCC)*, July 27th-30th, Guangzhou, China, 2019.

3. V. Giammarino, **M. Lv**, S. Baldi, P. Frasca, and M. L. Delle Monache, “On a Weaker Notion of Ring Stability for Mixed Traffic with Human-Driven and Autonomous Vehicles", *the 58th Conference on Decision and Control (CDC)*, December 11st-13rd, Nice, France, 2019.

2. D. Jagga, **M. Lv**, and S. Baldi, “Hybrid adaptive chassis control for vehicle lateral stability in the presence of uncertainty", *the 26th Mediterranean Conference on Control and Automation (MED)*, June 19th-22nd, Zadar, Croatia, 2018.

1. Y. Chen, **M. Lv**, S. Baldi, and Z. Liu, “Relaxing the Control-gain Assumptions of DSC Design for Nonlinear MIMO Systems", *the 12th Asian Control Conference (ASCC)*, June 9th-12nd, Kitakyusyu, Janpan, 2019.